Characterisation of Two Class V Myosins in the Fission Yeast *Schizosaccharomyces pombe*

Thein Zaw Win

A Thesis Submitted to the University of London
for the Degree of Doctor of Philosophy
October 2000

Department of Biology
University College London
Gower Street
London WC1E 6BT

ProQuest Number: U643836

All rights reserved

INFORMATION TO ALL USERS
The quality of this reproduction is dependent upon the quality of the copy submitted.

In the unlikely event that the author did not send a complete manuscript
and there are missing pages, these will be noted. Also, if material had to be removed,
a note will indicate the deletion.

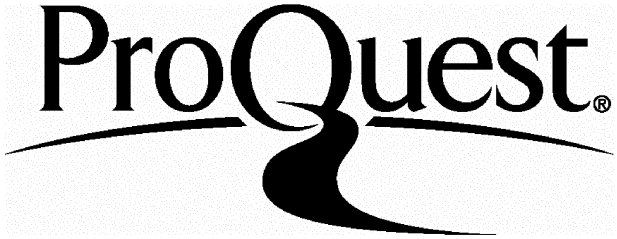

ProQuest U643836

Published by ProQuest LLC(2016). Copyright of the Dissertation is held by the Author.

All rights reserved.
This work is protected against unauthorized copying under Title 17, United States Code.
Microform Edition © ProQuest LLC.

ProQuest LLC
789 East Eisenhower Parkway
P.O. Box 1346
Ann Arbor, MI 48106-1346

for mum and dad

Acknowledgements

First and foremost I would like to thank the most important person in my research study my supervisor, Prof. Jerry Hyams. I am indebted to Jerry for his guidance, support, fairness and encouragement throughout this project. The one thing I would like to thank him most for, is his faith in me for which my heart felt and deepest gratitude goes out to Jerry and for which I will always remember.

I would also like to thank Dr Yannick Gachet for encouraging me to carry out important experiments and in particular teaching me how to do them. My thanks to Dr Daniel Mulvihill for teaching me how to perform certain experiments efficiently so that results can be obtained quickly. I would also like to express my gratitude to Dr Karen May for showing me how to carry out a Southern blot analysis and giving me support and motivation during my first year of research in Jerry's lab. My thanks to Mrs Vasanti Amin for teaching me immunofluorescence techniques and for her support throughout my research study. My thanks also goes to two former project students under my supervision, Panagiota Loli and Nalini Iyanger, for helping me in the localisation of Myo52 in fission yeast.

Finally, I would like to express my warm and humble gratitude to mum, dad, my brother and sisters and to all my teachers for filling my life with love, kindness and guidance.

ABSTRACT

The fission yeast *Schizosaccharomyces pombe* is a cylindrically-shaped cell which grows by tip elongation and divides by medial fission. The actin cytoskeleton is intimately associated with both of these processes. The actin-activated motor protein, myosin, is involved in cellular processes that require the function of the actin cytoskeleton. *S. pombe* has five myosin genes spread amongst three different myosin classes. This thesis describes the identification and characterisation of two of these genes, *myo51*$^+$ and *myo52*$^+$, both of which belong to the class V group of the myosin superfamily.

Gene inactivation studies reveal that *myo51Δ* cells display a phenotype that is indistinguishable from wild type whereas *myo52Δ* cells are temperature-sensitive with a rounded and pear-shaped morphology. The *myo51Δ myo52Δ* double mutant has the same characteristics as the *myo52Δ* single mutant. Overexpression of *myo51*$^+$ produce elongated cells with multiple nuclei whereas overexpression of *myo52*$^+$ produce branched cells with thickened septa. Preliminary localisation of Myo51 shows that the protein is localised to one of the cell poles. Detailed localisation studies of Myo52 shows that the protein is localised to the actin-rich poles during tip growth and is present at the equator in cells undergoing cytokinesis. The localisation of Myo52 is dependent on an intact actin cytoskeleton.

Further analysis of *myo52Δ* shows that the null mutant is resistant to cell wall digestion by Zymolyase. Immunoblot analysis of the α-glucan synthase, Mok1, shows that the protein is upregulated in *myo52Δ* cells. Localisation studies reveal that Mok1 colocalises with Myo52 at the cell poles during tip growth and to a certain extent at the equator during cytokinesis. Mok1 is delocalised in *myo52Δ* cells. These findings suggest that the function of Myo52 is to localise factors involved in growth, such as Mok1, to defined sites in the cell by virtue of its interaction with the actin cytoskeleton.

CONTENTS

Title Page 1
Acknowledgements 2
Abstract 3
Table of Contents 4
Figures and Tables 9
Abbreviations 11
A Note on Nomenclature 13

Chapter 1 Introduction
1.1 THE CYTOSKELETON 17
1.1.1 Introduction 17
1.1.2 Actin 17
1.1.3 Actin Binding Proteins 19
1.1.4 Microtubules 20
1.1.5 Microtubule Associated Proteins 22
1.1.6 Intermediate Filaments 22

1.2 MYOSINS 26
1.2.1 The Myosin Superfamily 26
1.2.2 Myosin Structure 29
a. Proteolytic Cleavage of Myosin II 29
b. Head Domain 30
c. Neck Domain 32
d. Tail Domain 34
1.2.3 The Myosin Catalytic Cycle and Force Production 40
a. The Catalytic Cycle 40
b. Force Production 41
1.2.4 Myosin Function 44
a. Class I Myosins 44
b. Class II Myosins 47
c. Class V Myosins 49
1.2.5 Myosins Participate in the Coordinated Transport of Cellular Cargo Along Actin and Microtubule Tracks 52

1.3 FISSION YEAST 55
1.3.1 Introduction 55
1.3.2 The Life Cycle of *Schizosaccharomyces pombe* 56
1.3.3 The Cell Division Cycle 58
1.3.4 Growth and Septation in Fission Yeast 60
1.3.5 The Fission Yeast Cytoskeleton 61
a. The Actin Cytoskeleton 61
b. The Microtubule Cytoskeleton 64
1.3.6 Cell Morphogenesis in *S. pombe* 67

1.3.7 Cytokinesis in *S. pombe* 70
a. Timing of Cell Division 70
b. Cleavage Plane Specification 72
c. Medial Ring Assembly 76
d. Medial Ring Contraction and Septation 81

1.4 OBJECTIVES OF THIS THESIS 89

Chapter 2 Materials and Methods
2.1 Identification and Analysis of Myosin Sequences 91
2.2 Chemicals 91
2.3 Strains and Media 91
2.4 Plasmids 92
2.5 Oligonucleotides 93
2.6 Preparation of Yeast Genomic DNA 94
2.7 Polymerase Chain Reaction (PCR) 95
2.8 Phenol:Chloroform Extraction of DNA 96
2.9 Ethanol Precipitation of DNA 96
2.10 Restriction Digest Analysis 96
2.11 Dephosphorylation of Plasmid DNA 96
2.12 Agarose Gel Electrophoresis 97
2.13 Recovery of DNA Fragments from Agarose Gels 97
2.14 Ligations 97
2.15 Transformation of *E. coli* 98
2.16 Recovery of Plasmid DNA from *E. coli* 98
2.17 Transformation of *S. pombe* 99
a. Method 1 99
b. Method 2 100
2.18 Southern Hybridisation Analysis of Genomic DNA 101
a. Preparation of Samples 101
b. Southern Transfer 101
c. Preparation of the Hybridisation Probe 101
d. Hybridisation of DNA 102
2.19 Re-isolation of Yeast Strains 102
2.20 Measuring Cell Concentration 102
2.21 Mating Cells 103
2.22 Yeast Classical Genetics 103
a. Tetrad Analysis 103
b. Random Spore Analysis 103
2.23 Overexpression of Genes 104
2.24 Treatment with Actin- and Microtubule-Depolymerising Drugs 104
2.25 Cell Fixation 104
a. Methanol Fixation 104
b. Formaldehyde-Glutaraldehyde Fixation 105
2.26 Nuclear Staining with DAPI 105
2.27 Cell Wall Staining with Calcofluor 105

2.28 Localisation of Specific Proteins by Immunofluorescence Microscopy 105
2.29 Microscopy and Photography 106
2.30 Zymolyase Cell Wall Digestion Assay 107
2.31 Immunoblot Analysis of Proteins 107
a. Protein Extraction 107
b. Sodium Dodecyl Sulphate Polyacrylamide Gel Electrophoresis (SDS- PAGE) 108
c. Protein Transfer 108
d. Probing with Antibody 109

Chapter 3 Identification of *myo51*$^+$ and *myo52*$^+$
3.1 INTRODUCTION 111

3.2 RESULTS 113
3.2.1 Identification of *myo51*$^+$ and *myo52*$^+$ 113
3.2.2 Myo51 and Myo52 are Class V Myosins 114
3.2.3 Features of Myo51 and Myo52 118
a. Head Domain 118
b. Neck Domain 119
c. Tail Domain 121

3.3 DISCUSSION 128

Chapter 4 Deletion of *myo51*$^+$ and *myo52*$^+$
4.1 INTRODUCTION 133

4.2 RESULTS 134
4.2.1 Construction of the *myo51*$^+$ and *myo52*$^+$ Integration Cassettes 134
4.2.2 Selection of the Null Mutants 135
4.2.3 *myo51Δ* Cells are Viable and Display Wild Type Morphology 138
4.2.4 *myo52Δ* Cells are Viable but Display an Aberrant Cell Morphology 138
4.2.5 Actin Organisation in *myo51Δ* and *myo52Δ* 139
4.2.6 Microtubule Oganisation in *myo51Δ* and *myo52Δ* 140
4.2.7 *myo52Δ* Cells are Temperature-Sensitive 141
4.2.8 *myo51Δ* and *myo52Δ* Exhibit a Genetic Interaction with the Temperature-Sensitive Actin Mutant *cps8*$^-$ but Not with Each Other 145
4.2.9 *myo52Δ* Cells do Not Grow Well After Prolonged Periods in the Same Medium 147

4.3 DISCUSSION 151

Chapter 5 Overexpression of *myo51*$^+$ and *myo52*$^+$
5.1 INTRODUCTION..... 156

5.2 RESULTS..... 157
5.2.1 Cloning of *myo51*$^+$ and *myo52*$^+$ into pREP Expression Vector..... 157
5.2.2 *myo51*$^+$ Gene is Correctly Expressed from Plasmids..... 161
5.2.3 *myo52*$^+$ Gene is Correctly Expressed from Plasmids..... 162
5.2.4 Overexpression of *myo51*$^+$ Produces Elongated..... 163
Multinucleate Cells
5.2.5 Overexpression of *myo52*$^+$ Produces Branched Cells with..... 164
Thickened Septa

5.3 DISCUSSION..... 169

Chapter 6 Localisation of Myo51 and Myo52
6.1 INTRODUCTION..... 174

6.2 RESULTS..... 176
6.2.1 Localisation of Myo51 by Indirect Immunofluorescence..... 176
Microscopy
6.2.2 Localisation of Myo52..... 177
a. Localisation of Myo52 by Indirect Immunofluorescence..... 177
Microscopy
b. Localisation of GFP-Myo52..... 178
c. Localisation of Myo52 Expressed from its Own Promoter..... 179
6.2.3 Localisation of Myo52 Correlates with the Distribution of Actin.... 185
6.2.4 Myo52 Relocates from the Poles to the Equator at Late Anaphase. 185
6.2.5 Myo52 Relocates to the Equator Before Septation 186
6.2.6 Myo52 Localises to Sites of Septation..... 187
6.2.7 Myo52 Localises to Growing Poles 188
6.2.8 Localisation of Myo52 is Dependent on an Intact Actin 195
Cytoskeleton
a. Treatment with Cytochalasin A..... 195
b. Localisation of Myo52 in cps8$^-$..... 195
c. Treatment with Latrunculin B..... 196
6.2.9 Polar Localisation of Myo52 is Dependent on an..... 196
Intact Microtubule Cytoskeleton

6.3 DISCUSSION..... 200
6.3.1 Myo51 Localisation..... 200
6.3.2 Myo52 Localisation..... 201
a. Myo52 and Polarised Growth..... 201
b. Myo52 and Cell Division..... 202
c. Myo52 and the Fission Yeast Cytoskeleton..... 203

Chapter 7 Myo52 and Cell Wall Synthesis
7.1 INTRODUCTION..... 206

7.2 RESULTS..... 208
7.2.1 *myo52Δ* Exhibits a Genetic Interaction with Components of the..... 208
Pathway that Regulates Septation
7.2.2 *myo52Δ* Cells Form Multiple Septa Upon Overexpression..... 209
with *spg1*$^{+}$
7.2.3 *myo52Δ* Exhibits a Genetic Interaction with Mutants that are..... 210
Defective in Actin Organisation
7.2.4 Moderate Expression of Myo52 is Toxic to *cdc4-8* Cells..... 211
7.2.5 Myo52 Colocalises with Mok1 α-Glucan Synthase..... 216
7.2.6 Mok1 is Delocalised in *myo52Δ* Cells..... 217
7.2.7 Myo52 Localisation does not Require Mok1..... 217
7.2.8 *myo52Δ* Exhibits a Synthetic Lethal Interaction with *pck2-8*..... 221
7.2.9 *myo52Δ* is Resistant to Zymolyase Cell Wall Digestion..... 221
7.2.10 Mok1 is Highly Abundant in *myo52Δ* Cells..... 223

7.3 DISCUSSION..... 227
7.3.1 Myo52 and Septation..... 227
7.3.2 Myo52 and Polarised Cell Growth..... 230

Chapter 8 Summary and Discussion..... 235

REFERENCES..... 242

FIGURES AND TABLES

Chapter 1

Figure 1.1 The Three Filament Types of the Cytoskeleton..... 24
Figure 1.2 Actin Binding Proteins.....25
Figure 1.3 The Myosin Superfamily..... 28
Figure 1.4 Structure of Myosin II and Myosin II Fragments.....37
Figure 1.5 The Domain Structure of Class I, II and V Myosins.....38
Figure 1.6 The Heptad Motif of Coiled-Coil Formation..... 39
Figure 1.7 The Myosin Catalytic Cycle..... 43
Figure 1.8 The Life Cycle of *Schizosaccharomyces pombe*.....57
Figure 1.9 Structural Rearrangements in Actin and Microtubules..... 66 in the Fission Yeast Cell Cycle
Figure 1.10 Localisation of Spg1 and Cdc7 in Fission Yeast..... 87
Figure 1.11 The Sid Pathway.....88

Chapter 2

Table 2.1 *S. pombe* strains used in this study..... 92
Table 2.2 Oligonucleotides used to delete *myo51*$^+$ (c2D10) and..... 93 *myo52*$^+$ (c1919)
Table 2.3 Oligonucleotides used to overexpress and tag *myo51*$^+$..... 94 (c2D10) and *myo52*$^+$ (c1919)
Table 2.4 Primary antibodies used for immunofluorescence..... 106

Chapter 3

Figure 3.1 The Gene Structure of *myo51*$^+$ and *myo52*$^+$..... 116
Figure 3.2 Phylogenetic Analysis of Myo51 and Myo52.....117
Figure 3.3 Features of Yeast and Vertebrate Class V Myosins..... 123
Figure 3.4 Sequence Analysis of Class V Myosin Head Domains..... 124
Figure 3.5 Class V Myosin Light Chain Binding Sites..... 126
Figure 3.6 Pair-Coil Predictions of Class V Myosins.....127

Chapter 4

Figure 4.1 Southern Blot Analysis of *myo51Δ* Cells..... 136
Figure 4.2 Southern Blot Analysis of *myo52Δ* Cells..... 137
Figure 4.3 Morphology of *myo51Δ* and *myo52Δ* Cells..... 142
Figure 4.4 Actin and Microtubule Organisation in *myo51Δ* and..... 143 *myo52Δ* Cells
Figure 4.5 Growth of *myo51Δ* and *myo52Δ* Cells..... 144
Figure 4.6 *myo51Δ* Exhibits a Genetic Interaction with the..... 148 Temperature-Sensitive Actin Mutant *cps8*$^-$
Figure 4.7 *myo52Δ* Exhibits a Genetic Interaction with the..... 149 Temperature-Sensitive Actin Mutant *cps8*$^-$
Figure 4.8 *myo52Δ* Cells do not Grow Well After Prolonged..... 150 Periods in the Same Medium

Chapter 5

Figure 5.1 Cloning of *myo51*$^+$ and *myo52*$^+$ into pREP1 and pREP41myc Expression Vectors 159

Figure 5.2 *myo51*$^+$ and *myo52*$^+$ are Expressed in the Correct Reading Frame 160

Figure 5.3 *myo51*$^+$ Plasmids Rescue the *myo51Δ cps8*$^-$ Phenotype 165

Figure 5.4 pREP41myc-*myo52*$^+$ Plasmid Rescues the Temperature-Sensitivity and Morphological Defects of *myo52Δ* Cells 166

Figure 5.5 Overexpression of *myo51*$^+$ 167

Figure 5.6 Overexpression of *myo52*$^+$ 168

Chapter 6

Figure 6.1 Localisation of Myo51 181

Figure 6.2 Localisation of Myo52 182

Figure 6.3 Construction of Myo52-GFP 183

Figure 6.4 Localisation of Myo52-GFP Expressed from the *myo52*$^+$ Promoter 184

Figure 6.5 The Localisation of Myo52 Correlates with the Distribution of Actin 189

Figure 6.6 Myo52 Relocates from the Poles to the Equator at Late Anaphase 190

Figure 6.7 Localisation of Myo52 in *cdc25-22* 192

Figure 6.8 Localisation of Myo52 in *cdc16-116* 193

Figure 6.9 Localisation of Myo52 in *tea1-3* 194

Figure 6.10 Localisation of Myo52 is Dependent on an Intact Actin Cytoskeleton 198

Figure 6.11 Polar Localisation of Myo52 is Microtubule-Dependent 199

Chapter 7

Figure 7.1 *myo52Δ* Exhibits a Genetic Interaction with Components of the Pathway that Regulates Septation 213

Figure 7.2 Overexpression of *spg1*$^+$ in *myo52Δ* and Wild Type Cells 214

Figure 7.3 Myo52 Exhibits an Interaction with Cdc4 215

Figure 7.4 Myo52 Colocalises with Mok1 in Fission Yeast Cells 218

Figure 7.5 Mok1 Localisation in *myo52Δ* Cells 219

Figure 7.6 Myo52 Localisation does not Require Mok1 220

Figure 7.7 *myo52Δ* Exhibits a Synthetic Lethal Interaction with *pck2-8* but not *mok1-664* 224

Figure 7.8 *myo52Δ* Cells are More Resistant to Zymolyase Cell Wall Digestion than Wild Type Cells 225

Figure 7.9 *myo52Δ* Cells have a Greater Abundance of the Mok1 α-Glucan Synthase than Wild Type Cells 226

ABBREVIATIONS

ADP	adenosine diphosphate
ATP	adenosine triphosphate
bp	base pairs
BSA	bovine serum albumen
cdc	cell division cycle
Cyt. A	cytochalasin A
DAPI	4'-6-diamido-2-phenylindole
DMSO	dimethyl sulphoxide
DNA	deoxyribonucleic acid
DTT	dithiothreitol
EDTA	ethylenediamine tetra-acetic acid
EGTA	ethylene glycol-bis(aminoethyl ether)-*NNN'N'* tetra-acetic acid
ELC	essential light chain
GDP	guanosine diphosphate
GFP	green fluorescent protein
GTP	guanosine triphosphate
HMM	heavy meromyosin
HMW	high molecular weight
hr	hour(s)
kb	kilo base pairs
kD	kilo Daltons
Lat. A	latrunculin A
Lat. B	latrunculin B
LMM	light meromyosin
Mb	mega base pairs
MBC	carbendazim
MHC	myosin heavy chain
min	minute(s)
MLC	myosin light chain
MM	minimal medium
μm	micro metres
mRNA	messenger ribonucleic acid
MW	molecular weight
NETO	new end take off
NTP	nucleoside triphosphate
PAGE	polyacrylamide gel electrophoresis
PBS	phosphate buffered saline
PCR	polymerase chain reaction
Pi	inorganic phosphate
PPB	preprophase band
RLC	regulatory light chain
rpm	revolutions per minute
S1	subfragment 1

S2	subfragment 2
SDS	sodium dodecyl sulphate
sec	seconds
SPB	spindle pole body
TBZ	thiabendazole
UV	ultraviolet
YES	supplemented yeast extract medium

A NOTE ON NOMENCLATURE

In the fission yeast, *Schizosaccharomyces pombe*, gene names are written in italics which consists of a three letter prefix followed by a number. For example, the gene that encodes a class II myosin in *S. pombe* is called *myo2*. Sometimes it is useful to distinguish a wild type version of the gene from a mutant allele. In these cases a '+' sign is added at the end of the name to show that it encodes a wild type gene whereas a '-' sign is added for a mutant allele. Thus, the wild type *myo2* gene is known as $myo2^{+}$ and a mutant version $myo2^{-}$. To describe null mutants of genes that have been disrupted or deleted a 'Δ' sign is placed at the end of the gene name. Therefore, a *myo2* null mutant is written as *myo2Δ*. Proteins, on the other hand, have the same name as the genes they are encoded by, but they are written in regular font and the first letter is capitalised. Thus, the protein encoded by the *myo2* gene is called Myo2.

Different conventions are used to name genes from other organisms. In these cases I have kept to the system employed to describe genes from these organisms. Sometimes two different proteins from two different organism have the same name. For example, Myo2, the fission yeast class II myosin, is also the name of a budding yeast class V myosin. In such cases I describe in the text the organism from which the protein is from.

Chapter 1
Introduction

1.1 THE CYTOSKELETON

1.1.1 Introduction

The cytoskeleton is a dynamic network of protein filaments that actively participate in many cellular processes such as polarised cell growth, motility, cytokinesis and nuclear division (Moreau and Way, 1999). The cytoskeleton consists of three filament types: actin filaments, microtubules and intermediate filaments (Figure 1.1). Components of the cytoskeleton have been identified in many phylogenetically distinct groups and seems to be present in all eukaryotic organisms of varying complexity from yeast to human (Salmon and Way, 1999). The three filament types and their associated proteins will be discussed briefly as an introduction to the major subject of this thesis, the actin associated motor protein myosin.

1.1.2 Actin

Actin is a ubiquitous molecule whose amino acid sequence and biochemical properties are highly conserved throughout eukaryotes (Kabsch and Vandekerckhove, 1992). It can exist as a monomeric globular protein, G-actin, or as a filamentous polymer, F-actin (Figure 1.1). The actin monomer consists of about 375 amino acid residues which comprises the 43 kD molecular weight of the protein. Actin is one of the most abundant proteins in eukaryotic cells and in motile cells such as amoebae can constitute 5% or more of the total cell protein. In vertebrate skeletal muscle cells, this figure can rise to 20% (Alberts et al., 1994). In these cells actin filaments activate the motor activity of its associated protein, myosin, to produce the force for muscle contraction (Kabsch and Vandekerckhove, 1992). Apart from its role in cell locomotion, actin is involved in many other cellular processes which include formation of the cytokinetic actin ring during cell division (Field et al., 1999) and providing the structural framework around which cells define their polarity and maintain their shape (Hall, 1998; Pruyne and Bretscher, 2000a, 2000b).

Structurally, the actin monomer is made up of two asymmetrical domains joined by a

short flexible loop. It has a nucleotide binding pocket which is located in the cleft formed by the two domains (Bremer and Aebi, 1992; Kabsch et al., 1990). This pocket binds one molecule of ATP or ADP. The assembly of monomeric ATP-actin into filaments is initiated by a nucleation step which requires the formation of an initiation complex, a nucleus of three monomers from which polymerisation can occur (Pollard and Craig, 1982). This is the rate limiting step of polymerisation and is highly dependent on monomer concentration. Actin filaments have a distinct polarity which can be seen under the electron microscope by the way the actin associated protein, myosin, binds to actin in a specific orientation. Decoration of actin filaments by myosin gives filaments an arrowhead-like appearance (Huxley, 1963). Consequently, one end of the actin filament is referred to as the 'pointed' or '-' end whereas the other end is referred to as the 'barbed' or '+' end of the polymer.

Subunits can be added at both ends of the actin filament, however, assembly occurs at a faster rate at the barbed (+) end than at the pointed (-) end. A certain critical concentration of assembly competent G-actin must be present for polymerisation to take place (Pollard and Craig, 1982). The critical concentration for the addition of subunits is different at the two ends of the actin filament. At the barbed end, this concentration is five fold lower than that of the pointed end and hence assembly at the barbed end is favoured. At a free monomer concentration that is intermediate between the critical concentrations at the barbed and pointed ends a phenomenon known as 'treadmilling' occurs. Treadmilling describes a situation in which there is a steady state of assembly at the barbed end and disassembly at the pointed end with no net change in filament length (Pollard, 1986).

ATP-actin associates with both ends of an actin filament at a faster rate than ADP-actin and is slower to dissociate than ADP-actin (Pollard, 1986). The pointed end is relatively stable as loss of both types of subunit is slower than at the barbed end. However, as the critical concentration for subunit assembly is higher at the pointed end there is a steady net loss of monomers in low concentrations of actin monomers.

After incorporation of an actin molecule into a filament, the bound ATP is hydrolysed into ADP (Kabsch and Vandekerckhove, 1992). The rate of subunit addition can be faster than the rate at which the bound nucleotide is hydrolysed. Consequently, in rapidly elongating filaments, a cap of ATP-actin subunits can be found at both ends of actin filaments.

1.1.3 Actin Binding Proteins

The assembly and disassembly of actin filaments and its organisation in the cell is controlled by a number of actin binding proteins (for reviews see Otto, 1994; Schafer and Schroer, 1999; Pollard et al., 2000). Different actin binding proteins have different effects on actin (Figure 1.2). For example, some actin binding proteins such as fimbrin and α-actinin cross link and bundle actin filaments. Whereas others, such as myosin, exhibit an ability to translocate along filaments of actin.

One important actin binding protein is profilin. Profilin is a small protein that forms a 1:1 complex with G-actin. It is thought that profilin inhibits actin filament formation by sequestering the pool of actin monomers available for polymerisation (Rozycki et al., 1994). Controversially, profilin is also suggested to promote actin filament assembly by lowering the critical concentration for polymerisation to take place (Pantaloni and Carlier, 1993). This may reflect its ability to facilitate the exchange of ATP for ADP when bound to actin monomers (Goldschmidt-Clermont et al., 1992).

Two classes of proteins which promote actin turnover in cells are those that belong to the gelsolin and cofilin/ADF (actin-depolymerising factor) families. The gelsolin family comprises of highly active actin filament severing proteins that can also cap barbed ends (Welch et al., 1997). The cofilin/ADF family, however, comprises of weaker severing proteins that also possess actin monomer binding ability. In contrast to gelsolin and cofilin/ADF, the structural protein tropomyosin has an opposite effect on actin filaments. Tropomyosin consist of two identical α-helical chains that wind around each other to form a coiled-coil protein (Kabsch and Vandekerckhove, 1992). It

binds along the length of actin filaments to stabilise and stiffen F-actin.

In the past decade a family of actin related proteins (Arps) have been identified. These proteins share between 17 - 60% amino acid identity to conventional actins although they do not function as actin. Actin related proteins usually form stable complexes with other proteins and as yet no Arp has been found to exist outside of these complexes (Schafer and Schroer, 1999). One Arp complex, known as the Arp2/3 complex consisting of Arp2, Arp3 and five other proteins is thought to be important for the nucleation of actin filaments. Purified Arp2/3 complex is a weak nucleator of actin but the modest nucleating activity can be stimulated 20 fold by ActA (Welch et al., 1998), a protein required for actin assembly on the surface of the intracellular pathogen *Listeria monocytogenes*.

1.1.4 Microtubules

Microtubules are formed from molecules of tubulin each of which is a heterodimer of two closely related and tightly linked polypeptides called α-tubulin and β-tubulin (Mandelkow and Mandelkow, 1994). Tubulin molecules associate with each other to form a single protofilament. A single microtubule is composed of thirteen protofilaments which form a wall around a hollow central core. This gives microtubules their cylinder-like structure (Figure 1.1). Microtubules have an inherent polarity because tubulin molecules are assembled onto a protofilament in a regular orientation (Alberts et al., 1994). Each protofilament is composed of alternating α- and β-tubulin subunits which results in a ring of α-tubulin subunits terminating one end of the microtubule ('+' end) and a ring of β-tubulin subunits terminating the other end ('-' end). Like actin filaments microtubule polymerisation occurs asymmetrically and microtubules preferentially extend from the (+) end while growth from the (-) end is slower (Wade and Hyman, 1997). Microtubules also undergo fluctuations in length, a phenomenon known as 'dynamic instability', in which individual microtubules alternate between periods of growth and periods of rapid disassembly.

Each of the α- and β-tubulin subunits of the heterodimeric tubulin molecule has a nucleotide binding site which binds GTP (Mandelkow and Mandelkow, 1994). When a tubulin molecule adds to the end of a microtubule the GTP bound to the β-tubulin subunit is hydrolysed to GDP (Erickson and O'Brien, 1992). The GTP nucleotide that is bound to the α-tubulin is not hydrolysed and can be considered to form a fixed part of the tubulin protein structure (Alberts et al., 1994). GTP hydrolysis is thought to contribute to the dynamic instability of microtubules. When a microtubule grows rapidly tubulin molecules add to a polymer faster than the GTP they carry is hydrolysed. This results in the presence of a GTP cap and because tubulin molecules that carry GTP bind to one another with higher affinity than to those with GDP, the GTP cap will encourage a growing microtubule to continue growing. However, in conditions in which the rate of polymerisation slows down a microtubule can lose its GTP cap and start shrinking.

In cells, the microtubule (-) end associates with the microtubule organising centre (MTOC). In animal cells this is the centrosome which is located close to the outer surface of the nuclear envelope (Alberts et al., 1994). In fungi and diatoms the spindle pole body is the microtubule organising centre which is embedded in the nuclear envelope. Despite these differences, all of the organising centres have a matrix which contain MTOC-specific proteins that facilitates microtubule polymerisation. The MTOCs also contain a third class of tubulin, γ-tubulin, which nucleate the growth of microtubules by interacting with αβ-tubulin heterodimers (Joshi, 1994; Erickson, 2000). High resolution microscopic methods have shown that a ring of γ-tubulin (named gamma-tubulin ring complex or gammaTuRC) is found at the minus end of microtubules. Components of the gammaTuRC localise to a narrow zone at the extreme minus end of microtubules to mediate microtubule nucleation (Keating and Borisy, 2000; Moritz et al., 2000) as well as to cap existing microtubules to block further minus end growth and prevent microtubule depolymerisation (Wiese and Zheng, 2000).

1.1.5 Microtubule Associated Proteins

Like actin, microtubules can also associate with a number of proteins. These proteins are commonly referred to as microtubule associated proteins or MAPs (Mandelkow and Mandelkow, 1995). Two major classes of proteins that associate with microtubules can be distinguished: the assembly MAPs and the motor proteins. The assembly MAPs are noted for their ability to promote the assembly of microtubules (Lee, 1993). They may do this by neutralising the charge repulsion between tubulin subunits or by changing the structure of tubulin into a conformation that favours assembly. As well as this MAPs are also known for their ability to stabilise microtubules against disassembly, to crosslink adjacent microtubules in the cytosol and to mediate their interaction with other cell components (Hirokawa et al., 1988; Obar et al., 1989; Friedrich and Azodi, 1991).

The second class of MAPs, the microtubule-dependent motor proteins, uses microtubules as tracks for the directed transport of vesicles and organelles. There are two types of microtubule-dependent motor proteins: the kinesins which generally move their cargo toward the plus end of microtubules and the cytoplasmic dyneins which move their cargo in the opposite direction (Skoufias and Scholey, 1993; Walker and Sheetz, 1993).

1.1.6 Intermediate Filaments

Intermediate filaments are tough and durable protein fibres which are found in the cytoplasm of cells. There are many different types of intermediate filament monomers and each monomer of an intermediate filament is a highly elongated molecule (Figure 1.1). Structurally, a subunit of an intermediate filament consists of an N-terminal head, a central rod domain and a C-terminal tail. The rod domain consists of an extended α-helical region which allows it to form a coiled-coil dimer with an identical subunit. In most cells, nearly all of the intermediate protein molecules are in the fully polymerised state. However, a cell can still regulate the assembly of intermediate filaments and determine their number, length and position. One mechanism of control involves

phosphorylation of specific serine residues in the N-terminal head domain of intermediate filament proteins. For example, phosphorylation of protein subunits that form the nuclear lamina causes them to disassemble at mitosis. This is reversed after mitosis by dephosphorylation of specific serine residues, resulting in the reformation of the nuclear lamina (for reviews see Alberts et al., 1994; Quinlan et al., 1995; Fuchs and Cleveland, 1998).

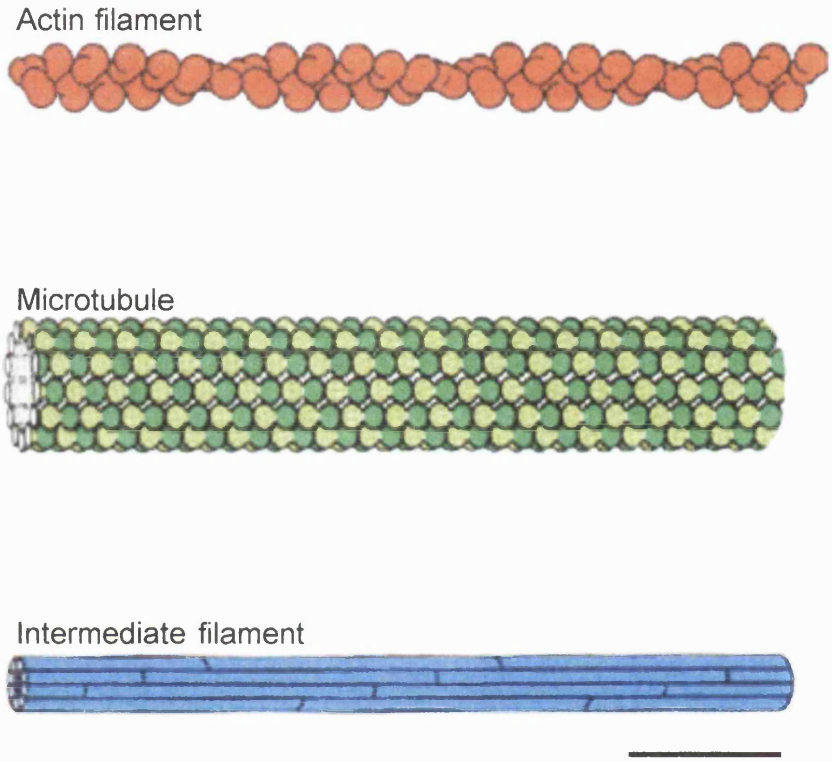

Figure 1.1 The Three Filament Types of the Cytoskeleton

The cytoskeleton is composed of three types of filaments: actin filaments, microtubules and intermediate filaments. Actin filaments are polymers of G-actin subunits whereas microtubules are constructed from α- and β- tubulin monomers. Intermediate filaments are polymers composed of intermediate filament proteins. A 25 μm scale bar is shown as a guide to their relative sizes. Figure modified from Alberts et al. (1994).

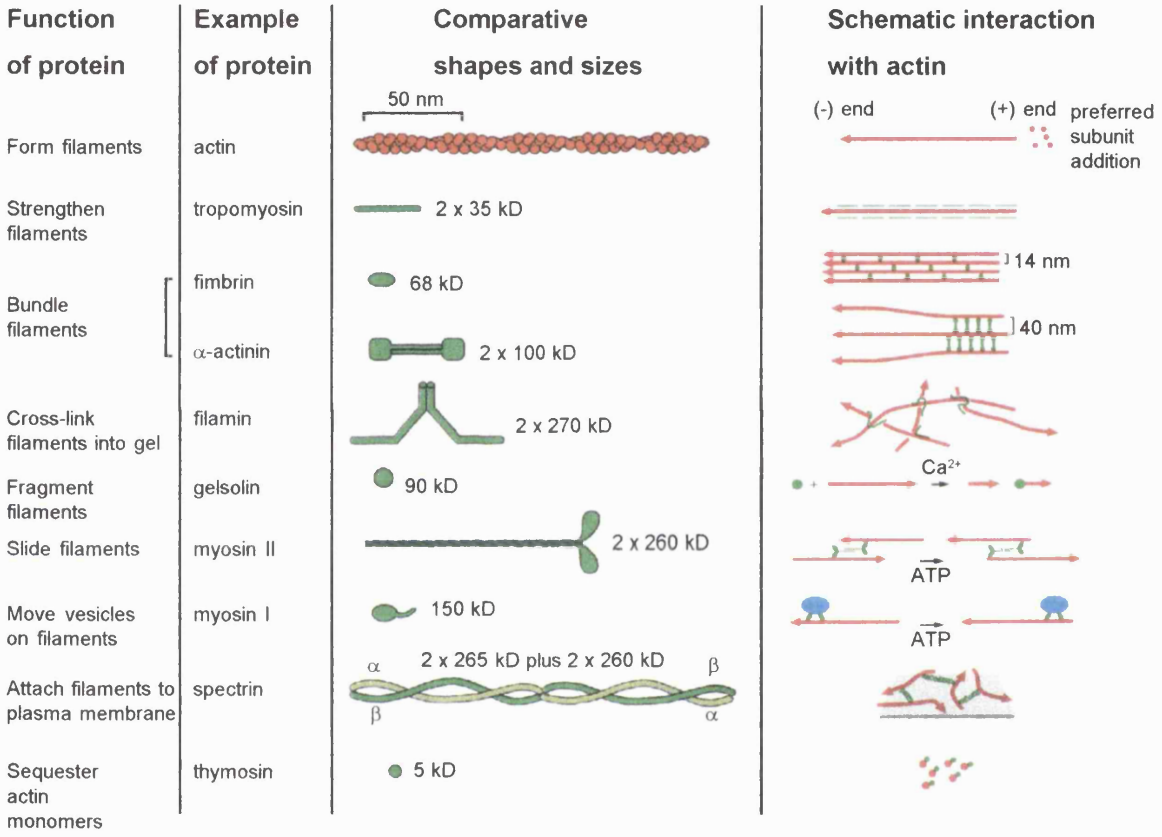

Figure 1.2 Actin Binding Proteins

Some of the major classes of actin binding proteins and their functions. Actin is shown in red while actin binding proteins are shown in green. Figure reproduced from Alberts et al. (1994).

1.2 MYOSINS

1.2.1 The Myosin Superfamily

The actin-dependent motor protein, myosin, was originally identified in skeletal muscle cells (Hanson and Huxley, 1953). Since then, numerous other myosins have been discovered in various eukaryotes including fungi, plants and invertebrates. Myosins now constitute a large and diverse superfamily of actin-activated molecular motors (Sellers, 2000). Traditionally, myosins have been divided into two classes based upon whether they form monomers (class I) or dimers (class II). The founding member of the myosin superfamily are the class II myosins and are also referred to as "conventional myosins" since this was the only class known for decades before the discovery of the first unconventional myosin (Pollard and Korn, 1973). As the number of newly identified myosins escalated it became clear that the simple method of classification into two classes was inadequate since many new myosins were too diverse to be grouped together (Cheney et al., 1993a; Goodson and Spudich, 1993). Nowadays myosins are classified on the basis of their similarity in the primary sequence of the conserved myosin head domain as proposed by Cheney et al. (1993a). Thus, all new classes of myosins discovered after the myosin I and II classes are assigned a Roman numeral in order of their discovery. At present, phylogenetic analysis of the motor domains have separated the myosin superfamily into 17 distinct classes (Hodge and Cope, 2000) (Figure 1.3). It is likely that the number of myosin classes will increase as new myosins are discovered.

The number of myosin genes present in mammals is conservatively estimated to be between 25 and 30 genes (Sellers, 2000). The latest count in humans indicate that there are approximately 30 different myosin genes (Cheney, 2000). Myosin genes from mammals belong to a broad spectrum of classes which include classes I, II, III, V, VI, VII, IX, X and XV. The large number of myosin genes in mammals can be seen to reflect the various functional roles they have in complex organisms and myosins have been implicated in numerous cellular tasks such as cytokinesis, phagocytosis,

endocytosis, polarised secretion, exocytosis and axonal transport (Soldati et al., 1999). Depending on the cell type, mammalian cells have the capacity to express between two and at least two dozen myosin genes (Soldati et al., 1999).

In the slime mould, *Dictyostelium discoideum*, which can undergo a complex developmental cycle, at least 12 myosin genes are known. These include seven class I myosins, a single class II myosin and four other genes that do not stringently group with the existing classes (Sellers, 2000). One of these has similarities to classes V and XI (Peterson et al., 1996) while another has similarities to classes VII and X (Sellers, 2000). No class of myosin appears to be universally expressed in all phyla, for example, no class II myosins have been found in plants. Indeed, some myosin classes are exclusively found in plants (VIII, XI and XIII).

In all animal cells examined representatives from classes I, II and V have been identified, particularly if the criteria for relatedness are relaxed (Sellers, 2000). These classes are also represented by the 5 myosin genes in the budding yeast, *Saccharomyces cerevisiae* (Brown, 1997). Budding yeast has two class I myosins *MYO3* and *MYO5* (Goodson and Spudich, 1995; Goodson et al., 1996), one class II myosin *MYO1* (Watts et al., 1987) and two class V myosins *MYO2* and *MYO4* (Johnston et al., 1991; Haarer et al., 1994). The *Schizosaccharomyces pombe* genome sequencing project is almost complete and, like budding yeast, *S. pombe* also contains 5 myosin genes from classes I, II and V. These include one class I myosin *myo1*$^+$ (D. Mulvihill, personal communication), two class II myosins *myo2*$^+$ and *myp2*$^+$ (Kitayama et al., 1997; May et al., 1997; Bezanilla et al., 1997; Motegi et al., 1997) and two class V myosins *myo51*$^+$ and *myo52*$^+$ (Win et al., 1999a, 1999b; this thesis). The fact that these three classes of myosins are found to be ubiqitous amongst animal and yeast cells indicates their importance in maintaining basic cellular functions.

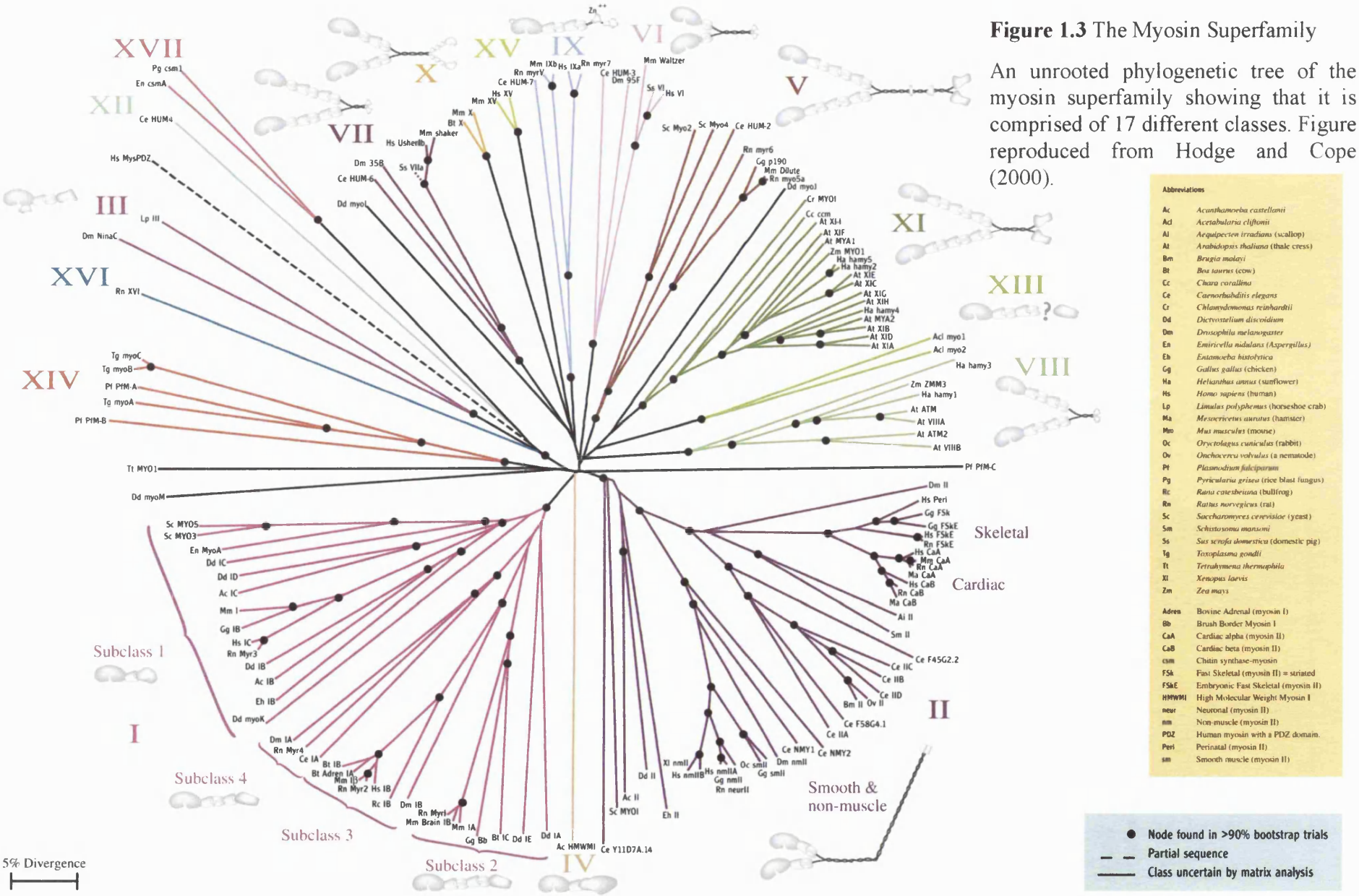

Figure 1.3 The Myosin Superfamily

An unrooted phylogenetic tree of the myosin superfamily showing that it is comprised of 17 different classes. Figure reproduced from Hodge and Cope (2000).

1.2.2 Myosin Structure

Three functional domains can be identified in a typical myosin heavy chain: (1) an N-terminal head or motor domain which interacts with actin and binds ATP, (2) a neck or regulatory domain that provides binding sites for regulatory proteins and (3) a C-terminal tail domain which differs in function between myosins of different classes (Mooseker and Cheney, 1995; Baker and Titus, 1998). Most of what is known about the structure of myosin has been obtained from the analysis of class II myosin from muscle. It is the most abundant of all myosins and can be purified relatively easily and in large quantities. Little is known about the structure of other myosin classes not only because of their late discovery but also due to their low abundance in cells (Sellers, 1999). However, class II myosins have been used as a model for the analysis of other myosins, especially in determining the structure of the head domain since this domain is the most highly conserved amongst all myosins (Cope et al., 1996).

a. Proteolytic Cleavage of Myosin II

The complete myosin II molecule is a hexameric enzyme composed of two heavy chains and four light chains (Figure 1.4). Each myosin heavy chain has a molecular weight between 171-244 kD and has a pair of light chain binding sites at the junction between the head and tail (Sellers, 2000). The C-terminal portion of the heavy chain consists of a long α-helical region which associates with the α-helical region of a second heavy chain to form a coiled-coil tail or rod. Dimerisation of the heavy chain tail at the C-terminus produces a two-headed structure at the N-terminus. Furthermore, these coiled-coil tails can form higher order structures by self associating to form filaments. Such filaments complicate the kinetic and biophysical characterisation of the enzymatic activity of the myosin molecule.

To overcome this complication, myosin II molecules are proteolytically cleaved to generate fragments which are soluble and easier to work with. Amazingly, the cleavage products are enzymatically active and retain similar properties to the native protein (Sellers, 1999). One cleavage site of the myosin II molecule occurs about 130 kD from

the N-terminus and produces two fragments, heavy meromyosin (HMM) and light meromyosin (LMM). HMM is the N-terminal portion of the cleaved myosin II molecule and consists of two heads with associated light chains and a small region of the coiled-coil tail. HMM can be further divided by proteolysis of the heavy chain at a point adjacent to the second light chain binding domain to generate subfragment 1 (S1) and subfragment 2 (S2). The enzymatically active S1 fragment is single-headed and is associated with one or two light chains depending on the conditions used for digestion.

The S1 region can be further cleaved at two proteolytically sensitive sites. Cleavage at both these sites generates three fragments of the head, an N-terminal 25 kD fragment, a central 50 kD fragment and a C-terminal 20 kD fragment. The three major proteolytic fragments of S1 are thought to be connected by two flexible surface loops (Rayment et al., 1993). The region between the 25 kD and 50 kD fragment is referred to as 'loop 1' and lies over the nucleotide binding pocket. The second loop which connects the 50 kD and 20 kD fragments termed 'loop 2' lies near the tip of the myosin head and is thought to contribute towards actin binding. The three proteolytic fragments of S1 only dissociate under denaturing conditions and are useful in describing structural domains within the head (Figure 1.4).

b. Head Domain

The three dimensional structures of the motor domain of myosin from chicken fast skeletal muscle (Rayment et al., 1993) and the myosin II of *Dictyostelium discoideum* (Fisher et al., 1995; Smith and Rayment, 1995; Smith and Rayment 1996; Bauer et al., 1997) have been determined. There is great similarity in the structure of the head domains from these phylogenetically diverse class II myosins (Sellers, 2000). Alignment of the myosin sequences from these myosins with those of other myosin classes strongly suggests that the structure of the myosin II head is a good template for the analysis of all myosin head domains (Sellers et al., 1996).

Analysis of the chicken fast skeletal myosin indicates that the nucleotide binding pocket has a relatively open structure and is formed by seven parallel β-sheets from each of the proteolytic fragments of S1 (Rayment et al., 1993). Some of the most conserved regions of amino acid sequence are present in loops that connect these β-sheets. This includes the highly conserved GESGAGKT motif which forms a P-loop (phosphate binding loop) at the base of the nucleotide binding pocket and is thought to be involved in nucleotide binding (Saraste et al., 1990; Vale, 1996).

Another region of conserved residues occurs at the lining of a prominent cleft that separates the 50 kD S1 fragment into two parts. The cleft separates the upper and lower parts of the 50 kD fragment and extends from the base of the nucleotide binding pocket to the opposite side of the head. The cleft closes slightly following nucleotide binding and may close more dramatically upon binding to actin (Houdusse et al., 1999). It has been suggested that residues from both the upper and lower domains of this region form part of the actin binding interface (Sellers, 1999). The flexible loop which connects the 50 kD and 20 kD fragments is found in close proximity to the body of protein spanning the cleft between the upper and lower 50 kD domains. This region has also been suggested to contribute toward the binding of actin. This is supported by the observation that this region can be cross-linked to actin (Sutoh, 1982) and that actin binding protects this region from proteolysis (Mornet et al., 1981; Blotnick and Muhlrad, 1992). Furthermore, cleavage of this region decreases the affinity of myosin for actin (Ikebe et al., 1993).

The 20 kD S1 fragment which begins near the tip of the head extends down the length of the molecule to form the neck domain at the base (Sellers, 1999). The 20 kD region is mostly α-helical and contains two highly reactive cysteine residues termed SH1 and SH2 which are located at the base of the α-helix, under the nucleotide binding pocket, immediately before the start of the second light chain binding domain. In the presence of nucleotide the two cysteine residues can be chemically cross-linked (Wells and Yount, 1979; Wells and Yount, 1980). However, in the absence of nucleotide the

cysteine residues lie with their active groups pointing in opposite directions with SH2 buried in the core of the protein (Rayment et al., 1993). This suggests that major rearrangements occur in this region upon binding to nucleotide to allow for their cross linking.

c. Neck Domain

The C-terminal portion of the 20 kD S1 fragment forms the regulatory or neck domain. It protrudes from the base of the globular head as a long single α-helix which is stabilised by binding to light chains (Sellers, 1999). A class II myosin heavy chain has two binding sites for light chains, the first of these provide a binding site for the essential light chain (ELC) and the second which is most distal from the head is the binding site of the regulatory light chain (RLC). In the chicken fast skeletal muscle and scallop myosins, both light chains are bound in the opposite polarity to that of the myosin heavy chain (Rayment et al, 1993; Xie et al., 1994). Two distortions are seen in the stabilised α-helix, a bend in the region between the bound light chains and a sharper 60° turn near the C-terminus (Rayment et al., 1993). In crystal structures, the essential light chain wraps around the heavy chain α-helix such that the N- and C-terminal regions of the light chain are in close proximity. The regulatory light chain also wraps around the heavy chain α-helix, however, it binds to the heavy chain in the region of the 60° turn.

Light chain binding is thought to be mediated by IQ motifs which are found in the primary sequence of myosin heavy chains (Mercer et al., 1991; Cheney and Mooseker, 1992). This motif has the consensus: IQXXXRGXXXR and has been suggested to be the binding site for calmodulin and myosin light chains (Rhoads and Friedberg, 1997). Calmodulin and myosin light chains belong to the EF hand superfamily of calcium modulated proteins which senses calcium levels in the cell and undergo conformational changes upon binding of Ca^{2+} (for review see Ikura, 1996). The number of IQ motifs present in the necks of different myosins can vary between zero and six (Sellers, 2000). For example, class II myosins have two IQ motifs

whereas class V myosins typically have six (Figure 1.5).

It is thought the IQ motifs in class V myosins mediate its binding to both calmodulin and myosin light chains (Reck-Peterson et al., 2000). Expression of truncated forms of a class V myosin (myosin Va) from chicken brain have shown that the neck region has the capability to associate with calmodulin (Espreafico et al., 1992). Biochemical studies indicate that chicken class V myosin copurifies with 4-5 calmodulin molecules per heavy chain (Cheney et al., 1993b). Furthermore, chicken class V myosin also copurifies with 17 kD and 23 kD proteins that correspond to the essential light chains found to associate with a class II myosin from chicken brain. Analysis of one of the budding yeast class V myosins (Myo2) have shown that it binds to calmodulin and a novel protein designated Mlc1 which may function as an essential light chain (Brockerhoff et al., 1994; Stevens and Davis, 1998). These results have led to the proposal that the class V myosin heavy chain has six IQ motifs, five of which may provide binding sites for calmodulin and a single IQ motif for binding to essential light chains (Reck-Peterson et al., 2000). It is not known which of the IQ motifs the essential light chain binds although the first N-terminal IQ motif has been suggested from analogy to class II myosins.

Various roles for calmodulin and myosin light chain binding have been proposed, one of which is to stabilise the neck which acts as a lever arm to increase the displacement of the power stroke during myosin motor activity (Uyeda et al., 1996). Analysis of skeletal muscle myosin II have shown that light chain binding is required to translocate actin filaments (Lowey et al., 1993). The speed of translocation is directly proportional to the length of the lever arm and it is possible that rearrangements in light chain binding may alter the neck to regulate lever arm movement (Barylko et al., 2000). In contrast to most target enzymes which are activated by calmodulin bound to Ca^{2+}, the vast majority of myosins characterised so far contain IQ motifs that bind with highest affinity to calmodulin in the absence of Ca^{2+} (Wolenski, 1995). This is supported by the observation that addition of calcium to brain myosin V has been

shown to result in the partial dissociation of calmodulin from the heavy chain (Nascimento et al., 1996). Thus, one mode of myosin regulation may be by altering the flexural rigidity of the neck domain either by calmodulin light chain dissociation or alteration in light chain binding affinity which occurs in response to changes in calcium levels in the cell.

d. Tail Domain

Of all the three major domains in a myosin heavy chain, the tail domain is the most diverse and vary widely in length and sequence between different classes (Sellers, 2000). Indeed, some myosins exhibit great variability in the tail domain even within members of the same class. For example, there is great diversity among class I myosins which is represented by the presence or absence of various functional motifs in their tails (Barylko et al., 2000) (Figure 1.5). Analysis of the class I myosin tails encoded by the *myoA*, *myoB*, *myoC*, *myoD* and *myoE* genes from *Dictyostelium discoideum* shows that they all have a domain just C-terminal to the neck which is rich in basic residues (Mooseker and Cheney, 1995). The basic residues present in class I myosins are thought to form a membrane binding domain and have been found to interact with acidic phospholipids (Pollard et al., 1991). The *Dictyostelium* myoA and myoE class I myosins, however, lack the GPA or GPQ domain which is present in the tails of myoB, myoC and myoD (Mooseker and Cheney, 1995). The GPA or GPQ domain have an amino acid sequence which is rich in glycine, proline and either alanine or glutamine and this region has been suggested to constitute a second actin binding site in these myosins. In addition, a src homology 3 (SH3) domain have also been identified in the tails of myoB, myoC and myoD from *Dictyostelium* as well as in some of the class I myosins from *Acanthamoeba castellanii* (Mooseker and Cheney, 1995), budding yeast (Goodson and Spudich, 1995; Goodson et al., 1996), *Aspergillus nidulans* (McGoldrick et al., 1995), mouse (Crozet et al., 1997) and human (Bement et al., 1994). The SH3 domain is found in many proteins involved in signal transduction or in proteins associated with the actin cytoskeleton and mediate protein-protein interactions by binding to proline-rich motifs. It has been suggested that the SH3

domain of class I myosins may target these molecules to their appropriate destinations in the cell or serve as a regulatory component which might fold back and interact intra-molecularly with a site within the proline rich GPA/Q domain to control access to the actin binding site in the tail (Mooseker and Cheney, 1995).

In contrast to class I myosins, which lack coiled-coil forming sequences in the tail and are consequently single-headed, the tails of class II and V myosins have sequences which allow them to dimerise to form two-headed motors (Sellers, 2000; Reck-Peterson et al., 2000). Sequence analysis of the coiled-coil forming sequences shows that it is largely α-helical which consists of a characteristic heptad repeat *a-b-c-d-e-f-g* in two turns of the α-helix (Figure 1.6). Hydrophobic residues predominate at the *a* and *d* positions which lie at the interface between the two heavy chains. These hydrophobic residues which lie within the coiled-coil form the basis for the interaction between the two heavy chains. The outermost positions *b*, *c* and *f* are occupied by highly charged residues with repeating negative and positive regions spaced 14 residues apart. These charged groups probably mediate the arrangement of myosin II rods into filaments where the interaction between neighbouring molecules is largely electrostatic (McLachlan and Karn, 1982; Atkinson and Stewart, 1991; Hoppe and Waterson, 1996). In most class II myosins, the coiled-coil forming sequence terminates shortly before the C-terminus which results in a non-helical tailpiece of unknown structure. Unlike class II myosins, myosin V molecules do not appear to be capable of forming higher order filamentous structures.

Analysis of the tail domains of class V myosins shows that the myosin V tails can be divided into two regions: an α-helical region of variable length and a C-terminal globular domain (Reck-Peterson et al., 2000). Like class II myosins, the α-helical region in the tail of a myosin V heavy chain is thought to mediate its dimerisation. Electron microscopy of myosin Va from chicken brain has shown that it dimerises and forms a two-headed motor which terminates in a globular tail (Cheney et al., 1993b). Two hybrid analysis of the budding yeast myosin V, Myo2, has shown that it also

dimerises with itself through the α-helical coiled-coil forming region in the tail (Beningo et al., 2000). Interestingly, Myo2 has not been found to associate with Myo4 (another budding yeast myosin V) indicating that Myo2 does not form a heterodimer with Myo4.

The globular domain at the C-terminus of myosin V tails is thought to be involved in cargo binding and/or localisation within the cell (Reck-Peterson et al., 2000). Analysis of the distribution of chicken myosin Va in cultured mammalian cells have shown that it localises to the centrosome in these cells (Espreafico et al., 1998; Tsakraklides et al., 1999). Truncation analysis of chicken myosin Va shows that the globular tail domain is required for the localisation of the protein to the centrosome. A study from the budding yeast class V myosin, Myo2, indicates that the globular tail domain is also important for binding to distinct cargoes (Catlett et al., 2000). Mutation analysis of the globular domain in the Myo2 tail suggests that the protein has two distinct subdomains, one of which may mediate binding to secretory vesicles and the other for vacuoles. The identification of these subdomains indicates that a single class V myosin motor is capable of moving multiple cargoes.

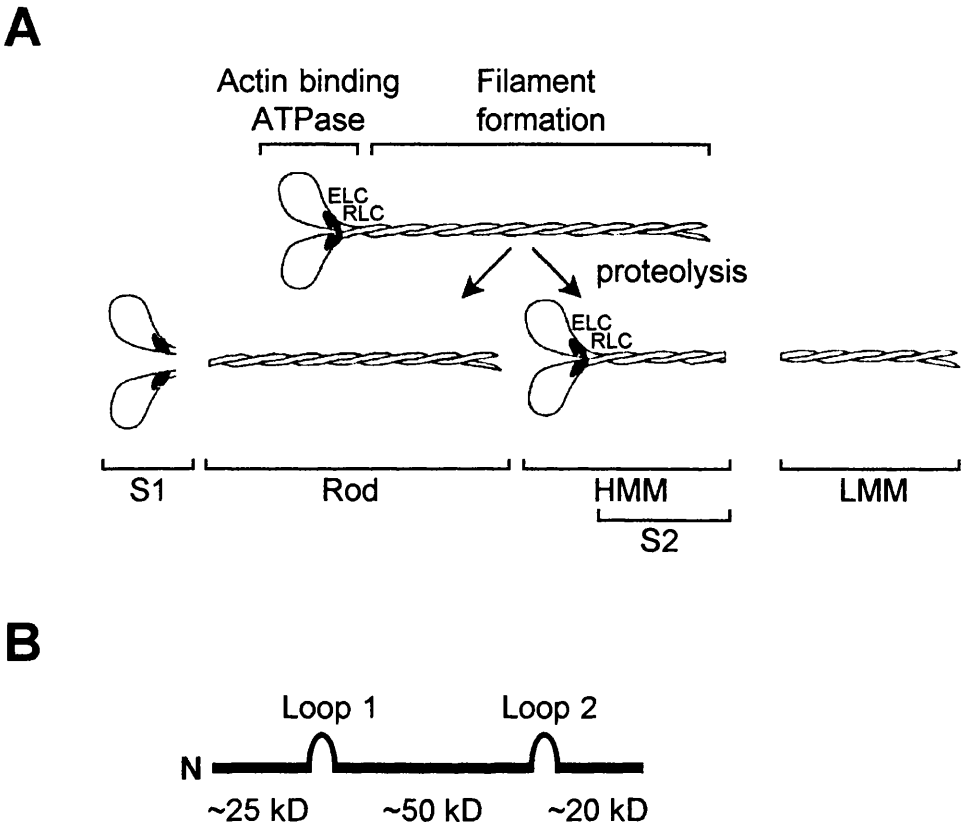

Figure 1.4 Structure of Myosin II and Myosin II Fragments

(A) Various proteases cleave myosin II molecules at the S1/S2 junction to produce S1 and rod, or at the HMM/LMM junction to produce HMM and LMM. The schematic S1 fragment is drawn with both light chains intact. However, under some conditions the regulatory light chain (RLC) is lost.

(B) There are also two major cleavage sites within the head region of myosin II. One of these is about 25 kD from the N-terminus and the other about 75 kD from the N-terminus.

Figure reproduced from Sellers (1999).

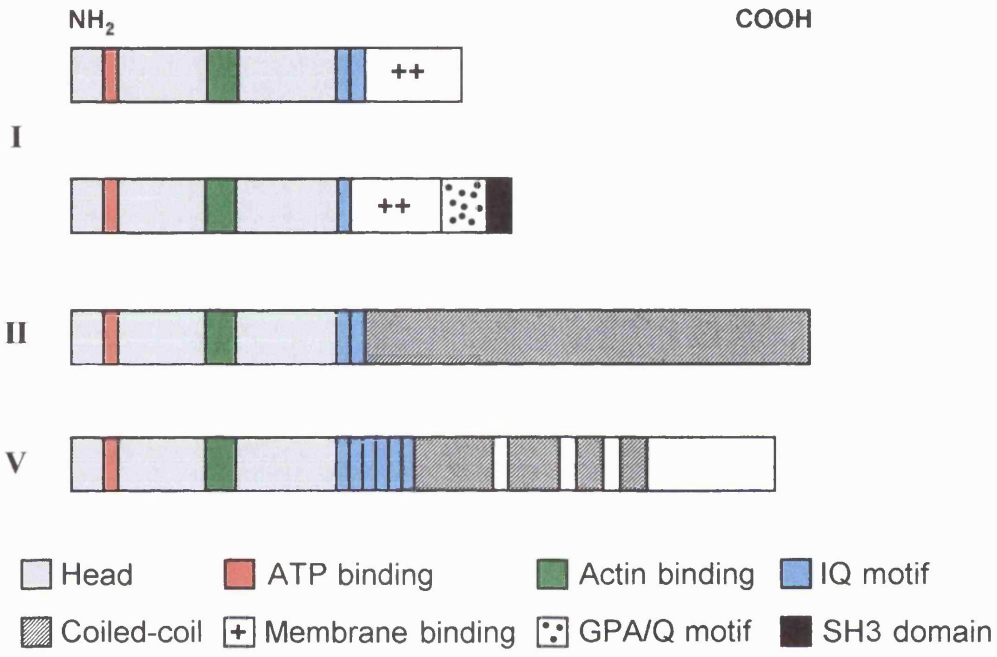

Figure 1.5 The Domain Structure of Class I, II and V Myosins

The domain structure of typical class I, II and V myosins. Class I myosins exhibit intra-class variation, some possess a GPA/Q motif and a SH3 domain in their tail whereas some lack these domains. In addition, class I myosins have a variable number of IQ motifs in their neck region (usually between 1-6 light chain binding sites). Note the presence of an ATP and an actin binding site in the head domain of all myosins.

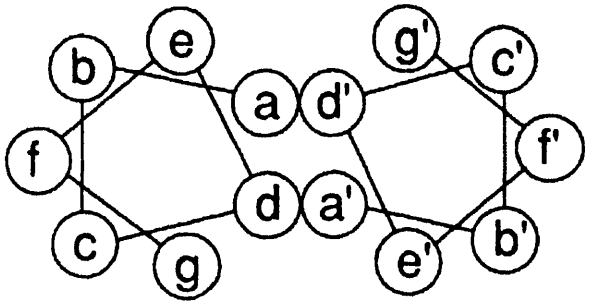

Figure 1.6 The Heptad Motif of Coiled-Coil Formation

Heptad wheels showing the sequence motif of a coiled-coil α-helix. The positions (a-g) mark positions along the α-helix. Positions (a) and (d) are typically occupied by hydrophobic residues while positions (b), (c) and (f) are often charged. Figure reproduced from Sellers (1999).

1.2.3 The Myosin Catalytic Cycle and Force Production

Most of the work on the catalytic activity of myosins and how this translates to movement have been carried out on class II myosins from muscle. It is thought that some aspects of the motor activity of class II myosins may be transferable to other myosins although some class specific variation from the myosin II model is expected to occur between myosins of different classes (Volkmann and Hanein, 2000).

a. The Catalytic Cycle

The salient characteristic of myosins is their ability to reversibly bind actin and exhibit MgATPase activity (Sellers, 2000). During part of the ATP hydrolysis cycle the myosin head is firmly attached to actin (strong binding states). In order to move relative to the actin filament the myosin head needs to detach from the actin filament at some point (weak binding states). It is thought that the binding and release of actin is controlled by a cleft running from the nucleotide binding pocket to the actin binding site (Rayment et al., 1993).

In the strong binding state the myosin head is tightly bound to actin, the cleft is closed and the nucleotide binding pocket is open (Figure 1.7). When ATP binds, the phosphate moiety first binds to the P-loop at the base of the active site. The putative γ-phosphate binding site is located at the base of the cleft and binding of the γ-phosphate causes the cleft to open which dissociates the myosin-ATP complex from actin (Ruppel and Spudich, 1996). ATP is hydrolysed while myosin is detached from actin, generating a stable intermediate complex of myosin, ADP and inorganic phosphate (Pi). In the intermediate state in which the products of hydrolysis (ADP and Pi) are bound to myosin, the lower cleft domain move towards the upper domain and thus partially closes the cleft. It is thought that this movement provides the source of the conformational change to allow the myosin head to reorientate for binding to a new actin monomer (Rayment et al., 1993; Fisher et al., 1995; Ruppel and Spudich 1995). Release of ADP and Pi occurs whilst myosin is tightly bound to actin. The power stroke which results in the displacement of the actin filament is thought to

occur at this stage when Pi is released from the myosin head (Volkmann and Hanein, 2000). Release of ADP and Pi enables a new catalytic cycle to begin with the binding of ATP to the open nucleotide binding pocket (Figure 1.7).

b. Force Production

Muscle contraction and non-muscle cell motility results from the relative sliding of actin and myosin filaments (Yanagida et al., 2000). The heads of myosin molecules project from myosin filaments to form links with actin. These links are referred to as cross-bridges which cyclically attach and detach from actin filaments with biochemical cycles of ATP hydrolysis. To account for the movement of actin and myosin filaments, the 'cross-bridge' model was proposed in which actin filaments were pulled by the swing of the cross-bridges (Huxley, 1969; Huxley and Simmons, 1971).

Recently, many studies have shown that the neck region of the myosin head undergoes major conformational changes. Using different nucleotide analogues to reflect the different stages of ATP hydrolysis, changes in the angle of the myosin head relative to the neck region has been observed in crystal structures (Rayment et al., 1993; Fisher et al., 1995; Smith and Rayment, 1996; Houdusse et al., 1999). On the basis of these findings the 'cross-bridge' model of force generation has been refined into the 'lever arm' model in which the neck region of the myosin head has been hypothesised to act as a lever arm (for reviews see Spudich, 1994; Block, 1996; Goldman, 1998; Highsmith, 1999; Vale and Milligan, 2000).

In the lever arm model, force generation involves small conformational changes in the nucleotide binding pocket which transduces the chemical energy released from ATP hydrolysis into mechanical force (Volkmann and Hanein, 2000). The conformational changes in the nucleotide binding pocket are thought to be communicated through a subdomain in the head known as the 'converter' to the base of the long helix that make up the neck domain. The small changes in the nucleotide binding pocket are translated by the converter into rotation of the neck. The neck acts as a lever arm and moves by

several nanometres during a power stroke while the rest of the motor domain remains tightly attached to actin and does not move significantly.

A region that has been implicated to be the pivot point for lever arm movement is located within the motor domain close to two short helices containing two reactive cysteines (SH1 and SH2). Crystal structures place the reactive thiols in the two cysteine residues about 17-19 angstroms apart (Rayment et al., 1993; Fisher et al., 1995; Smith and Rayment, 1996; Gulick et al., 1997; Dominguez et al., 1998). This distance, however, does not account for results from cross linking experiments that indicated that the thiols can be as close as 2 angstroms to each other in the presence of nucleotide (Wells and Yount, 1980). Recent studies indicate that multiple conformational states occur which allow the distance between SH1 and SH2 to vary from 2-20 angstroms (Nitao and Reisler, 1998; Kliche et al., 1999). These results indicate that the distance between the reactive thiols is determined by the nucleotide state of the myosin head such that the thiols are brought closer together when bound by nucleotide. Mutation studies indicate that a conserved glycine residue that lies between SH1 and SH2 may be a possible candidate as a pivot point to allow rotation of the lever arm (Batra et al., 1999).

One of the remaining questions is the size of the displacement, the power stroke, that a single ATP hydrolysis event can achieve. For class II myosins this has been suggested to be about 10 nm (Spudich, 1994). There is also evidence that the size of the power stroke is dependent on the length of the lever arm since removal of the regulatory region of the neck domain results in a decrease in filament velocity (Uyeda and Spudich, 1993) whereas addition of a light chain binding site increases filament velocity (Uyeda et al., 1996). This implies that different myosin classes with different lever arm lengths will display differing sizes of displacements. Indeed, myosin I has been found to have a power stroke of approximately 12 nm (Veigel et al., 1999) and myosin V exhibits a power stroke in the 30-38 nm range (Mehta et al., 1999).

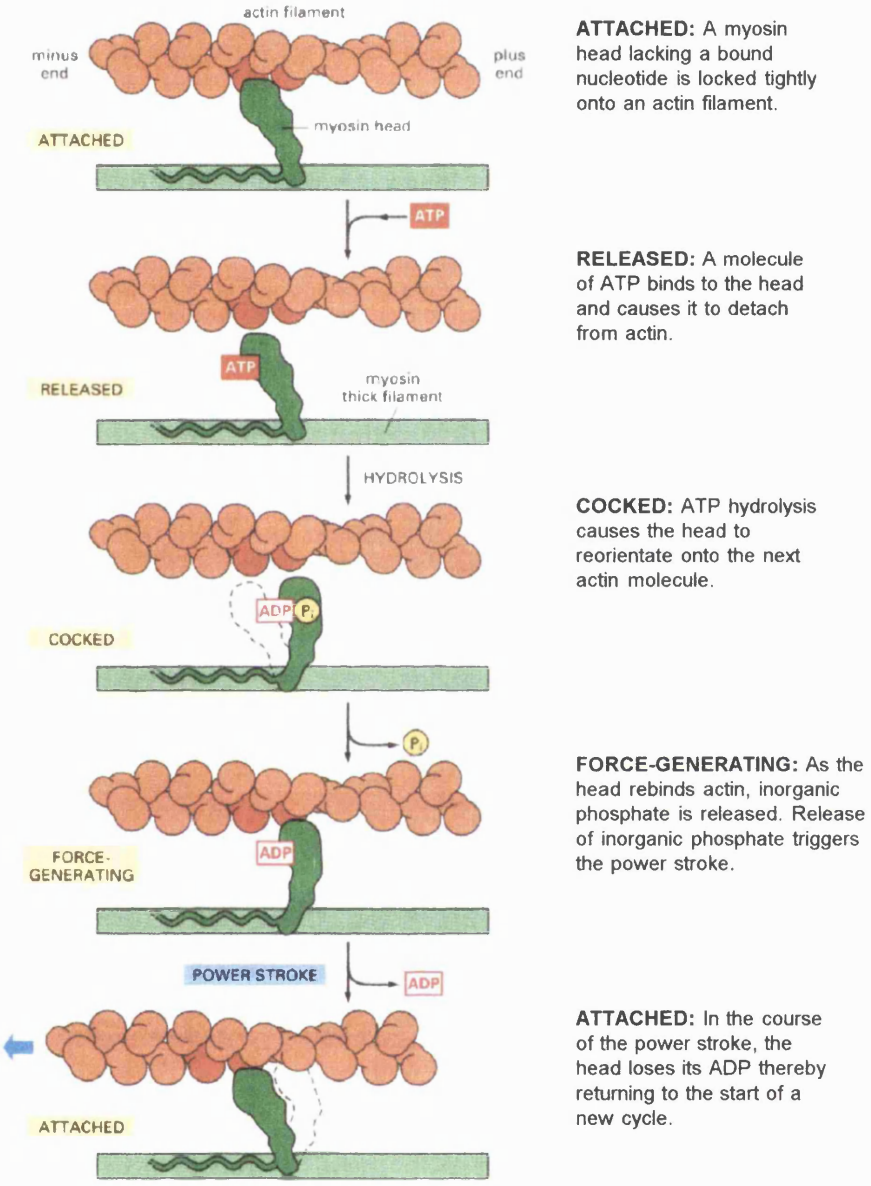

Figure 1.7 The Myosin Catalytic Cycle

The cycle of changes by which a myosin molecule moves along an actin filament. Figure reproduced from Alberts et al. (1994).

1.2.4 Myosin Function

Myosins have been implicated to perform various functions in the cell. These include cytokinesis, organelle positioning, secretion, endocytosis, signal transduction and mRNA localisation. Functional analysis of myosins from phylogenetically diverse organisms reveal a common theme, that particular processes seem to be carried out by specific myosin classes. This is not surprising given the structural diversity between myosins of different classes indicating that certain myosins are particularly suited to perform a specific function (for reviews see Yamashita and May, 1998; Bahler, 2000; Barylko et al., 2000; Reck-Peterson et al., 2000; Sellers, 2000; Steinberg, 2000; Wu et al., 2000). Class I, II and V myosins are the only myosins that have been identified in budding yeast and fission yeast (see section 1.2.1). These myosins are also ubiquitous amongst animal cells and as such the functional role of these three classes will be discussed in this section. Particular attention will be focused on the function of class V myosins since *myo51*$^{+}$ and *myo52*$^{+}$ are the subject of this thesis and belong to this myosin class.

a. Class I Myosins

Studies from a variety of organisms indicate that myosin I plays a critical role in endocytic and exocytic membrane traffic (Mermall et al., 1998). Multiple myosin I isoforms are expressed in *Dictyostelium* and results of gene knockout studies suggests that these myosins may be functionally redundant in the process of endocytosis (Novak et al., 1995). Analysis of two *Dictyostelium* myosin I double mutants (*myoA*$^{-}$*/myoB*$^{-}$ and *myoB*$^{-}$*/myoC*$^{-}$) revealed that they exhibit conditional defects in one form of endocytosis (fluid phase pinocytosis). Double mutants grown in suspension culture were impaired in their ability to take in nutrients from the medium whereas they were indistinguishable from wild type and single mutant strains when grown on a solid surface. These results led Novak et al. (1995) to suggest that myoA, myoB and myoC may be important in controlling the formation and retraction of membrane projections by the cell's actin rich cortex to effect pinosome internalisation while in suspension. Overexpression studies also show that increased levels of myoB inhibited pinocytosis

which is accompanied by a decrease in growth rate (Novak and Titus, 1997). Perhaps the slow growth rate reflects the defect of myoB overexpressing cells to take in nutrients.

In *Aspegillus nidulans* a single class I myosin gene, *myoA*, has been identified (McGoldrick et al., 1995). Disruption of *myoA* indicates that it encodes an essential gene. Analysis of a conditionally null *myoA* strain in which *myoA* expression was regulated by the alcohol dehydrogenase promoter showed that, under conditions in which the promoter was induced, the strain displayed polarised growth by apical extension similar to wild type strains. However, under repressed conditions *myoA* null cells were enlarged and incapable of hyphal extension. These cells also showed a reduction in the level of secreted acid phosphatase indicating that myoA is involved in polarised growth and secretion. Interestingly, myoA also seems to have a function in endocytosis (Yamashita and May, 1998). A mutation in *myoA* which results in the constitutive activation of the protein has been generated. Analysis of this mutant showed that it accumulated intracellular membranes in growing hyphae. This accumulation has been suggested to be a consequence of a higher rate of plasma membrane internalisation by endocytosis in these constitutively active myoA mutants.

In budding yeast there are two genes, *MYO3* and *MYO5*, that encode class I myosins (Goodson and Spudich, 1995; Goodson et al., 1996). Deletion of either gives no obvious phenotype and single mutants display normal morphology and growth rates indicating, that Myo3 and Myo5 may have overlapping or redundant functions (Goodson et al., 1996). However, Geli and Riezman (1996) isolated a temperature-sensitive *myo5* mutant that is defective for endocytosis indicating that Myo3 and Myo5 are not entirely functionally redundant. Combination of *myo3Δ* with *myo5Δ* results in a double mutant that has severe defects in growth and polarisation of actin patches and cables. These results led Goodson et al. (1996) to propose that Myo3 and Myo5 are important in organising the actin cytoskeleton in budding yeast.

Consistent with this, *myo3Δ myo5Δ* double mutants exhibit phenotypes associated with actin disorganisation which include defects in bud site selection, cell wall deposition, secretion and endocytosis (Goodson et al., 1996). Truncation analysis indicates that the SH3 domain of Myo5 is critical for the Myo5-dependent actin organisation in budding yeast (Anderson et al., 1998). Ectopic expression of various forms of Myo5 show that full length Myo5 rescues the defects associated with actin disorganisation in *myo3Δ myo5Δ* double mutants. However, truncated forms of Myo5 which lack the SH3 domain fails to rescue the actin associated defects of *myo3Δ myo5Δ*. In two hybrid tests the SH3 domain of Myo3 and Myo5 interacts with the proline rich protein, Vrp1 (verprolin). The interaction between the class I myosins with verprolin has been suggested to mediate the polarisation of actin patches in budding yeast (Anderson et al., 1998). Recently, the SH3 domain has also been reported to be the site of interaction with Bee1/Las17, the budding yeast homologue of the human Wiskott-Aldrich syndrome protein (WASP) (Evangelista et al., 2000). Members of the WASP family of proteins and the Arp2/3 complex have been shown to be key factors involved in the nucleation of actin filaments in a number of diverse eukaryotic organisms (Lechler et al., 2000). In budding yeast, Bee1/Las17 controls actin nucleation by interacting with components of the Arp2/3 complex through its acidic domain. Interestingly, the C-terminal tail of budding yeast class I myosins contain an acidic domain that displays sequence similarity to the Arp2/3-interacting domain of Bee1/Las17 (Evangelista, 2000). Like Bee1/Las17, the budding yeast class I myosins also interact with the Arp2/3 complex through their acidic domain (Lechler et al., 2000). Combined deletions of the Arp2/3-interacting domain of Bee1/Las17 and the acidic domains of Myo3 and Myo5 abolish actin nucleation at the cell cortex. These results indicates that Bee1/Las17 and class I myosins function redundantly in the activation of the Arp2/3 complex in budding yeast.

b. Class II Myosins

Class II myosins have been implicated to perform many functions in the cell which include providing the force needed to contract muscle and to close the actomyosin ring during cytokinesis (Sellers, 2000). Many class II myosins have been identified in different cell types and throughout diverse organisms. For these reasons they are often subclassified into the following groups: (1) vertebrate skeletal and cardiac muscle myosin II; (2) vertebrate smooth muscle and nonmuscle myosin II; (3) invertebrate muscle myosin II; and (4) protozoan myosin II. Sequence analysis of class II myosins from yeast suggest that a distinct fifth subclass of myosin II may exist in fungi (May et al., 1998).

A unique characteristic of myosin II proteins is their ability to form filaments via the association of the rod-like tail. Bipolar filaments such as those found in skeletal muscle are formed by a combination of antiparallel interaction at the middle of the filament followed by parallel interactions along most of the filament length (Sellers, 2000). A central bare zone is found in the myosin filaments of skeletal muscle which is not populated by motor domains. These myosin filaments interdigitate between and interact with actin filaments. The motor domains at the end of myosin filaments provides the force necessary to move the myosin and actin filaments to slide past each other, thus resulting in muscle contraction.

Invertebrate muscle is also specialised for contraction. However, variations in filament structure and size do exist. Invertebrate muscle filaments have been found to contain paramyosin, a coiled-coil α-helical rod-like protein, at the core of the myosin thick filament (Cohen et al., 1971; Hoppe and Waterson, 1996). The ratio of paramyosin to myosin varies greatly from muscle to muscle, as does the length and diameter of the filament (Levine et al., 1976). Some molluscan muscle filaments can be as long as 50 μm in length, compared with the 1.6 μm length seen in vertebrate skeletal muscle (Szent-Gyorgyi et al., 1971). Variations in filament structure between vertebrate skeletal muscle and smooth muscle myosins are also observed. For example, analysis

of myosins from smooth muscle indicates that they form side polar filaments which result from antiparallel interactions between the tails of myosin molecules (Craig and Megerman, 1977).

In nonmuscle cells the abundance of myosin II is much less than that in muscle cells and appears to form transient filaments in different locations as needed by the cell (Verkhovsky et al., 1995; Moores et al., 1996). In cultured vertebrate cells, nonmuscle myosin II is largely found in stress fibres (Conrad et al., 1993; Maupin et al., 1994). Myosin II has also been associated with a select population of vesicles budding from the trans Golgi network although the exact identity and destination of these vesicles have yet to be resolved (Stow et al., 1998). Studies in mammalian tissue culture cells have also shown the recruitment of myosin II to the cleavage furrow where it is thought to mediate actomyosin ring contraction during cytokinesis (Field et al., 1999).

Studies from invertebrates, protozoa and yeast also implicate myosin II in cytokinesis. Myosin II is required for division of the *Caenorhabditis elegans* embryo (Guo and Kemphues, 1996). In *Drosophila melanogaster*, mutants which lack myosin II function are defective in cytokinesis and morphogenesis (Young et al., 1993). In addition, mutations in the *Drosophila* myosin regulatory light chain have been found to give cytokinesis defects (Karess et al., 1991). In *Dictyostelium discoideum* and budding yeast, myosin II localises to the division plane (Moores et al., 1996; Bi et al., 1998). Interestingly, in certain conditions *Dictyostelium* myosin II mutants are able to divide indicating that there may be an alternative cleavage mechanism in this organism that might involve other myosins (for reviews see Field et al., 1999; Gerisch and Weber, 2000). Studies from budding yeast also indicates that there may be a myosin II independent mechanism of cytokinesis since myosin II null mutants are viable and are able to divide, albeit defectively (Bi et al., 1998). Budding yeast myosin II has also been implicated in the generation of cell polarity since cells that lack myosin II have an altered budding pattern (Watts et al., 1987; Rodriguez and Paterson, 1990). The two fission yeast class II myosins, Myo2 (Kitayama et al., 1997; May et al., 1997) and

Myp2 (Bezanilla et al., 1997; Motegi et al., 1997), have been shown to be involved in cytokinesis. Their role in fission yeast cytokinesis is discussed in more detail in section 1.3.7c.

c. Class V Myosins

Functional analysis of class V myosins from various model systems indicate that these motors participate in the directed transport of a number of distinct cargoes to polarised regions of the cell (Titus, 1997a, 1997b). This is consistent with the finding that a class V myosin from chicken has been demonstrated to move towards the barbed (+) end of actin filaments. In contrast, a class VI myosin motor from pig has recently been found to move in the opposite direction along actin tracks (Wells et al., 1999; for review see Cheney, 2000).

Studies from mouse indicate that melanosomes could be one of the cargoes carried by myosin V motors (Reck-Peterson et al., 2000). Two class V myosins have been identified in mouse: Myo5A and Myo5B (Sellers, 1999). One of them, Myo5A, is encoded by the *dilute* locus (Mercer et al., 1991). As the name suggests, *dilute* mutants display a lightened coat colour. Normally, pigmentation in mammals depends on pigment synthesis by melanocytes and transfer of the pigment-containing organelles, the melanosomes, via dendritic processes to keratinocytes of the epidermis and hair follicles (Nascimento et al., 1997). Transfer of melanosomes to keratinocytes results in a uniform distribution of pigment granules throughout the hair shaft and epidermis. Thus, proper pigmentation requires the melanosomes to be transported from their site of synthesis at the perinuclear region to the cell periphery of melanocytes. Analysis of melanocytes from *dilute* mice indicate that their lightened coat colour is not a consequence of abnormal dendritic processes or melanosomes since they are similar to those from wild type cells. Instead, the coat colour defect in *dilute* mice appears to be a consequence of their failure to localise melanosomes to dendritic processes (Provance et al, 1996). This is supported by the observation that cultured melanocytes from *dilute* mice display melanosomes which are clustered around the

nucleus. In contrast, melanosomes from wild type melanocytes are evenly distributed throughout the cytoplasm. Interestingly, the product of the *dilute* locus, Myo5A, colocalises with the melanosome marker protein α-tyrosinase in cultured wild type melanocytes (Provance et al., 1996). Furthermore, immunoblot analysis has shown that the Myo5A is enriched in subcellular fractions containing melanosomes from a murine melanoma cell line (Nascimento et al., 1997). These results are consistent with the hypothesis that Myo5A plays a role in the intracellular localisation of melanosomes in melanocytes, either by directly transporting the melanosomes to the cell periphery or by anchoring them in these regions.

In addition to their coat colour defect, *dilute* mutants also have neurological disorders which causes their death within three weeks of birth (Huang et al., 1998). Expression analysis of *dilute* transcripts indicate that they are highly abundant in neurons (Mercer et al., 1991). Examination of brains from *dilute* mice has revealed that the dendritic spines of Purkinje cells lack smooth endoplasmic reticulum (SER). This has led to the suggestion that the neurological disorders observed in *dilute* mice could be a result of lack of SER transport to the dendritic spines or a failure to anchor the SER in these regions (Reck-Peterson et al., 2000). Furthermore, Myo5A has also been found to colocalise with a synaptic vesicle protein (SV2) in neurons (Bridgman, 1999) and a homologue of Myo5A from rat has been observed to associate with synaptic vesicles (Prekeris and Terrian, 1997). These results indicate that class V myosins are involved in the localisation of a variety of cellular cargoes.

Studies of the budding yeast class V myosins, Myo2 and Myo4, have shown that these motors may have distinct functions (for review see Brown, 1997). The budding yeast *MYO2* gene encodes an essential protein and a *myo2-66* temperature-sensitive mutant produces unbudded, enlarged cells at the restrictive temperature (Johnston et al., 1991). Furthermore, *myo2-66* mutants accumulate vesicles in the mother cell and *myo2-66* mutants have been shown to exhibit a synthetic lethal genetic interaction with mutants defective at a post Golgi stage of the secretory pathway (Govindan et

al., 1995). These phenotypes suggest that Myo2 may be involved in the localisation of secretory vesicles in budding yeast. Myo2 also seems to be important in the localisation of vacuoles since *myo2-66* mutants exhibit a vacuole inheritance defect and daughter cells receive little or no vacuoles, even at the permissive temperature (Hill et al., 1996). Consistent with a role for Myo2 in vacuole localisation is the finding that the protein is enriched in cell fractions containing vacuoles (Catlett and Weisman, 1998). Localisation studies have shown that Myo2 localises to sites of polarised growth such as the bud tip of small budded cells and then later to the mother-bud neck (Lillie and Brown, 1994). Taken together, these results indicate that Myo2 may be the motor that delivers vacuoles (Catlett and Weisman, 2000) and secretory vesicles (Pruyne et al., 1998) to the growing bud and the observation that *myo2-66* mutants undergo isotropic growth may be a consequence of their failure to localise components required for cell growth to polarised sites. Actin cables which connect the mother cell to the bud may be used as tracks for the Myo2 dependent transport since actin and tropomyosin mutants which disrupt actin cables also exhibit defects in the targeting of vacuoles and secretory vesicles to the bud (Hill et al., 1996; Pruyne et al., 1998).

Unlike Myo2, the other budding yeast class V myosin, Myo4, does not seem to be involved in cell growth since *myo4Δ* mutants displays normal morphology and growth characteristics (Haarer et al., 1994). Instead, Myo4 is involved in the establishment of developmental asymmetry that prevents daughter cells from switching mating type (Jansen et al., 1996; for review see Bloom and Beach, 1999). In budding yeast, mating type switching is induced by the *HO* endonuclease which creates double stranded breaks at the *MAT* locus. The *HO* gene is only transcribed in mother cells and therefore allows mother cells to switch mating type. Interestingly, Myo4 is preferentially localised to the growing bud and is required for the accumulation of the nuclear protein Ash1 (for asymmetric synthesis of *HO*) to prevent *HO* expression in daughter cells (Bobola et al., 1996). Thus, it might appear that Myo4 may be a motor that transports a factor, possibly along actin cables, to promote *HO* repression from the mother cell into its bud. This factor was later found to be the mRNA for the Ash1

protein itself (Long et al., 1997; Takizawa et al., 1997). Four other proteins are also required for the asymmetric localisation of *ASH1* mRNA to the growing bud, two of which, She2 and She3, appear to mediate the interaction between Myo4 and *ASH1* mRNA (Munchow et al., 1999). She3 has been shown to bind to Myo4 in the absence of RNA (Takizawa and Vale, 2000). She2 on the other hand is required for binding She3-Myo4 to *ASH1* mRNA. These results indicate that She3 may act as an adapter protein that docks the myosin motor onto an *ASH1*-She2 ribonucleoprotein complex.

1.2.5 Myosins Participate in the Coordinated Transport of Cellular Cargo Along Actin and Microtubule Tracks

In the past, the actin and microtubule cytoskeletons have been viewed as constituting separate filament systems which perform distinct functions. However, in recent years a growing number of evidence have shown that the two filament systems cooperate functionally during a variety of cellular processes (for review see Goode et al., 2000). One of these processes is the directed transport of vesicles and organelles to distinct cellular sites. In general, microtubules have been likened to train tracks which are used for the long range transport of cellular cargoes (Schliwa, 1999). However, microtubules do not reach to all parts of the cell which necessitates the use of actin filaments which acts as roads for the final delivery of cellular cargoes to their target destination.

Studies into intracellular transport have shown that various cargoes could move along both actin and microtubule tracks. For example, observation of single organelles in squid axoplasm showed that they could move along both actin and microtubule tracks, seamlessly switching between the two filament systems (Kuznetsov et al., 1992). In fission yeast, a structure known as the 'Cdc12 spot' has also been shown to exhibit actin- and microtubule-dependent movement (Chang, 1999; see section 1.3.7c for more details).

Much of our understanding in intracellular transport has come from the analysis of the movement of melanosomes in the melanophores of various organisms. Melanophores

are present in the dermal layers of fish and amphibians. The role of these cells is to aggregate pigmented organelles (melanosomes) to the centre of the cell or disperse them throughout the cytoplasm to effect colour changes in the animal's skin (Haimo and Thaler, 1994). Previously it was thought that a balance of activities between the '+' and '-' end directed microtubule-based motors, kinesin and dynein respectively, were responsible for the uniform dispersal of melanosomes throughout the cytoplasm. However, it has been demonstrated that actin filaments are required for their uniform dispersal in fish melanophores (Rodionov et al., 1998). Analysis of living cells showed that melanosomes frequently detach from their microtubule tracks and continue to move along irregular tracks, indicating the presence of a microtubule-independent transport system. Upon closer examination the melanosomes were shown to be associated with actin filaments which underwent an ATP-dependent shuttling motion. Treatment of cells with actin depolymerising drugs, however, caused the shuttling motion to stop and led to the accumulation of melanosomes at the cell margin, thus altering their normal uniform cellular distribution. Therefore, it appears that microtubules may be required for the outward transport of melanosomes to the cell periphery and actin filaments are required for their even dispersal throughout the cytoplasm. A complementary study has shown that purified frog melanosomes exhibit directed movement along microtubules and actin filaments *in vitro* and that the actin-based motor, myosin V, is associated with these organelles (Rogers and Gelfand, 1998).

The ability of various cargoes to be transported along actin and microtubule tracks is dependent on the association of the cargo with actin- and microtubule-based motors. Evidence is emerging which shows that single vesicles and organelles can possess simultaneously both actin and microtubule motors (Goode et al., 2000). Moreover, these motors have been shown to physically associate to form a 'hetero-motor' complex. Analysis of mouse brain extracts have shown that a class V myosin (MyoVA) and a kinesin-like motor protein (KhcU) coimmunoprecipitate and that the two proteins interact in yeast and mammalian two hybrid assays (Huang et al., 1999).

These results indicate that mouse myosin V and kinesin physically associate. Molecular analysis of the two proteins suggests that the interaction is mediated through an association between the rod domain of kinesin and the tail of myosin. Furthermore, localisation studies show that the two proteins colocalise in the cell in a punctate staining pattern in the cytoplasm. Two recent reports have shown that the budding yeast class V myosin, Myo2, also exhibits a physical interaction with a kinesin-like motor protein, Smy1 (Beningo et al., 2000) and a microtubule-associated protein, Kar9 (Yin et al., 2000).

1.3 FISSION YEAST

1.3.1 Introduction

Schizosaccharomyces pombe has been utilised as a model system for the investigation of various fundamental cellular processes. In recent years this organism has given valuable insights into the regulation of the cell cycle (Nurse, 1997), the mechanism of cytokinesis (Balasubramanian et al., 2000), the determination of cell polarity (Mata and Nurse, 1998; Verde, 1998) and the role of the cytoskeleton in these processes (May and Hyams, 1998). Much of what is learnt from this simple organism has turned out to be applicable to more complex organisms, including human beings (Nurse, 1997).

S. pombe has a small genome of about 14 Mb contained within three chromosomes (Alfa et al., 1993). Our understanding of gene function has been facilitated by advances in molecular biology (Russell, 1989). Like budding yeast, *S. pombe* genes can be easily manipulated such that they can be knocked out (Bahler et al., 1998), ectopically expressed (Maundrell, 1990) or epitope tagged (Craven et al., 1998). As well as these techniques *S. pombe* is also amenable to genetic (Munz et al., 1989), biochemical (Moreno et al., 1991) and cytological (Robinow and Hyams, 1989) analysis. The *S. pombe* genome sequencing project is nearly complete, the focus of attention now is to understand the role of the gene products and their interactions in cellular processes. The fact that *S. pombe* is amenable to a variety of research techniques makes it a powerful organism with which to dissect the function of these genes.

1.3.2 The Life Cycle of *Schizosaccharomyces pombe*

Schizosaccharomyces pombe, also commonly known as fission yeast, is a eukaryotic organism that normally exists in the haploid state. Each cell is rod-shaped in morphology which has a constant diameter of approximately 4 μm (Zhao and Lieberman, 1995). Cells grow by tip extension and depending on how far they have progressed in the growth cycle the length of fission yeast cells can vary from 7-15 μm. When cells reach a certain size they divide by medial fission to produce two equal sized daughter cells (Figure 1.8). Newly born cells continue this mitotic cycle so long as conditions remain favourable. However, when *S. pombe* experience nitrogen starvation haploid cells of opposite mating types conjugate to form a diploid zygote. Occasionally, diploid zygotes develop into diploid cells when the nitrogen stress is removed and these cells propagate vegetatively by mitosis (Munz et al., 1989). However, under continued nitrogen starvation the diploid zygote undergoes meiosis to produce an ascus containing four haploid ascospores. When favourable conditions return the dormant ascospores germinate to form haploid cells which resume the haploid mitotic cycle of propagation.

S. pombe cells can be of two mating types, "plus" or "minus". In heterothallic strains the plus or minus mating types are stable and perpetuated almost indefinitely (Egel, 1989). However, in homothallic strains the mating types frequently switch from one type to the other such that sister cells are often of different mating types. The vast majority of fission yeast strains that are used for laboratory research are descendants of three strains, one homothallic (strain: *968* h^{90}) and two heterothallic (strains: *972* h^{-S} and *975* h^{+N}), Munz et al. (1989). All three strains were originally isolated from grape juice and the monolithic origin provides a high degree of homogeneity in the genetic background of *S. pombe* strains used in research. In contrast to other yeast and moulds, where wild type strains have been isolated from a wide variety of different sources, the isogenic nature of *S. pombe* laboratory strains enables data to be fairly compared between different laboratories.

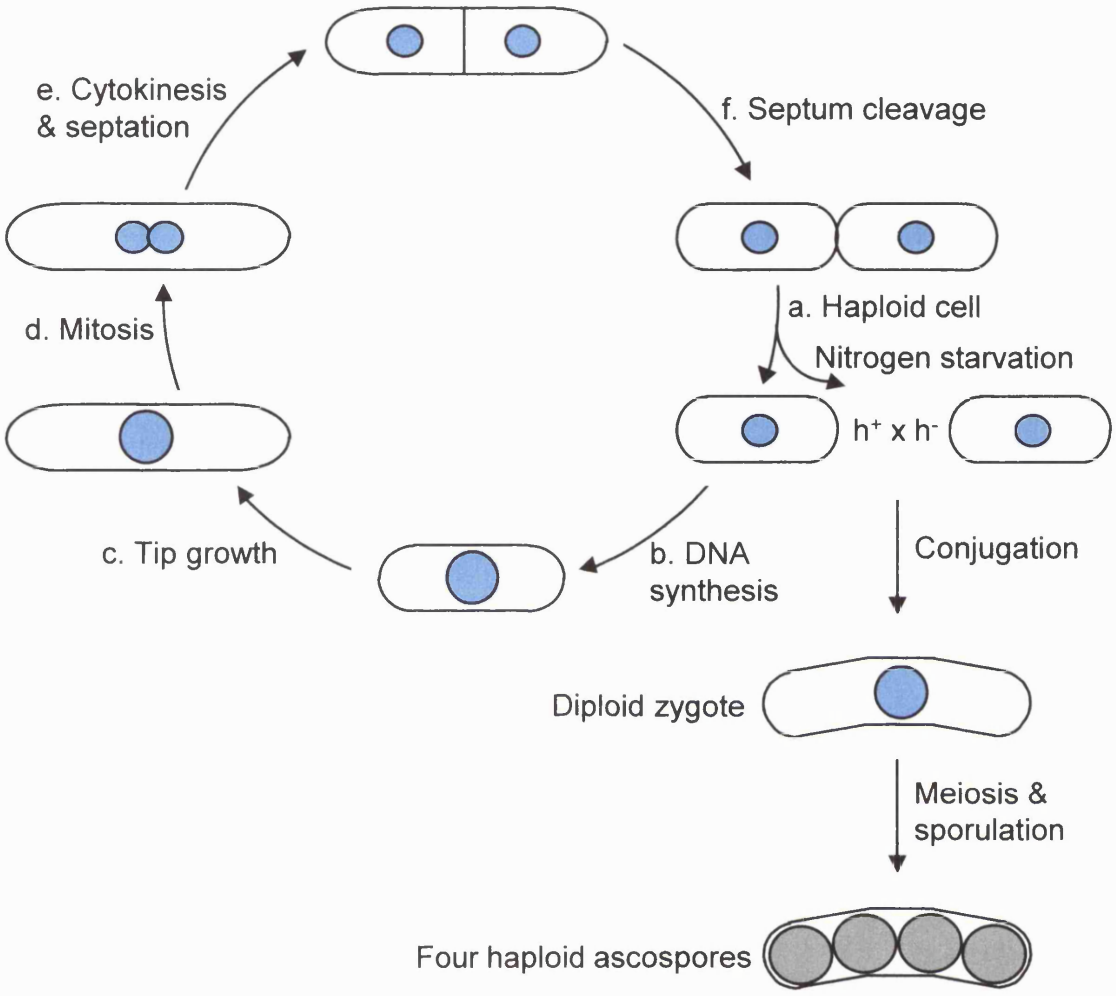

Figure 1.8 The Life Cycle of *Schizosaccharomyces pombe*

During vegetative growth, a haploid fission yeast cell (a) undergoes DNA replication (b). After DNA synthesis, it spends most of its time growing (c). Once it reaches a certain size, a fission yeast cell initiates mitosis (d). Cytokinesis and septation ensues following chromosome segregation (e). The septum is hydrolysed to release two separate daughter cells (f).

In conditions of nitrogen starvation, a haploid fission yeast cell exits from this cycle and follows a different path. Under these conditions a haploid cell can mate with another cell of the opposite mating type (h^+ or h^-) to form a diploid cell. Under continued nitrogen starvation they undergo meiosis and sporulation to produce a tetrad of haploid spores. These spores remain dormant until favourable conditions return when they germinate into haploid cells and re-enter the mitotic life cycle. In the diagram, blue circles represents nuclei and grey circles represents spores.

1.3.3 The Cell Division Cycle

The cell division cycle of *S. pombe*, like that of other eukaryotes, is comprised of four phases: (1) G1 phase, (2) S phase, (3) G2 phase and (4) M phase. DNA synthesis takes place during S phase, upon completion results in the duplication of the genome. The products of DNA synthesis are segregated into each daughter cell during M phase (mitosis) such that each daughter cell receives a single set of chromosomes containing the organism's entire genome. The cell division cycle is marked by two major transition points - one at late G1, just before S phase and the other late in G2, just before M phase. These transition points act as brakes and delay cell cycle progression until certain internal and environmental conditions have been fulfilled. For example, passage through the transition point at G2 requires replication of DNA before entry into mitosis or M phase. Thus, progression through the cell cycle is dependent upon the successful completion of previous events (for reviews see Fantes, 1989; Murray, 1992; D'Urso and Nurse, 1995; Elledge, 1996).

Exponentially growing *S. pombe* cells spend most of their time growing in G2 phase which can occupy as much as three quarters of the cell division cycle. The remainder being spent roughly equally among G1, S and M phases. Under optimal growth conditions, one cell cycle takes about 2 hours to complete although this is greatly extended at low temperatures and in poor growth media (Alfa et al., 1993). Due to its mode of growth by tip elongation, cell length can provide a visible measure of a cell's position in the cell cycle (Mitchison and Nurse, 1985). Thus, a newly born cell usually has completed G1 upon septum cleavage and has an average length of approximately 7 μm when they enter S phase. After passing through S phase, cells are in G2 during which most of the growth of a *S. pombe* cell takes place. Growth stops when cells reach a length of approximately 14-15 μm and mitosis is initiated. Towards the end of mitosis a septum is formed in the middle to bisect the two daughter cells. A new cell cycle begins and daughter cells are in G1 upon septum formation.

A number of temperature-sensitive mutants which affect the cell division cycle have

been isolated (Nurse et al., 1976). These mutants (called *cdc* mutants) progress normally through the cell cycle until shifted to the restrictive temperature where upon the cells arrest at a specific point in the cell cycle which require the function of the product of the *cdc* gene in order to proceed to the next stage. Analysis of *cdc* mutants have shown that they fall into three classes depending on when they are required during the cell cycle. Thus, some of the *cdc* gene products are required in order to pass through the transition point at G1, whilst others are required to pass through the transition point at G2. *Cdc* mutants which arrest in G1 have unreplicated DNA and have a nucleus with a 1C DNA content. *Cdc* mutants which arrest in G2, however, have passed through S phase and therefore have a single nucleus with a 2C DNA content. The third group classified as 'septation mutants' define genes that are involved in septation and cytokinesis. These mutants complete nuclear division but are either unable to form septa or have aberrant septa and so, unable to divide, arrest as elongated cells with multiple nuclei (see section 1.3.7c).

The fact that *cdc* mutants arrest at specific points in the cell cycle can be utilised as a way of synchronising a population of *S. pombe* cells (Alfa et al., 1993). This is usually achieved by shifting an asynchronous culture of *cdc* mutants to the restrictive temperature until nearly all of the cells in the population arrest at the point in the cell cycle which require the function of the gene product. Cells are then released from their cell cycle arrest by shifting the culture back down to the permissive temperature and the population of cells proceed to the next stage of the cell cycle in a synchronous fashion.

1.3.4 Growth and Septation in Fission Yeast

S. pombe is a rod-shaped organism which grows by tip extension. In a newly divided cell growth occurs exclusively at the old end of the cell which was present before cell division. Growth at the new end, formed by the splitting of the division septum, is activated at a point in G2 called 'NETO' (new end take off). NETO takes place about one third of the way through the cell cycle from which point growth occurs at both ends of the cell. Growth stops at the so called 'constant volume stage' of the cell cycle while the cell undergoes mitosis and cytokinesis. Both NETO and the onset of mitosis are regulated by a size control such that a critical volume must be attained before either is initiated (Mitchison and Nurse, 1985).

In order to grow a fission yeast cell must be able to extend its cell wall. The fission yeast cell wall is composed of galactomannan, α-1,3-linked glucans, β-1,3-linked glucans and β-1,6-linked glucans (Osumi et al., 1998). The exact mechanism by which a fission yeast cell extends its cell wall is unknown but it has been suggested that hydrolytic enzymes first cut a portion of the existing glucan structure. Turgor pressure pushes the weakened cell wall allowing room for the covalent insertion of new oligosaccharides (Johnson et al., 1989).

The septum that forms at the equator of a dividing cell is also composed of cell wall polysaccharides. Biosynthesis of the septum occurs by forming a primary septum that is laid down centripetally from the cell cortex (Johnson et al., 1973). As this is laid down a secondary septum forms on either side of the primary septum. Thus, the completed septum has a three layered structure composed of an inner primary septum which is flanked by a secondary septum. The primary septum can be visualised by the fluorescent cell wall dye, Calcofluor (Streiblova et al., 1984). Separation of the two daughter cells occurs by first degrading the outer cell wall at the site of septation and is completed by centripetal degradation of the primary septum (Johnson et al., 1973).

1.3.5 The Fission Yeast Cytoskeleton

The fission yeast cytoskeleton consists of a dynamic network of microtubules, F-actin patches and F-actin cables which undergo major rearrangements throughout different stages of the cell cycle. *Schizosaccharomyces pombe* is an excellent model organism with which to study the role of the cytoskeleton in basic cellular processes. This is partly due to the fact that the *S. pombe* cytoskeleton is almost exclusively concerned with growth and division and does not have to accommodate gross changes in cell shape and/or cell locomotion (May and Hyams, 1998). This section describes the role of the actin and microtubule cytoskeletons in *S. pombe*.

a. The Actin Cytoskeleton

Actin is encoded by a single gene, *act1*$^+$, in *S. pombe* (Mertins and Gallwitz, 1987). Disruption of *act1*$^+$ shows that the gene product performs essential functions in the cell. However, a temperature-sensitive mutant of actin, called *cps8*$^-$, which exhibits defects in growth and septation has been isolated (Ishiguro and Kobayashi, 1996). In addition, several cold-sensitive actin mutants have been constructed in order to determine the functional role of actin in *S. pombe* (McCollum et al., 1999).

The distribution of actin in *S. pombe* can be observed by indirect immunofluorescence microscopy using antibodies which recognise both G-actin and F-actin. The F-actin binding compound, phalloidin, conjugated to a fluorescent dye such as rhodamine has also been used as a method to visualise the actin cytoskeleton in *S. pombe*. The first detailed analysis of the distribution of actin in *S. pombe* was carried out by Marks and Hyams (1985) using this method. They showed that the *S. pombe* actin cytoskeleton consists mainly of actin patches and to a lesser extent actin cables. This study revealed a close correlation between the distribution of actin patches and polarised cell growth. They showed that at the beginning of the cell cycle actin localises as patches at the old end of a newly divided cell (Figure 1.9). This is consistent with the monopolar growth pattern as observed by Mitchison and Nurse (1985) during the first third of the cell cycle. Later on in the cell cycle, actin patches are also seen at the

new end of the cell which represents the switch from monopolar growth to bipolar growth at new end take off (NETO). As cells enter mitosis and cease growth, actin patches disappear from the cell ends and relocalise as an equatorial ring of actin that anticipates the formation of the division septum (Marks and Hyams, 1985; Alfa and Hyams, 1990; Jochova et al., 1991). Following cytokinesis and septum formation the equatorial ring of actin diminishes and actin patches are observed on either side of the septum. After septum digestion actin patches are once again seen at the old end of the cell and a new growth cycle begins (Figure 1.9).

The spatial and temporal coincidence between actin patches and growth indicates that the actin cytoskeleton is closely associated with growth and cell wall deposition. The nature of this relationship is still unclear, partly due to the fact that the structure of the actin patches remain unresolved. However, it is thought that actin patches may be associated with vesicles used for cell wall synthesis. Consistent with this, electron microscopy studies have shown that the poles and equator of fission yeast cells are rich in vesicles where cell wall deposition takes place (Kanbe et al., 1989). Immunofluorescence microscopy studies indicate that one of the roles of the actin cytoskeleton is to localise factors involved in cell wall synthesis. Analysis of the distribution of the Mok1 α-glucan synthase shows that it requires an intact actin cytoskeleton for its localisation to the growth sites of a fission yeast cell (Katayama et al., 1999). When the actin cytoskeleton is disrupted, Mok1 delocalises from these sites and exhibits a random distribution in the cell.

Immunofluorescence microscopy studies indicate that cortical actin patches consist of a number of proteins, which includes components of the Arp2/3 complex (McCollum et al., 1996; Arai et al., 1998; Morrell et al., 1999). In addition some actin patches, although not all, are associated with the fission yeast actin binding protein, Cdc8 tropomyosin (Arai et al., 1998). Cdc8 also localises to actin cables which run along the length of the cell from one end to the other. These cables are attached to some actin patches and have been suggested to play a role in the supply of actin patches and/or

cell wall materials to the cell ends during tip growth and to the equator during cell division (Arai et al., 1998).

As an alternative method of studying actin function, drugs that disrupt the actin cytoskeleton have been used to study the role of actin in various cellular processes. Cytochalasins are one class of compounds which have been shown to reversibly disrupt the actin cytoskeleton (Cooper, 1987). Cytochalasins are thought to disrupt actin filaments by capping the barbed (+) end of growing filaments and thereby inhibiting the association and dissociation of subunits at that end. However, there is also evidence that cytochalasins may disrupt nucleation of filaments by binding to actin monomers and dimers. In addition, cytochalasins may sever existing filaments by binding to a subunit in the interior of the filament and thereby break the filament in two. *In vivo*, treatment of *S. pombe* with one form of cytochalasin (cytochalasin A) has shown that it prevents actin ring formation and subsequent septum deposition (Kanbe et al., 1993). The relocalisation of actin is also inhibited and actin remains trapped at the cell ends. Electron micrographs show actin filaments amassed at the cell ends in cytochalasin A treated cells. Vesicles carrying cell wall material, which are usually localised to the growing sites, are found to be dissociated from actin filaments and accumulate in the cytoplasm. A similar study using cytochalasin D on another fission yeast (*Schizosaccharomyces japonicus var. versatilis*) also showed that cytochalasin interferes with actin ring formation and septation in this organism (Gabriel et al., 1998).

Other drugs which have also proved to be of considerable utility are latrunculin A (Lat-A) and latrunculin B (Lat-B). Analysis of the effects of Lat-A on the actin cytoskeleton shows that it disrupts actin filament polymerisation by forming an assembly incompetent complex with monomeric actin (Ayscough et al., 1997). In budding yeast, Lat-A causes a rapid (2-5 minutes) and complete disruption of the actin cytoskeleton such that no actin structures (patches or cables) persist after treatment with the drug. Treatment of budding yeast and fission yeast with either Lat-

A or Lat-B shows that these drugs are effective in inhibiting the growth of yeasts. Like cytochalasin treatment, treatment of cells with latrunculin is reversible and cells resume growth if the drug is washed out of the medium (Petersen et al., 1998).

b. The Microtubule Cytoskeleton

As in all eukaryotes, fission yeast microtubules are polymers of α- and β-tubulin subunits. The related molecule, γ-tubulin, is localised at microtubule organising centres (Horio et al., 1991) where it functions in the nucleation of microtubules (Paluh et al., 2000). In *S. pombe*, the microtubule organising centre is known as the spindle pole body (SPB). Most of the fission yeast SPB is located on the outside of the nuclear envelope during interphase (Ding et al., 1997). However, upon commitment to mitosis the SPB duplicates and is found within the nuclear membrane until anaphase.

Four tubulin genes have been identified in *S. pombe*: two α (*nda2*$^+$, *atb2*$^+$), one β (*nda3*$^+$) and one γ (*gtb1*$^+$/*tug1*$^+$) (for review see Hagan, 1998). One of the two α-tubulin genes, *atb2*$^+$, is non-essential (Adachi et al., 1986). Analysis of microtubule function in *S. pombe* have been greatly assisted by the isolation of cold-sensitive mutations in *nda2*$^+$, *nda3*$^+$ and *gtb1*$^+$/*tug1*$^+$ (Umesono et al., 1983; Hiraoka et al., 1984; Toda et al., 1984; Paluh et al., 2000). In addition to these, temperature-sensitive mutations in *atb2*$^+$ and *nda3*$^+$ have also been isolated (Radcliffe et al., 1998). Although a number of tubulin mutants have been found, tubulin-binding compounds that disrupt microtubules have also been used to understand microtubule function (Umesono et al., 1983; Mata and Nurse, 1997). Drugs such as thiabendazole (TBZ) and carbendazim (MBC) have been shown to be effective in depolymerising microtubules in *S. pombe* (Sawin and Nurse, 1998; Brunner and Nurse, 2000). Like actin-disrupting compounds, microtubule-depolymerinsing drugs such as TBZ and MBC have a reversible effect and microtubules reform if these compounds are removed from the growth medium.

In fission yeast, microtubules have been reported to execute several distinct functions which includes the distribution of organelles such as mitochondria and Golgi

(Ayscough et al., 1993; Yaffe et al., 1996); the determination of cell polarity (Toda et al., 1983; Mata and Nurse, 1997; Hirata et al., 1998) and chromosome segregation. Analysis of α- and β-tubulin mutants indicates that the essential function of fission yeast microtubules is in the segregation of chromosomes. Indeed, the *nda2*$^+$ and *nda3*$^+$ genes were so named because mutants in these genes exhibited a nuclear division arrest phenotype (Umesono et al., 1983). At the restrictive temperature these mutants fail to form a proper mitotic spindle and arrest in early metaphase with condensed chromosomes. Some of these mutants also exhibit aberrant cell morphology indicating the importance of microtubules in cell polarity (Toda et al., 1983) (see section 1.3.6).

The distribution of microtubules throughout the cell cycle of *S. pombe* has been extensively characterised by indirect immunofluorescence microscopy (Hagan and Hyams, 1988). In wild type cells between four to eight linear tubulin staining elements, each probably a bundle of two or three microtubules, extend between the cell ends during interphase. These microtubule arrays forms a basket that embraces and positions the nucleus to the middle of the cell (Hagan and Yanagida, 1997) (Figure 1.9). At the onset of mitosis, cytoplasmic microtubules depolymerise and a short intranuclear spindle is formed between the two SPBs associated with the nuclear envelope (Hagan and Hyams, 1988). Spindle elongation separates the daughter nuclei to the ends of the cell, from where they subsequently relocate to the centres of the two daughter cells as the spindle breaks down (Hagan et al., 1990). After cell separation the interphase array of microtubules reforms (Hagan and Hyams, 1988).

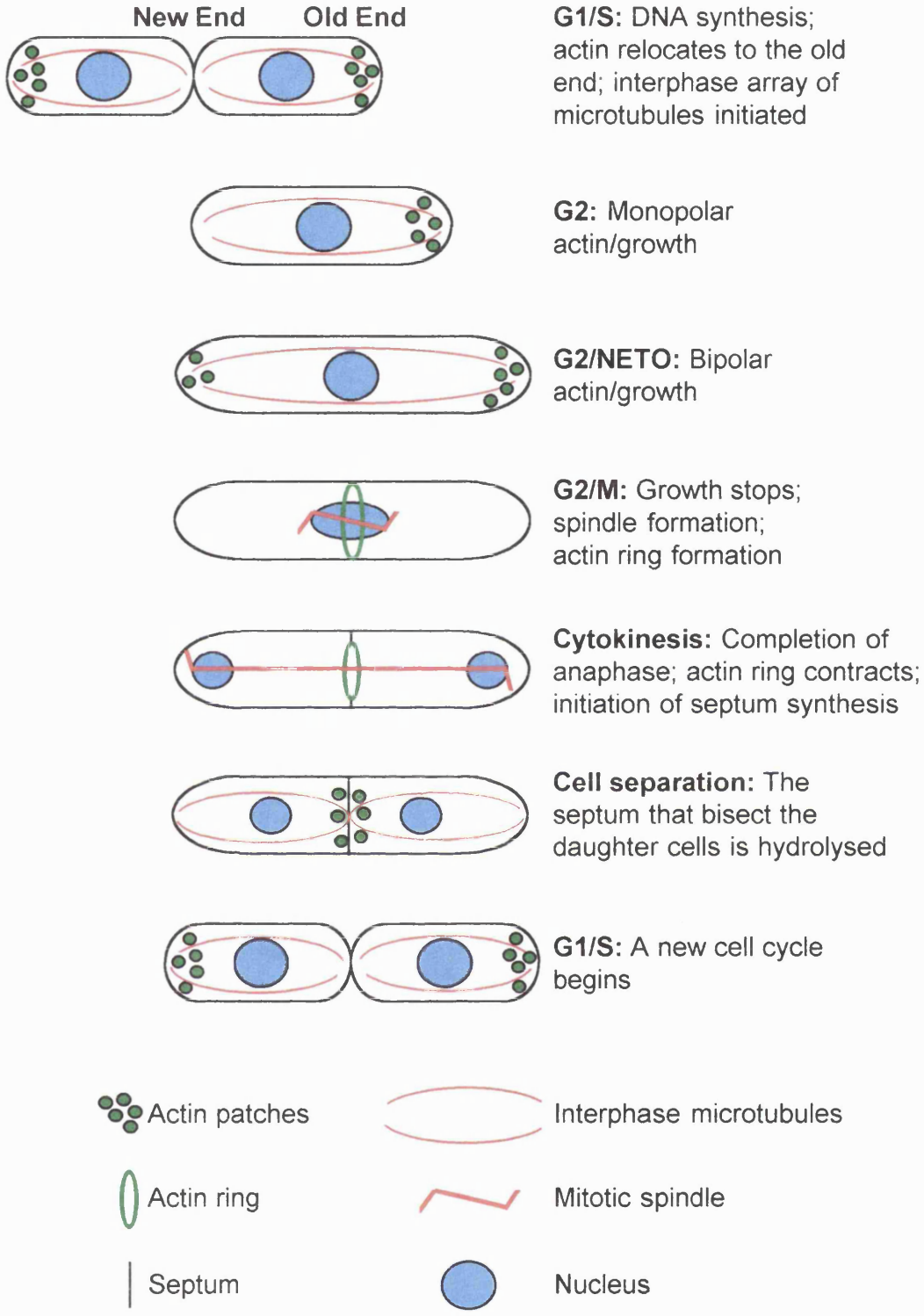

Figure 1.9 Structural Rearrangements in Actin and Microtubules in the Fission Yeast Cell Cycle

Rearrangements in the actin and microtubule cytoskeletons in the fission yeast cell cycle is shown diagramatically. The cycle begins at the top and progresses down the page. For the sake of clarity actin cables which run along the main axis of fission yeast cells have been omitted from this diagram.

1.3.6 Cell Morphogenesis in *S. pombe*

The Rho family of GTP-binding proteins which consists of Rho, Rac and Cdc42 subfamilies have been shown to be key regulators of the actin cytoskeleton in mammalian cells (Hall, 1998). Homologues of these proteins have been found in budding yeast. Analysis of the function of the budding yeast Cdc42 GTPase and its GTP/GDP exchange factor, Cdc24, have shown that these proteins are critical for bud emergence and in establishing cell polarity (Madden and Snyder, 1998). Temperature-sensitive mutants in these genes fail to properly localise many polarised components important for yeast budding including actin patches and a class of proteins known as 'septins' (see section 1.3.7b). Consequently these mutants form large, round and unbudded cells with multiple nuclei at the restrictive temperature.

Fission yeast with its well defined cell shape and amenability to genetic analysis provides another ideal system to study cell morphogenesis. This is because mutations which perturb the fission yeast cylindrical morphology can be easily identified and the corresponding genes cloned. In *S. pombe* three Rho-related proteins Cdc42 (Miller and Johnson, 1994), Rho1 and Rho2 (Nakano and Mabuchi, 1995) have been identified. The *S. pombe* Cdc42 GTPase displays 85% and 83% amino acid identity to its homologues in budding yeast and humans respectively (Miller and Johnson, 1994). Like in other eukaryotes, the *S. pombe* Cdc42 GTPase modulates the actin cytoskeleton and is a key protein that regulates polarised cell growth in fission yeast (Verde, 1998). The *S. pombe cdc42*$^{+}$ gene is essential for cell viability and null mutants arrest as small, round cells consistent with its implicated role in controlling cell polarity. Overproduction of Cdc42, however, results in an abnormal morphological phenotype of large misshapen cells (Miller and Johnson, 1994). In fission yeast, Cdc42 is found in a complex with the GTPase Ras1, the putative Cdc42 GTP/GDP exchange factor Scd1/Ral1 and the SH3 domain containing protein Scd2/Ral3 (Chang et al., 1994). Ras1 is thought to associate with and activate Cdc42.

A serine/threonine kinase, Pak1/Shk1 which associates with Cdc42 and is homologous

to the mammalian PAK kinases (p21 activated kinases) is thought to be an important mediator of the Ras1/Cdc42 signalling complex (Marcus et al., 1995; Ottilie et al., 1995). A temperature-sensitive allele of the *pak1/shk1* gene known as '*orb2*' has been found (Verde et al., 1998). The *orb2*$^-$ mutant was originally isolated in a screen to identify *S. pombe* genes involved in cell morphogenesis (Verde et al., 1995). A number of *orb* or spherical mutants were identified in this screen. Like other *orb* mutants, *orb2*$^-$ displays a number of morphological defects which includes a rounded cell shape and delocalised actin patches. Interestingly, *orb2*$^-$ displays a genetic interaction with another *orb* mutant, *orb6*$^-$. It has been suggested that Orb6 might act downstream or parallel to the morphogenetic pathway controlled by Cdc42 (Verde et al., 1998; Verde 1998). Cloning of *orb6*$^+$ has shown that it encodes a serine/threonine kinase similar to mammalian Rho kinase and myotonic dystrophy kinase.

Rho1 (Nakano et al., 1997) and Rho2 (Hirata et al., 1998) and two protein kinase C related proteins Pck1 and Pck2 (Toda et al., 1993; Kobori et al., 1994) are also important for the control of cell shape in *S. pombe*. Disruption of *rho1*$^+$ shows that it encodes an essential gene (Arellano et al., 1997; Nakano et al., 1997). However, disruption of *rho2*$^+$, *pck1*$^+$ and *pck2*$^+$ results in viable cells with several defects in the cell wall which includes an increased sensitivity to compounds that inhibit the synthesis of cell wall glucans (Hirata et al., 1998; Arellano et al., 1999). These mutants also have a lower amount of α- and β-glucan incorporated into their cell wall (Arellano et al., 1999; Katayama et al., 1999) and an increased sensitivity to cell wall lytic enzymes (Hirata et al., 1998; Katayama et al., 1999). Analysis of Rho1 and Pck2 indicates that they may modify the fission yeast cell wall through their ability to activate the 1,3-β-D-glucan synthase (Arellano et al., 1996; Arellano et al., 1999). A study by Katayama et al. (1999) also provides evidence that Pck2 may additionally modify the fission yeast cell wall by positively regulating the 1,3-α-D-glucan synthase encoded by the *mok1*$^+$ gene.

Two hybrid and coimmunoprecipitation assays have shown that Pck1 and Pck2 are

targets of the Rho GTPases and interact with the active, GTP-bound form of Rho1 and Rho2 (Arellano et al., 1999). Both Pck1 and Pck2 have two HR1 motifs at their N-termini and it is thought that these motifs, which are present in other Rho-binding proteins, mediate their interaction with Rho1 and Rho2 (Arellano et al., 1999; Sayers et al., 2000). Interestingly, several PEST sequences (which marks a protein to destruction by the proteasome) are also found at the N-terminus of Pck1 and Pck2. Expression of a constitutively active form of Rho1 (GTP-Rho1) has been shown to increase the stability of Pck1 and Pck2 (Arellano et al., 1999). These results indicate that binding of the Rho GTPases to Pck1 and Pck2 is important for the stabilisation of the protein kinases.

It is not known whether Rho1 or Rho2 interacts with the pathway defined by Cdc42 to effect cell morphogenesis (Verde et al., 1998). However, consistent with their role in the control of polarised cell growth, some of the components known to interact with Cdc42 such as Ras1, Scd1/Ral1 and Scd2/Ral3 have been localised to the actin-associated growing tips (Sawin and Nurse, 1998; Verde, 1998). Thus, these proteins are found at the old end prior to NETO and at both ends after activation of bipolar growth. The same localisation pattern has been observed with Rho1 (Arellano et al., 1997) and Rho2 (Hirata et al., 1998) and their effectors Pck1 and Pck2 (Katayama et al., 1999; Sayers et al., 2000).

Interestingly, Rho1, Rho2 and Orb6 are only found at the single growing tip in *tea1*$^{-}$ mutant cells which fail to undergo NETO (Verde et al., 1998). Mutants in *tea1*$^{+}$ often mislocalise their site of growth and consequently produce bent and branched cells (Mata and Nurse, 1997). In wild type cells, Tea1 is localised at the tips of both poles and its tip localisation requires the function of microtubules although not actin. Furthermore, Tea1 localises to the new end of the cell long before actin reorganisation and activation of bipolar growth. Tea1 also exhibits differential localisation at the two poles and appears to be more abundant at the old end. In contrast, Pom1, another protein which exhibits microtubule-dependent tip localisation is highly enriched at the

new end (Bahler and Pringle, 1998). Like *tea1*$^{-}$, *pom1*$^{-}$ mutants also display branched cells but may act in a different way to Tea1 to effect cell polarity (Verde et al., 1998).

The differential presence of Tea1 and Pom1 at the old and new ends have led to a model of how the order of growth activation may be established in fission yeast (Verde et al., 1998). The model suggests that following mitosis components of the Cdc42-dependent pathway, Rho1, Rho2 and actin localise to the old end and activate it for growth. This process may be facilitated by a complex of proteins involving Tea1 which remains at the cell tips during mitosis. At the same time, newly synthesised Tea1 is transported to the new end in a microtubule-dependent manner. In early G2, the Tea1 complex at the new end is modified, possibly by the activity of the cell cycle regulator, Cdc2 kinase. Modification of Tea1 complex may allow components of the growth machinery including Cdc42-associated proteins to localise at the new end and control the recruitment of actin and consequently activation of bipolar growth.

1.3.7 Cytokinesis in *S. pombe*

Cytokinesis, the division of one cell into two daughters, is a complex event that must be performed in a coordinated manner to ensure the survival of daughter cells. Cytokinesis appears to proceed as a single, well-orchestrated process, but can be separated into several distinct events: (a) timing of cell division, (b) cleavage plane specification, (c) medial ring assembly, (d) medial ring contraction and septation. These events have to be accurately executed so that each daughter cell receives a single complement of the duplicated genome and organelles.

a. Timing of Cell Division

Cell division occurs at a precise moment in the cell cycle such that cells divide after they have gone through a period of growth and after they have replicated their DNA. Thus, cytokinesis is prevented in cells with an unduplicated genome. One of the earliest signs that a cell is about to divide is the appearance of a medial ring comprised of actin and various other components (Marks and Hyams, 1985; for reviews see

Fankhauser and Simanis, 1994; Le Goff et al., 1999; Balasubramanian et al., 2000). Entry into mitosis rather than attainment of a certain size seems to be critical to initiate the process of medial ring assembly. This is supported by the observation that *cdc2*$^-$ and *cdc25*$^-$ mutants continue to elongate with a single nucleus without forming an actin ring when arrested at a point in the cell cycle just prior to mitosis (Snell and Nurse, 1994). It is possible that the initial cell cycle trigger for medial ring assembly is the Cdc2 mitotic kinase since ring formation is an early event in mitosis and requires activation of the Cdc2 mitotic kinase. Two potential effectors which may act downstream of Cdc2 to mediate actin ring assembly are the products of the *plo1*$^+$ and *cdc15*$^+$ genes (Balasubramanian et al., 2000).

Plo1 is a homologue of the conserved polo kinase family which have been shown to play roles in mitosis in several organisms (Ohkura et al., 1995). Like other polo kinases, Plo1 of fission yeast also seems to regulate mitotic events since cells deleted for *plo1*$^+$ have defects in spindle assembly and actin ring formation. Interestingly, overexpression of *plo1*$^+$ induces actin ring assembly and septation in G1 and G2 arrested interphase cells in the absence of mitotic Cdc2 kinase activity. Thus, Plo1 which may normally act downstream of Cdc2 may bypass the requirement of Cdc2 activity when *plo1*$^+$ is overexpressed to initiate actin ring assembly. Localisation studies have shown that Plo1 exhibits no particular localisation during interphase (Bahler et al., 1998; Mulvihill et al., 1999). However, in late G2 or early mitosis Plo1 localises to the spindle pole body and remains associated to the spindle poles as they separate during anaphase. In addition, Plo1 exhibits nuclear localisation at the onset of mitosis and is seen to be present at the mitotic spindles during spindle elongation. Interestingly, an equatorial ring of Plo1 is also observed during early mitosis which has been suggested to mark the site at which the medial ring will form (Bahler et al., 1998).

Cdc15 is a novel protein which is essential for septum formation (Fankhauser et al., 1995). It has been suggested that the septation defect of *cdc15* mutants lies in their inability to mobilise actin patches to the medial region of the cell (Balasubramanian et

al., 1998). Localisation studies have shown that Cdc15 exhibits diffuse cytoplasmic localisation during interphase but forms a ring during mitosis which coincides with the actin ring (Fankhauser et al., 1995). Interestingly, Cdc15 is a phosphoprotein which exists in its phosphorylated form during most of the cell cycle and becomes dephosphorylated during actin ring formation. Like *plo1*$^+$, overexpression of *cdc15*$^+$ in G2 arrested interphase cells promotes the formation of a medial actin ring, although not septation. These observations have led to the proposal that Cdc15 may act as medial ring nucleating protein which is subject to cell cycle regulation by protein kinases and phosphatases (Chang and Nurse, 1996). The regulators of Cdc15 are not known although the Plo1 and Cdc2 kinases or their downstream targets have been suggested to be involved in the regulation of Cdc15 (Chang and Nurse, 1996).

b. Cleavage Plane Specification

In fission yeast the actin ring and septum is precisely positioned in the middle of the cell such that upon cell separation each daughter cell is approximately equal in size. Just how the cleavage plane is specified in fission yeast is a subject of ongoing debate. In other organisms, however, different mechanisms seems to operate to determine the site of division (for review see Field et al., 1999). In animal cells the cleavage plane is thought to be determined by the position of the mitotic spindle in late metaphase or early anaphase of the cell cycle (Glotzer et al., 1997). The cleavage plane is therefore positioned to bisect the axis of chromosome segregation during mitosis in animal cells. The observation that in certain developmentally important divisions the spindle is rotated or positioned asymmetrically prior to cytokinesis in order to generate daughter cells of different sizes and different fates supports the model that the mitotic spindle is important for cleavage plane specification in animal cells (for reviews see Strome, 1993; White and Strome, 1996).

In other eukaryotes, the cleavage plane is specified prior to mitosis independently of spindle location. For example, in budding yeast a landmark established prior to spindle assembly determines the bud neck as the site of division (Chant, 1996). This landmark

consists of a group of proteins known as septins which defines the cleavage plane at the beginning of G1. The ring of septins encircles the mother-bud junction and persists for the duration of the cell cycle where it acts as a scaffold for the proteins that ultimately execute the mechanics of cytokinesis. During mitosis, however, the spindle is positioned in such a way that it conforms to the location of the bud neck and aligns through the opening of the septin ring and elongates to segregate a set of chromosomes into the mother and daughter cells. Cytokinesis then occurs in the plane of the septin ring.

In plants, the location of the division plane is also established prior to mitosis and is determined by a structure known as the preprophase band (PPB). The PPB is a transient cortical microtubule array that overlays the nucleus prior to the formation of the mitotic spindle (Field et al., 1999). The PPB marks the site at which the phragmoplast, a cytoplasmic structure composed of microtubules, will form. The phragmoplast is responsible for the localisation of vesicles for the synthesis of the cell plate which divides the plant cell.

Several models have been proposed for the positioning of the division site in *S. pombe* (Chang and Nurse, 1996). One model suggests that the cleavage plane may be specified by the mitotic spindle similar to the proposed mechanism of cleavage plane specification in animal cells. However, numerous observations in *S. pombe* have shown that the mitotic spindle is not required for the placement of the actin ring. For example, a mutation in the *nda3* gene which encodes for β-tubulin causes cells to arrest in mitosis with a correctly positioned medial ring even in the complete absence of a mitotic spindle (Chang et al., 1996). As discussed earlier, overexpression of either *cdc15*$^+$ or *plo1*$^+$ induces the formation of medially placed actin rings in interphase cells with no mitotic spindles (Fankhauser et al., 1995; Ohkura et al., 1995). These observations indicate that the position of the division site can be determined even before a cell enters mitosis and forms a mitotic spindle.

The model that is most consistent with observations in *S. pombe* is the nuclear model which proposes that the position of the premitotic nucleus may determine the site of medial ring formation in fission yeast. The evidence that supports this model comes from the observation that the positions of the nucleus prior to chromosome segregation and the actin ring always coincide. For example, in wild type cells the actin ring forms in the middle of the cell in early mitosis on the cortex that overlays the nucleus prior to nuclear division. This model is further supported from the pattern of multiple actin rings in the *cdc11*$^-$ mutant. C*dc11*$^-$ undergoes repeated nuclear cycles and forms highly elongated cells containing multiple nuclei (Nurse et al., 1976). Interestingly, the position of the actin rings coincide with the position of nuclei in this mutant (Marks et al., 1987). The most convincing support for the nuclear model of cleavage plane specification comes from the recent observation of a *ste12*$^-$ mutant (Morishita and Shimoda, 2000). In *ste12*$^-$, the nucleus is eccentrically positioned possibly because of the large vacuoles that are present which displaces the nucleus from the cell equator. Despite this the cortical actin ring is always found to overlay the displaced nucleus.

In *S. pombe*, several mutants have been identified to be defective in the placement of the actin ring (for review see Le Goff et al., 1999). Cells with mutations in the *mid1*$^+$ gene (Chang et al., 1996; also known as *dmf1*$^+$, Sohrmann et al., 1996) have correctly positioned nuclei but the position of the division septum is aberrant ranging from a slightly eccentric placement which produces daughter cells of unequal size to more extreme phenotypes such as the formation of a septum along the main axis of the cell. Actin and other cytokinesis components always colocalise with the misplaced septum indicating that the defect lies not in forming the cytokinetic actin ring but rather the placement of the cleavage plane may be uncoupled from the nuclear positioning signal in the *mid1*$^-$ mutant. In wild type cells Mid1 is localised in the nucleus during interphase. However, Mid1 exits the nucleus at the onset of mitosis to form a diffuse cortical band in the region of the nucleus which becomes a tight ring around metaphase or early anaphase (Sohrmann et al., 1996; Bahler et al., 1998). Interestingly, actin rings

are observed at the medial cortex before metaphase and precede the formation of the Mid1 rings. However, the early actin rings are faint and sometimes branched or slightly misplaced in comparison to the actin rings in metaphase or anaphase cells (Bahler et al., 1998). Before mitosis, actin is primarily localised at the growing cell poles (Marks and Hyams, 1985). It has been suggested that the exit of Mid1 from the nucleus early in mitosis to form a broad equatorial band may recruit actin or actin binding proteins to this zone to facilitate the formation and maturation of the actin ring (Bahler et al., 1998).

Several lines of evidence indicate that Plo1 may be a regulator of Mid1. Exit of Mid1 from the nucleus at the onset of mitosis correlates with increased phosphorylation of the protein (Sohrmann et al., 1996). Interestingly, overexpression of the Plo1 kinase causes Mid1 to exit the nucleus prematurely in the cell cycle and Mid1 displays a reduced mobility on gels similar to that of the hyperphosphorylated form in mitotic cells (Bahler et al., 1998). Genetic interactions between *plo1*$^-$ and *mid1*$^-$ mutants have also been observed and the proteins interact in a two hybrid assay. Furthermore, temperature-sensitive mutants of *plo1*$^-$ exhibit defects in the localisation of the division plane similar to that observed in *mid1*$^-$ mutants. These results indicate that one of the roles of Plo1 is to phosphorylate Mid1 to cause it to exit the nucleus and thus mediate the positioning of the cytokinetic actin ring (Bahler et al., 1998).

Another protein that is important for the correct placement of the medial ring is the product of the *pom1*$^+$ gene. *Pom1*$^+$ encodes a putative protein kinase which appears to provide positional information for both polarised growth and cell division (Bahler and Pringle, 1998). Mutants in *pom1*$^+$ have several defects which include the inability to distinguish new from old ends resulting in the initiation of growth with equal frequency from the old or new end after cell division. This is in contrast to wild type cells which first resume growth from the old end immediately after cell division (Mitchison and Nurse, 1985). Furthermore, *pom1*$^-$ mutants fail to activate bipolar growth and grow from the same end that has been designated for growth after cell

division. Mutants in *pom1*$^-$ also misplace their septum and is often seen to be located near the non-growing end of the cell resulting in daughter cells of unequal sizes (Bahler and Pringle, 1998). In wild type cells, Pom1 mainly localises to the new cell end during interphase. In mitotic cells, Pom1 localises to both ends and some are also present at the equator during early mitosis. The equatorial localisation of Pom1 increases with mitotic progression and a band of Pom1 localises to the septum at the end of mitosis. It is not clear how Pom1 is involved in the positioning of the cleavage plane although it has been suggested that it may receive or transmit a signal that emanates from the nucleus, perhaps carried by Mid1, to direct the positioning of the division site (Bahler and Pringle, 1998).

c. Medial Ring Assembly

Once a division site has been specified numerous proteins are assembled at the site of division to form a medial ring which actually carries out the mechanics of cytokinesis. The medial ring consists of actin and a number of proteins which are important for its assembly and/or integrity. Some of the proteins required for the organisation of the medial ring have been identified and these include the product of the *cdc3*$^+$ and *cdc8*$^+$ genes which encode the actin binding proteins, profilin and tropomyosin respectively (Balasubramanian et al., 1992, 1994). During interphase Cdc3 localises to the growing poles where actin patches are concentrated while Cdc8 is observed as discrete patches at the cell cortex, though not all of these coincide with actin patches (Arai et al., 1998). In addition, cables of Cdc8 are seen at all stages of the cell cycle which seems to coincide with cables of actin (Arai et al., 1998). During mitosis, Cdc3 localises to the medial region as a broad band which has been suggested to promote the formation of the contractile actin ring (Balasubramanian et al., 1994). In contrast, an equatorial ring of Cdc8 is thought to form after the formation of the actin ring since the Cdc8 ring is observed at a later stage of mitosis than the ring of actin (Balasubramanian et al., 1992). Mutants in *cdc3*$^+$ and *cdc8*$^+$ exhibit delocalised actin patches and disorganised actin rings suggesting that they are important for the general organisation of actin in the cell (Chang and Nurse, 1996). Despite the abnormalities in actin patch

distribution, *cdc3*$^+$ and *cdc8*$^+$ null mutants are still able to maintain polarised growth but die because they fail to assemble a medial ring and undergo cytokinesis indicating that this step is the most sensitive to their absence (Le Goff et al., 1999).

In contrast to *cdc3*$^+$ and *cdc8*$^+$ which are required for the general organisation of actin, mutants in *cdc4*$^+$, *cdc12*$^+$, *myo2*$^+$, *myp2*$^+$ and *rng2*$^+$ show defects in the formation of the medial ring but display normal distribution of actin patches (Balasubramanian et al., 2000). This suggests that their main function is to assemble or maintain the integrity of the medial ring. The product of the *cdc4*$^+$ gene encodes a myosin light chain that has been demonstrated to associate with the two class II myosins Myo2 and Myp2 (Naqvi et al., 1999; Motegi et al., 2000). Temperature-sensitive and null mutants of *cdc4*$^+$ die as elongated cells with multiple nuclei that fail to complete cytokinesis (McCollum et al., 1995). In wild type cells Cdc4 forms an equatorial ring during mitosis which appears to shorten in diameter as mitosis proceeds (Balasubramanian et al., 1997). Cdc4 exhibits no particular localisation during interphase. In cells that have yet to form a Cdc4 ring treatment of cells with the actin depolymerising drug, latrunculin A, prevents the Cdc4 ring from forming (Naqvi et al., 1999). However, in cells where a Cdc4 ring has established latrunculin A treatment has no effect on the integrity of the Cdc4 ring. These results suggests that the initial assembly of Cdc4 to the medial ring requires an intact actin cytoskeleton but once the Cdc4 ring has established actin is no longer required for the maintenance of the Cdc4 ring.

Interestingly, the localisation of Myo2 to the division site is dependent on the function of Cdc4 although accumulation of Cdc4 to the division site is independent of Myo2 (Naqvi et al., 1999). Myo2 has two IQ domains for myosin light chain binding (May et al., 1997). The first IQ domain of class II myosins typically binds the essential light chain whereas the second IQ domain binds the regulatory light chain. It has been shown that a point mutation that changes the conserved arginine to an alanine residue of the first IQ domain reduced the ability of Myo2 to bind to Cdc4 (Naqvi et

al., 1999). Thus, it appears that Cdc4 functions in a manner similar to myosin essential light chains and sequence analysis have indicated that Cdc4 has homology to these class of light chains (May et al., 1998). The second fission yeast class II myosin, Myp2, also contains two IQ domains (Bezanilla et al., 1997). It is possible that the observed association of Myp2 with Cdc4 is also mediated through the IQ domains (Motegi et al., 2000) although no mutational or biochemical studies have been carried out so far to confirm this.

Like Cdc4, the two class II myosins exhibit cytoplasmic localisation during interphase. During mitosis a ring of Myo2, which colocalises with actin, is observed and is seen to decrease in diameter as mitosis progressed (Kitayama et al., 1997). Similarly, a ring of Myp2 that exhibit similar dynamics to Myo2 is also observed during mitosis (Bezanilla et al., 1997). However, the localisation of Myo2 and Myp2 to the medial ring appear to be a sequential process since a Myo2 ring is observed at metaphase/anaphase A whereas the Myp2 ring forms much later, at the end of anaphase B (Bezanilla et al., 2000). Thus, at some point in mitosis the Myo2 and Myp2 rings are seen to colocalise (Motegi et al., 2000). The observation that both the Myo2 and Myp2 rings decreased in diameter and disappeared into a small dot can be seen to represent the contractile nature of the medial ring which serves to divide the parent cell into two daughter cells.

At present it is not clear why *S. pombe* should require two class II myosins for cytokinesis since budding yeast has a single class II myosin, Myo1, to achieve contraction of the actin ring (Bi et al., 1998). Interestingly, the slime mould, *Dictyostelium discoideum*, also has a single class II myosin and null mutants of myosin II are still able to divide in conditions in which cells are anchored to a substrate (for review see Gerisch and Weber, 2000). However, they fail to divide when cultured in suspension indicating that in *Dictyostelium*, cell separation can be driven by two mechanisms which have been termed Cytokinesis A which requires myosin II and Cytokinesis B which is cell adhesion dependent (Zang et al., 1997).

In fission yeast Myo2 appears to be the more important of the two class II myosins since *myo2Δ* mutants die as elongated cells with improperly formed actin rings (Kitayama et al., 1997; May et al., 1997). Null mutants of *myp2*$^+$, on the other hand, are viable but display cytokinetic defects when cells are exposed to stress (Bezanilla et al., 1997; Motegi et al., 1997) although Mulvihill et al. (2000) have reported that *myp2Δ* cells display cytokinetic defects even in normal conditions. Analysis of the actin rings of *myp2Δ* mutants show that the actin rings are improperly formed and appear as a broad band during cytokinesis (Motegi et al., 1997). When the *myp2Δ* mutation is in the genetic background of a temperature-sensitive mutation in *myo2*$^+$ (*myo2-E1*) the *myo2-E1 myp2Δ* double mutant displays an exaggerated cytokinetic defect as a result of its failure to form a functional actin ring (Bezanilla and Pollard, 2000; Motegi et al., 2000; Mulvihill et al., 2000). These results indicate that both class II myosins are important in organising or maintaining the integrity of the actin ring.

Another protein which is important for the assembly of the actin ring is the product of the *cdc12*$^+$ gene. Cdc12 is a multidomain protein that is a member of the formin family of proteins that have been implicated in cytokinesis and cell polarity (Chang et al., 1997). Deletion of *cdc12*$^+$ is lethal and cells die with up to four nuclei without forming an actin ring indicating that mitosis occurs in the absence of cytokinesis. Instead actin dots are concentrated in zones where the actin ring would have formed in mitotic *cdc12Δ* cells. In wild type cells Cdc12 localises as a thin, faint ring at the equator early in mitosis which becomes more intense during anaphase. After completion of anaphase the Cdc12 ring appears to contract to a single dot indicating that Cdc12 is part of the complex of proteins, that includes actin and myosin II, that is involved in the closure of the plasma membrane to separate the two daughter cells. Interestingly, Cdc12 is found as a discrete cytoplasmic spot in interphase (Chang, 1999). Moreover, the Cdc12 spot moves during interphase but relocates to the incipient site of cell division just before mitosis. During mitosis, however, the

intensity of the spot progressively decreases as the Cdc12 spot turns into a Cdc12 ring.

The product of the *rng2*$^+$ gene is also required for the organisation of the actin ring. Like Cdc12, Rng2 is a large multidomain protein that belongs to a family of proteins (IQGAPs) which has been found to be involved in cytokinesis (Eng et al., 1998). Rng2 most closely resembles the human IQGAP protein, IQGAP1 (Hart et al., 1996) but is less similar to the budding yeast IQGAP, Iqg1/Cyk1 (Epp and Chant, 1997; Lippincott and Li, 1998). Primary sequence analysis of Rng2 shows that it has a putative actin-binding domain; coiled-coil domains, six IQ motifs and a GAP domain. Deletion of *rng2*$^+$ is lethal and cells accumulate up to eight nuclei before they lyse (Eng et al., 1998). Interestingly, actin staining reveals the presence of a large actin spot in the region of the cell where the first actin ring would normally have formed. Temperature-sensitive mutants of *rng2*$^+$, however, exhibit medially placed actin cables that sometimes seem to originate from a spot. These cables fail to organise into a ring indicating that the primary defect of *rng2*$^-$ mutants is the inability to compose an actin ring from medially positioned actin cables. Localisation studies show that Rng2 is present on the spindle pole body throughout the entire cell cycle but also forms an equatorial ring early in mitosis. Like other contractile ring components the diameter of the ring decreases as cytokinesis proceeds.

Genetic screens have also uncovered another two *rng* genes (*rng3*$^+$ and *rng4*$^+$) which are also important for organising a medial actin ring (Balasubramanian et al., 1998). The product of the *rng3*$^+$ gene has been cloned, however, the molecular identity of the *rng4*$^+$ gene product has yet to be found. Sequence analysis of Rng3 indicates that it contains a motif known as the 'UCS' domain (Wong et al., 2000). Proteins which contain this motif have been reported to be required in processes that involve myosin and actin function. Interestingly, localisation studies have failed to detect Rng3 staining in wild type cells during any part of the cell cycle. However, Rng3 localises to the division site in the *myo2-E1* mutant but not in any other cytokinesis mutants

tested. These results led the authors to propose that Rng3 levels at the medial ring in wild type cells may be far below the limits of detection by fluorescence microscopy (Wong et al., 2000). However, in the *myo2-E1* mutant, Rng3 might accumulate at the division site as a consequence of the mutant's failure to form a functional medial ring. The fact that Rng3 is seen only in *myo2-E1* and not in any other cytokinesis mutants suggests that Rng3 detects a specific change in the medial ring of the *myo2-E1* mutant.

The medial ring of *S. pombe* is a complex of a number of proteins which requires the function of actin, myosin II, Cdc3, Cdc4, Cdc8, Cdc12, Rng2 and Rng3 for its organisation and stability. All of these proteins appear to be part of the medial ring itself with the possible exception of Cdc3 and Rng3. Cdc3 localises as a broad equatorial band in cells undergoing mitosis and has not been detected in any ring-like structure. The localisation of Rng3 to the medial ring is unclear since it has not been detected in wild type cells but is present at the division site in the *myo2-E1* mutant. The medial ring is formed early in mitosis and contracts after nuclear segregation to partition a complete set of chromosomes into each daughter cell. By analogy to mammalian cells, the presence of Myo2 and Myp2 at the medial ring suggests that ring contraction may be driven by the motor activity of class II myosins (Field et al., 1999). A mutant in *rng4*$^+$ also exhibit defects in actin ring organisation suggesting that the known inventory of medial ring components is still incomplete.

d. Medial Ring Contraction and Septation

Late in mitosis, at the end of anaphase, the assembled medial ring constricts and the division septum is formed. A group of genes, collectively referred to as the *sid* genes (for septum initiation defective), are thought to couple medial ring contraction and septum synthesis with the completion of mitosis (for review see Balasubramanian et al., 2000). The *sid* genes include *cdc7*$^+$, *cdc11*$^+$, *cdc14*$^+$, *sid1*$^+$, *sid2*$^+$, *sid4*$^+$ and *spg1*$^+$. Mutants in these genes display normal rearrangements in actin such as the assembly of an actin ring at mitosis and accumulation of actin patches at the cell poles during interphase. However, these mutants fail to undergo medial ring contraction and

septation indicating that the *sid* genes are required to activate this process. Moreover, *sid* mutants continue through the nuclear cycle and proceed with S and M phases in the absence of cell division. This results in the formation of highly elongated, multinucleate cells which eventually lyse.

Molecular analysis of the *sid* genes reveal that they encode three protein kinases, Cdc7, Sid1 and Sid2 (Fankhauser and Simanis, 1994; Sohrmann et al., 1998; Guertin et al., 2000; Sparks et al., 1999); a GTPase, Spg1 (Schmidt et al., 1997) and two novel proteins with no significant sequence similarity to any known proteins, Cdc14 and Sid4 (Fankhauser and Simanis, 1993; Chang and Gould, 2000). The identity of the protein encoded by the other *sid* gene, *cdc11*$^{+}$, is not yet known (Le Goff et al., 1999). It has been suggested that the product of the *sid* genes form an elaborate signal transduction network that regulates cell division and that the Spg1 GTPase is a key component in activating this signalling cascade (Guertin et al., 2000).

The nucleotide state of the Spg1 GTPase appears to be of critical importance in triggering medial ring contraction and septum synthesis (Schmidt et al., 1997). Spg1 exists in two forms during the cell cycle (Figure 1.10). During interphase it localises to the spindle pole body in an inactive GDP-bound form. Upon entry into mitosis, Spg1 is converted into its active GTP-bound state until anaphase, when conversion of Spg1-GTP to Spg1-GDP occurs at one of the two spindle poles (Sohrmann et al., 1998). Interestingly, the Cdc7 protein kinase shows no discrete localisation during interphase but early in mitosis it associates with both spindle poles until at a point in anaphase when it is seen at only one spindle pole body. Spg1 and Cdc7 have been shown to physically interact (Schmidt et al., 1997) and that Cdc7 preferentially associates with the active form of Spg1 (Sohrmann et al., 1998). Taken together, these results indicate that Spg1-GTP is the protein that recruits Cdc7 to the spindle poles from its cytoplasmic localisation during mitosis and that the asymmetric localisation of Cdc7 to only one of the two spindle poles at anaphase is a consequence of the asymmetric conversion of Spg1-GTP to Spg1-GDP at the spindle poles (Figure 1.10).

Conversion of Spg1 to its inactive form is mediated by a two component GTPase activating protein (GAP) consisting of Cdc16 and Byr4 (Furge et al., 1998). Absence of either protein promotes septum formation and mutants display a multiseptate phenotype (Fankhauser et al., 1993; Song et al., 1996) indicating that the Cdc16-Byr4 GAP negatively regulate Spg1 to inhibit septation. Biochemical analysis has shown that Cdc16 binds Byr4 but does not bind Spg1 or affect the nucleotide bound to Spg1 in the absence of Byr4. This has lead to the proposal that Cdc16 may be the catalytic subunit of the Cdc16-Byr4 GAP and that Byr4 may act to hold Spg1 and Cdc16 together to allow Cdc16 to activate GTP hydrolysis by Spg1 (Furge et al., 1998). Recently it has been shown that Byr4 has one binding site for Cdc16 and four binding sites for Spg1 (Furge et al., 1999). Localisation studies have revealed that Cdc16 and Byr4 are localised to the spindle pole body throughout interphase and disappear from the spindle poles early in mitosis (Cerutti and Simanis 1999; Li et al., 2000). During this early period of mitosis when discrete localisation of Cdc16 and Byr4 is no longer seen, Cdc7 is seen to be present at both spindle poles. However, during anaphase when Cdc7 disappears from one of the spindle poles, Cdc16 and Byr4 reappears at the spindle pole where Cdc7 is absent. Collectively, these results indicate that the localisation of the Cdc16-Byr4 GAP to the spindle poles is important in regulating the activity of Spg1 which in turn controls the localisation of Cdc7.

Spg1 is a member of the ras superfamily of GTPases, the activity of which are negatively regulated by GAPs (as discussed) and also by proteins, known as GEFs, which promote the active GTP form of GTPases by facilitating the exchange of GTP for GDP on the GTPase (Schmidt et al., 1997). Thus, the two different forms of GTPases are controlled by a balance of GAP and GEF activity. Genetic studies have shown that *cdc11*$^{-}$ mutants can be rescued by loss of function mutations in *cdc16*$^{-}$ (Marks et al., 1992) and that increased expression of *cdc7*$^{+}$ and *spg1*$^{+}$ rescue mutations in *cdc11*$^{+}$ (Fankhauser and Simanis, 1994; Schmidt et al., 1997). This has led to the proposal that Cdc11 may act as the GEF that activates Spg1 (Schmidt et al., 1997). Since localisation of Cdc7 to the spindle pole body depends on Spg1-GTP, the

recent finding that Cdc7 does not localise to the spindle poles in *cdc11*$^{-}$ mutants is consistent with the proposed function of Cdc11 as an activator of Spg1 (Guertin et al., 2000). Whether Cdc11 is the GEF for Spg1, or a regulator of it, awaits its molecular cloning and characterisation.

The reason for the asymmetric inactivation of Spg1 and therefore the asymmetric localisation of Cdc7 to the mitotic spindle poles is unclear. Asymmetric localisation of Cdc7 does not seem to be necessary for medial ring contraction and septum formation since Cdc7 remains at both spindles poles in *cdc16*$^{-}$ mutants that undergo repeated rounds of septation (Guertin et al., 2000). However, the observation that Cdc7 does not localise to the spindle poles in *spg1*$^{-}$ mutants that do not undergo septation indicate that localisation of Cdc7 to the spindle poles is important in triggering septation (Sohrmann et al., 1998).

Recently it has been shown that the localisation of Spg1, Cdc7 and Byr4 is dependent on the function of the *sid4*$^{+}$ gene product (Chang and Gould, 2000). In *sid4*$^{-}$ mutants these key regulators of the septation initiation pathway fail to localise at the spindle poles. Sid4 itself localises to the spindle poles at all stages of the cell cycle in wild type cells and in *sid* mutants indicating that localisation of Sid4 is independent of other Sid proteins. Biochemical analysis of Sid4 shows that it is a 76 kD protein which has an N-terminal domain that is important for spindle pole localisation and a C-terminal domain through which it associates with itself. Overproduction of an N-terminal truncated form of Sid4 acts as a dominant negative and prevents wild type Sid4 from localising at spindle poles. Interestingly, overproduction of the truncated form of Sid4 inhibits septation and cells fail to localise Spg1 at the spindle poles. These results indicate that Sid4 localisation at the spindle poles is a prerequisite for the execution of the Spg1 septation initiation pathway.

Localisation of the other *sid* gene product, Sid1, correlates with the localisation of Cdc7 (Guertin et al., 2000). During interphase Sid1 exhibits diffuse localisation,

however, during metaphase and early anaphase Sid1 localises to both spindle poles. As mitosis proceeds Sid1 disappears from one of the spindle poles and is seen on only one spindle pole body during late anaphase and telophase, prior to the appearance of the division septum. Colocalisation studies show that Sid1 and Cdc7 are present on the same spindle pole body during late mitosis. Localisation studies of Sid1 in *cdc7*$^-$, *cdc11*$^-$, *cdc14*$^-$, *sid2*$^-$, *sid4*$^-$ and *spg1*$^-$ mutants show that Sid1 does not localise to the spindle poles in these mutants with the exception of the *sid2*$^-$ mutant. This indicates that Sid1 functions upstream of Sid2 but downstream or parallel to other Sid proteins in the signalling cascade. Biochemical studies have shown that Sid1 displays a physical association with Cdc14. Moreover, Cdc14 colocalises with Sid1 and that localisation of Cdc14 to the spindle poles is disrupted in *sid1*$^-$ mutants. The fact that Sid1 and Cdc14 physically associate and depend on each other for their localisation indicates that Sid1 and Cdc14 may function together in the septation initiation pathway.

The function of Sid2 appears to be required late in the signalling cascade and seems to be downstream of other *sid* gene products, just after Sid1-Cdc14 (Guertin et al., 2000). Localisation studies show that Sid2 is present at the spindle poles at all stages of the cell cycle, including the two spindle poles during mitosis (Sparks et al., 1999). Interestingly, Sid2 also localises to the division site during medial ring contraction and septation. Localisation of Sid2 to the division site seems to require the function of the medial ring since Sid2 does not form an equatorial band in *cdc3*$^-$ mutants in which the medial ring is disrupted. Biochemical studies show that Sid2 is a protein kinase the activity of which peaks during medial ring contraction and septation. Furthermore, localisation of Sid2 to the division site and its kinase activity depend on the function of all other septation initiation genes: *cdc7*$^+$, *cdc11*$^+$, *cdc14*$^+$, *sid1*$^+$, *sid4*$^+$ and *spg1*$^+$.

From these results a model for the chain of events that occur to initiate septation has been proposed (Balasubramanian et al., 2000) (Figure 1.11). Central to the model is the nucleotide state of the Spg1 GTPase. During interphase Spg1 is maintained in the

inactive GDP-bound form by the activity of a two component GAP comprised of Cdc16-Byr4. The activity of Cdc16-Byr4 is balanced by Cdc11, a potential GTP/GDP exchange factor (GEF) which converts Spg1 to its active GTP-bound form. At the onset of mitosis the Cdc16-Byr4 GAP disappears from the spindle poles which enables Spg1 to become activated. Activation of Spg1 causes Cdc7 to be recruited to the spindle poles. The presence of Cdc7 at the spindle poles initiates the localisation of Sid1-Cdc14. Sid2 which is constitutively localised at the spindle poles throughout the cell cycle becomes activated with the localisation of Sid1-Cdc14. The process of medial ring contraction and septum synthesis is then triggered following the localisation of Sid2 to the division site.

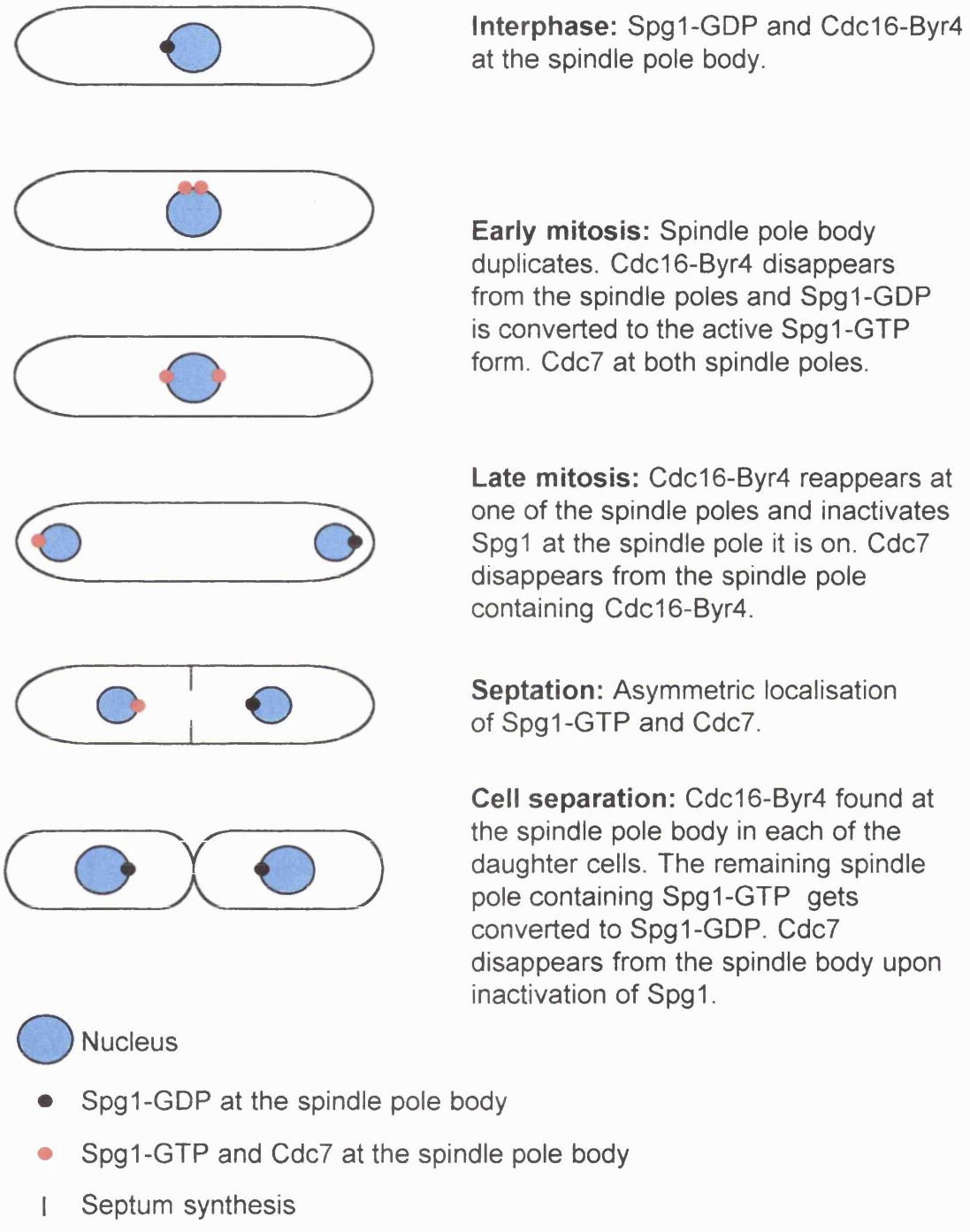

Figure 1.10 Localisation of Spg1 and Cdc7 in Fission Yeast

Spg1-GTP and Cdc7 localises asymmetrically at the spindle poles during mitosis. The cell cycle begins at the top and progresses down the page. See text for details.

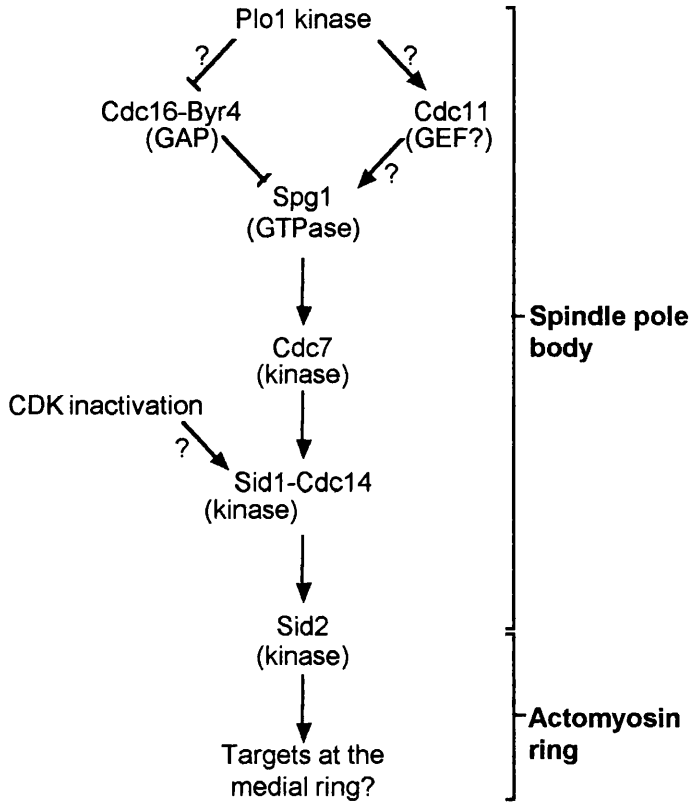

Figure 1.11 The Sid Pathway

The Sid pathway regulates the timing of actomyosin ring contraction and septum assembly in response to signals originating from the spindle pole body following mitotic exit. Figure reproduced from Balasubramanian et al. (2000).

1.4 OBJECTIVES OF THIS THESIS

This thesis describes the identification and characterisation of two class V myosins (Myo51 and Myo52) in the fission yeast, *Schizosaccharomyces pombe*. As this is the first characterisation of Myo51 and Myo52, I will show justifications in placing these proteins in the class V group of the myosin superfamily (Chapter 3). In Chapter 4, I present the phenotypes of *myo51Δ* and *myo52Δ* cells and show that one of them (*myo52Δ*) exhibits defects in cell morphology. The effects of Myo51 and Myo52 overproduction in wild type cells is shown in Chapter 5. In Chapter 6, I present the initial localisation of Myo51 in fission yeast. A detailed analysis of the localisation of Myo52 is also presented showing that Myo52 localises to sites of cell wall deposition. The functional relationship between Myo52 and cell wall synthesis is presented in Chapter 7. Finally, I discuss the roles of Myo51 and Myo52 in Chapter 8 and show that they have distinct functions in *S. pombe*.

Chapter 2
Materials and Methods

2.1 Identification and Analysis of Myosin Sequences

Myosin sequences were identified by searching the Sanger Centre Fission Yeast Genome Sequencing Project (www.sanger.ac.uk/Projects/S_pombe) for proteins containing the myosin GESGAGKT motif. Protein sequences were analysed using DNASTAR software (DNASTAR Inc., Wisconsin, USA) or by using the package of programs available at Swiss-Prot (www.expasy.ch/sprot/sprot-top.html). Phylogenetic analysis of protein sequences were performed using Phylip computer software (http://evolumeution.genetics.washington.edu/phylip.html).

2.2 Chemicals

All chemicals were purchased from Sigma or BDH unless otherwise indicated. All media reagents were purchased from Difco.

2.3 Strains and Media

The *E. coli* strains JA226 (*recBC leuB6 trpE5 HsdR⁻ HsdM⁺ lacY* E600, a gift from P. Fantes) or DH5α (*supE44 Δlac* U169 *hsdR17 recA1 endA1 gyrA96 thi-1 relA1*, a gift from J. Millar) were used in bacterial plasmid transformation reactions. These strains were maintained on Luria-Bertani (LB) medium (10 g/l bactotryptone, 10 g/l NaCl, 5 g/l yeast extract) prior to transformation. Ampicillin (100 μg/ml) was supplemented to the LB medium to select for and maintain transformants.

All *Schizosaccharomyces pombe* strains used in this study were derived from those listed in Table 2.1. Fission yeast strains without plasmids were maintained on supplemented yeast extract (YES) (5 g/l yeast extract and 30 g/l glucose supplemented with 75 mg/l adenine). Fission yeast strains used for gene replacement and plasmid transformations were selected on minimal medium (MM) (3 g/l KH phthalate, 2.2 g/l Na_2HPO_4, 5 g/l NH_4Cl, 20 g/l glucose) containing 10,000X minerals stock, 1000X vitamins stock (Alfa et al., 1993) and supplemented with 75 mg/l adenine, leucine or uracil as required. In strains containing the pREP series of plasmids repression of the *nmt1*$^+$ promoter was achieved by the addition of 7.5 μg/ml thiamine.

Solid media was made by the addition of 20 g/l agar.

Table 2.1 *S. pombe* strains used in this study.

Genotype	Source
972 h⁻	P. Nurse
ade6-210 leu1-32 ura4-D18 h⁻ / ade6-216 leu1-32 ura4-D18 h⁺	P. Fantes
ade6-210 leu1-32 ura4-D18 h⁻	P. Fantes
ade6-216 leu1-32 ura4-D18 h⁺	P. Fantes
myp2::ura4⁺ ade6-210 leu1-32 ura4-D18 h⁺	T. Win
myo51::ura4⁺ ade6-210 leu1-32 ura4-D18 h⁻ /ade6-216 leu1-32 ura4-D18 h⁺	This study
myo51::ura4⁺ ade6-216 leu1-32 ura4-D18 h⁺	This study
myo52::ura4⁺ ade6-210 leu1-32 ura4-D18 h⁻ /ade6-216 leu1-32 ura4-D18 h⁺	This study
myo52::ura4⁺ ade6-216 leu1-32 ura4-D18 h⁻	This study
myo52::ura4⁺ ade6-216 leu1-32 ura4-D18 h⁺	This study
myo52-GFPS65T ade6-210 leu1-32 ura4-D18 h⁻	This study
cam1-E14 ade1-D25 ade6-210 leu1-32 ura4D18 h⁻	T. Davis
cps8⁻ ura4-D18 h⁻	J. Ishiguro
cps8⁻ leu1-32 h⁺	J. Ishiguro
tea1-3 leu1-32 h⁻	P. Nurse
mok1-664 leu1-32 h⁻	T. Toda
pck2::LEU2 leu1-32 h⁻	T. Toda
pck2-8 leu1-32 h⁻	T. Toda
spg1-B8 ura4-D18 h⁻	V. Simanis
cdc3-6 ura4-D18 h⁻	V. Simanis
cdc4-8 ura4-D18 h⁻	V. Simanis
cdc7-24 ura4-D18 h⁻	V. Simanis
cdc8-110 ura4-D18 h⁻	V. Simanis
cdc16-116 ura4-D18 h⁻	V. Simanis
cdc25-22 leu1-32 h⁻	P. Fantes

2.4 Plasmids

The modified plasmids pSL1180 and pSL1180-*ura4*$^+$ (kind gifts from T. Chappell) were used for subcloning and gene replacement experiments. The TOPO II plasmid (Invitrogen) was used as a vector to maintain amplified PCR products. For gene expression in fission yeast the plasmids pREP1 (a gift from P. Nurse; Maundrell, 1990; Basi et al., 1993) and pREP41myc (a gift from I. Hagan; Craven et al., 1998) carrying the repressible *nmt1*$^+$ promoter were used. Overexpression of *spg1*$^+$ was

carried out using pREP41-*spg1*$^+$ (a gift from V. Simanis; Schmidt et al., 1997). The GFP coding sequence from pGEM-GFP plasmid (a gift from I. Hagan; Craven et al., 1998) was used to create pREP41GFP-*myo52*$^+$ whereas the pFA6a-GFP(S65T)-kanMX6 plasmid (a gift from J. Bahler; Bahler et al., 1998) was used as a PCR template to amplify a GFP integration module which was targeted at the 3' end of the *myo52*$^+$ chromosomal locus.

2.5 Oligonucleotides

The oligonucleotides used in this study were synthesised by Perkin-Elmer and are listed in Tables 2.2 and 2.3.

Table 2.2 Oligonucleotides used to delete *myo51*$^+$ (c2D10) and *myo52*$^+$ (c1919). Engineered restriction sites are underlined.

Name	Sequence (5' ⇒ 3')	Restriction site
c2D10-ApaI-up	CTTCGTGGGCCCGGAGGCTCTCACAG	ApaI
c2D10-AscI-up	GAAGGCGCGCCTGATTGACCGATGTTTC	AscI
c2D10-AscI-down	ATCGGCGCGCCTGATGAGAACACAACAC	AscI
c2D10-PstI-down	TGCTTTCCTGCAGTTACTATATGATGCTTTGA	PstI
c1919-ApaI-up	ATTATAGGGCCCAAGGAAAGCTCACCGCA	ApaI
c1919-AscI-up	AACGGCGCGCCGTTTCTTCCTTCATAATTT	AscI
c1919-AscI-down	AGTGGCGCGCCGGAAGCTTATTTGCAGCT	AscI
c1919-PstI-down	GCTAACGCTGCAGGAGACTTCGTACTTCAAT	PstI

Table 2.3 Oligonucleotides used to overexpress and tag *myo51*$^+$ (c2D10) and *myo52*$^+$ (c1919). Engineered restriction sites are underlined.

Name	Sequence (5' ⇒ 3')	Restriction site
c2D10-start	AATTAAAGTCGACTATGAGTCATGCAAGATTAC	SalI
c2D10-end	ATATGGATCCGGTGTAACGTTTAATGATACTTG	BamHI
c1919-start	AATTTCTGTCGACCATGACATCGGGGATTTATTAC	SalI
c1919-end	TTAAAACGTCGACGGAAACTAAGGCCCAGCTCC	SalI
myo52C-forward	TCACTGTAGGCAACGTAGCCGACAATGATGTACAG AACTCGAGCGACGAAGAAAATCAAGTACCAAATGG TATTAAAGTTCGGATCCCCGGGTTAATTAA	None
myo52C-reverse	AGCTCCAAATTTTGAAAGTAAAACCCCTAATTAGG GAATAAATAAGTAGGCAGAGCACCTTGAAAAATAA CTAGATATTAGAATTCGAGCTCGTTTAAAC	None

2.6 Preparation of Yeast Genomic DNA

Fission yeast cells were grown in 20 ml of YES medium overnight at 25°C or 29°C until saturation in a shaking incubator at 150 rpm. The culture was harvested bycentrifugation at 3,000 rpm for 5 min. The pellet was resuspended in 1 ml SP1 solution (1.2 M sorbitol, 50 mM sodium citrate, 50 mM sodium phosphate, 40 mM EDTA) containing 3 mg/ml Zymolyase-20T (ICN) and incubated at 37°C for 60 min to digest the cell walls. The spheroplasts were microfuged and resuspended in 0.5 ml 5X TE (50 mM Tris.HCl pH 8.0, 20 mM EDTA) after which they were lysed by the addition of 50 µl 10% SDS. The sample was left to incubate at 65°C for 20 min. After incubation, 200 µl 5M potassium acetate was added to the suspension and left on ice for 30 min. The tube contents were then spun in a microfuge at 13,000 rpm and the supernatant containing the genomic DNA was transferred into a clean Eppendorf tube. The supernatant was extracted with 400 µl phenol:chloroform to remove any contaminating protein. The aqueous phase was transferred into another Eppendorf

tube which was subsequently filled with 100% ethanol and left at -20°C for 30 min to precipitate the genomic DNA. The tube was spun and the supernatant removed, following which the DNA pellet was left to air dry. The DNA pellet was resuspended in 300 µl TE (10 mM Tris.HCl pH 8.0, 1 mM EDTA) and left to dissolve overnight at room temperature. To remove contaminating RNA 50 µl 1 mg/ml RNase A was added to the DNA solution and left to incubate at 37°C for 60 min. The DNA solution was then precipitated with the addition of 0.5 ml isopropanol and spun in a microfuge. The DNA pellet was washed with 70% ethanol and resuspended in 100 µl TE. The purity and quantity of genomic DNA obtained was determined by running a 5 µl sample on a 0.7% agarose gel.

2.7 Polymerase Chain Reaction (PCR)

All polymerase chain reactions (PCRs) were performed using the Expand High Fidelity PCR System (Boehringer Mannheim) using the manufacturer's recommended conditions. Wild type (*972 h⁻*) genomic DNA was used as template unless otherwise indicated. Each PCR was carried out in a final volume of 50 µl containing 2-10 ng of template DNA, 300 nM of forward and reverse primers, 200 µM of dATP, dCTP, dGTP and dTTP nucleotides (Pharmacia) in Expand HF buffer and Expand HF enzyme mix (2.6 units). Thermal cycling was performed using a Techne Progene thermocycler. In all PCRs template DNA was initially denatured at 94°C for 2 min. This was followed by the main cycling protocol which consisted of 20 to 30 cycles of the following regime: template denaturation at 94°C for 15-30 sec, primer annealing at 50-65°C (depending on the primers used) for 1 min and DNA synthesis at 68°C for 1-8 min (depending on the length of DNA being amplified). A final extension phase at 68°C for 5-10 min was used to complete a PCR. The yield of PCR product obtained was checked by running a 2 µl sample on a 1% agarose gel.

To amplify the GFP integration module for C-terminal tagging of Myo52 the PCR conditions described above were modified such that 0.1 µg of pFA6a-GFP(S65T)-

kanMX6 plasmid was used as template DNA and the PCR performed in a final volume of 100 µl.

2.8 Phenol:Chloroform Extraction of DNA

Contaminating proteins were removed from DNA solutions by the addition of an equal volume of phenol:chloroform (1:1). The organic and aqueous mixture was separated into two phases by centrifugation at 13,000 rpm for 10 min. The upper aqueous phase containing the purified DNA solution was transferred into a clean Eppendorf tube.

2.9 Ethanol Precipitation of DNA

DNA was precipitated from aqueous solutions by adding 0.1 volume 3M sodium acetate (pH 5.2) to the DNA solution to be precipitated. This was followed by the addition of two volumes of –20°C ethanol. The entire mixture was then kept at -20°C for at least 30 min. Precipitated DNA was pelleted by centrifugation at 13,000 rpm for 10 min. The pellet was washed with 1 ml of 70% ethanol and left to air dry, after which the DNA pellet was dissolved in an appropriate volume of TE.

2.10 Restriction Digest Analysis

DNA was cut using restriction enzymes from New England Biolabs or Gibco BRL. DNA restriction was performed using the supplied buffers and the manufacturers' recommended conditions. To avoid 'star activity' (DNA restriction at non-canonical sites), the glycerol concentration was never allowed to be more than 5% (v/v) in each reaction. After most reactions the digests were placed in a 65°C water bath for 10 min to heat inactivate the restriction enzyme.

2.11 Dephosphorylation of Plasmid DNA

Following restriction enzyme digestion plasmid DNA was treated with calf intestinal alkaline phosphatase (New England Biolabs) to remove the 5' phosphate groups thus preventing it from self-ligating in ligation reactions. This was done by adding 1 unit of

the phosphatase directly into the restriction digest. Dephosphorylation was carried out at 37°C for 15 min after which the DNA was electrophoresed through an agarose gel for purification.

2.12 Agarose Gel Electrophoresis

DNA was separated according to size through agarose gels. The DNA to be electrophoresed was mixed with 0.5 volume FOG loading buffer (15% (w/v) Ficoll, 0.25% (w/v) Orange G) prior to loading into agarose gels. Electrophoresis was carried out either at 10 mA overnight or 40 mA for 2 hr to ensure good separation of DNA. A 1 kb DNA ladder (Gibco BRL) or λ DNA (Boehringer Mannheim) cut with HinDIII and HinDIII/EcoRI were used as DNA size markers. DNA was visualised by illumination with ultraviolet light (302 nm). As well as separating DNA, agarose gel electrophoresis was also used to estimate the quantity of DNA in a sample as judged by the intensity of fluorescence emitted when illuminated with ultraviolet light.

2.13 Recovery of DNA Fragments from Agarose Gels

The required DNA fragment was excised from the rest of the gel using a clean razor blade with minimal exposure to ultraviolet light. The DNA was purified from the gel piece using the GENECLEAN II kit (Bio 101, Anachem) following the recommended procedure. The amount of DNA recovered was checked by running a sample through an agarose gel.

2.14 Ligations

Ligations were performed on gel-purified vector and insert DNA following the GENECLEAN II DNA purification process. Ligations were adjusted such that the ratio of vector:insert was 1:5. Ligations were carried out in a 20 µl reaction volume using 5 units of T4 ligase (New England Biolabs) and the supplied ligase buffer, at 16°C overnight. Control ligations were also carried out; these included a vector only reaction to determine the background of uncut or religated vector and an insert only ligation to show that no contaminating vector was present.

2.15 Transformation of *E. coli*

A colony of *E. coli* JA226 or DH5α cells that had grown overnight on LB medium was inoculated into 20 ml SOB (20 g/l bactotryptone, 5 g/l yeast extract, 0.5 g/l NaCl, 0.2 g/l KCl, 10 mM $MgCl_2$). Cells were incubated at 37°C for approximately 4 hr until a density of $OD_{650} = 0.45$ was obtained. Cells were then spun at 3,000 rpm for 10 min and the pellet washed in 7 ml of ice-cold TFB (10 mM MES pH 6.2, 100 mM KCl, 45 mM $MnCl_2$, 10 mM $CaCl_2$, 3 mM hexamine cobalt chloride). Cells were spun once more and resuspended in 1.6 ml cold TFB after which 56 µl of DMSO was added. Cells were left to incubate on ice for 5 min. This was followed by the addition of 56 µl 1 M DTT and a further incubation of 10 min. A second aliquot of 56 µl DMSO was added and the cells incubated for a further 5 min. At this stage the cells were competent to receive DNA and 200 µl of competent cells were aliquoted out for each plasmid transformation. To each 200 µl aliquot of competent cells 8 µl of plasmid DNA from a ligation reaction was added and incubated on ice for 30 min. To determine the efficiency of transformation 0.1 ng of pGEX2T plasmid DNA (Pharmacia) was also added to an aliquot of competent cells as a positive control. Cells were heat shocked at 42°C for 90 sec after which they were put back on ice for 2 min. To each transformation 800 µl of SOC (SOB containing 20 mM glucose) was added and the cells left to recover in a shaking incubator at 37°C for 1 hr. Cells were spread onto LB medium containing 100 µg/ml ampicillin and incubated at 37°C overnight to select for transformants.

2.16 Recovery of Plasmid DNA from *E. coli*

Plasmid DNA was recovered from *E. coli* by inoculating a single colony from a transformation plate or from cells woken up from a freezer stock into 10 ml of LB containing ampicillin. Cells were incubated overnight at 37°C. Plasmid DNA was then recovered from these cells by either using the QIAprep Spin Miniprep kit (Quiagen) or by using the procedure outlined below.

Into an Eppedorf tube 1 ml of overnight culture was added and spun at 13,000 rpm. The pellet of cells was resuspended in 150 µl of P1 solution (50 mM Tris.HCl pH 8.0, 10 mM EDTA) containing 0.1 µg/µl RNase A. The cell suspension was then lysed with the addition of 150 µl P2 solution (200 mM NaOH, 1% SDS) and the tube contents mixed by inversion. The lysis reaction was neutralised by the addition of 150 µl P3 solution (2.55 M KAc pH 4.8). At this point cellular debris precipitated out of solution which was removed by the addition of 350 µl phenol:chloroform and centrifugation of the tube at 13,000 rpm for 10 min. The upper aqueous layer containing plasmid DNA was transferred into a clean Eppendorf tube and purified by ethanol precipitation. The precipitated DNA was dissolved in 30 µl of TE.

2.17 Transformation of *S. pombe*

Two lithium acetate transformation methods were used to transform *S. pombe*. The first, described below, was a simple and quick procedure used to transform plasmid DNA into *S. pombe* or to integrate linear fragments of DNA to delete genes. The second method was a modified and more efficient version of the first which was used to integrate a GFP module at the 3' end of the *myo52*$^{+}$ locus.

a. Method 1

S. pombe cells were grown at 25°C or 29°C overnight in 50 ml YES medium until they were at a density of 5 x 10^6 cells/ml. Cells were spun at 3,000 rpm for 10 min and the resulting pellet was washed with 20 ml sterile distilled water. The cells were spun again and the pellet washed with 20 ml TE. After a final spin the cells were resuspended in 450 µl TE after which 50 µl of 1 M lithium acetate (pH 8.4) was added. The cell suspension was distributed into 45 µl aliquots into Eppendorf tubes for each plasmid or DNA fragment to be transformed. To each aliquot of competent *S. pombe* cells approximately 0.5 µg of DNA and 240 µl of 50% PEG 3350 was added. The mixture was vortexed to obtain an even cell suspension and incubated at room temperature for 30 min. Following this the cells were heat shocked at 42°C for 15 min

and spun at 3,000 rpm for 2 min. The supernatant was removed and the pellet resuspended in 200 µl sterile distilled water. The entire cell suspension was then spread onto minimal medium plates containing appropriate supplements. Transformation plates were left to incubate at either 25°C or 29°C until colonies were observed (usually 5 days).

b. Method 2

This method was used only on one occasion when integration of a GFP module into wild type *S. pombe* at the 3' end of the *myo52*$^{+}$ locus was not achieved by other transformation methods. Wild type *S. pombe* cells were grown in 50 ml YES at 25°C overnight until a density of 5 x 10^6 cells/ml was obtained. From this a 20 ml aliquot was taken and spun at 3,000 rpm for 10 min. The resulting pellet was resuspended in 1 ml sterile distilled water and transferred into a Eppendorf tube. The cells were spun at 3,000 rpm for 2 min and the pellet washed with 0.1 M lithium acetate (pH 4.9). The washed cells were spun again before being finally resuspended in 300 µl of 0.1 M lithium acetate. A 50 µl aliquot of the cell suspension was transferred into a clean microfuge tube which was followed by the addition of 240 µl 50% PEG 3350, 36 ul 1 M lithium acetate (pH 8.4), 25 µl 10 mg/ml denatured salmon sperm DNA stock and 15 µg of the integrating DNA module. The tube contents were mixed and incubated at room temperature for 30 min and then heat shocked for 20 min at 42°C. Cells were spun at 3,000 rpm for 2 min and resuspended in 200 µl of sterile distilled water. The entire cell suspension was spread onto a YES plate and incubated at 29°C overnight. Cells were replica plated onto a YES plate supplemented with Geneticin (Life Technologies) at a concentration of 100 mg/l to select for transformants containing the GFP module which confers resistance to Geneticin. This plate was incubated at 29°C for 2 days until colonies were observed. To check for stable integrants each colony was streaked onto another YES plate supplemented with Geneticin.

2.18 Southern Hybridisation Analysis of Genomic DNA

a. Preparation of Samples

Approximately 2 µg of genomic DNA was digested with 20 units of the appropriate restriction enzyme and incubated at 37°C overnight. A further 20 units of restriction enzyme was added the next day and incubated for 2 more hr to complete the digestion. The digested DNA was electrophoresed in a large (15 cm x 13 cm) 0.7% agarose gel at 100 mA for 6 hr. A photograph of the gel with a ruler was taken as a reference.

b. Southern Transfer

Following electrophoresis and photography the gel was rinsed briefly in distilled water. The Southern blot apparatus (Bios Corporation, USA) was set up by covering the platform with two sheets of 3MM CHR chromatography paper (Whatman) such that it extended beyond the platform and into the reservoir containing 0.4 M NaOH. The gel was placed on the centre of the platform and wetted with 0.4 M NaOH. Hybond-N+ membrane (Amersham) cut to the same size as the gel was placed on top of the gel and any air bubbles were rolled out with a plastic pipette. Two pieces of 3MM CHR chromatography paper cut to the same size as the gel were placed on top of the membrane which was then covered with a stack of green paper hand towels. The weighted lid of the Southern blot apparatus was placed on top of the stack and the DNA left to transfer onto the membrane overnight. After transfer the membrane was briefly rinsed in distilled water and then baked in an oven at 80°C for 1 hr to fix the DNA onto the membrane.

c. Preparation of the Hybridisation Probe

A 550 bp fragment from the *ura4*$^+$ gene was used as a probe. This was labeled with α-^{32}P-CTP (10 µCi/µl, Amersham) using the Prime-It II random primer labeling kit (Stratagene) according to the manufacturer's instructions. The labeled probe was denatured by boiling for 5 min just prior to hybridisation of the membrane.

d. Hybridisation of DNA

The membrane was pre-incubated in 70 ml of hybridisation solution (5X SSPE (750 mM NaCl, 45 mM NaH_2PO_4, 20 mM EDTA, pH 7.4), 5X Denhardt's solution (50X stock solution: 2.5 g/l Ficoll, 2.5 g/l polyvinylpyrrolidone, 2.5 g/l BSA), 0.5% SDS) and incubated in a hybridisation oven (Hybaid) at 65°C for 1 hr in a Hybaid hybridisation tube. The solution was removed and 30 ml of hybridisation solution containing the denatured labeled probe was added. The membrane was left to incubate with the probe in the hybridisation oven at 65°C overnight. The hybridisation solution was then removed and the membrane was washed twice in 50 ml of 2X SSC (300 mM NaCl, 30 mM sodium citrate, pH 7.0) with each wash lasting for 15 min. This was followed by a 20 min wash with 50 ml of 2X SSC containing 1% SDS and two 15 min washes with 50 ml of 0.1X SSC. The membrane was then covered in thin plastic (Saran wrap) and exposed to Bio Max film (Kodak) in a light-proof cassette at -70°C overnight after which the film was developed.

2.19 Re-isolation of Yeast Strains

Yeast strains were stored as frozen glycerol stocks at -70°C and were re-isolated by streaking some of the stock onto a YES or minimal medium plate with the appropriate supplements. Depending on the strain re-isolated, the plate was incubated at 25°C, 29°C or 36°C for 3-5 days until colonies appeared. The auxotrophy of the strain was determined by streaking a single colony onto minimal medium lacking the required supplement for each auxotrophic marker being tested. Temperature-sensitivity and cold-sensitivity of strains were determined by growth at the appropriate temperature.

2.20 Measuring Cell Concentration

The cell concentration of a yeast culture was measured by taking a 10 µl sample and placing it in the square grid of an Improved Neubauer haemocytometer. Cells were observed with phase contrast optics at X400 magnification using an Olympus light microscope.

2.21 Mating Cells

This was performed to determine the mating type of a strain by crossing to a strain of known mating type or to create a strain with the desired genotype by classical genetic methods. Cells were conjugated on malt extract (ME) medium (30 g/l malt extract, 20 g/l agar) by mixing a loopful of each of the two strains with 10 µl sterile distilled water. The plate was then incubated at 25°C or 29°C for 2-3 days after which a sample was observed under the microscope for the presence of zygotes and asci.

2.22 Yeast Classical Genetics

a. Tetrad Analysis

Tetrads were dissected from 2-3 day old mating mixes on ME or from diploid cells sporulated on minimal medium. A small loopful of sporulated cells was spread thinly over one side of a YES plate. Using a Singer MSM micromanipulator individual asci were picked with a glass needle and placed in another area of the YES plate away from the initial streak. After several asci were picked the plate was incubated at 25°C or 29°C for 4-7 hr to allow the asci walls to break down and release the tetrad of spores. Individual spores were then separated and placed in an ordered array. After tetrad dissection the plate was incubated at 25°C or 29°C until colonies appeared (usually 5-7 days).

b. Random Spore Analysis

A loopful of mating mix was inoculated into 500 µl of sterile distilled water into which 2.5 µl of β-glucuronidase (Sigma) was added to digest the cell walls of asci and vegetative cells. The mixture was incubated at 29°C or 36°C overnight after which the enzyme was removed by washing the released spores three times in sterile distilled water. The spore concentration was estimated using an Improved Neubauer haemocytometer and approximately 200 spores were spread onto an appropriate agar plate. Plates were incubated at 25°C or 29°C until colonies appeared.

2.23 Overexpression of Genes

Genes were overexpressed from the pREP series of plasmids which carry the thiamine-repressible *nmt1*$^+$ promoter. Fission yeast strains bearing the required plasmid were maintained in 10 ml of supplemented minimal medium containing 7.5 μg/ml thiamine at 25°C or 29°C. De-repression of the *nmt1*$^+$ promoter was achieved by removing the thiamine from the growth medium which was carried out by washing the cells three times in 10 ml of minimal medium. An appropriate volume of the cell suspension was inoculated into flasks containing 50-100 ml supplemented minimal medium without thiamine such that following overnight incubation in a shaking water bath at 25°C or 29°C the cell density was between 1-5 x 10^6 cells/ml.

2.24 Treatment with Actin- and Microtubule-Depolymerising Drugs

The fission yeast actin cytoskeleton was depolymerised by treating cells for 5 min with a final concentration of either 10 μM latrunculin B (Molecular Probes) or 5 μg/ml cytochalasin A (Sigma) at room temperature. To depolymerise microtubules cells were treated for 1 hr with 300 μg/ml thiabendazole (Sigma) at 25°C. For both actin- and microtubule-depolymerisation DMSO alone (1%) was used as the control.

2.25 Cell Fixation

Two methods were used to fix cells: methanol fixation or formaldehyde-glutaraldehyde fixation (Hagan and Hyams, 1988). A particular method was chosen for its ability to best preserve the cell structure being examined.

a. Methanol Fixation

A sample of fission yeast culture was taken and transferred into a 50 ml Falcon tube and centrifuged at 3,000 rpm for 5-10 min. The growth medium was then removed and the pellet of cells was resuspended in 5-20 ml of -70°C methanol and left for at least 8 min. The fixed cells were then washed twice with PEM (100 mM PIPES, 1 mM EGTA, 1 mM $MgSO_4$, pH 6.9) before being resuspended in an appropriate volume of PEM.

b. Formaldehyde-Glutaraldehyde Fixation

To 50 ml of yeast culture 5 ml of 37% freshly prepared formaldehyde was added, followed by the addition of 100 µl of 25% glutaraldehyde. Cells were left to fix at 25°C for 1 hr in a shaking water bath, after which they were transferred into a 50 ml Falcon tube. Cells were then spun at 3,000 rpm for 5-10 min and washed with 20 ml PEM. This was repeated twice before a final resuspension in an appropriate volume of PEM.

2.26 Nuclear Staining with DAPI

A 10 µl volume of methanol fixed cell suspension in PEM was smeared onto a glass microscope slide and dried with a hair dryer. A 1-2 µl drop of DAPI mounting medium (0.01 mg/ml DAPI, 10 mg/ml *p*-phenylenediamine) was placed on the smear. A cover slip was then placed on the DAPI mounting medium such that it spread evenly over the smear of cells. The edges of the cover slip were then sealed with clear nail varnish.

2.27 Cell Wall Staining with Calcofluor

A 500 µl sample of methanol fixed cells in PEM was mixed with 2 µl of 5 mg/ml Calcofluor stock. The cell suspension was incubated at room temperature for 5 min after which the excess Calcofluor was removed by two washes with 1 ml PEM. Cells were resuspended in a small volume of PEM, 10 µl of which was mounted onto a glass slide with DAPI mounting medium as described previously.

2.28 Localisation of Specific Proteins by Immunofluorescence Microscopy

Cells fixed by the methanol fixation method or following fixation with formaldehyde-glutaraldehyde were spun at 3,000 rpm for 5-10 min and resuspended in 5 ml PEMS (PEM containing 1M sorbitol) containing 5 mg lysing enzyme (Sigma) and 1.5 mg Zymolyase-20T (ICN). The suspension was incubated at 37°C for 5-10 min to digest the cell walls. Digestion was stopped by filling the tube with PEMS and centrifugation at 3,000 rpm for 5 min. The supernatant was removed and the cells

washed three times in PEMS, after which the pellet was resuspended in 10 ml 1% Triton X-100 in PEM and incubated at room temperature for 30 sec. This was followed by three washes in PEMS. The pellet was then resuspended in 5 ml of PEMBAL (PEM with 1% BSA, 0.1% sodium azide and 0.1 M L-lysine) and incubated for at least 30 min at room temperature. A 1 ml sample of the cell suspension was transferred into an Eppendorf tube for each protein being localised. The cell suspension was spun at 3,000 rpm for 1 min and the pellet resuspended in 30-100 µl of PEMBAL containing the primary antibody at an appropriate dilution. The primary antibodies used for immunofluoresence and their working dilutions are listed in Table 2.4. Following overnight incubation with primary antibody the cell suspension was washed three times with 1 ml PEMBAL. Depending on the primary antibody used the pellet was resuspended in 30-100 µl of PEMBAL containing either rhodamine-conjugated anti-mouse or anti-rabbit (Sigma) or fluorescein-conjugated anti-mouse (Vector Laboratories) secondary antibody. All of the secondary antibodies were used at a dilution of 1:100 and were incubated at room temperature in the dark for at least 4 hr. After incubation the cells were washed three times with 1 ml of PEMBAL before being resuspended in 30-100 µl of PEMBAL. A 10 µl sample of the cell suspension was smeared onto a glass slide and dried with a hair dryer after which it was mounted with 1 µl of DAPI mounting medium.

Table 2.4 Primary antibodies used for immunofluorescence.

Antibody	Origin	Dilution	Source
N-350 anti-actin	mouse	1:100	Amersham
TAT1 anti-tubulin	mouse	1:100	a gift from K. Gull
9E10 anti-myc	mouse	1:100	a gift from N. Pringle
Anti-mok1	rabbit	1:10	a gift from T. Toda

2.29 Microscopy and Photography

Cells were viewed with a Zeiss Axiophot photomicroscope fitted with epifluorescence optics using a planachromat 63X 1.25 NA Neofluor objective. Nuclei and cell wall staining were observed using the DAPI filter whilst other cell structures

were observed using the rhodamine or FITC filter. Images were captured with a Hamamatsu digital camera and analysed using OpenLab computer software (Improvision Ltd., Coventry, UK).

2.30 Zymolyase Cell Wall Digestion Assay

To test the sensitivity of fission yeast cell walls to the enzyme Zymolyase, cells were grown in YES medium at 25°C to exponential phase and centrifuged to obtain a pellet of 1 x 10^7 cells. The pellet was resuspended in 1 ml 300 μg/ml Zymolyase-20T (ICN) solution and incubated at room temperature. The change in optical density (OD_{600}) with time was used as a measure of the progress of cell wall digestion. The viability of Zymolyase-digested cells was also quantified by plating out approximately 1500 cells onto YES plates in duplicate. Plates were incubated at 25°C for 4 days before they were scored for colonies.

2.31 Immunoblot Analysis of Proteins

a. Protein Extraction

Fission yeast cells were grown in 50 ml YES at 25°C to mid-exponential phase after which they were spun at 3,000 rpm for 10 min. The cell pellet was resuspended in 4 M urea containing 5 mM Tris pH6.8 in a microfuge tube. The cells were smashed by filling the tube with 425-600 μm diameter glass beads (Sigma) to the meniscus level of the cell suspension and shaking the tube vigorously at 4°C using an IKA-VIBBRAX-VXR cell disruptor for 12 min. The cell suspension was then transferred into a clean Eppendorf tube and spun at 13,000 rpm at 4°C for 5 min after which the supernatant containing the protein extract was transferred into another Eppendorf tube. A 5 μl sample of the protein extract was taken to determine protein concentration using the Bradford protein assay (Bio-Rad). To the rest 20 μl of 5X sample buffer (250 mM Tris.HCl pH 6.8, 10% SDS, 50% glycerol, 25% β-mercaptoethanol, 0.1% bromophenol blue) was added for every 80 μl of the protein extract. The protein

sample was then boiled for 3 min.

b. Sodium Dodecyl Sulphate Polyacrylamide Gel Electrophoresis (SDS-PAGE)

SDS-PAGE was performed using a mini-gel electrophoresis apparatus. Each mini-gel consisted of a lower 7% resolving layer and an upper 5% stacking layer. The lower 7% resolving layer was made by mixing 1.34 ml LGB (182 g/l Tris, 4 g/l SDS, pH 8.8), 2.5 ml distilled water, 1.16 ml 30% acrylamide (National Diagnostics), 10 µl 25% ammonium persulphate and 10 µl TEMED. This liquid mixture was transferred into the mini-gel electrophoresis apparatus with a glass pipette and left to polymerise at room temperature for approximately 30 min. The upper 5% stacking layer was made by mixing 0.61 ml UGB (60 g/l Tris, 4 g/l SDS, pH 6.8), 1.5 ml distilled water, 0.4 ml 30% acrylamide, 10 µl 25% ammonium persulphate and 10 µl TEMED. This solution was added on top of the resolving layer and left to set for approximately 30 min at room temperature. The running buffer consisted of 25 mM Tris.HCl, 200 mM glycine and 0.1% SDS. Broad range molecular weight protein markers (Bio-Rad) were used to determine the size of protein bands. Electrophoresis was performed at 10 mA until the first marker reached the bottom of the gel.

c. Protein Transfer

Proteins were transferred from polyacrylamide gels by using a Semi-dry blotting apparatus (Millipore). In this method three 17 CHR chromatography paper sheets (Whatman) were cut to the same size as the gel, pre-soaked in transfer buffer (25 mM Tris, 193 mM glycine) and placed on the centre of the blotting apparatus. An Immobilon-P membrane (Millipore) cut to the same size as the gel and briefly rinsed in methanol was placed on top of the chromatography paper. This was followed by the gel itself and three further pieces of 17 CHR paper. Air bubbles were rolled out with a glass pipette after which the lid was placed on the stack. Transfer of proteins was carried out at 20 volts for 2 hr after which the membrane was briefly rinsed in 1X PBS (137 mM NaCl, 3 mM KCl, 8 mM Na_2HPO_4, 1 mM KH_2PO_4, pH 7.2).

d. Probing with Antibody

Following transfer the membrane was blocked with 1% Marvel dried milk (w/v) in 1X PBS for 1 hr at room temperature. The membrane was then sealed in a plastic bag containing 1:1000 dilution of primary antibody in 1% Marvel in 1X PBS. The membrane was incubated with the primary antibody at 4°C overnight after which the membrane was treated to three 10 min washes with 20 ml 1X PBS. Depending on the primary antibody the membrane was incubated with either a 1:1000 dilution of anti-mouse or anti-rabbit secondary antibody conjugated to horse radish peroxidase (Sigma) in 1% Marvel in 1X PBS. Incubation with secondary antibody was carried out at room temperature for 4 hr following which the membrane was washed three times with 1X PBS as described previously. The membrane was then treated with the ECL chemiluminescent kit (Amersham) after which it was covered in Saran wrap. Protein bands were detected by exposing Bio Max film (Kodak) to the membrane in a light-proof cassette and the film was developed using an X-OGRAPH Compact X2 developer (Xograph Imaging Systems).

Chapter 3
Identification of *myo51*$^{+}$ and *myo52*$^{+}$

3.1 INTRODUCTION

Myosins are actin-activated molecular motors that are found in high abundance in muscle tissue. The involvement of actin and myosin in forming the distinct striation pattern of skeletal muscle caused by the partially overlapping arrays of actin and myosin filaments was described as long ago as 1953 by Hanson and Huxley. The finding that actin and myosin filaments were linked through cross-bridges, which we now know as myosin heads, was used to develop the idea that myosin and actin filaments could slide past each other to effect muscle contraction (Huxley, 1969). It was not until in 1973 that Pollard and Korn showed that other types of myosins can exist outside of muscle tissue when they identified the first unconventional myosin, as opposed to the conventional myosins of muscle, in *Acanthamoeba.* Since then numerous other myosins have been identified throughout the animal, plant and fungal kingdoms. Myosins now constitute a large and diverse superfamily of actin-activated molecular motors (Sellers, 2000). To make sense of the diverse and numerous myosins that exist in eukaryotes, members of the myosin superfamily are grouped according to the similarity in their head domains (Cheney et al., 1993a). Thus, the founding members of the myosin superfamily (the conventional myosins) are grouped together as class II myosins. All other myosin classes (unconventional myosins) are classified in the order they were discovered. At present, phylogenetic analysis of the head domains have separated the myosin superfamily into 17 distinct classes (Hodge and Cope, 2000).

The fact that myosins are ubiquitous throughout eukaryotes indicates that these proteins existed early in evolutionary history (Cheney et al., 1993a) and the fact that they are present in the organisms of today suggests that they have been maintained because of their importance to cell function. Indeed, myosins have been implicated in many cellular processes which include cytokinesis, endocytosis, polarised secretion and signal transduction (Soldati et al., 1999; Bahler, 2000). Various model systems have been used to understand the role of myosin in cellular processes. For example, the motile amoebae of *Dictyostelium discoideum*, have been used to study the role of

myosin in cell locomotion (Novak and Titus, 1997) whereas fish and frog pigment cells have proven useful in the study of intracellular transport (Rodionov et al., 1998; Rogers et al., 1999). In the budding yeast model system, three classes of myosins have been identified (classes I, II and V) each of which is specialised for a particular cell process (Brown, 1997). For example, the budding yeast class I myosins, Myo3 and Myo5, have been suggested to be involved in endocytosis and actin organisation (Geli and Riezman, 1996; Goodson et al., 1996) whereas the two class V myosins, Myo2 and Myo4, are involved in intracellular transport (Govindan et al., 1995; Long et al., 1997; Takizawa et al., 1997). The single budding yeast class II myosin, Myo1, on the other hand, has been implicated in the contraction of the actin ring at the mother-bud neck to achieve cytokinesis (Bi et al., 1998) (see Chapter 1, section 1.2.4).

The fission yeast, *Schizosaccharomyces pombe*, offers another model system with which to understand the role of myosins in cellular processes. The fission yeast model system complements that of budding yeast and other systems, and in many respects may be better for studying certain cellular processes. For example, *S. pombe* divides by medial fission which is analogous to the process of cytokinesis in most animal cells (Chang and Nurse, 1996). This is in contrast to budding yeast which divides asymmetrically to produce cells of unequal size (Madden and Snyder, 1998). Furthermore, BLAST analysis of the available *S. pombe* genomic sequences indicates that fission yeast contains similarity to at least 169 human proteins for which there are no similar proteins in budding yeast (L. Robertson, personal communication).

Prior to the start of this project only two myosins have been described in *S. pombe*, Myo2 (Kitayama et al., 1997; May et al., 1997) and Myp2/Myo3 (Bezanilla et al., 1997; Motegi et al., 1997). Both Myo2 and Myp2/Myo3 are class II myosins and like their budding yeast homologue, the fission yeast proteins localise to the division plane to execute cytokinesis (Kitayama et al., 1997; May et al., 1997; Bezanilla et al., 2000; Motegi et al., 2000; Mulvihill et al., 2000). During the course of this project a single class I myosin gene, *myo1*$^+$, was identified (Mulvihill and Hyams, in

preparation). In this chapter, I report the first identification of two class V myosin genes, *myo51*$^+$ and *myo52*$^+$, in *S. pombe*. I present sequence analysis of their gene products to justify their classification into the class V group of the myosin superfamily and show that the fission yeast class V myosins are similar to those in budding yeast and vertebrates.

3.2 RESULTS

3.2.1 Identification of *myo51*$^+$ and *myo52*$^+$

In an attempt to identify new myosin genes in *S. pombe*, the ongoing Sanger Centre Fission Yeast Genome Sequencing Project (www.sanger.ac.uk/Projects/S_pombe) was searched for proteins that contained the conserved GESGAGKT motif that is present in the nucleotide binding pocket of the myosin head domain (Saraste et al., 1990; Vale, 1996). Using the TBlastN search algorithm, the *S. pombe* genome was fished for protein sequences that displayed similarity to a 200 amino acid sequence that encompasses the nucleotide binding site of the previously identified fission yeast class II myosin, Myo2 (Kitayama et al., 1997; May et al., 1997). This search revealed four protein sequences that displayed similarity to the Myo2 bait: Myo2 itself, Myp2 (another previously identified class II myosin: Bezanilla et al., 1997; Motegi et al., 1997; May et al., 1998) and two new protein sequences that had not been characterised before. Analysis of the genes encoding the two new protein sequences showed that one of the genes resided on chromosome 2 (from cosmid c2D10, EMBL accession number: AL031788) whereas the second gene resided on chromosome 3 (from cosmid c1919, EMBL accession number: AL035075). Interestingly, both genes contain three exons separated by two introns. In both genes the first intron starts at an identical position: after 30 bases of the protein coding sequence (Figure 3.1).

To verify that the two new genes encoded for bona fide myosins, the entire primary sequence of their gene products was obtained and analysed for the existence of signature motifs, other than the nucleotide binding domain, that are hallmarks of a

myosin heavy chain. Two conserved regions downstream of the GESGAGKT motif have been used as diagnostic indicators of a myosin molecule. The first of these, the so called LEAF motif, starts shortly after the nucleotide binding motif and has the consensus: LEAFGNAKTV (Garces and Gavin, 1998). The second region which lies approximately 300 amino acids C-terminal to the nucleotide binding motif contains a conserved sequence of residues (GILSLLDEE) which is thought to constitute part of the actin binding interface (Cope et al., 1996). Interestingly, both proteins showed significant homology to the LEAF motif as well as complete identity to the GILSLLDEE actin binding sequence. From these results it was concluded that two previously unidentified myosins had been discovered in *S. pombe*.

3.2.2 Myo51 and Myo52 are Class V Myosins

The finding that the two newly discovered proteins contained several motifs that are characteristics of an actin binding ATPase showed that these proteins were indeed myosins. However, it was still not clear which class of myosins these proteins belonged to. Cheney et al. (1993a) have proposed a method of classification of the myosin superfamily in which myosins are grouped according to their similarity within the head domain, essentially the first 800 amino acids. This method of classification was adopted in order to classify the new fission yeast myosins. The analysis was performed by obtaining the primary sequence of the myosin head domain from members representing all the known classes of the myosin superfamily (Swiss-Prot: www.expasy.ch/sprot/sprot-top.html). The sequences were aligned using the ClustalW sequence alignment program from which similarity between myosins was calculated using the Phylip suite of phylogenetic analysis software created by Joseph Felsenstein (http://evolution.genetics.washington.edu/phylip.html). A phylogenetic tree of the relationship between the two new fission yeast myosins and all the representative members of the myosin superfamily was drawn. The tree was bootstrapped or redrawn 100 times to calculate the percentage of times a particular branch point occurred in the bootstrapping trials. This was used to estimate the confidence in branching pattern of the tree at branch points or nodes.

The completed tree revealed that the two new fission yeast myosins grouped with members of the class V division of the myosin superfamily which included Myo5D from chick, Myo5A from mouse and the budding yeast class V myosins, Myo2 and Myo4. Bootstrap analysis showed that this part of the phylogenetic tree containing members of the class V myosins was able to be regenerated in greater than 95% of the bootstrapping trials (Figure 3.2). The high level of confidence in branching pattern indicated that the two new fission yeast myosins were both class V myosins. Interestingly, closer examination of the tree showed that the fission yeast class V myosins were on the same branch as their budding yeast homologues whereas the vertebrate myosins formed a separate branch (Figure 3.2). This indicated that the fission yeast class V myosins were more similar to their budding yeast homologues than their vertebrate counterparts. The finding that the two new fission yeast myosins were class V myosins enabled them to be named. The gene encoding the class V myosin from chromosome 2 was subsequently called *myo51*$^+$ and the gene encoding the second class V myosin, from chromosome 3, was called *myo52*$^+$ (for fission yeast myosin V1 and fission yeast myosin V2 respectively).

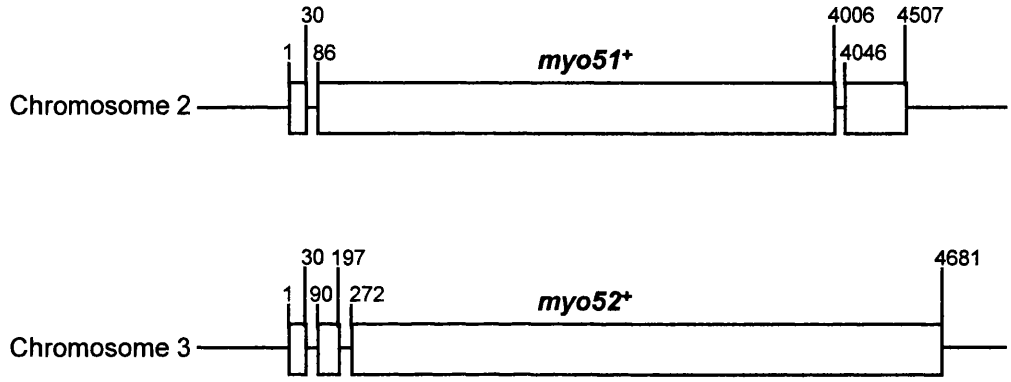

Figure 3.1 The Gene Structure of *myo51*$^+$ and *myo52*$^+$

Both *myo51*$^+$ and *myo52*$^+$ have three exons (white boxes) separated by two introns. Interestingly, the first intron in both genes occurs after 30 bases of coding sequence. Numbers denote position from the start codon, where '1' represents the position of the adenine (A) base of the start codon (ATG).

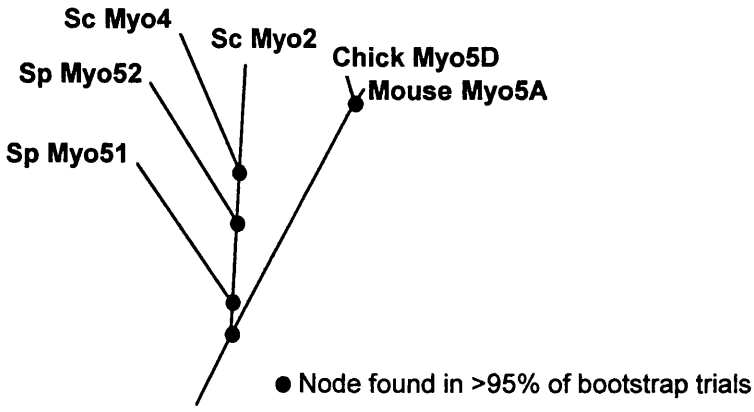

Abbreviations: Sp (*Schizosaccharomyces pombe*); Sc (*Saccharomyces cerevisiae*).

Accession numbers: Myo51(AL031788); Myo52 (AL035075); Myo2 (P19524); Myo4 (P32492); Myo5A (Q99104); Myo5D (Q02440). Fission yeast myosin sequences are available from the Sanger Centre web site (www.sanger.ac.uk/Projects/S_pombe), all other proteins sequences are available from the Swiss-Prot web site (www.expasy.ch/sprot/sprot-top.html).

Figure 3.2 Phylogenetic Analysis of Myo51 and Myo52

Phylogenetic tree showing that Myo51 and Myo52 groups with class V myosins from vertebrates and budding yeast. Interestingly, the fission yeast and budding yeast class V myosins are on the same branch of the tree. Myosin head sequences were aligned using the ClustalW software. The phylogenetic tree was constructed from aligned protein sequences using the Neighbor joining method. The Neighbor algorithm is available from the Phylip suite of programs (http://evolution.genetics.washington.edu/phylip.html). To estimate the degree of confidence in branching, the tree was bootstrapped 100 times.

3.2.3 Features of Myo51 and Myo52

Comparison of the sequences of Myo51 and Myo52 shows that they are proteins predicted to consist of 1471 and 1516 amino acids respectively (Figure 3.3). The predicted molecular weight of Myo51 is 168 kD and the predicted molecular weight of Myo52 is 175 kD. Interestingly, these sizes are comparable to that of the corresponding proteins in budding yeast in which Myo2 is a protein consisting of 1574 amino acids and Myo4 has an identical number of amino acids as Myo51 (1471 amino acids). This is in contrast to the sizes of the vertebrate class V myosins which are longer proteins of over 1800 amino acids in length. Like other myosins, the class V myosin heavy chain can be separated into three functional domains: the head, neck and tail domains. What now follows is a discussion of each of the class V myosin domains.

a. Head Domain

Extensive regions of homology that span the entire head domain of yeast and vertebrate myosin V's can be identified (Figure 3.4). In particular, long regions of amino acid identity can be found at critical points in the head domain which include the nucleotide and actin binding interfaces as well as the LEAF motif as discussed above. In Myo51, the GESGAGKT, LEAF and part of the actin binding interface occur at residues 159-166, 203-212 and 506-514 respectively. The corresponding regions in Myo52 occurs at residues 167-174, 218-227 and 524-532.

Another region of the head domain that is critical for its function is the active thiol region (Johnston et al., 1991). This region mediates major structural changes when nucleotide binds to the head. In chicken fast skeletal muscle myosin, the active thiol region contains two short α-helices each containing a cysteine residue with a highly reactive sulfhydryl group (Rayment et al., 1993). These cysteine residues occur at positions 707 and 697 in chicken fast skeletal muscle myosin and have been termed SH1 and SH2 respectively in the order of their chemical reactivity. Extrapolation of the information obtained from chicken fast skeletal has been used to identify the corresponding regions in other myosin classes (Cope et al., 1996). Using this strategy

the active thiol region in Myo51 occurs between residues 644-685, and in Myo52 the region occurs between residues 663-704. In chicken fast skeletal muscle myosin a highly conserved glycine residue at position 703 separates the two α-helices of the active thiol region and is thought to form the pivot point to allow rotation of the lever arm (Batra et al. 1999). In Myo51, this corresponds to glycine 670 and in Myo52 it is glycine 689. Corresponding glycine residues are also found in the amino acid sequence of budding yeast Myo2 and Myo4 as well as mouse Myo5A (Figure 3.4) and chick Myo5D (data not shown), thus reflecting the conserved nature of this residue. Interestingly, two cysteine residues are found in close proximity on either side of this conserved glycine in Myo52. These cysteine residues which occur at positions 698 and 688 of Myo52 have been tentatively marked SH1 and SH2 respectively in Figure 3.4 since they may be analogous to the reactive sulfhydryl groups of chicken fast skeletal muscle myosin. Myo51, on the other hand, has a single cysteine residue near the conserved glycine at position 669. The second cysteine residue is missing in Myo51 and instead is replaced by a serine residue at position 679. Interestingly, this cysteine residue is also absent in mouse Myo5A (Figure 3.4) and chick Myo5D (data not shown) and is replaced by an alanine residue in both cases.

b. Neck Domain

The neck domain is the site of light chain binding in myosins. Light chain binding is mediated by a special sequence of about 25 residues called the 'IQ motif' which is found repeated tandemly in the heavy chain of many myosins including myosin V's (Cheney and Mooseker, 1992). The core consensus sequence of the IQ motif has the form IQXXXRGXXXR where X represents any amino acid (Rhoads and Friedberg, 1997). This sequence can be separated into two parts, the first part (IQXXXR) is the most critical part of the IQ motif since it plays a role in determining the conformation of the light chain and consequently affects the ability of the light chain to grip the myosin heavy chain (Houdusse and Cohen, 1995; Houdusse et al., 1996). This part of the motif also positions the light chain onto the heavy chain. The second part of the IQ motif core (GXXXR), however, plays a minor role in fixing the position of the

light chain on the heavy chain and does not affect the major conformational changes that occur in the light chain that determines its ability to bind the heavy chain. Sequence analysis of the IQ motifs in class II myosins has shown that the site of binding of the regulatory light chain (RLC) is not well conserved. In the cases examined, the IQ motif that binds the RLC has been found to be incomplete in which the second part of the IQ core (GXXXR) is missing (Houdusse et al., 1996).

In many IQ motifs the amino acids that occupy conserved positions are substituted with other residues. For example, the isoleucine in the first position is frequently a different branched chain amino acid such as a leucine (L) or a valine (V) residue (Rhoads and Friedberg, 1997). Occasionally, a phenylalanine (F), threonine (T) or a methionine (M) residue has been seen to occupy this position (Rhoads and Friedberg, 1997; Jurado et al., 1999). The glutamine that occupies the second position of the IQ motif is sometimes replaced by an alanine (A), arginine (R) or serine (S) in certain class I myosins (Houdusse et al., 1996). The arginines in both the sixth and the terminal position are sometimes replaced by a lysine (K) or histidine (H) residue and less frequently by a leucine (L) residue. The seventh position glycine is frequently not conserved (Jurado et al., 1999). These observations indicate that variation from the core consensus sequence of the IQ motif exists between different myosins and indeed between different IQ motifs of the same myosin heavy chain. This may consequently affect the affinity or type of light chain that associates with a given light chain binding site on a myosin molecule (Houdusse et al., 1996).

In class V myosins, six IQ motifs can be found in the neck domain of these proteins (Reck-Peterson et al., 2000). Alignment of the neck domains of Myo51 and Myo52 with that of other class V myosins shows that the fission yeast myosins align well with most of the six IQ motifs of their budding yeast and vertebrate homologues, showing either amino acid identity or similarity at key positions of an IQ motif (Figure 3.5). Using the information that the first part of the core consensus sequence of the IQ motif is critical for light chain binding and that some of the conserved amino

acids are substituted by other residues in some IQ motifs, five potential light chain binding sites can be identified in the neck domains of both Myo51 and Myo52. These five sites are identified as IQ motifs 1, 3, 4, 5 and 6 in Myo51, using the search criterion: I(LVFTM)Q(ARS)XXXR(KHL). In Myo52, the five sites are labelled as IQ motifs 2, 3, 4, 5 and 6 (Figure 3.5).

c. Tail Domain

Comparison of the sizes of the class V myosins between yeasts and vertebrates show that the vertebrate myosins are longer proteins with some additional 300 amino acid residues (Figure 3.3). Alignment of the entire protein sequences of the yeast and vertebrate class V myosins shows the presence of an insertion which occurs after the head and neck domains that accounts for most of the size difference between the yeast and vertebrate myosins. In both mouse Myo5A and chick Myo5D the insertion occurs approximately between residues 1100 and 1400: which starts shortly after the neck domain and ends well before the C-terminus of the proteins (Figure 3.3).

Class V myosins are noted for having a coiled-coil region in their tail that mediates dimerisation between two heavy chains (Reck-Peterson et al., 20000). Pair-coil predictions using the method of Berger et al. (1995) shows that fission yeast Myo51 and Myo52 both have a region in their tail that is predicted to form a coiled-coil (Figure 3.6). Curiously, comparison of the pair-coil predictions between the yeast class V myosins shows that fission yeast Myo51 has a similar (though not identical) pair-coil prediction to that of the budding yeast Myo4 protein whereas Myo52 has a similar prediction to that of Myo2. Thus, not only do Myo51 and Myo4 have an identical number of amino acids in their primary sequence (1471) but coincidentally they also seem to share a similar coiled-coil structure. Whether these similarities extend to protein function awaits to be seen.

Vertebrate class V myosins have a longer region of predicted coiled-coil, which spans over 500 amino acid residues. This is in contrast to the 50-200 amino acids that are

predicted to form a coiled-coil in yeasts. In mouse Myo5A and chick Myo5D the region of the predicted coiled-coil start around residue 900 and ends shortly after residue 1400. Interestingly, the pair-coil region of vertebrate class V myosins coincides with the 300 or so amino acid insertion that occurs between residues 1100-1400. Thus, the reason for the larger size of vertebrate class V myosins can be accounted for by their more extensive region of coiled-coil in their tail.

Interestingly, a short region of coiled-coil has also been predicted in the head domains of budding yeast Myo2, mouse Myo5A and Chick Myo5D (Figure 3.6). This may represent an artefact of the pair-coil algorithm (Berger et al., 1995) used for the coiled-coil predictions. Whether these coiled-coil predictions genuinely occur in the myosin V structure can only be resolved experimentally.

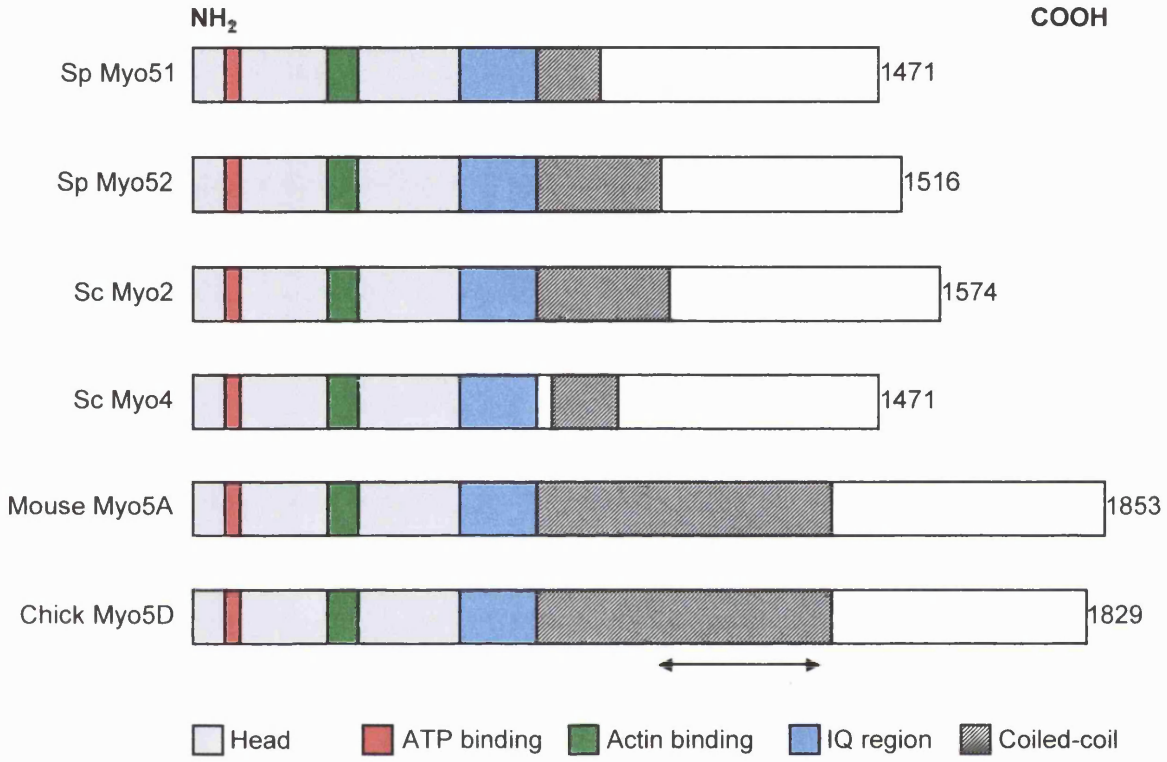

Figure 3.3 Features of Yeast and Vertebrate Class V Myosins

Schematic representation of class V myosins from yeasts and vertebrates. Like the vertebrate myosins, yeast class V myosins possess a neck region (shown here in blue as an IQ region) which provides binding sites for light chains. Class V myosins typically have six IQ motifs for light chain binding. Immediately C-terminal to the neck region is a domain which is predicted to form a coiled-coil. In both fission yeast and budding yeast the coiled-coil domain is relatively short compared to that of vertebrate myosin V's. Vertebrate class V myosins have an insertion of approximately 300 amino acids in this coiled-coil domain which accounts for most of the size difference observed between the yeast and vertebrate myosin V's. The location of the insertion in the vertebrate class V myosins is shown as a double headed arrow.

Figure 3.4 Sequence Analysis of Class V Myosin Head Domains

Class V myosin head domains from yeasts and mouse were aligned using the ClustalW sequence alignment program available at the Swiss-Prot web site (www.expasy.ch/sprot/sprot-top.html). The GESGAGKT motif which constitutes part of the nucleotide binding site is marked with asterisks. The LEAF motif is indicated with a dotted line. An overhead line marks the GILSLLDEE protein sequence which is thought to form part of the actin binding interface. Overhead arrows are used to indicate the location of the active thiol region. The conserved glycine residue which separates two reactive sulfhydryls in the active thiol region is marked with a '+'. The cysteine residues that are thought to occupy the positions of the reactive sulfhydryl groups, SH1 and SH2, have been designated '1' and '2' respectively. The position of the first IQ motif is shown boxed. Shaded letters represent amino acid identity between sequences. Letters shown in grey represent amino acid similarity between sequences. Numbers on the left side of a protein sequence show amino acid position from the N-terminus.

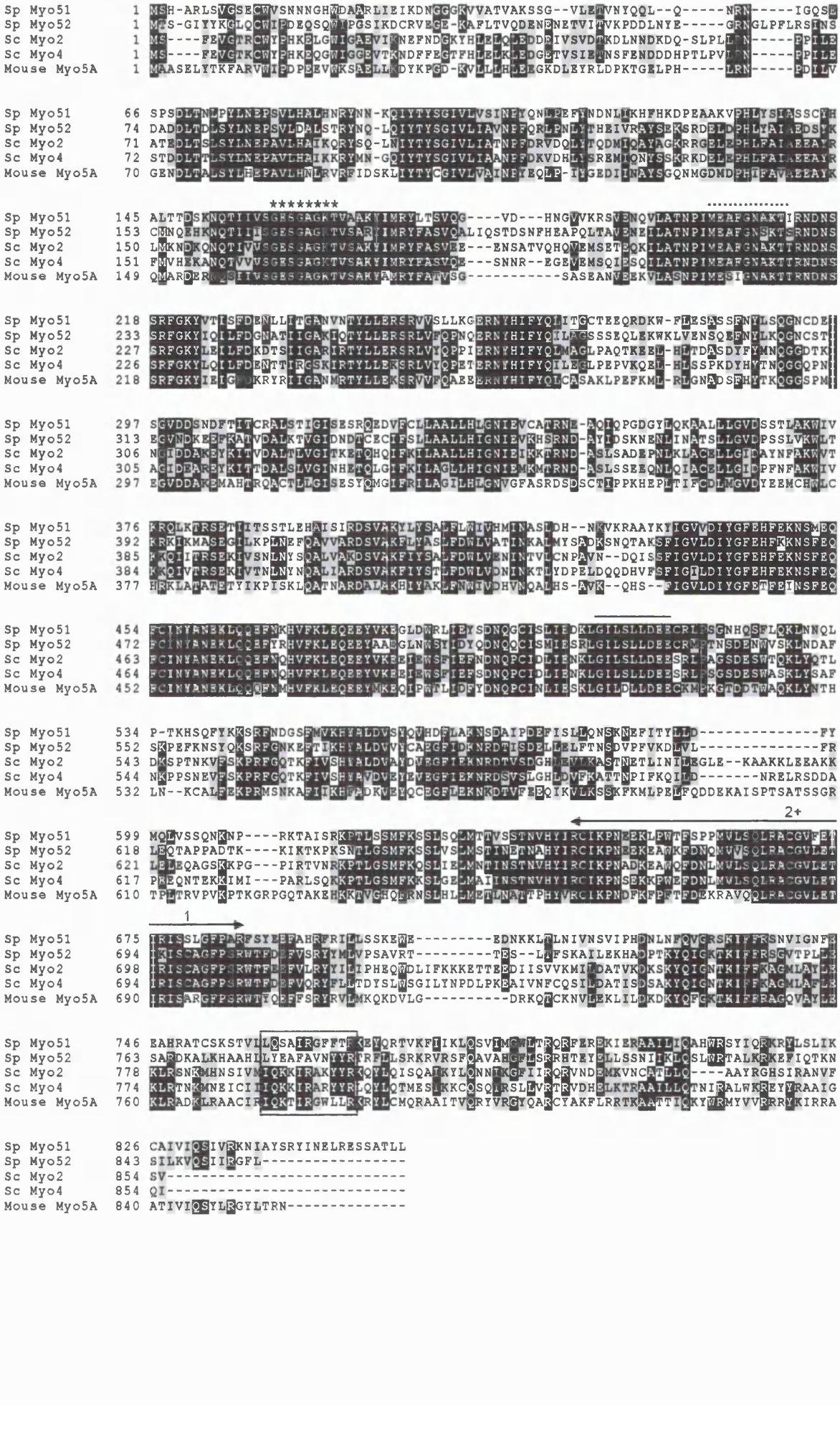
Sp Myo51
Sp Myo52
Sc Myo2
Sc Myo4
Mouse Myo5A
****
2+
1

Figure 3.5 Class V Myosin Light Chain Binding Sites

ClustalW analysis showing the alignment of the neck region of Myo51 and Myo52 with budding yeast and mouse class V myosins. IQ motifs (IQXXXRGXXXR) are found in the neck region to mediate binding to light chains. In Myo51 and Myo52, five IQ motifs can be recognised using the search criterion I(LVFTM)Q(ARS)XXXR(KHL) (see text for details). In the case of Myo51, these potential light chain binding sites are labelled as IQ motifs 1, 3, 4, 5 and 6. In Myo52, these are IQ motifs 2, 3, 4, 5 and 6. Boxes show the positions of the six IQ motifs in class V myosins. Amino acid residues that occupy conserved positions of an IQ motif are written in bold.

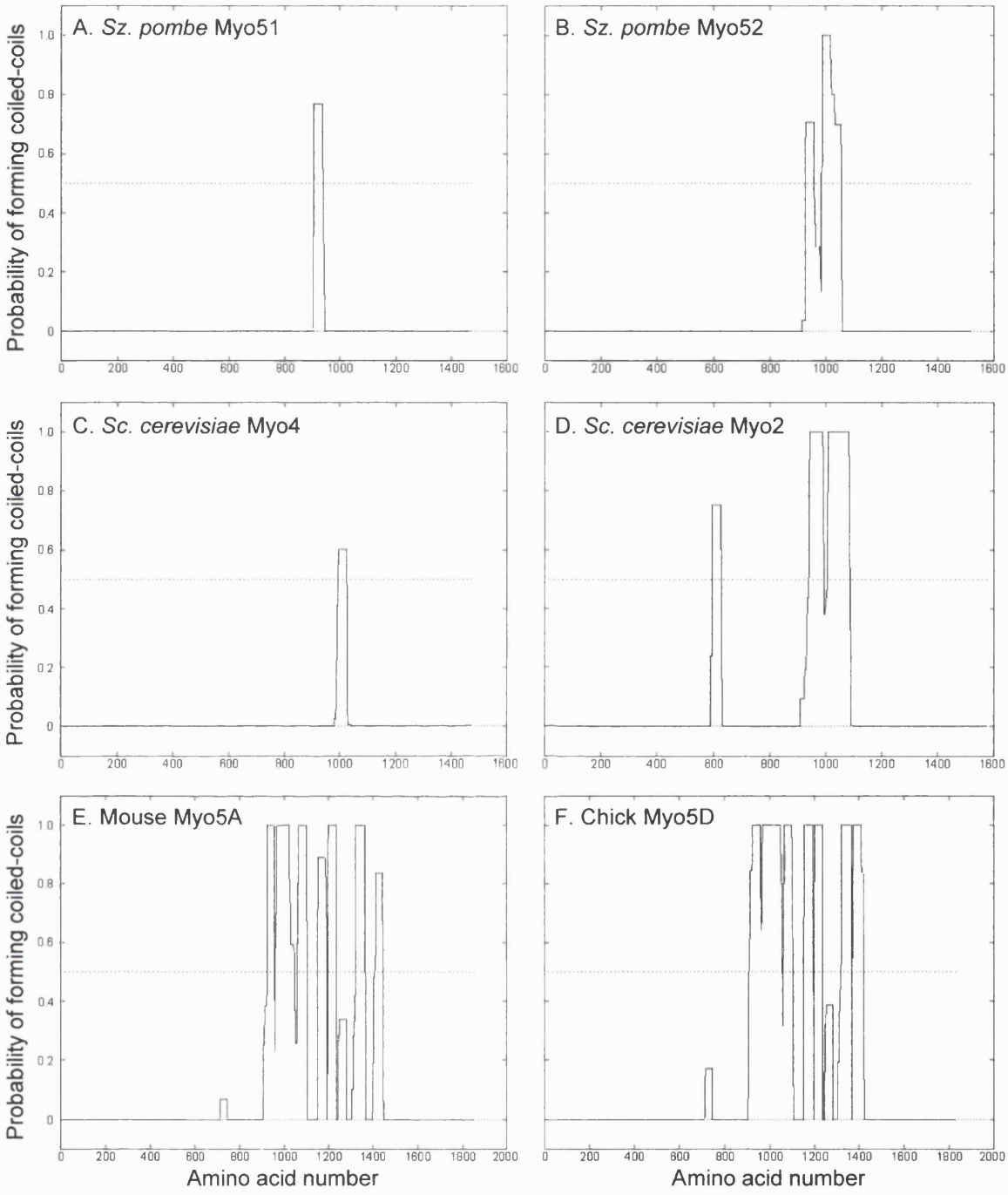

Figure 3.6 Pair-Coil Predictions of Class V Myosins

Pair-coil analysis of class V myosins using the algorithm of Berger et al. (1995). The program is available at Swiss-Prot (http://www.expasy.ch/sprot/sprot-top.html). Interestingly, the fission yeast and budding yeast myosins show similar pair-coil predictions: Myo51 displays a similar prediction to that of Myo4, and Myo52 has a similar pair-coil prediction to that of Myo2. The vertebrate myosins have a longer region of predicted coil-coil compared to that of their yeast homologues. Note the change in scale of the X-axis between the yeast and vertebrate plots which emphasises the difference in sizes between yeast and vertebrate myosin V's.

3.3 DISCUSSION

In this chapter I have reported the identification of two new myosin genes in *Schizosaccharomyces pombe* which have been designated *myo51*$^+$ and *myo52*$^+$ (Win et al., 1999a, 1999b). Phylogenetic analysis of the predicted gene products shows that *myo51*$^+$ and *myo52*$^+$ encode class V myosins. This is in contrast to the previously identified fission yeast myosin genes, *myo2*$^+$ (Kitayama et al., 1997; May et al., 1997) and *myp2*$^+$ (Bezanilla et al., 1997; Motegi et al., 1997), which encode class II myosins. During the course of this study a fifth myosin gene, *myo1*$^+$, that encodes a class I myosin has been identified (Mulvihill and Hyams, in preparation). The tally of *S. pombe* myosin genes currently stands at five: one encoding a myosin I, two encoding class II myosins and two encoding class V myosins. The *S. pombe* genome sequencing project is almost complete and it is unlikely that further myosin genes exist in fission yeast. The same number of myosin genes is also found in budding yeast (Brown, 1997). Interestingly, these genes also encode class I, II and V myosins suggesting that these classes of myosins may be the minimum requirement needed for performing basic cellular processes in a non-motile, unicellular eukaryote. More complex eukaryotes may require additional myosins to cope with the more numerous processes that occur in these organisms. Consistent with this, twelve myosin genes have been identified in the motile organism, *Dictyostelium discoideum* (Sellers, 2000). In humans, this number dramatically rises to thirty different myosin genes (Cheney, 2000).

Sequence analysis of Myo51 and Myo52 shows that they are more similar to their budding yeast homologues than their vertebrate counterparts. Alignment of Myo51 with the budding yeast class V myosins, Myo2 and Myo4, shows that Myo51 exhibits a 34% amino acid identity over the entire sequence of both its budding yeast homologues. In the case of Myo52, the amino acid identity with either of its budding yeast homologues is 38%. When the two fission yeast class V myosins themselves are aligned, an amino acid identity of 35% is seen. In contrast, comparison of either Myo51 or Myo52 with either of the vertebrate myosin V's (mouse Myo5A or chick

Myo5D) shows that an amino acid identity of just under 30% is observed between them. Most of the amino acid identity is observed in the head domain which contains regions that define the myosin molecule, namely, the nucleotide and actin binding sites and regions that are important for the mechanical activity of the molecule such as the active thiol region.

Immediately, C-terminal to the head domain is the neck region which is the domain of light chain binding. Six IQ motifs, of the consensus IQXXXRGXXXR, are present in a typical class V myosin (Reck-Peterson et al., 2000). However, in either Myo51 or Myo52 only five IQ motifs have been determined. In Myo51, the second IQ motif does not conform to consensus sequence and has a methionine residue in the sixth position that is usually occupied by an arginine. In Myo52, however, the first IQ motif is different from that of the consensus sequence at two positions, both in the critical first part of the IQ motif (IQXXXR). In this motif, a tyrosine residue is present at the second position usually occupied by a glutamine and an alanine residue is found at the sixth position usually occupied by arginine. The fact that an IQ motif in Myo51 and Myo52 does not conform to the consensus sequence does not necessarily imply that these sites are incapable of binding light chains since a number of IQ motifs have been found to vary from the consensus sequence (Houdusse et al., 1996; Rhoads and Friedberg, 1997; Jurado et al., 1999). Perhaps differences in IQ motifs may be required for differential binding to myosin light chains such that some IQ motifs are occupied first whereas others provide a low affinity binding site for light chains. Alternatively, fission yeast class V myosins may have binding sites for unique light chains that do not recognise a typical IQ motif.

In class II myosins, two binding sites are found in the neck domain, the first of these binds the essential light chain and the second, the regulatory light chain (Xie et al., 1994). The binding site for the essential light chain is different from that of the regulatory light chain in which only the first part of the IQ motif is usually present in the regulatory light chain binding domain (Houdusse et al., 1996). In class V myosins,

the IQ motifs are complete and are similar to that of the essential light chain binding site of myosin II. Most of the IQ motifs in a class V myosin molecule bind calmodulin (Reck-Peterson et al., 2000). Biochemically purified chicken class V myosin has been shown to copurify with 4-5 calmodulin molecules per heavy chain (Cheney et al., 1993b). However, in addition to binding calmodulin, chicken brain myosin V has also been found to be associated with low molecular weight proteins of 17 kD and 23 kD in size. These proteins correspond to the sizes of the essential light chains that are components of chicken brain non-muscle myosin II. In budding yeast, the class V myosin, Myo2, also associates with more than one type of light chain. Myo2 has been found to be associated with calmodulin and a protein designated Mlc1 which has characteristics of an essential light chain (Brockerhoff et al., 1994; Stevens and Davis, 1998). In fission yeast, a gene encoding calmodulin, *cam1*$^+$, and a gene encoding a novel myosin light chain, *cdc4*$^+$, have been identified (Moser et al., 1997; May et al., 1998). Biochemical analysis of Cdc4 have shown that it associates with both of the fission yeast class II myosins, Myo2 and Myp2 (Naqvi et al., 1999; Motegi et al., 2000). Recently, a protein with homology to a myosin regulatory light chain has been identified by the *S. pombe* Genome Sequencing Project but is as yet biochemically uncharacterised. The observation that class V myosins from vertebrates and budding yeast bind to more than one type of light chain and the finding that at least two myosin light chains exists in *S. pombe* opens the possibility that fission yeast class V myosins may also be associated with a number of different light chains.

The tail domain of class V myosins can be separated into two functional regions: the first is a region predicted to form an α-helical coiled-coil, followed by a globular C-terminal domain that is thought to be involved in cargo binding and/or localisation within the cell (Reck-Peterson et al., 2000). Yeast class V myosins are much shorter than their vertebrate homologues which is attributable to an insertion of about 300 amino acids in the tail of the vertebrate myosins. This insertion extends the predicted coiled-coil region, which in vertebrate class V myosins is approximately 500 amino acids in length. In yeasts, however, this region is considerably shorter and is about 50-

200 amino acids in length. Despite this, the budding yeast class V myosin, Myo2, is able to self associate and form a dimer consisting of two heavy chains (Beningo et al., 2000). Electron microscopy has shown that a chicken class V myosin from brain tissue is also a two headed motor with a globular tail domain (Cheney et al., 1993b). The size of the region that is thought to form a globular domain at the C-terminus of class V myosins is about the same in both yeasts and vertebrate myosin V proteins.

In this chapter, I have compared the sequences of the fission yeast class V myosins with that of their budding yeast and vertebrate homologues. I have shown that the fission yeast class V myosins are more similar to the budding yeast myosins in terms of their primary sequence compared to that of their vertebrate counterparts. In budding yeast, the class V myosins have been reported to be involved in the localisation of secretory vesicles, vacuoles and mRNA (Govindan et al., 1995; Hill et al., 1996; Long et al., 1997; Takizawa et al., 1997). In the following chapters I will present experimental results that attempt to elucidate the functional role of the class V myosins in *S. pombe*.

Chapter 4
Deletion of *myo51*$^{+}$ and *myo52*$^{+}$

4.1 INTRODUCTION

An important technique used to understand the role of a gene in an organism is to inactivate the gene by disruption or deletion. By observing the phenotype of the organism in the absence of a functional gene an idea of the gene's role can be discerned.

In *Schizosaccharomyces pombe*, creation of a null mutation is particularly easy because fission yeast can undergo homologous recombination at a high frequency, such that specific genes can be targeted for disruption or deletion (Zhao and Lieberman, 1995). This involves construction of an integration cassette which consists of a selection marker gene flanked by DNA sequences from the gene of interest so that the cassette will integrate into the target site by homologous recombination upon transformation into fission yeast (Moreno et al., 1991). Depending on the way the integration cassette was designed a gene could be disrupted when a selection marker is inserted into the gene or deleted when some or all of the gene sequence is replaced by the selection marker. In either method the function of the gene is abolished with the integration of the selection marker into the chromosomal locus.

There are a number of markers available for the disruption and deletion of genes in *S. pombe*. These are usually biosynthetic marker genes which allow fission yeast auxotrophs to grow in the absence of the required supplement when they are integrated into the chromosome (Moreno et al., 1991). Biosynthetic markers commonly used in these experiments include *S. pombe* genes such as *ura4*$^+$, *his7*$^+$ and *ade2*$^+$. The *Saccharomyces cerevisiae LEU2* gene has also been used successfully in fission yeast because of its ability to complement the *S. pombe leu1-32* mutation and allows such auxotrophs to grow in the absence of the amino acid leucine in the culture medium (Russell, 1989). The bacterial *kan*^{r} gene has also been developed as a heterologous marker, conferring resistance in *S. pombe* cells containing this marker to the drug Geneticin (Bahler et al., 1998). The multitude of selection markers available in fission yeast allows more than one gene to be disrupted or deleted in a cell. This is

especially useful when studying a family of genes which are functionally redundant and when disruption or deletion of any one member gives no clue to its function.

Transformation of the integration cassette is usually performed in a diploid strain to select for heterozygous diploids which contain one copy of the intact gene and one copy of the disrupted or deleted allele. By doing it this way, diploid cells disrupted in a gene whose function is essential remain viable in the presence of the wild type gene. The phenotype of the disruption is unmasked when the heterozygous diploid is sporulated. If the gene is essential then only two members of the four haploid meiotic products remain viable.

In an attempt to elucidate the function of *myo51*$^+$ and *myo52*$^+$, both genes were deleted with the *ura4*$^+$ marker. This chapter describes the construction of the integration cassettes and their integration into the *myo51*$^+$ and *myo52*$^+$ loci. Following this, the phenotypic characterisation of the deleted cells by microscopic, physiological and genetic methods are presented. Finally, the results of these analyses are discussed and compared to those obtained from other model systems.

4.2 RESULTS

4.2.1 Construction of the *myo51*$^+$ and *myo52*$^+$ Integration Cassettes

Approximately 80% of the *myo51*$^+$ and 85% of the *myo52*$^+$ coding sequence was deleted in the null mutants. This was performed by constructing a cassette which consisted of the *ura4*$^+$ gene flanked by sequences upstream and downstream of the gene targeted for deletion.

To delete *myo51*$^+$, the upstream sequence was obtained by PCR of wild type genomic DNA using the primers c2D10-ApaI-up and c2D10-AscI-up (Materials and Methods Table 2.2) whereas the downstream sequence was obtained using the primers c2D10-

AscI-down and c2D10-PstI-down. The upstream and downstream PCR products, each 1 kb in size, were sequentially cloned into the modified vector pSL1180 as an Apa/AscI and an AscI/PstI fragment respectively. This was then used to insert the *ura4*$^+$ gene into the AscI restriction site that lies between the *myo51*$^+$ sequences.

The same strategy was used to construct the *myo52*$^+$ integration cassette but using primers specific for the *myo52*$^+$ locus (c1919-ApaI-up, c1919-AscI-up, c1919-AscI-down and c1919-PstI-down). The *myo51*$^+$ and *myo52*$^+$ integration cassettes were then cut from the vector and separately transformed into the diploid *leu1-32 ura4-D18 ade6-210 h*$^-$ */ leu1-32 ura4-D18 ade6-216 h*$^+$.

4.2.2 Selection of the Null Mutants

After transforming a diploid strain in separate reactions with the *myo51*$^+$ and *myo52*$^+$ integration cassettes, homologous recombination at these loci were selected by growing the diploid transformants in supplemented minimal medium lacking uracil. To test for stable integration of the *ura4*$^+$ marker, six diploid colonies from each transformation were randomly chosen for further analysis and subcultured onto a non-selective YES plate to promote loss of the marker in transformants that had not integrated the *ura4*$^+$ marker into the genome. All six colonies from the transformation of the *myo51*$^+$ integration cassette and four out of the six colonies from the transformation of the *myo52*$^+$ cassette were found to have inherited a stable *ura4*$^+$ gene upon subculture onto minimal medium lacking uracil. The integrated *ura4*$^+$ diploid transformants were then sporulated and the haploid progeny examined by tetrad analysis. To check that the *ura4*$^+$ marker had integrated at the target locus, a Southern blot analysis was performed. For each gene, correct integration of the cassette was confirmed by Southern analysis with a 550 bp *ura4*$^+$ probe using genomic DNA obtained from a heterozygous diploid transformant and its *ura4*$^+$ and *ura4*$^-$ haploid progeny (Figures 4.1 and 4.2).

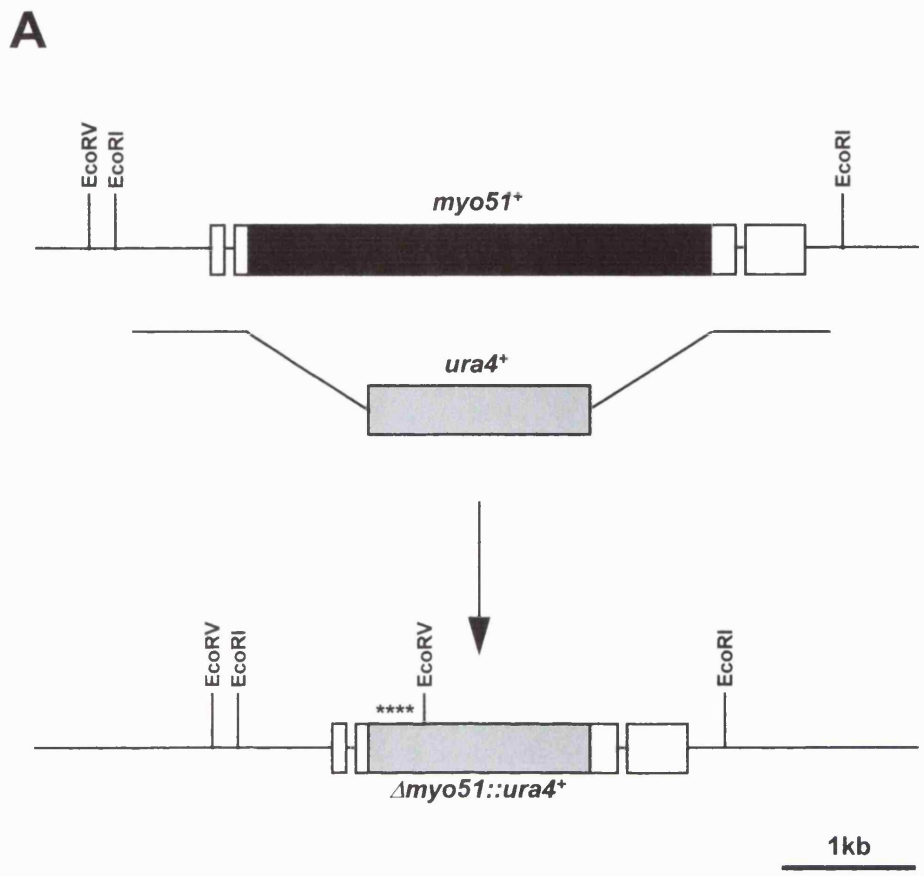

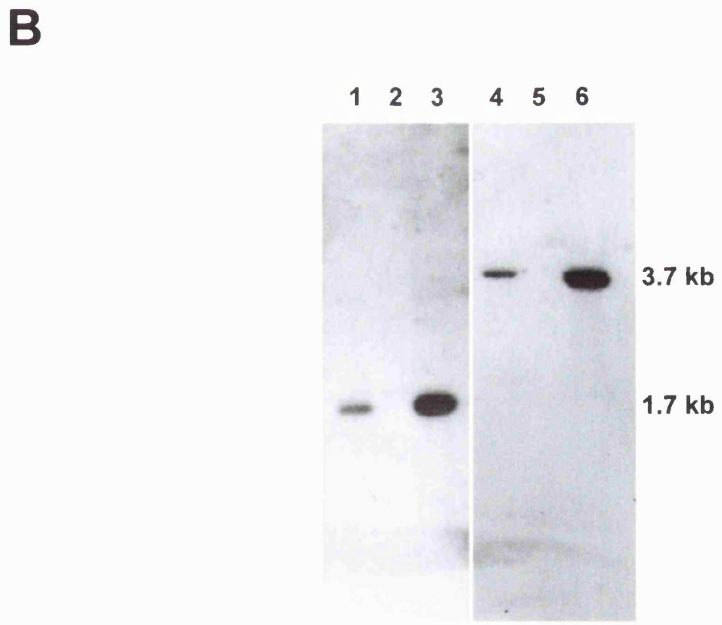

Figure 4.1 Southern Blot Analysis of *myo51Δ* Cells

(A) *myo51*$^{+}$ is encoded in three exons (white boxes). The region of exon 2 deleted in *myo51Δ* cells is shown in black. The *ura4*$^{+}$ gene used to delete *myo51*$^{+}$ is shown in grey. The 550 bp *ura4*$^{+}$ fragment used as a probe for Southern analysis is indicated with asterisks.

(B) Southern blot of genomic DNA from a *myo51::ura4*$^{+}$ / *myo51*$^{+}$ heterozygous diploid (lanes 1 and 4) and its *ura4*$^{-}$ (lanes 2 and 5) and *ura4*$^{+}$ (lanes 3 and 6) haploid progeny. Samples 1-3 were digested with EcoRV and samples 4-6 were digested with EcoRI.

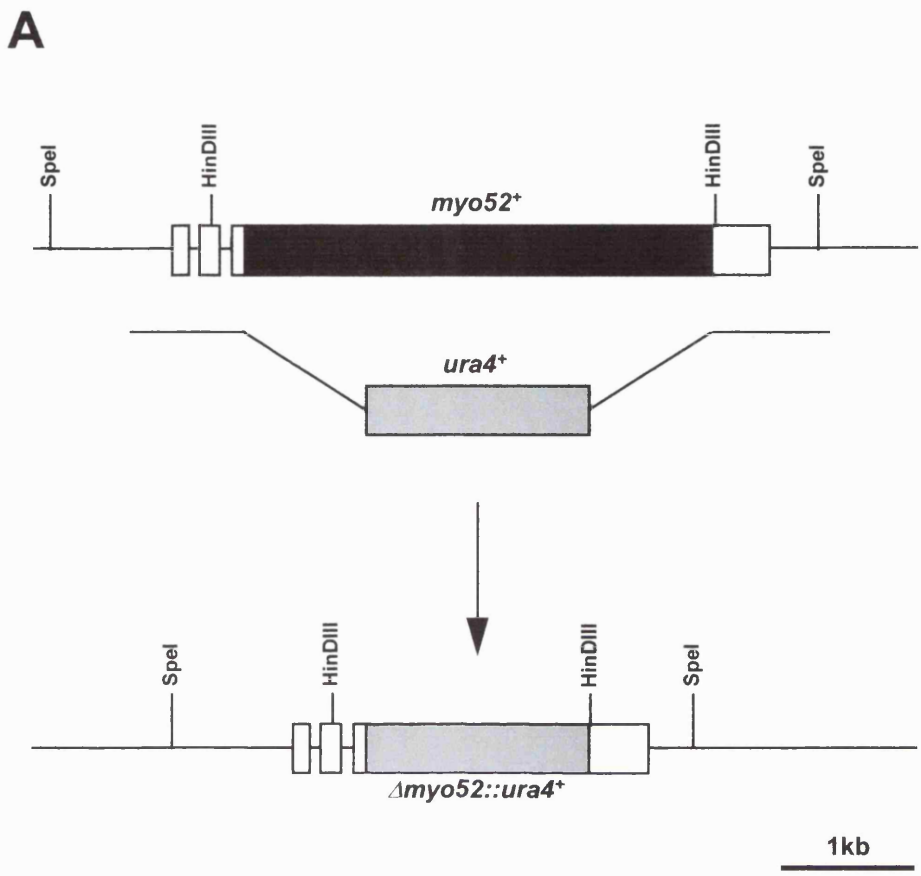

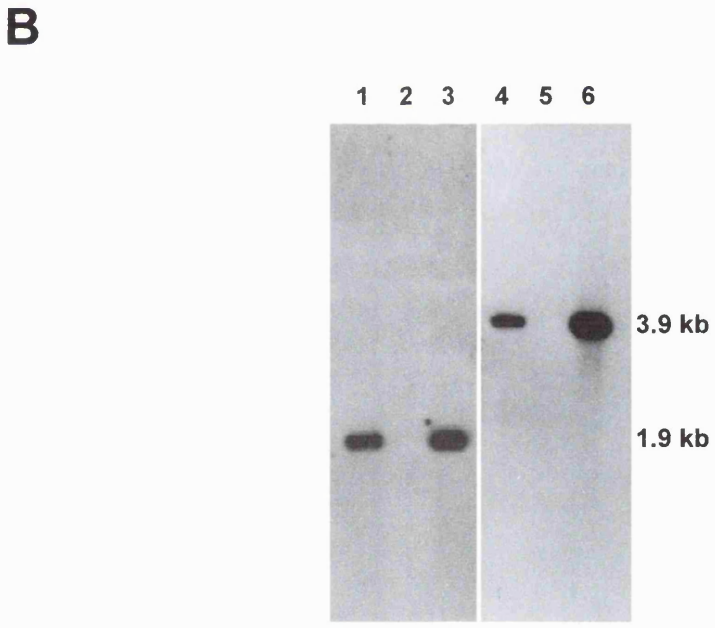

Figure 4.2 Southern Blot Analysis of *myo52Δ* Cells

(A) *myo52*$^+$ is encoded in three exons (white boxes). The region of exon 3 deleted in *myo52Δ* cells is shown in black. The *ura4*$^+$ gene used to delete *myo52*$^+$ is shown in grey. A 550 bp *ura4*$^+$ fragment was used as a probe for Southern analysis.

(B) Southern blot of genomic DNA from a *myo52::ura4*$^+$ / *myo52*$^+$ heterozygous diploid (lanes 1 and 4) and its *ura4*$^-$ (lanes 2 and 5) and *ura4*$^+$ (lanes 3 and 6) haploid progeny. Samples 1-3 were digested with HinDIII and samples 4-6 were digested with SpeI.

4.2.3 *myo51Δ* Cells are Viable and Display Wild Type Morphology

When the *myo51::ura4*$^+$ / *myo51*$^+$ heterozygous diploid transformant was sporulated and the spores from each tetrad dissected, it was found that all of the four haploid members from each tetrad were able to form colonies. The auxotrophy of each tetrad was tested and, as expected, the *ura4*$^+$ gene segregated in a ratio of 2:2. Thus, each tetrad gave rise to two viable *myo51Δ* colonies and two viable *myo51*$^+$ colonies. To see if there were any morphological difference between the *myo51Δ* and *myo51*$^+$ cells, each was grown to mid-exponential phase in YES medium at 25°C and stained with DAPI and Calcofluor to visualise nuclei and cell wall respectively by fluorescence microscopy. No difference in morphology was observed; both *myo51Δ* and *myo51*$^+$ cells maintained the rod shaped morphology that is characteristic of wild type fission yeast cells (Figure 4.3). To confirm that this was not a peculiarity of the diploid transformant that was chosen for analysis, other heterozygous *myo51::ura4*$^+$ / *myo51*$^+$ diploid transformants were analysed. All of these independent transformants also gave the same result: two viable *myo51Δ* and two viable *myo51*$^+$ progeny with wild type morphology from each tetrad dissected.

4.2.4 *myo52Δ* Cells are Viable but Display an Aberrant Cell Morphology

When the *myo52::ura4*$^+$ / *myo52*$^+$ diploid was examined by tetrad analysis, it too produced four viable colonies. However, for each tetrad dissected two of the colonies were smaller and grew more slowly. When these slow growing cells were examined under the microscope they appeared as cells with a short cell axis but with a wide diameter (Figure 4.3). Pear-shaped and completely round cells were also occasionally observed. The auxotrophy of the tetrads were tested and it was found that the *ura4*$^+$ gene segregated in a 2:2 ratio. All of the cells with the aberrant cell morphology segregated with the *ura4*$^+$ marker whereas the *ura4*$^-$ cells were of normal appearance. Thus, each tetrad produced two viable *myo52Δ* colonies with cells that display morphological defects and two *myo52*$^+$ colonies with cells of wild type appearance.

The same result was found when two other *myo52::ura4*$^+$ / *myo52*$^+$ diploid transformants were analysed.

Closer examination of *myo52Δ* cells showed that their mean dimension was 10.0 x 4.9 μm (n = 407) compared to the wild type dimension of 13.2 x 4.2 μm (n = 400). As well as having an abnormal morphology, *myo52Δ* cells also exhibited a difference in the frequency of septating cells. Whereas wild type cells had a septation index (percentage of cells with septa) of 5.3% (n = 400) *myo52Δ* cells had a septation index of 8.1% (n = 407), approximately 50% higher. In addition, approximately 1% of *myo52Δ* cells had two or more septa, a situation which was not found in wild type cells.

4.2.5 Actin Organisation in *myo51Δ* and *myo52Δ*

To investigate whether actin organisation was disrupted in *myo51Δ* and *myo52Δ* cells the actin cytoskeleton was stained with an anti-actin antibody and observed by immunofluorescence microscopy (Figure 4.4A). The actin cytoskeleton in *myo51Δ* cells was similar to that of wild type: *myo51Δ* cells displayed actin-staining at both ends in cells undergoing bipolar growth and monopolar staining of actin patches was observed in cells which had yet to activate growth at the new end. In *myo51Δ* cells undergoing mitosis the actin patches at the ends of the cells disappeared to form an equatorial ring of actin. These results indicate that the dynamics of actin relocation during major events in the fission yeast cell cycle (new end take off and mitosis) was unaffected in *myo51Δ* cells.

Actin-staining in *myo52Δ* cells showed that the actin cytoskeleton was disrupted. Unlike *myo51Δ* and wild type cells where fluorescence was localised at discrete places in the cell (i.e. at the poles and equator), fluorescence was observed throughout the cytoplasm. This diffuse staining pattern was more apparent in *myo52Δ* cells that were

completely round. In these round cells dots of fluorescence was found mostly at the cell periphery and the staining pattern followed the circular shape of the cells. In pear-shaped *myo52Δ* cells fluorescence was at its most intense at the pointed end. In some cells where the poles could not be easily defined, actin was present as random deposits. In cells where the rod-shaped morphology was still apparent, fluorescence was observed at both poles. In these rod-shaped cells fluorescence was more intense at one end than the other, enabling the old end to be distinguished from the new end. Thus, in *myo52Δ* cells the relationship between the old and new ends has not been completely lost. However, unlike wild type cells undergoing bipolar growth, where fluorescence is observed only at the cell poles, in *myo52Δ* fluorescence was also observed in the middle such that there was a continuity of actin-staining from one end of the cell to the other.

These results indicate that *myo52Δ* cells attempt to polarise their actin cytoskeleton, as exemplified by the intense fluorescence at the pointed end of pear-shaped cells and the bipolar distribution of actin patches in rod-shaped cells. However, the process of actin localisation is less efficient since actin-staining was observed in places other than the poles in growing cells or the equator in dividing cells.

4.2.6 Microtubule Oganisation in *myo51Δ* and *myo52Δ*

Microtubules play an important role in determining cell polarity in fission yeast (Sawin and Nurse, 1998). Therefore, *myo52Δ* cells were stained with an anti-tubulin antibody and observed by immunofluorescence microscopy to study whether the microtubule cytoskeleton was affected in these morphologically compromised cells.

The results of the microtubule-staining showed that *myo52Δ* cells contained short interphase microtubules that reflected the short size of these cells (Figure 4.4B). Unlike wild type cells, where microtubules were distributed in a parallel array along the length of the cell from one tip to the other, in *myo52Δ* the microtubules were often

obliquely oriented with microtubules extending diagonally from tip to tip. In some *myo52Δ* cells microtubules did not extend to the very tips of cells.

When *myo51Δ* cells were examined, the microtubule organisation was similar to that of wild type with interphase microtubules distributed in a parallel array along the length of cells extending to the tips. Both *myo51Δ* and *myo52Δ* had mitotic spindle microtubules that were indistinguishable from wild type cells (data not shown).

4.2.7 *myo52Δ* Cells are Temperature-Sensitive

Since *myo52Δ* cells produced smaller colonies upon tetrad analysis, a quantification of their growth rate was carried out in liquid YES medium and compared to that of wild type and *myo51Δ* cells (Figure 4.5A). Both *myo51Δ* and wild type cells grew at comparable rates with a generation time of approximately 3 hours at 29°C but the generation time of *myo52Δ* cells was much slower, taking over twice the time as wild type cells to double in population. When *myo51Δ*, *myo52Δ* and a strain deleted for a class II myosin (*myp2Δ*) were grown at various temperatures, it was found that the *myo52Δ* cells were unable to grow at 36°C (Figure 4.5B). *myo51Δ*, *myp2Δ* and wild type cells, however, were able to grow vigorously at all temperatures tested. Thus, *myo52Δ* cells are temperature-sensitive as well as slow-growing.

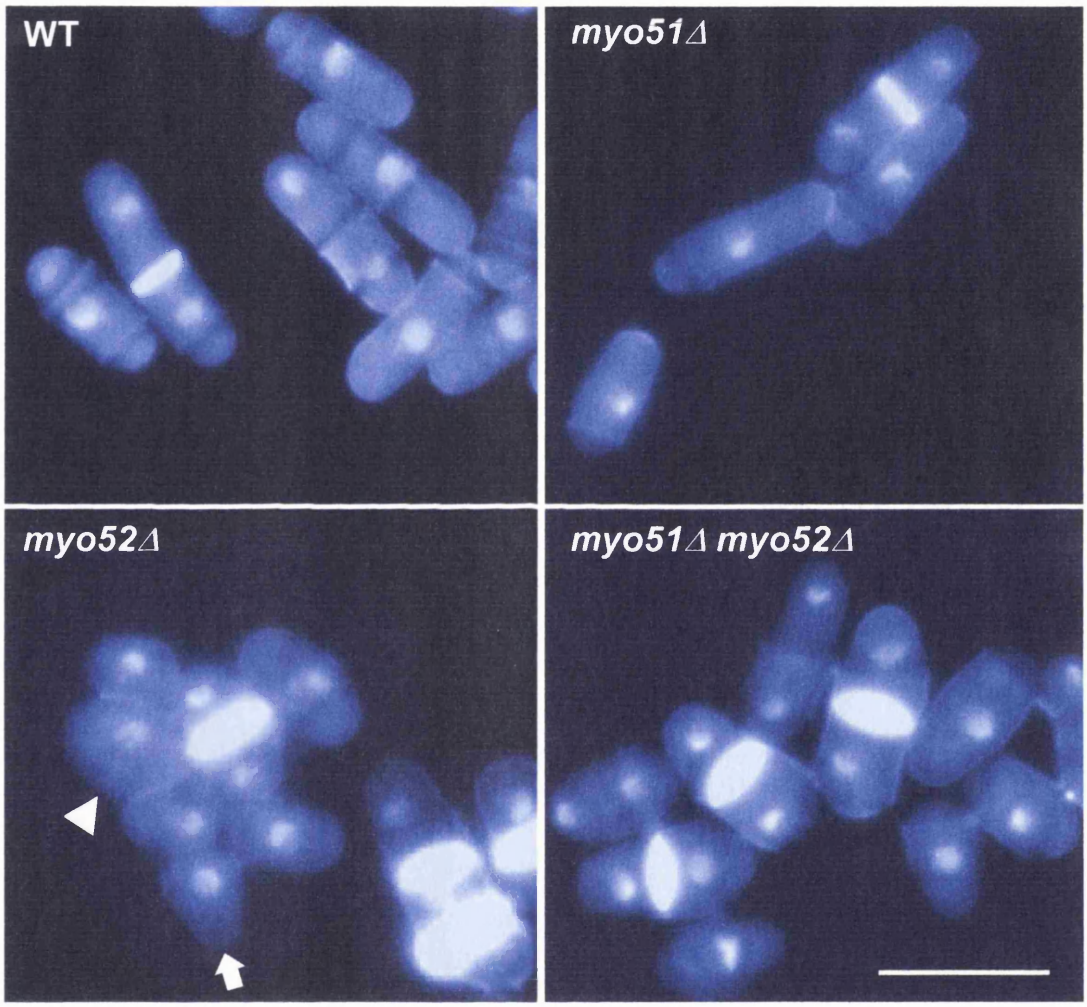

Figure 4.3 Morphology of *myo51Δ* and *myo52Δ* Cells

DAPI (nuclear) and Calcofluor (cell wall) staining of *myo51Δ* and *myo52Δ* cells show that *myo51Δ* cells maintain the rod-shaped morphology of wild type fission yeast cells whereas *myo52Δ* cells have a defect in cell polarity and septation. *myo52Δ* cells are fatter than wild type and in some cases appear completely round (arrow head) or pear-shaped (arrow), multiseptate cells are also observed. The *myo51Δ myo52Δ* double mutant is viable and has a similar phenotype to the *myo52Δ* single mutant. Cells were taken from cultures grown in liquid YES medium at 29°C. Bar = 10 μm.

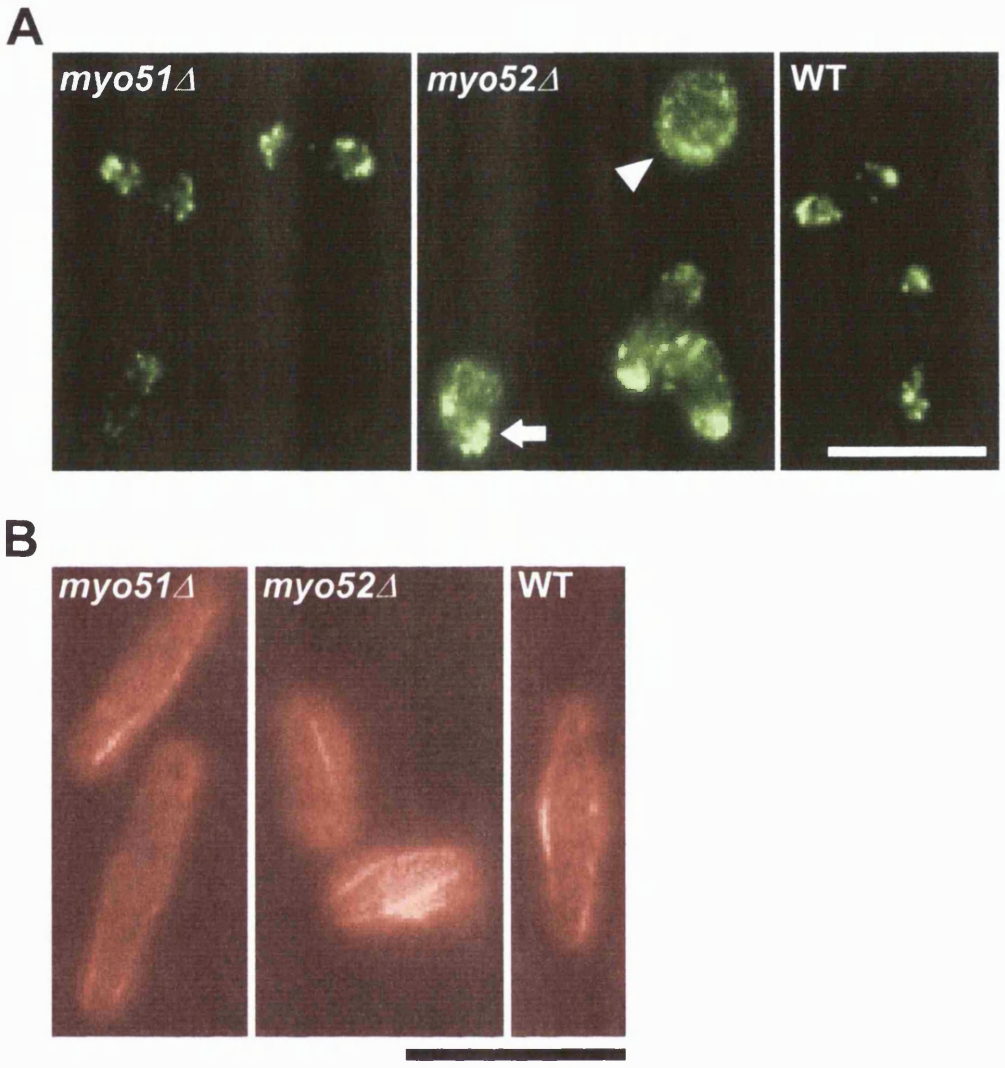

Figure 4.4 Actin and Microtubule Organisation in *myo51Δ* and *myo52Δ* Cells

(A) Immunofluorescence microscopy of *myo51Δ* and *myo52Δ* cells stained with anti-actin antibody. *myo52Δ* cells exhibit abnormal actin organisation with actin patches (green dots) diffusely distributed throughout the cytoplasm. This is particularly apparent in round cells (arrow head). Localised deposits of actin are also found in *myo52Δ* cells (arrow). *myo51Δ* cells, however, exhibit bipolar actin distribution similar to that of wild type cells undergoing bipolar growth.

(B) Immunofluorescence microscopy of *myo51Δ* and *myo52Δ* cells stained with anti-tubulin antibody. *myo51Δ* cells have an interphase array of microtubules similar to that of wild type with microtubules distributed along the length of cells. *myo52Δ* cells, however, have shorter microtubules that appear to be obliquely oriented.

Cells were processed for immunofluorescence microscopy from cultures grown in liquid YES medium at 29°C. Bar = 10 μm.

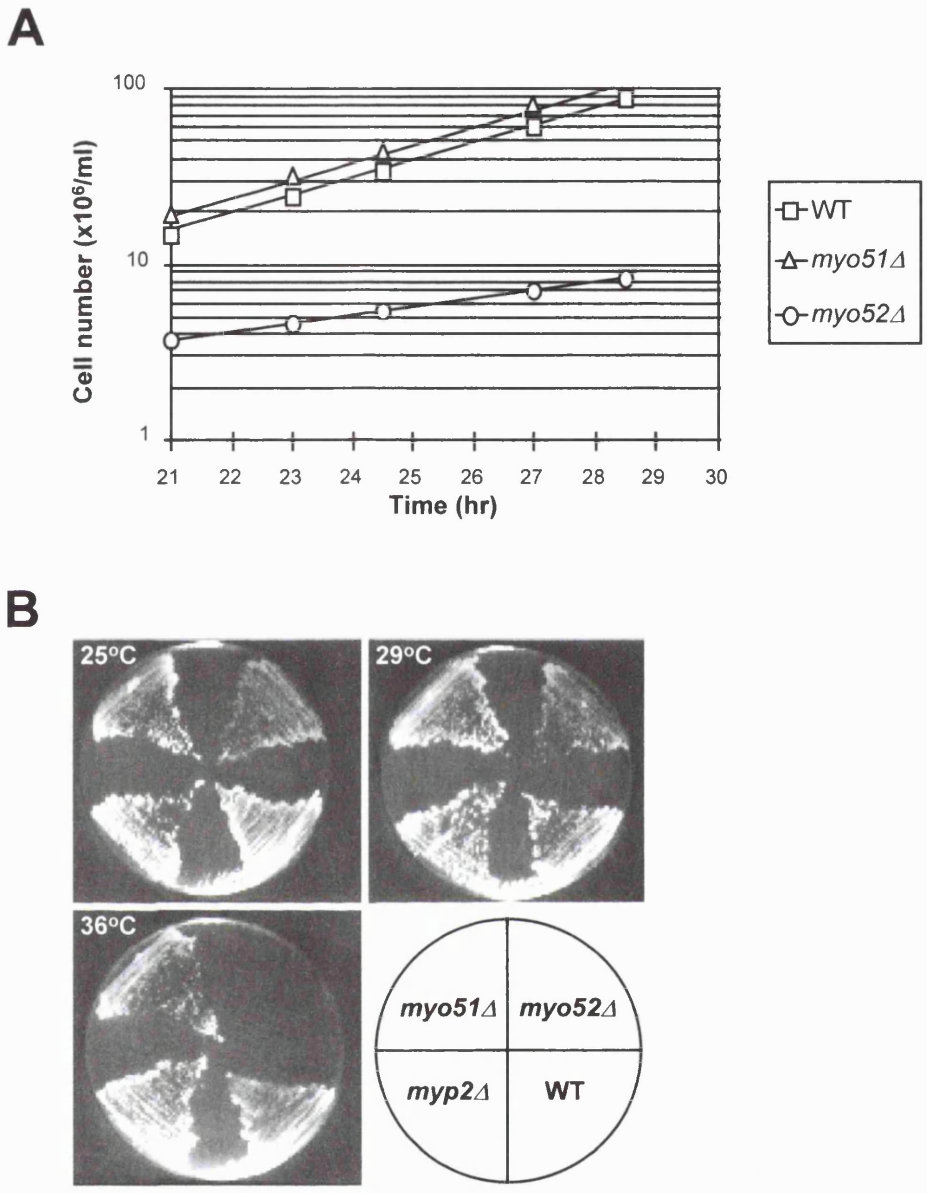

Figure 4.5 Growth of *myo51Δ* and *myo52Δ* Cells

(A) Log graph showing the increase in cell number with time of *myo51Δ*, *myo52Δ* and wild type fission yeast strains in liquid culture. The graph shows that *myo51Δ* cells grow at a similar rate to wild type but *myo52Δ* cells exhibit slow growth rates. Experiment performed in liquid YES medium at 29°C. Note, the graph shows the first results after 21 hours following inoculation of cells into medium.

(B) *myo52Δ* cells are temperature-sensitive at 36°C. At other temperatures they are able to grow, albeit slowly. Fission yeast cells deleted for the other class V myosin (*myo51Δ*), a class II myosin (*myp2Δ*) and a wild type strain are shown for comparison. Cells were incubated on YES plates for three days.

4.2.8 *myo51Δ* and *myo52Δ* Exhibit a Genetic Interaction with the Temperature-Sensitive Actin Mutant *cps8*$^-$ but Not with Each Other

Since *myo51Δ* cells were of normal appearance and showed wild type growth characteristics, no clue to the function of the gene was found. It was hoped that by performing yeast classical genetics with a variety of fission yeast mutants some clue might emerge to suggest a function for *myo51*$^+$ and *myo52*$^+$.

First, the functional redundancy of the two fission yeast class V myosins was tested by constructing a *myo51Δ myo52Δ* double mutant. Since both *myo51Δ* and *myo52Δ* parental strains were deleted using the *ura4*$^+$ gene, the *myo51Δ myo52Δ* double mutants were taken from tetrads that exhibited a non-parental ditype segregation of the loci concerned, that is, from tetrads that produced two *ura4*$^+$ (*myo51Δ myo52Δ*) and two *ura4*$^-$ (*myo51*$^+$ *myo52*$^+$) colonies. For all tetrads dissected, asci from the cross between the *myo51Δ* and *myo52Δ* parental strains resulted in four viable colonies. Microscopic inspection of each of the tetrads revealed two colonies of wild type phenotype and two colonies with cells of abnormal appearance, similar to that already described for *myo52Δ* (Figure 4.3). To confirm that the abnormal cells were the *myo51Δ myo52Δ* double mutant, the strain was back-crossed with a *ura4*$^-$ wild type strain which segregated out the *ura4*$^+$ markers at the *myo51Δ* and *myo52Δ* loci to produce tetrads some of which contained more than two *ura4*$^+$ progeny.

The fact that the phenotype of the *myo51Δ myo52Δ* double mutant was no different from that of the *myo52Δ* single mutant indicated that the *myo51*$^+$ and *myo52*$^+$ genes have non-overlapping functions and that these functions are not essential for the viability of the cell in normal growth conditions.

To investigate whether *myo51Δ* and *myo52Δ* exhibited a genetic interaction with the temperature-sensitive actin mutant *cps8*$^-$, *myo51Δ cps8*$^-$ and *myo52Δ cps8*$^-$ double

mutants were constructed. Tetrad analysis of the cross *myo51Δ* x *cps8*$^-$ produced four viable colonies at 25°C. However, when these colonies were subcultured onto YES plates and incubated at various temperatures it was found that the *myo51Δ cps8*$^-$ strain was unable to grow at 29°C, the permissive temperature for the growth of both parental strains (Figure 4.6A). This indicated that these mutations resulted in the synthetic lethality of the *myo51Δ cps8*$^-$ double mutant. Even at 25°C the *myo51Δ cps8*$^-$ double mutant was morphologically distinct from the *myo51Δ* and *cps8*$^-$ parental strains which were of wild type appearance at this temperature (Figure 4.6A). DAPI and Calcofluor staining of the *myo51Δ cps8*$^-$ double mutants showed that these cells were highly enlarged with multiple septa that failed to cleave. In this double mutant the septa also appeared abnormally formed. Rather than forming a single band that spanned the width of the cell as in wild type cells, septa were often obliquely oriented and sometimes failed to span the entire width of the cell. Occasionally, more than one septum emanated from the same point on the cell surface. Branching was observed when growth occurred at a point where septa failed to cleave.

Tetrad analysis of the cross *myo52Δ* x *cps8*$^-$ frequently produced incomplete tetrads. The colonies that failed to grow were of the *myo52Δ cps8*$^-$ genotype. Occasionally, viable *myo52Δ cps8*$^-$ colonies were observed but these were very slow growing and grew more slowly than the *myo52Δ* and *cps8*$^-$ single mutants. When these *myo52Δ cps8*$^-$ double mutants were subcultured onto YES plates at various temperatures no growth was observed at 29°C, the permissive temperature for the growth of the *myo52Δ* and *cps8*$^-$ single mutants (Figure 4.7A), indicating that *myo52Δ* also exhibited a synthetic lethal interaction with *cps8*$^-$. Even at 25°C growth of the *myo52Δ cps8*$^-$ double mutant was so slow that a streaking pattern was not observed.

DAPI and Calcofluor staining of the *myo52Δ cps8*$^-$ double mutant grown at 25°C showed that these cells were enlarged with a rounded shape (Figure 4.7B). The septa in these cells were misplaced and did not form in the middle. This resulted in some

cells with multiple nuclei and some which were anucleate. Often the septa were incompletely formed, resulting in deposits of septal material along the sides of cells.

4.2.9 *myo52Δ* Cells do Not Grow Well After Prolonged Periods in the Same Medium

During the course of this study it was unintentionally discovered that *myo52Δ* cells died if they were not replated frequently. Usually, fission yeast cells were subcultured approximately every four days onto a new YES plate so that a fresh culture of cells was available for experiments. However, when the *myo51Δ* and *myo52Δ* strains were left for more than a week before being subcultured onto a new YES plate, the *myo52Δ* strain was unable to form colonies (Figure 4.8).

This result was verified by inoculating *myo52Δ* and control strains which had been incubated for a week in YES into fresh liquid YES medium and following the increase in cell number. No increase in cell number was observed in *myo52Δ* cells whereas *myo51Δ* and wild type cells under the same conditions exhibited growth with a generation time of 3 hours at 29°C.

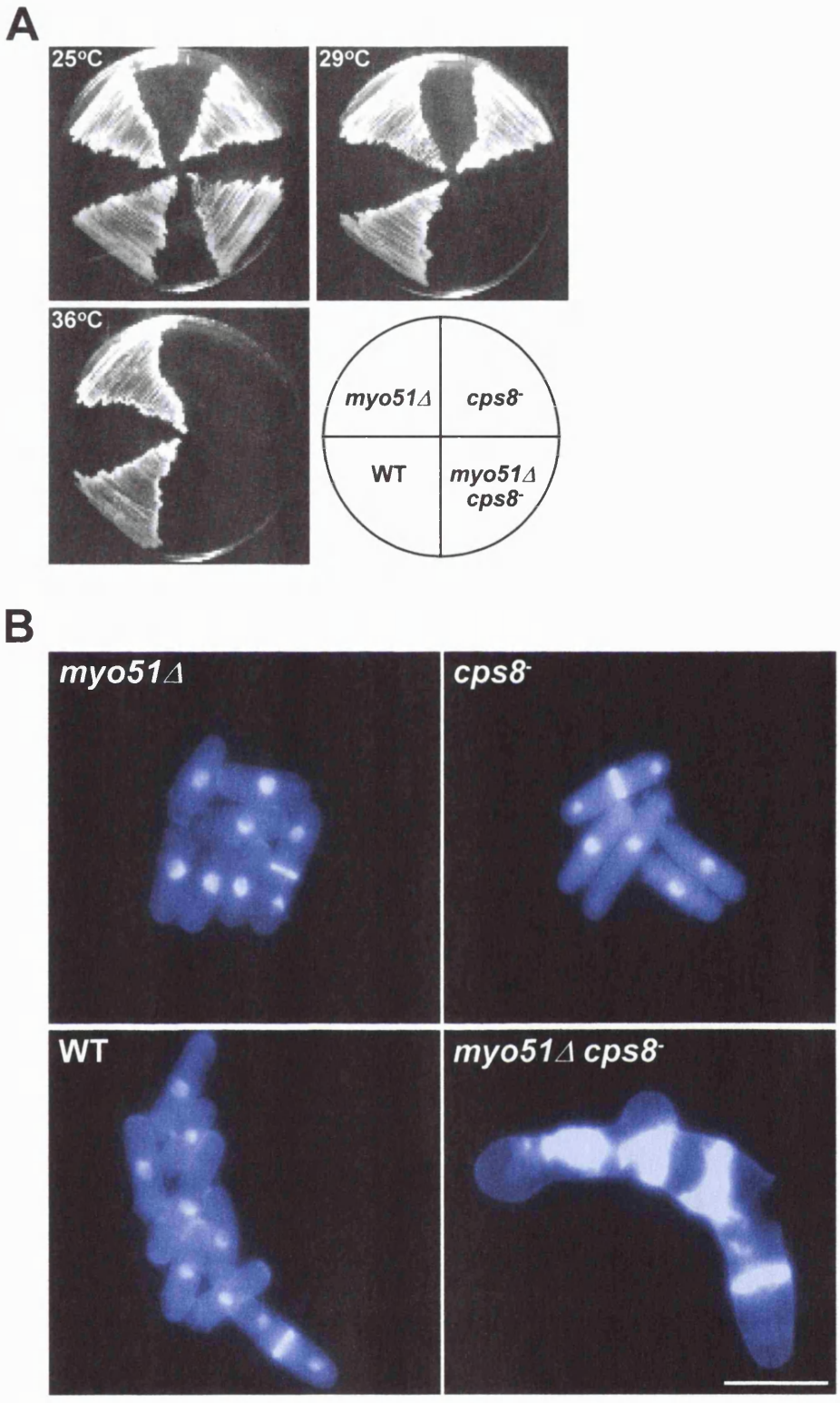

Figure 4.6 *myo51Δ* Exhibits a Genetic Interaction with the Temperature-Sensitive Actin Mutant *cps8-*

(A) The *myo51Δ cps8-* double mutant is unable to grow at 29°C a temperature which is permissive for the growth of *myo51Δ* and *cps8-* single mutants. Cells were incubated on YES plates for three days.

(B) Even at 25°C, DAPI and Calcofluor staining show that the *myo51Δ cps8-* double mutant cells are highly enlarged with multiple, thickened septa. Cells were taken from cultures grown in liquid YES medium grown at 25°C. Bar = 10 μm.

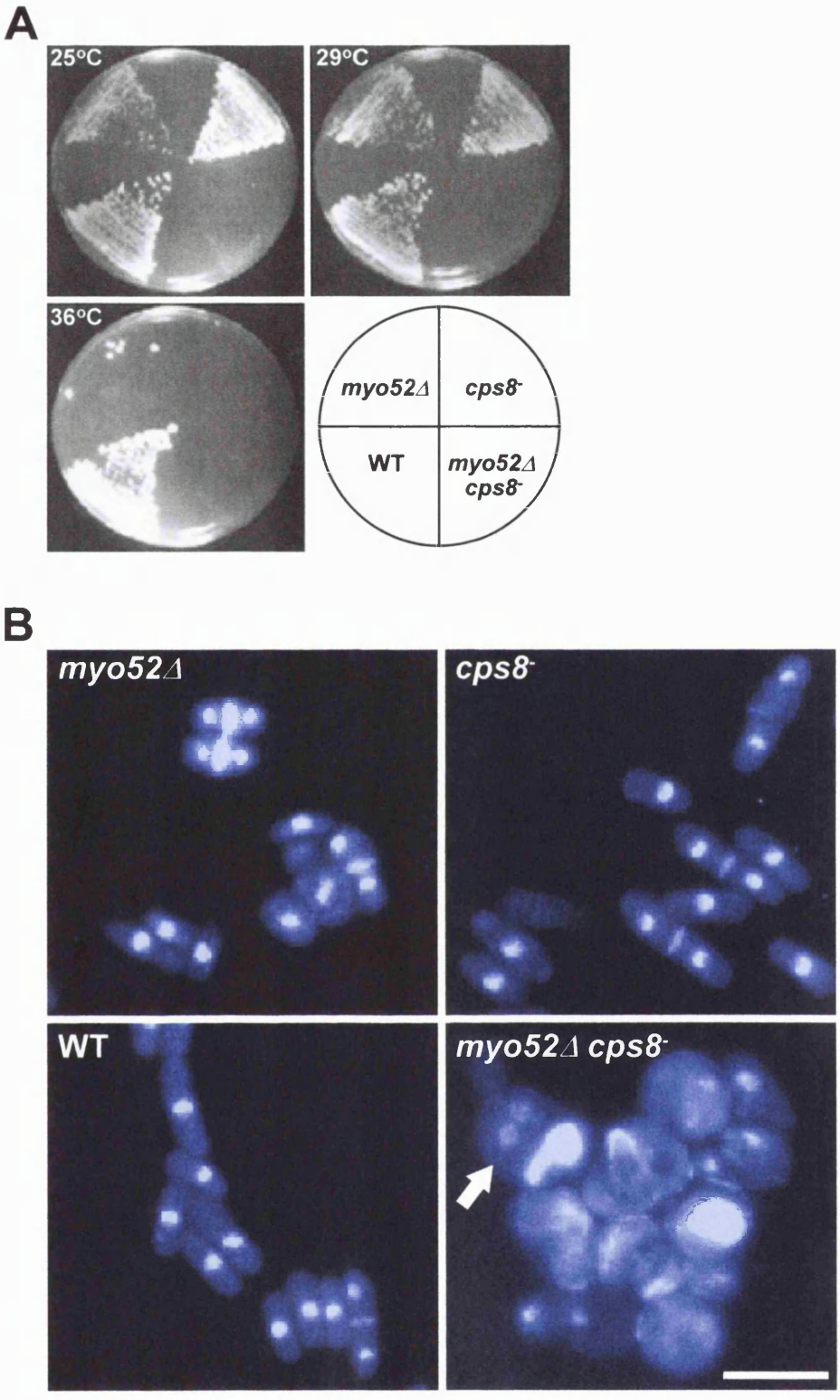

Figure 4.7 *myo52Δ* Exhibits a Genetic Interaction with the Temperature-Sensitive Actin Mutant *cps8-*

(A) The growth of the *myo52Δ cps8-* double mutant is virtually abolished even at 25°C, a temperature which is permissive for the growth of *myo52Δ* and *cps8-* single mutants. Cells were incubated on YES plates for three days.

(B) DAPI and Calcofluor staining show that the *myo52Δ cps8-* double mutant cells are highly enlarged and round with multiple nuclei (arrow). Cells were taken from cultures grown in liquid YES medium grown at 25°C. Bar = 10 μm.

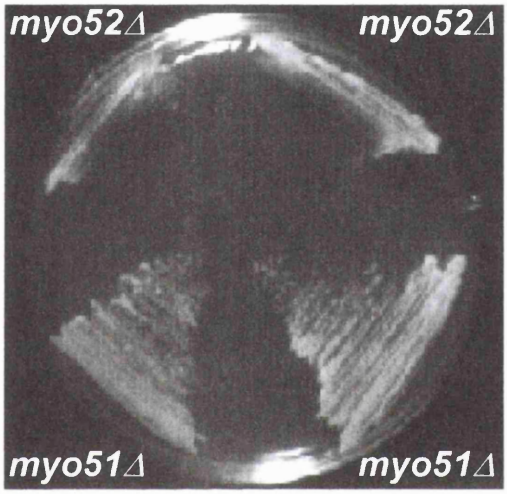

Figure 4.8 *myo52Δ* Cells do not Grow Well After Prolonged Periods in the Same Medium

Two *myo51Δ* and two *myo52Δ* strains were subcultured onto a fresh YES plate from a culture that have been incubating at 29°C for eight days. When this new plate was incubated the *myo52Δ* cells grew poorly. The photograph shows the plate after three days incubation at 29°C.

4.3 DISCUSSION

Deletion of *myo51*$^+$ and *myo52*$^+$ does not affect the viability of cells under laboratory conditions. However, *myo52*$^+$ is required for the efficient growth of fission yeast cells since *myo52Δ* cells display slow growth rates at 25°C and 29°C in comparison to wild type and *myo51Δ* cells. At 36°C *myo52Δ* cells are unable to grow. In addition to their slow growth rates, *myo52Δ* cells have morphological defects with cells that are pear-shaped and round, indicating that *myo52*$^+$ has a role in cell polarity. However, complete loss of cell polarity was not observed since rod-shaped cells were still present although these cells were shorter and broader than wild type cells. This is in contrast to the *orb* class of fission yeast mutants which displays a complete loss of polarity at the restrictive temperature (Verde et al., 1995).

Actin-staining of *myo52Δ* cells showed a close correlation between cell morphology and actin distribution. When actin was delocalised, round cells were observed but when actin was partially localised, pear-shaped and rod-shaped cells were observed. Marks and Hyams (1985) have shown that the distribution of actin and cell growth are closely correlated. During tip growth actin patches are found at the growing poles whereas in cells undergoing cytokinesis an actin ring is found at the equator that anticipates the formation of the division septum. Perhaps the morphological defects observed in *myo52Δ* cells reflects their inability to polarise the actin cytoskeleton. Alternatively, the disruption in the actin cytoskeleton may be secondary to the growth defects of *myo52Δ* cells. Observations in *cdc3*$^+$ and *cdc8*$^+$, which encode profilin and tropomyosin respectively (Balasubramanian et al., 1992, 1994), may be useful in distinguishing between these two possibilities. The function of *cdc3*$^+$ and *cdc8*$^+$ has been suggested to be required for the general organisation of the actin cytoskeleton (Chang and Nurse, 1996) because mutants in these genes display abnormalities in the distribution of actin patches and fail to assemble an actin ring. Consequently, *cdc3*$^-$ and *cdc8*$^-$ mutants die as cells fail to form a division septum (Balasubramanian et al., 1992, 1994). In contrast to these mutants *myo52Δ* cells are

able to form septa, indicating at least, that Myo52 is not essential for the organisation of the actin ring which guides the formation of the division septum.

Although *myo52Δ* cells exhibit morphological defects resulting in round cells in the most severe cases, in rod-shaped *myo52Δ* cells the old and new ends could still be distinguished as judged by the differential distribution of actin patches. However, actin patches were also present other than at the growing poles even in these rod-shaped cells, indicating that actin was not efficiently localised in all *myo52Δ* cells.

As well as having a partially organised actin cytoskeleton, microtubule-staining of *myo52Δ* cells showed that the interphase microtubule arrays were also disorganised as they existed as short microtubules that were obliquely oriented with respect to the main axis of fission yeast cells. Spindle microtubules, however, appeared unaffected in *myo52Δ* cells since they were able to form and segregate chromosomes during mitosis. *myo52Δ* cells also retained the ability to recognise the cell middle since a septum was always formed exactly midway between the ends of both rod-shaped and pear-shaped cells. Cell division in round cells also produced daughter cells of equal size. However, a proportion of *myo52Δ* cells contained two or more septa with a nucleus in each cellular compartment indicating that the *myo52*$^+$ gene might play a role for the proper synthesis or cleavage of the septum.

Conjugation of *myo51Δ* and *myo52Δ* cells showed that neither *myo51*$^+$ nor *myo52*$^+$ genes were essential for mating since the null mutants were able to mate with each other and to other fission yeast mutants. Neither were they required for spore germination since spores from the cross between *myo51Δ* and *myo52Δ* germinated normally. Tetrad analysis of crosses between the null mutants yielded four viable progeny. The phenotype of *myo51Δ myo52Δ* double mutant was indistinguishable from the *myo52Δ* single mutant indicating that *myo51*$^+$ and *myo52*$^+$ have non-overlapping functions in fission yeast. This is in contrast to the two fission yeast

class II myosins, *myo2*$^+$ and *myp2*$^+$, which are both involved in cytokinesis and mutants in these genes have been shown to exhibit a synthetic lethal interaction (Bezanilla and Pollard, 2000; Motegi et al., 2000; Mulvihill et al., 2000).

In budding yeast, the class V myosins, Myo2 and Myo4, have been implicated in the directed movement of different types of cargo to target sites in the cell. Myo2 has been reported to be responsible for the targeting of vacuoles and secretory vesicles to the growing bud (Hill et al., 1996; Catlett and Weisman, 1998; Pruyne et al., 1998; Schott et al., 1999) whereas Myo4 has been implicated in the movement of *ASH1* mRNA to the bud to repress mating-type switching in daughter cells (Bobola et al., 1996; Jansen et al., 1996; Long et al., 1997; Takizawa et al., 1997; Munchow et al., 1999). It is interesting to speculate that the fission yeast class V myosins, Myo51 and Myo52, might also operate in the same fashion transporting different types of cargo around the cell. This might explain why the *myo51Δ myo52Δ* double deletion shows no more severe phenotype than the single null mutants particularly since the budding yeast *myo2 myo4* double mutants also show no genetic interaction (Haarer et al., 1994).

Both *myo51Δ* and *myo52Δ*, however, exhibit a synthetic lethal interaction with the temperature-sensitive actin mutant *cps8*$^-$ (Ishiguro and Kobayashi, 1996) at 29°C indicating that the function of these class V myosins is required when the actin cytoskeleton is compromised. At 25°C the *myo52Δ cps8*$^-$ double mutants were barely viable and displayed morphological defects more severe than the *myo52Δ* and *cps8*$^-$ single mutants alone resulting in highly enlarged and rounded cells. This indicates that even at the permissive temperature of 25°C the *cps8*$^-$ mutation is such that the actin cytoskeleton or actin dynamics is altered in some way that exacerbates the polarity defect of *myo52Δ* cells.

The observation that *myo52Δ* cells are unable to survive prolonged incubation in the same medium suggests that these cells are sensitive to the condition of the medium. Interestingly, deletion of one of the fission yeast class II myosins, *myp2*$^+$, causes *myp2Δ* cells to be sensitive to different types of media (Bezanilla et al., 1997; Motegi et al., 1997). In rich medium these cells grow and divide like wild type cells but in minimal medium or malt extract medium the *myp2Δ* mutant displays cytokinetic defects (Bezanilla et al., 1997). In addition, *myp2Δ* cells exhibit a heightened sensitivity to salts, being unable to grow in medium containing 0.2 M magnesium chloride (Motegi et al., 1997). These results have led to the suggestion that Myp2 is required in conditions of stress and that the protein is dispensable in favourable growing conditions (Bezanilla et al., 1997; Motegi et al., 1997). Myo52 on the other hand is not a dispensable protein since *myo52Δ* cells are temperature-sensitive and displays morphological defects in all tested growing conditions. Furthermore, the morphological defects of these cells are not alleviated by the addition of 1 M sorbitol to provide osmotic stability (Win et al., 2001). Like *myp2Δ*, *myo52Δ* cells are also sensitive to medium containing 0.2 M magnesium chloride (T. Z. Win, unpublished results). The findings that *myo52Δ* cells are temperature and salt-sensitive, together with the observation that these cells are unable to survive prolonged incubation in the same medium suggests that *myo52Δ* cells are highly sensitive to environmental conditions.

Chapter 5
Overexpression of *myo51*$^{+}$ and *myo52*$^{+}$

5.1 INTRODUCTION

Another way by which an aspect of a gene's function can be determined is through carrying out gene overexpression studies. This technique complements that of gene inactivation because it investigates the effects of a functional gene when the gene dosage is increased. Overexpression studies, when combined with data from other experimental procedures, has been successfully applied to understand the role of many fission yeast genes. For example, it was found that overexpression of *cdc7*$^+$ (Fankhauser and Simanis, 1994) and *spg1*$^+$ (Schmidt et al., 1997) caused cells to form multiple septa, implicating these genes in the positive regulation of septum formation whereas overexpression of *byr4*$^+$ (Song et al., 1996) inhibited cytokinesis implicating *byr4*$^+$ in the negative regulation of cytokinesis.

Several promoters are available for the expression of genes in fission yeast, these include the SV40, *adh* and *nmt1*$^+$ expression systems (Forsburg, 1993). Recently, an inducible gene expression system has been reported (Iacovoni et al., 1999) which utilises the *inv1*$^+$ promoter for the expression of genes in glucose deficient medium. The most common method of gene overexpression, however, employs the thiamine-regulatable *nmt1*$^+$ promoter, so called because it produces no message in the presence of thiamine (Maundrell, 1990) and therefore offers a way in which gene expression can be controlled. The induced *nmt1*$^+$ promoter is a powerful promoter of transcription, which is up to 7 and 30 times more active at initiating transcription than the *adh* and SV40 constitutive promoters respectively (Basi et al., 1993). However, a similar study by Forsburg (1993) has reported that the *nmt1*$^+$ promoter is about 2 and 900 times more active than the the *adh* and SV40 constitutive promoters respectively. Comparison of the *nmt1*$^+$ and *inv1*$^+$ promoters show that they exhibit similar levels of activity in transcription initiation (Iacovoni et al., 1999).

As the original *nmt1*$^+$ promoter was highly active in the absence of thiamine and was not completely repressed in its presence, Basi et al. (1993) have created attenuated versions of *nmt1*$^+$ to provide varying levels of gene expression. These modifications

have been incorporated to create the pREP family of expression plasmids which include pREP1 (containing the wild type *nmt1*$^+$ promoter), pREP41 and pREP81 plasmids which provide high, moderate and low levels of gene expression respectively (Basi et al., 1993). These plasmids have been further modified by others (Craven et al., 1998) by incorporating sequences into the plasmid so that the expressed proteins are tagged with short peptides such as the myc and haemagglutinin epitopes. This kind of strategy enables tagged proteins to be analysed using well characterised commercially available antibodies when specific antibodies to the protein of interest have not been raised.

In this chapter I report the cloning of *myo51*$^+$ and *myo52*$^+$ into pREP1 and pREP41myc plasmids containing the thiamine-repressible *nmt1*$^+$ promoter. I will present evidence that the cloned genes are correctly expressed from these plasmids by their functional complementation of the *myo51Δ* and *myo52Δ* phenotypes. Following this, their overexpression in wild type cells will be presented and discussed.

5.2 RESULTS

5.2.1 Cloning of *myo51*$^+$ and *myo52*$^+$ into pREP Expression Vector

The *myo51*$^+$ gene was cloned by PCR of wild type genomic DNA using the primers c2D10-start and c2D10-end (Materials and Methods Table 2.3). The forward primer (c2D10-start) contained an engineered SalI restriction site immediately upstream of the *myo51*$^+$ start codon and the reverse primer (c2D10-end) contained an engineered BamHI restriction site to facilitate cloning into plasmids. This produced a 4.5 kb PCR product which was subsequently cloned into the SalI and BamHI unique restriction sites of pREP1 and pREP41myc to yield pREP1-*myo51*$^+$ and pREP41myc-*myo51*$^+$ plasmids (Figure 5.1). The junction between plasmid DNA and the start of the *myo51*$^+$ gene showing that the gene was expressed in the correct reading frame is shown in Figure 5.2A.

Similarly, the *myo52*$^+$ gene was cloned by PCR using the primers c1919-start and c1919-end both of which contained an engineered SalI restriction site. A 4.8 kb PCR product was obtained and cloned into the SalI restriction site of pREP41myc plasmid. The orientation of the *myo52*$^+$ gene in pREP41myc was verified by restriction analysis and those that contained the gene in the correct orientation (pREP41myc-*myo52*$^+$) were used in experiments. The junction between plasmid DNA and the start of the *myo52*$^+$ gene is shown in Figure 5.2B.

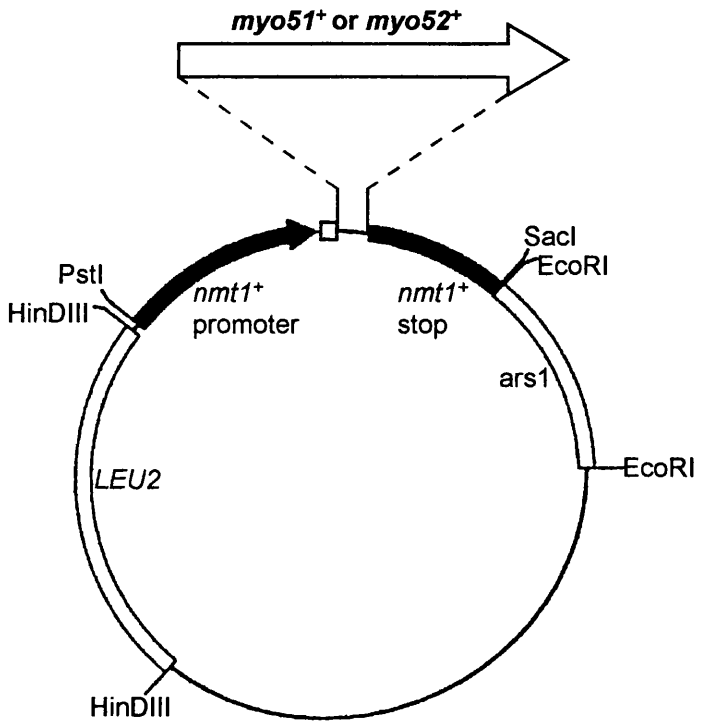

Figure 5.1 Cloning of *myo51*$^+$ and *myo52*$^+$ into pREP1 and pREP41myc Expression Vectors

myo51$^+$ and *myo52*$^+$ were both cloned into the multiple cloning site which lies between the *nmt1*$^+$ promoter and stop sequences of pREP41myc plasmid. The grey box represents the location of the coding sequence for the myc epitope. The same approach was also used to clone *myo51*$^+$ into pREP1 plasmid. The *LEU2* gene provided the nutritional marker to select for transformants. Figure modified from Craven et al. (1998).

A

DNA 5' ATG TCG ACT **ATG AGT CAT GCA AGA TTA**.....3'

PROTEIN NH_2 M S T **M S H A R L**.....COOH

B

DNA 5' ATG TCG ACC **ATG ACA TCG GGG ATT TAT**.....3'

PROTEIN NH_2 M S T **M T S G I Y**.....COOH

Figure 5.2 *myo51*$^+$ and *myo52*$^+$ are Expressed in the Correct Reading Frame

(A) The junction between plasmid DNA and the start of the *myo51*$^+$ gene in pREP1-*myo51*$^+$ and pREP41myc-*myo51*$^+$. The *myo51*$^+$ coding sequence and the corresponding Myo51 protein sequence are shown in bold.

(B) The junction between plasmid DNA and the start of the *myo52*$^+$ gene in pREP41myc-*myo52*$^+$. The *myo52*$^+$ coding sequence and the corresponding Myo52 protein sequence are shown in bold.

For both (A) and (B) the SalI restriction site of plasmid DNA is underlined and the few amino acid residues that are fused at the N-terminus of Myo51 and Myo52 are also shown.

5.2.2 *myo51*$^+$ Gene is Correctly Expressed from Plasmids

The first fission yeast class V myosin to be cloned was *myo51*$^+$. It was decided to clone the gene in both pREP1 and pREP41myc, because they provided two different levels of gene expression, high levels of expression from pREP1 and moderate levels of expression from pREP41myc. Different expression levels were needed in an attempt to create the physiological concentrations of Myo51 in the cell to test whether the cloned gene was functional. This was performed by transforming the plasmids bearing the *myo51*$^+$ gene into the *myo51Δ cps8*$^-$ double mutant to test their ability to complement the synthetic lethality of the double mutant at 29°C. It was found that both pREP1-*myo51*$^+$ and pREP41myc-*myo51*$^+$ were able to rescue the lethality of the double mutant at 29°C in minimal medium supplemented with thiamine whereas control cells transformed with plasmids not carrying the *myo51*$^+$ gene were not able to grow at this temperature (Figure 5.3A). This indicated that both pREP1-*myo51*$^+$ and pREP41myc-*myo51*$^+$ were expressed even in the presence of thiamine, suggesting that the *nmt1*$^+$ promoter was not fully repressed and was initiating some basal level of transcription. Furthermore, this basal level of transcription from both the high-strength and moderate-strength *nmt1*$^+$ promoters was enough to create the approximate physiological concentrations of Myo51 protein to rescue the *myo51Δ cps8*$^-$ double mutant but did not reach high enough levels to cause toxicity.

In addition to complementing the lethality of the double mutant at 29°C, both pREP1-*myo51*$^+$ and pREP41myc-*myo51*$^+$ also reversed the morphological defects of the double mutant (Figure 5.3B). Empty vector control cells revealed the septation and branching defects typical of the *myo51Δ cps8*$^-$ double mutant. The fact that both pREP1-*myo51*$^+$ and pREP41myc-*myo51*$^+$ rescued the temperature-sensitivity and morphological defects of the double mutant indicated that the *myo51*$^+$ gene was correctly expressed from these plasmids and that the expressed protein was functional.

To confirm that the phenotype of the double mutant was rescued because of the presence of the pREP1-*myo51*$^+$ or pREP41myc-*myo51*$^+$ plasmids and not because of a suppressing mutation in the genome, plasmid loss was promoted in these cells. This was carried out by plating plasmid-bearing cells on non-selective medium (YES) seven times at 25°C by which time they had lost their plasmid because they were unable to grow on medium that selected for the plasmid. These cells were unable to grow at 29°C and when examined microscopically were found to show the morphological defects of the *myo51Δ cps8*$^-$ double mutant. Thus, the complementing activity of the double mutant resided in the pREP1-*myo51*$^+$ and pREP41myc-*myo51*$^+$ plasmids and not from a suppressing mutation in the genome.

5.2.3 *myo52*$^+$ Gene is Correctly Expressed from Plasmids

Since *myo51*$^+$ was expressed in thiamine-supplemented medium from both the high and moderate-strength *nmt1*$^+$ promoters it was decided to clone the second class V myosin, *myo52*$^+$, into pREP41myc only. This was because the plasmid provided a way of tagging the Myo52 protein with two copies of the myc epitope and thus allowing the protein to be localised in the cell using anti-myc antibodies by immunofluorescence microscopy and also allowed *myo52*$^+$ to be overexpressed from the *nmt1*$^+$ promoter when thiamine is removed from the culture medium.

To test that pREP41myc-*myo52*$^+$ correctly expressed *myo52*$^+$, the plasmid was transformed into *myo52Δ* cells and the ability of the plasmid to rescue the morphological defects and temperature-sensitivity of the *myo52Δ* strain was assayed. Upon transformation with pREP41myc-*myo52*$^+$, *myo52Δ* cells assumed a rod-shaped morphology and were able to grow at 36°C whereas empty vector control cells retained the typical *myo52Δ* morphology and temperature-sensitivy (Figure 5.4). This indicated that the potein expressed by pREP41myc-*myo52*$^+$ was fully functional.

To confirm that the complementing activity resided in pREP41myc-*myo52*$^+$ and not from a suppressing mutation in the genome, cells were subcultured onto YES until they had lost the plasmid. When these cells were observed microscopically and tested for their ability to grow at 36°C, they were found to have morphological defects and were temperature-sensitive. Thus, the *myo52Δ* strain used in these experiments did not pick up a suppressing mutation that allowed it to grow like wild type cells.

5.2.4 Overexpression of *myo51*$^+$ Produces Elongated Multinucleate Cells

To overexpress *myo51*$^+$, wild type cells transformed with pREP41myc-*myo51*$^+$ were grown in liquid minimal medium in the absence of thiamine for 24 hours. Maximum induction of the *nmt1*$^+$ promoter does not take place until 16 hours after inoculation into thiamine-free medium (Maundrell, 1990). After allowing the *myo51*$^+$ gene to overexpress and accumulate more than physiological levels of Myo51 protein, cells were fixed and stained with DAPI and Calcofluor. Fluorescence microscopy showed that *myo51*$^+$ overexpressing cells were longer than control cells grown in the presence of thiamine which displayed wild type morphology (Figure 5.5A). Cells of varying lengths were often observed, which may reflect the variation in *myo51*$^+$ expression as a consequence of differences in plasmid copy number between cells. In some cases, cells of up to 30 μm in length was observed, approximately three times the size of a wild type cell. DAPI and Calcofluor staining revealed the presence of up to four nuclei in the most highly elongated cells. The presence of multiple nuclei probably resulted from the failure of these cells to form a proper division septum between daughter nuclei after each mitosis. This is shown in Figure 5.5A by the absence of septum staining in some cells and the formation of improperly organised or oriented septa in others.

The morphological defects caused by *myo51*$^+$ overexpression had an inhibitory effect on cell growth since cells grown in the absence of thiamine grew at a slower rate than those grown in the presence of thiamine. Figure 5.5B shows that control cells grown in

the presence of thiamine doubled in population every three hours whereas cells overexpressing *myo51*$^+$ grew with a generation time of approximately six hours.

5.2.5 Overexpression of *myo52*$^+$ Produces Branched Cells with Thickened Septa

To overexpress *myo52*$^+$ wild type cells transformed with pREP41myc-*myo52*$^+$ were grown in liquid minimal medium under conditions that induced the *nmt1*$^+$ promoter. Following 24 hours growth cells were stained with DAPI and Calcofluor. Fluorescence microscopy revealed a mixture of cell morphology with some cells that displayed a branched phenotype whilst others were rod-shaped in appearance (Figure 5.6A). Analysis of the branched cells showed that branching occurred at points where the septum failed to cleave and as a consequence, protrusions were made as daughter cells reinitiated tip growth despite their failure to separate.

Overexpression of *myo52*$^+$ also resulted in cells with multiple septa. The septa that formed separated daughter nuclei into different cellular compartments such that a single nucleus was present in each compartment of a multiseptate cell. Thus, *myo52*$^+$ overexpression did not appear to affect septum placement. However, Calcofluor staining indicated that some septa were abnormally thick as judged by the intense fluorescence from the septal bands. Interestingly, the most prominent septum in multiseptate cells was the first one that formed whereas subsequent septa were less prominent. This might indicate that components of septum deposition were unevenly distributed in the construction of different septa in multiseptate cells or that subsequent septa were still in the process of being made.

Growth studies showed that, unlike cells grown in the presence of thiamine which doubled in population approximately every 3 hours, cells overexpressing *myo52*$^+$ showed little increase in cell number in thiamine-free medium (Figure 5.6B).

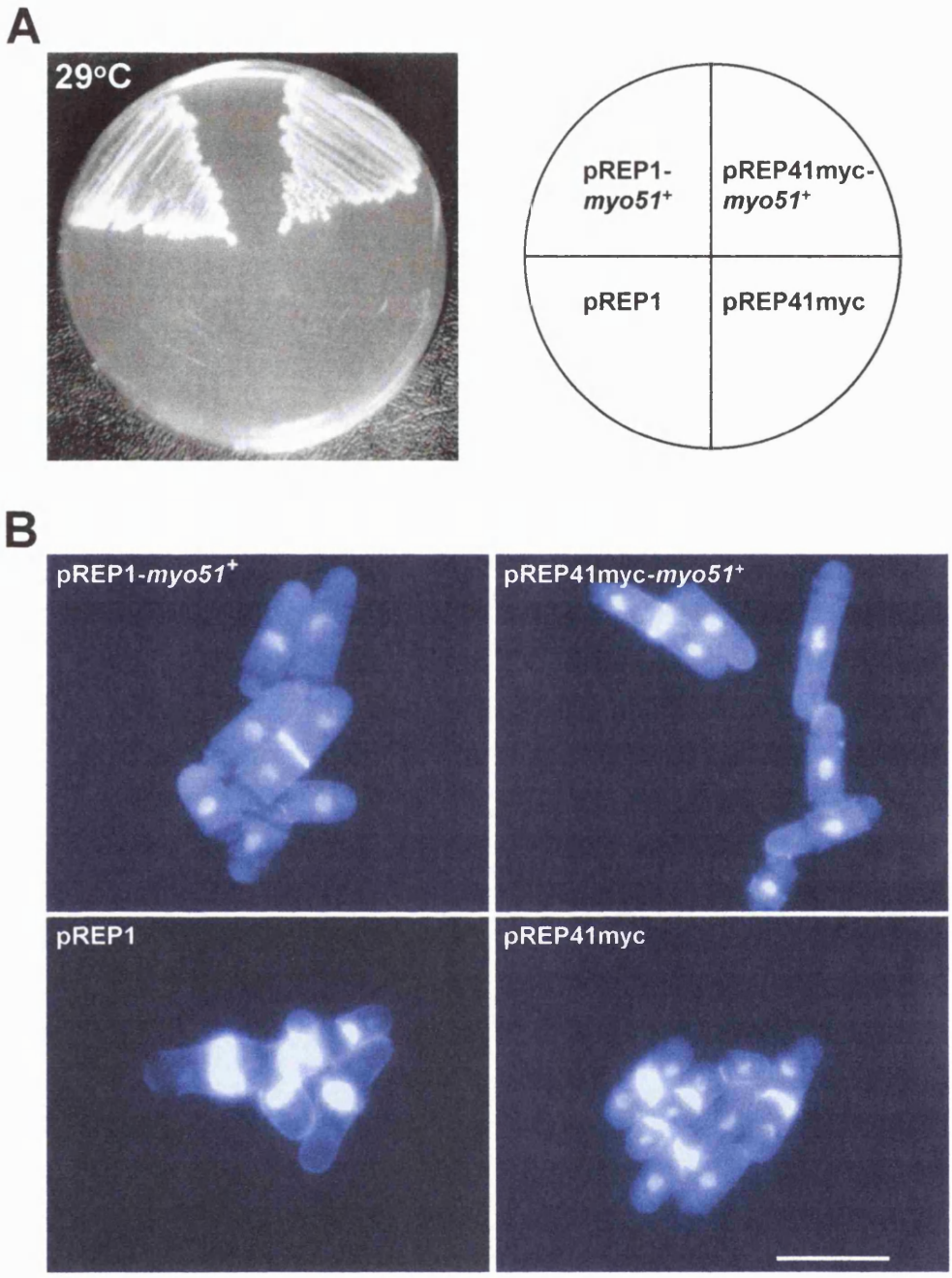

Figure 5.3 *myo51*$^{+}$ Plasmids Rescue the *myo51Δ cps8*$^{-}$ Phenotype

(A) Both pREP1-*myo51*$^{+}$ and pREP41myc-*myo51*$^{+}$ plasmids rescue the lethality of *myo51Δ cps8*$^{-}$ double mutant at 29°C. Empty vector controls did not rescue the double mutant. The plate was incubated for five days.

(B) DAPI and Calcofluor staining of *myo51Δ cps8*$^{-}$ cells transformed with *myo51*$^{+}$ plasmids and empty vector controls. Both pREP1-*myo51*$^{+}$ and pREP41myc-*myo51*$^{+}$ plasmids also rescue the morphological defects of *myo51Δ cps8*$^{-}$ double mutant at 25°C. Bar = 10 μm.

Cells in (A) and (B) were grown in appropriately supplemented minimal medium in the presence of thiamine and relied on the basal level of transcription initiation by the *nmt1* promoter for the expression of *myo51*$^{+}$ in these conditions.

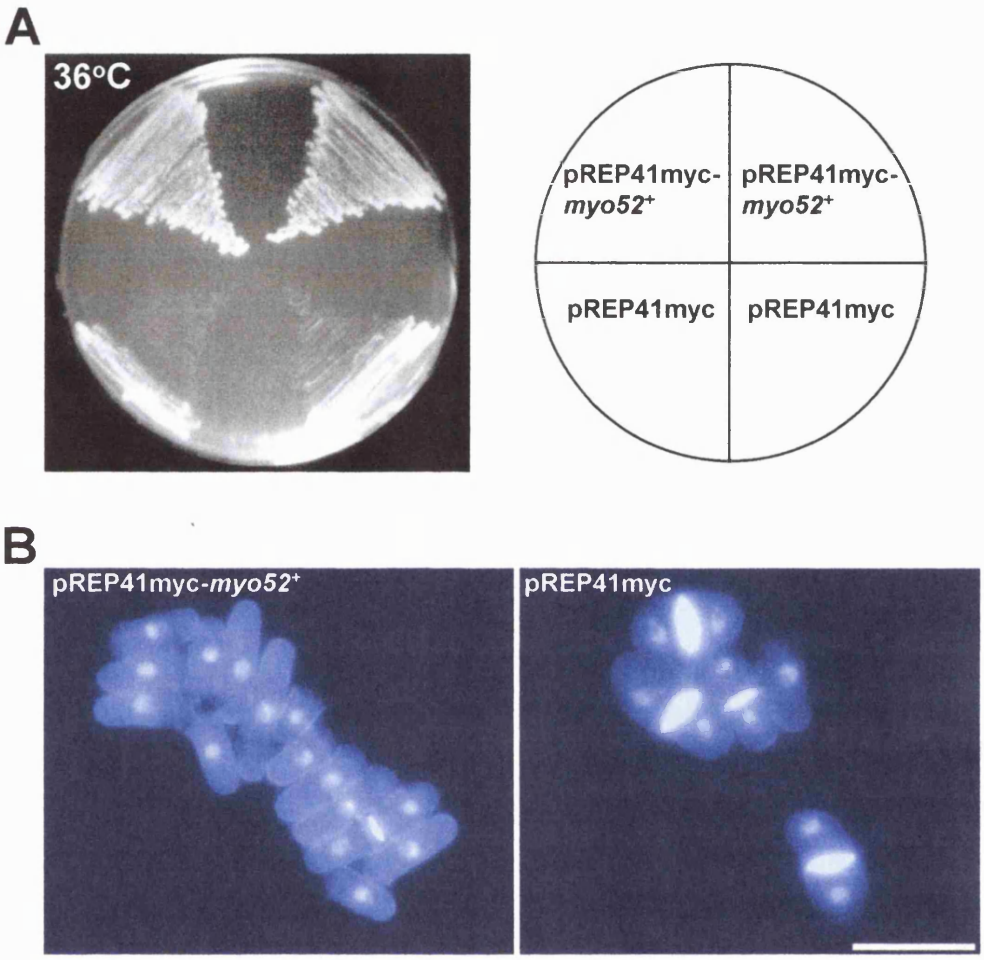

Figure 5.4 pREP41myc-*myo52*$^+$ Plasmid Rescues the Temperature-Sensitivity and Morphological Defects of *myo52Δ* Cells

(A) pREP41myc-*myo52*$^+$ plasmid rescue the temperature-sensitivity of *myo52Δ* cells at 36°C. Empty vector control did not rescue the temperature-sensitivity of *myo52Δ*. The plate was incubated for three days.

(B) DAPI and Calcofluor staining of *myo52Δ* cells transformed with pREP41myc-*myo52*$^+$ and empty vector control. pREP41myc-*myo52*$^+$ plasmid also rescue the morphological defects of *myo52Δ*. Cells were grown at 29°C. Bar = 10 μm.

Cells in (A) and (B) were grown in appropriately supplemented minimal medium in the presence of thiamine and relied on the basal level of transcription initiation by the *nmt1* promoter for the expression of *myo52*$^+$ in these conditions.

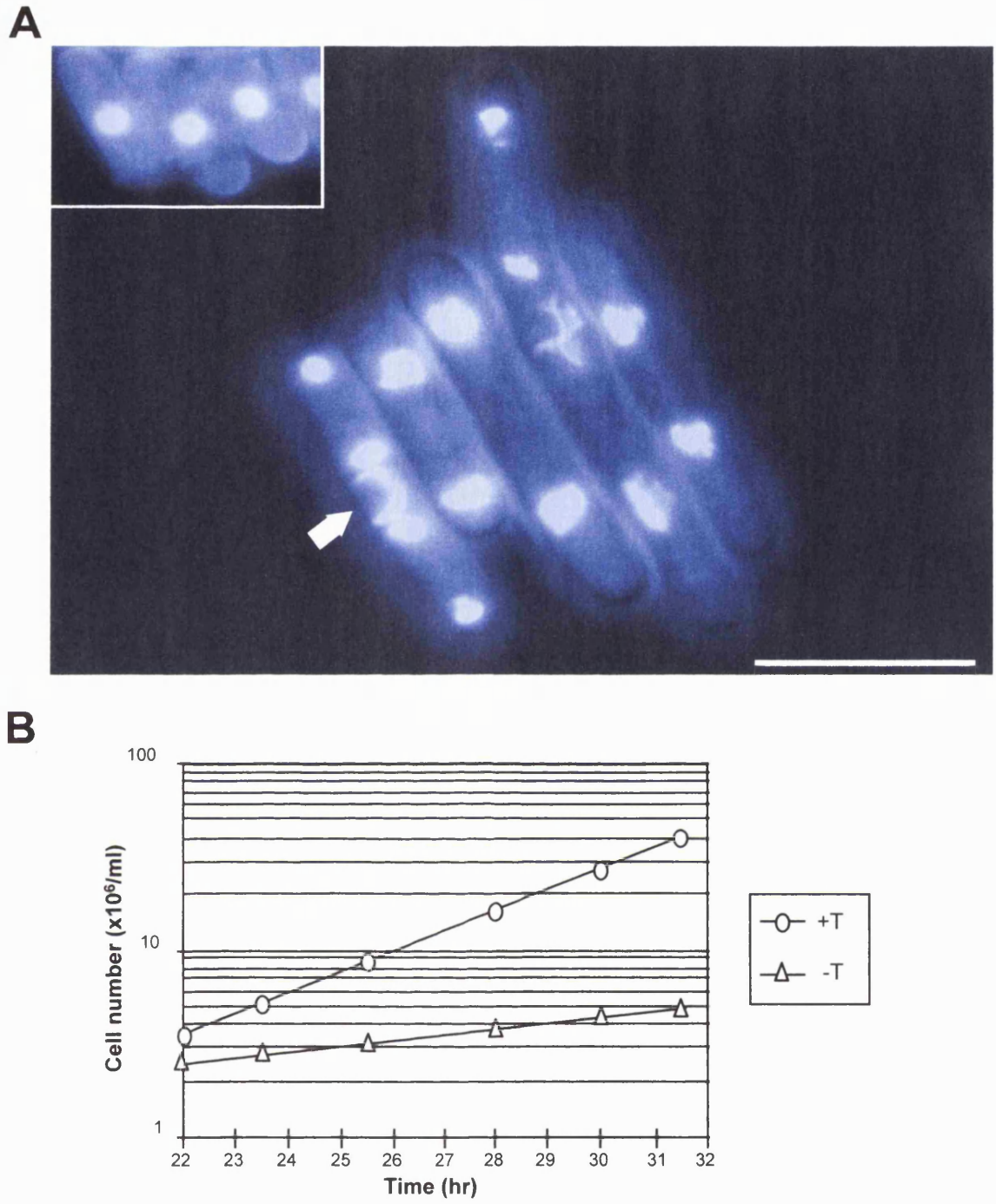

Figure 5.5 Overexpression of *myo51*$^+$

(A) DAPI and Calcofluor staining of wild type cells overexpressing *myo51*$^+$ from the pREP41myc-*myo51*$^+$ plasmid 24 hours after removal of thiamine from the growth medium. Cells overexpressing *myo51*$^+$ are elongated with multiple nuclei and form aberrant septa (arrow). Control cells grown in repressed conditions in the presence of thiamine display wild type morphology (inset). Bar = 10 μm.

(B) Log graph showing the increase in cell number with time of wild type cells transformed with pREP41myc-*myo51*$^+$ grown either in the presence (+T) or absence (-T) of thiamine. Note, the graph shows the first results after 22 hours following inoculation of cells into medium. Overexpression of *myo51*$^+$ (-T) inhibits the increase in cell number.

Cells in (A) and (B) were grown in appropriately supplemented minimal medium at 29°C.

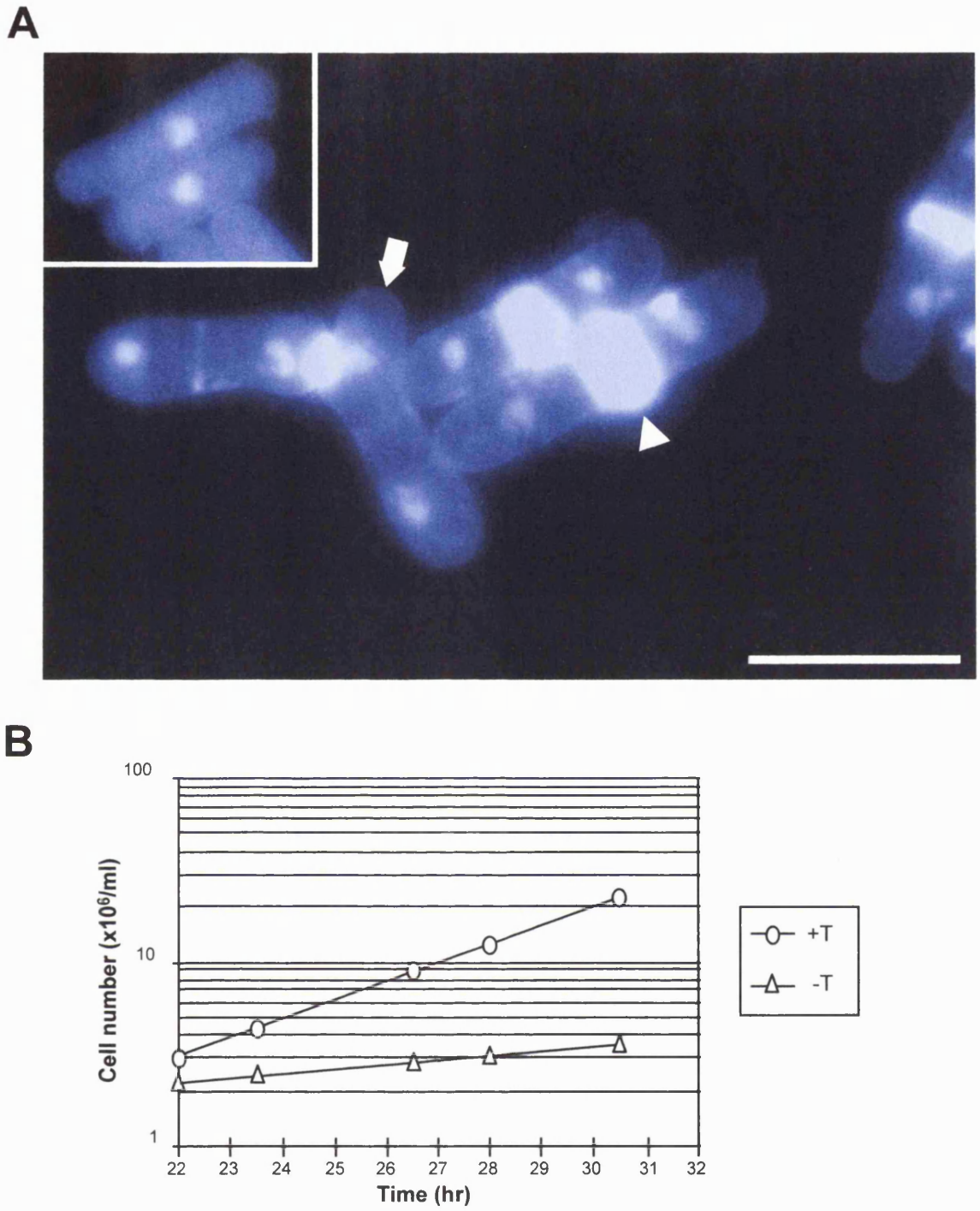

Figure 5.6 Overexpression of *myo52*$^{+}$

(A) DAPI and Calcofluor staining of wild type cells overexpressing *myo52*$^{+}$ from the pREP41myc-*myo52*$^{+}$ plasmid 24 hours after removal of thiamine from the growth medium. Cells overexpressing *myo52*$^{+}$ exhibit thickened septa (arrow head) and frequently branch (arrow). Control cells grown in repressed conditions in the presence of thiamine display wild type morphology (inset). Bar = 10 μm.

(B) Log graph showing the increase in cell number with time of wild type cells transformed with pREP41myc-*myo52*$^{+}$ grown either in the presence (+T) or absence (-T) of thiamine. Note, the graph shows the first results after 22 hours following inoculation of cells into medium. Overexpression of *myo52*$^{+}$ (-T) inhibits the increase in cell number.

Cells in (A) and (B) were grown in appropriately supplemented minimal medium at 29°C.

5.3 DISCUSSION

The cloned *myo51*$^+$ and *myo52*$^+$ genes were functional as judged by their ability to rescue the phenotypes of the *myo51Δ cps8*$^-$ and *myo52Δ* strains respectively. The presence of two copies of the myc epitope at the N-terminus of Myo51 and Myo52 did not appear to affect the function of either protein. For example, both the tagged (pREP41myc-*myo51*$^+$) and untagged (pREP1-*myo51*$^+$) versions of Myo51 were equally effective in rescuing the phenotype of the *myo51Δ cps8*$^-$ double mutant when expressed at low levels.

Distinct phenotypes were obtained when *myo51*$^+$ and *myo52*$^+$ were overexpressed in wild type cells. Overexpression of *myo51*$^+$ produced long cells in which proper septum formation was suppressed whilst overexpression of *myo52*$^+$ produced branched cells with abnormally thick septa that failed to cleave. The morphological defects arising from myosin overexpression may be a consequence of their effects on factors involved in cell growth and division. Perhaps the absence of a properly organised septum in cells overexpressing *myo51*$^+$ may be due to the disruption of the actin ring which marks the site of septation in fission yeast (Marks and Hyams, 1985). This could be envisaged if excess levels of Myo51 sequestered actin or formed inappropriate complexes with components involved in the organisation of the actin ring. Interestingly, overexpression of the class II myosins, *myo2*$^+$ (Kitayama et al., 1997; May et al., 1997) and *myp2*$^+$ (Bezanilla et al., 1997; Motegi et al., 1997) produces a phenotype similar to that of *myo51*$^+$ overexpression, indicating that high levels of either Myo2, Myp2 or Myo51 causes a disruption in the same cellular processes. Overexpression of *myo52*$^+$ did not appear to prevent the formation of actin rings since cells were able to form discrete septa. However, septa in these cells appeared thicker, indicating that the mechanisms that normally control the termination of septation were not functioning correctly.

The most likely explanation for the differences in phenotype between *myo51*$^+$ and *myo52*$^+$ overexpression is through their interaction with different proteins. Class V

myosins have several domains through which they interact with other proteins. The head domain, which bind actin, is unlikely to contribute much to the observed differences in phenotype since the two proteins share extensive homology in primary sequence in this domain (Chapter 3). The neck domain which is the region of light chain binding may contribute to some of the observed differences in overexpression phenotype. Five potential light chain binding sites have been determined in the neck domains of Myo51 and Myo52 (Chapter 3). A sixth binding site may exist in either protein that binds a light chain with low affinity or binds a unique type of light chain (Chapter 3). Most of the light chains associated with a class V myosin are calmodulin molecules (Reck-Peterson et al., 2000) and a calmodulin gene, *cam1*$^+$, has been identified in fission yeast (Moser et al., 1997). Other types of light chains have also been found to associate with class V myosins (Cheney et al., 1993b; Stevens and Davis, 1998). Some of these light chains associate with other classes of myosins, indicating that some light chains are shared amongst myosins. In fission yeast, a novel myosin light chain, Cdc4, has been identified as the light chain for both of the class II myosins, Myo2 and Myp2 (Naqvi et al., 1999; Motegi et al., 2000). Interestingly, Cdc4 is localised at the equator during cytokinesis and is essential for the organisation of the actin ring (McCollum et al., 1995). Perhaps the absence of septa in cells overexpressing *myo51*$^+$ is a consequence of the disruption in the Cdc4 mediated assembly of the actin ring either through a direct or indirect interaction between Myo51 and Cdc4. Whether Myo51 and Myo52 binds Cdc4, calmodulin or any other light chain awaits further investigation.

The tail domain of class V myosins provides other sites of protein-protein interaction. Two functional subdomains can be distinguished in the myosin V tail: an α-helical region and a C-terminal globular domain (Reck-Peterson et al., 2000). The α-helical region is the domain through which myosin V molecules self-dimerise by forming coiled-coil tails (Beningo et al., 2000). It is possible that some of the myosin V overexpression phenotypes may result from an interaction of this domain with the α-helical region of other proteins. The C-terminal globular tail domain is thought to be

involved in cargo binding and/or localisation in the cell (Reck-Peterson et al., 2000). Analysis of one of the budding yeast class V myosins, Myo2, has shown that it contains two distinct regions in the globular tail domain that are required for the movement of different cargoes, one of which is required for vacuole transport whereas the other is required for polarised growth (Catlett et al., 2000). Catlett et al. (2000) have proposed that Myo2 uses the C-terminal globular domain to associate with specific receptors on secretory vesicles and vacuoles to effect their localisation in the cell. The other budding yeast myosin V, Myo4, is involved in the targeting of *ASH1* mRNA to the growing bud (Long et al., 1997; Takizawa et al., 1997). Recently, Myo4 has been shown to associate with *ASH1* mRNA through an adapter protein, She3 (Takizawa and Vale, 2000). The observation that budding yeast class V myosins associate with distinct cellular cargoes provides an explanation for the distinct phenotypes of *myo51*$^+$ and *myo52*$^+$ overexpression in fission yeast. Perhaps, like their budding yeast homologues, fission yeast class V myosins also interact with different cellular cargoes.

The results presented in this chapter represent the phenotypes of overproducing entire myosin V molecules. It is possible that the different domains of a myosin V heavy chain will contribute their effects to the overall overexpression phenotype of a myosin V molecule. A better understanding to the role of these domains may be gained by expressing truncated forms of a myosin V molecule. This approach will enable the dissection of a myosin heavy chain such that the effects of expressing individual domains can be discerned. This strategy can also be used to investigate the domains which are important for gene function by testing their ability to complement the *myo51Δ cps8*$^-$ and *myo52Δ* phenotypes. Another strategy is to express chimeras of Myo51 and Myo52 to determine the domain that is important for gene specific functions. For example, a fusion protein consisting of the Myo51 head with the Myo52 tail can be expressed in a *myo52Δ* mutant to investigate the ability of the Myo51 head to complement the *myo52Δ* phenotype. If the fusion protein complements the *myo52Δ* phenotype, this will suggest that the Myo51 and Myo52

heads are functionally exchangeable and is not the domain which determine gene specific functions. This approach has been carried out in the characterisation of the two fission yeast class II myosins which has revealed that the tail of Myo2 and Myp2 confer their unique functions (Bezanilla and Pollard, 2000). Another suggested experiment is to determine the levels of Myo51 and Myo52 when they are overproduced and investigate their stability in cells.

Chapter 6
Localisation of Myo51 and Myo52

6.1 INTRODUCTION

So far I have shown that *myo51*$^+$ and *myo52*$^+$ encode two class V myosin genes which exhibit distinct phenotypes when they are deleted or overexpressed. To further investigate the function of Myo51 and Myo52, the localisation of these proteins in fission yeast cells was carried out.

A protein's localisation throughout different stages of the cell cycle can reveal much about where in the cell it performs its activities and when it does so. This can be illuminating if a protein of unknown function can be colocalised with a protein in which the function has already been established, suggesting that they may be involved in the same cellular processes. For example, this approach helped to implicate the product of the *mok1*$^+$ gene, which shows sequence homology to α-glucan synthase, in cell growth (Katayama et al., 1999) because it colocalised with actin structures which are associated with the growth of fission yeast (Marks and Hyams, 1985): to actin patches at the cell poles during interphase and to the equatorial ring during mitosis.

A widely used and well established method by which proteins are localised in the cell is by indirect immunofluorescence microscopy. This technique has been used to localise a number of proteins in fission yeast since its pioneering use to examine the organisation of actin (Marks et al., 1986) and microtubules (Hagan and Hyams, 1988) in this organism. In this technique a specific antibody is used to probe the distribution of the protein of interest in the cell and the localisation of the primary antibody is visualised using a secondary antibody conjugated to a fluorescent molecule by fluorescence microscopy. Traditionally, this involved raising antibodies to the protein of interest which can be time consuming and provides no guarantee to the specificity of the raised antibody. This has led researchers to seek alternative methods which could complement or substitute for protein specific antibodies. One method is to fuse the protein of interest with small antigenic tags such as the myc and haemagglutinin epitopes for which antibodies are commercially available. Once the protein of interest has been epitope tagged, it can be localised in the cell and biochemically characterised.

A number of plasmids have been developed for this purpose which can be used to tag an epitope at the N- or C-terminus to the protein of interest (Craven et al., 1998; Iacovoni et al., 1999).

Another way by which proteins are localised is by tagging the protein with green fluorescent protein (GFP). The GFP molecule has intrinsic fluorescent activity and emits green light when it is excited by blue light (Cubitt et al., 1995) and as a consequence any proteins tagged to GFP can be localised in the cell by observing the distribution of green fluorescence. The advantage of this technique is that the localisation of the GFP tagged protein can be followed in living cells without having to fix the cells which is required when performing protein localisation by immunological detection. However, one disadvantage of using GFP is that it may affect protein function since it is a relatively large tag with a molecular weight of 27 kD (Prasher et al., 1992). Despite this GFP has been used to tag a number of proteins (Moser et al., 1997; Eng et al., 1998; Bezanilla et al., 2000) and plasmids have been developed for the N- and C-terminal tagging of proteins with GFP in fission yeast (Craven et al., 1998; Iacovoni et al., 1999).

The vectors used to tag proteins with an epitope or a GFP molecule employ a heterologous promoter such as the *nmt1*$^+$ and *inv1*$^+$ promoters to induce expression of the tagged protein and consequently gene expression from the native promoter cannot be studied. To overcome this problem Bahler et al. (1998) has constructed a series of modules for the production of C-terminally tagged proteins in which the gene is tagged at the chromosomal locus and expression is thus controlled by the native promoter. The method is a PCR based gene targeting technique which involves integration of a module containing homologous sequences to the 3' end of the gene of interest at the chromosomal locus. The remarkable feature of this technique is that the tagging module is obtained directly from PCR of template DNA in which homologous sequences to target the module is provided by the primers used to amplify it. The template DNA, however, has all the other necessary information to create the gene

fusion by providing the tag coding sequence and the *kan*^{r} selection marker for the isolation of transformants. A variety of template modules are available for epitope and GFP tagging and, since the homologous sequences to target the amplified module are provided by the primers, a variety of genes could be tagged by designing primers specific to the gene of interest, thus providing a versatile way to manipulate a number of genes with the tag of choice (Bahler et al., 1998). A necessary feature of this technique, however, is that the primers are long, up to 100 bases, to provide enough homology for the successful integration of the module to the target gene.

In this chapter I report the preliminary localisation of Myo51 by indirect immunofluorescence microscopy. The localisation of Myo52 will be presented in more detail using a variety of techniques which includes localisation by immunological detection and by N- and C-terminal tagging of the protein with GFP. The localisation of Myo52 in several fission yeast mutants will also be shown. Finally, I will present evidence that the localisation of Myo52 is actin and microtubule dependent.

6.2 RESULTS

6.2.1 Localisation of Myo51 by Indirect Immunofluorescence Microscopy

Myo51 was localised using the pREP41myc-*myo51*$^+$ plasmid as described in Chapter 5. To localise Myo51, wild type cells transformed with the plasmid were incubated in minimal medium in the absence of thiamine at 29°C for 20 hours to allow enough time for the myc-Myo51 fusion protein to be expressed but not long enough so as to give the overexpression phenotype observed in the previous chapter. Cells were fixed by the formaldehyde-glutaraldehyde method (Materials and Methods, section 2.25) and processed for immunofluorescence microscopy using the 9E10 anti-myc antibody to probe the localisation of myc-Myo51.

Microscopic observation revealed the presence of diffuse myc-staining that was asymmetrically distributed in cells (Figure 6.1). Occasionally, the staining covered

almost one half of the cell which extended from one pole to the equatorial region of the cell. Interestingly, the intensity of myc-Myo51 staining differed from cell to cell and some cells were left unstained which usually occurred in small cells of about 8 μm in length. Perhaps this may have been a result of a newly born cell that received no myc-Myo51 upon cell division due to the asymmetric distribution of the protein. Longer cells, however, had more staining indicating that myc-Myo51 may have been accumulated in these cells.

The differences in staining between cells probably reflects the variability in plasmid copy number and expression levels of the fusion protein that occurs from cell to cell due to the inherent limitations of a plasmid-based gene expression system. A better understanding of the localisation of Myo51 would be possible from localising the protein expressed from its own promoter (Win et al., 2001).

6.2.2 Localisation of Myo52

Myo52 was localised using three distinct approaches. The first was to use a similar method to that described for the localisation of Myo51 by indirect immunofluorescence microscopy. The second was to use a plasmid to tag the protein with GFP so that the localisation of the protein could be followed in living cells. The final method was to integrate a GFP tagging module at the 3' end of the *myo52*$^{+}$ gene so that a tagged Myo52 protein was expressed from the native promoter.

a. Localisation of Myo52 by Indirect Immunofluorescence Microscopy

Localisation of Myo52 by immunofluorescence microscopy was performed in wild type cells transformed with the previously described pREP41myc-*myo52*$^{+}$ plasmid (Chapter 5). Expression of the gene was achieved by growing cells in minimal medium in the absence of thiamine after which they were fixed with formaldehyde-glutaraldehyde. Cells were then processed and probed for the distribution of myc-Myo52 using the 9E10 anti-myc antibody.

Microscopic examination of cells showed that myc-Myo52 was localised to two distinct places in the cell: the poles and equator (Figure 6.2A). Polar localisation was observed in cells undergoing tip growth whereas equatorial staining was observed in dividing cells. In contrast to the monopolar staining pattern of myc-Myo51, myc-Myo52 localised to both poles of fission yeast cells. Furthermore, the localisation of myc-Myo52 was more discrete being present at the very tips of growing fission yeast cells unlike the diffuse localisation of myc-Myo51. Comparison of the staining at cell poles show that one end was more intensely stained than the other indicating that there was an assymetric distribution of myc-Myo52 at the cell poles.

b. Localisation of GFP-Myo52

Myo52 was tagged at the N-terminus with GFP by inserting the GFP coding sequence from pGEM-GFP (Craven et al., 1998) as a NdeI/NdeI fragment into the NdeI restriction site of pREP41myc-*myo52*$^+$ to create pREP41GFP-*myo52*$^+$ plasmid. To test whether the GFP tagged protein was functional, pREP41GFP-*myo52*$^+$ was transformed into *myo52Δ* to examine its ability to rescue the temperature-sensitivity and morphological defects of *myo52Δ* cells. Indeed, the plasmid was able to rescue the defects of *myo52Δ* cells similar to that shown in Chapter 5 by pREP41myc-*myo52*$^+$ (Figure 5.4). Plasmid loss experiments were also carried out similar to that described in the previous chapter to confirm that the complementing activity resided in pREP41GFP-*myo52*$^+$ and not from a suppressing mutation in the genome.

After showing that the protein was functional, the localisation of GFP-Myo52 was performed in *myo52Δ* cells. Microscopic examination of these cells showed that GFP-Myo52 localised to the poles of growing cells and to the equator of cells undergoing cell division (Figure 6.2B), similar to the localisation of myc-Myo52. GFP-Myo52 also localised to the very tips of growing cells and appeared to cap the cells at both poles.

c. Localisation of Myo52 Expressed from its Own Promoter

Myo52 was tagged at the C-terminus with GFP by constructing a GFP tagging module from PCR using the primers myo52C-forward and myo52C-reverse (Materials and Methods Table 2.3). These primers each contained approximately 80 bases of homology to the 3' end of the *myo52*$^+$ locus and 20 bases of homology to the pFA6a-GFP(S65T)-kanMX6 template DNA which contained the coding sequence for GFP and the bacterial *kan*^{r} gene that confers Geneticin resistance (Bahler et al., 1998). The primers were designed in such a way so that the amplified PCR product would integrate precisely at the 3' end of the *myo52*$^+$ locus and that the protein coding sequence of Myo52 continued in frame with that of GFP without interruption by a stop codon between the two sequences. Integration of the GFP module at the *myo52*$^+$ locus is illustrated in Figure 6.3A.

After construction of the tagging module, it was transformed into wild type cells and stable integrants were selected by growing cells in YES medium supplemented with Geneticin. Eight integrants that had integrated the tagging module were found. Correct integration of the module at the *myo52*$^+$ locus was checked by PCR of genomic DNA extracted from the integrants using the primers c1919-start and c1919-end. These primers were used to amplify the entire 4.8 kb *myo52*$^+$ coding sequence and a band shift of 2.6 kb that corresponded to the size of the tagging module was expected in cells which had correctly integrated the module. Out of the eight integrants, six had integrated the module at the *myo52*$^+$ locus since a band shift from 4.8 kb to 7.4 kb was found in these cells (Figure 6.3B).

Microscopic examination of the six strains that had correctly integrated the GFP tagging module showed that all exhibited the previously observed bipolar and equatorial localisation of Myo52. The two integrants that did not integrate the module at the correct locus did not show this staining pattern (data not shown).

Figure 6.4 shows the localisation of Myo52-GFP from one of the integrants that had correctly integrated the module at the *myo52*$^{+}$ locus. Like before, fluorescence was observed at the very tips of growing cells and at the equator of cells undergoing division. However, the intensity of fluorescence was less than that observed from plasmid-based expression of *myo52*$^{+}$ indicating that cells contained less of the tagged protein when expression was from the native promoter. In newly born small cells the tagged protein was seen to localise at one cell end, perhaps reflecting the distribution of actin at the old end in cells yet to undergo new end take off (Marks and Hyams, 1985). Closer examination of cells with a bipolar distribution of Myo52-GFP showed that the intensity of fluorescence at the two poles was again unequal, indicating that the protein was preferentially localised to one pole which might also reflect the unequal distribution of actin in cells undergoing bipolar growth. This kind of monopolar and bipolar staining was also found in cells when it was expressed from plasmids but occurred less frequently since the subtle staining patterns may have been obscured by the high levels of the protein when it was expressed from plasmids.

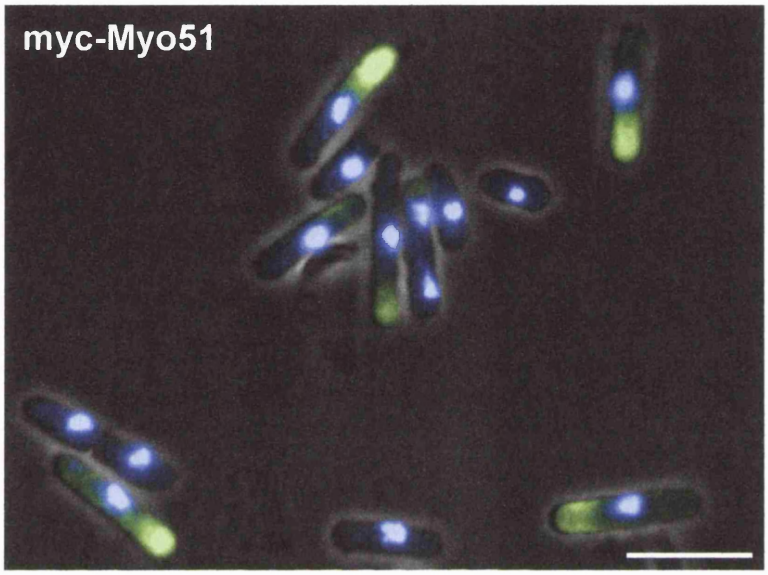

Figure 6.1 Localisation of Myo51

Immunofluorescence microscopy of wild type cells transformed with pREP41myc-*myo51*$^+$ plasmid. myc-Myo51 is observed as diffuse pale green staining that is asymmetrically distributed in fission yeast cells. DAPI staining is also shown to reveal the location of nuclei. Cells were grown at 29°C in liquid minimal medium in the absence of thiamine for 20 hours to induce the expression of the gene from the *nmt1*$^+$ promoter before processing for immunofluorescence microscopy. The 9E10 anti-myc antibody was used to localise myc-Myo51. Bar = 10 μm.

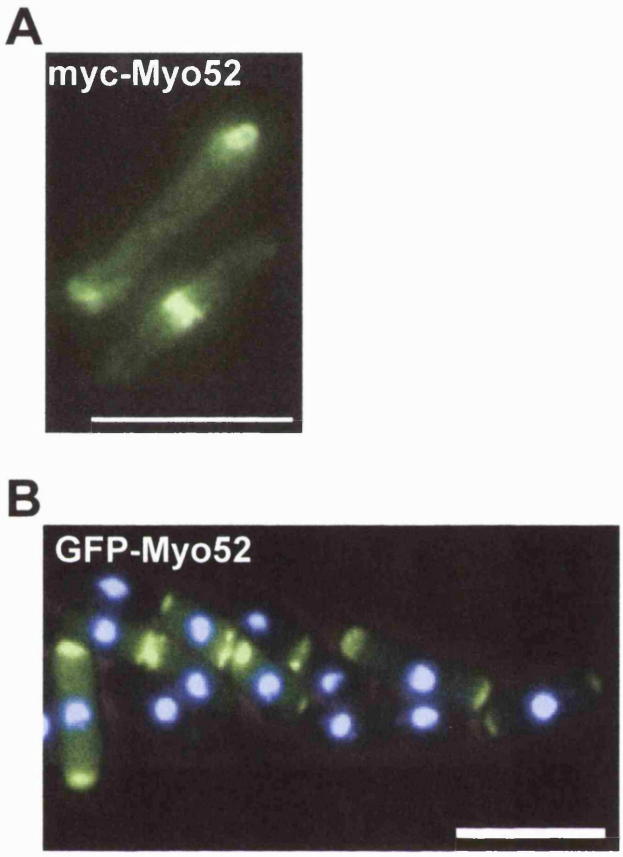

Figure 6.2 Localisation of Myo52

(A) Immunofluorescence microscopy of wild type cells transformed with pREP41myc-*myo52*$^{+}$ plasmid. myc-Myo52 localises to the poles and equator of fission yeast cells. The 9E10 anti-myc antibody was used to localise myc-Myo52.

(B) *myo52Δ* cells transformed with pREP41GFP-*myo52*$^{+}$ display the rod-shaped morphology of wild type fission yeast. GFP-Myo52 also localises to the poles and equator in *myo52Δ*. DAPI staining is also shown to reveal the location of nuclei.

Cells in (A) and (B) were grown at 29°C in liquid minimal medium in the absence of thiamine for 20 hours to induce expression of the tagged *myo52*$^{+}$ gene from plasmids. Bars = 10 μm.

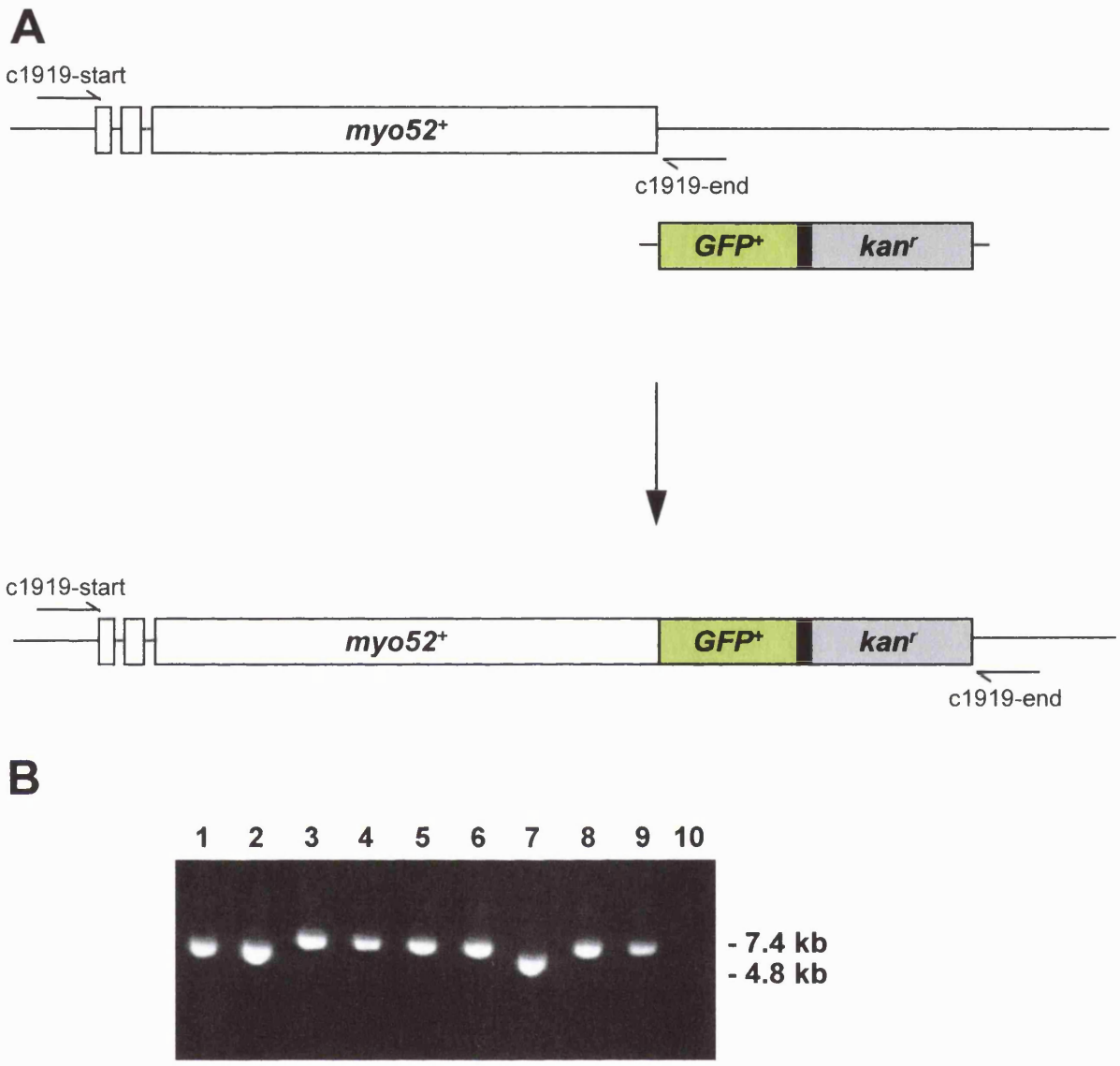

Figure 6.3 Construction of Myo52-GFP

(A) A GFP tagging module containing homologous sequences to the 3' end of *myo52*$^+$ was transformed into wild type cells. The tagging module also contained the *kan*^{r} gene (grey box) in addition to the GFP coding sequence (green box) to select for transformants. *myo52*$^+$ is encoded in three exons (white boxes). The primers (c1919-start and c1919-end) used to check for the integration of the GFP tagging module at the *myo52*$^+$ locus is also shown.

(B) PCR was performed on genomic DNA extracted from untransformed wild type cells (lane 1) and transformants containing the tagging module (lanes 2-9). A no DNA control was also performed (lane 10). Six lanes show a band of 7.4 kb in size and corresponds to transformants with the GFP tagging module correctly integrated at the *myo52*$^+$ locus (lanes 3, 4, 5, 6, 8 and 9).

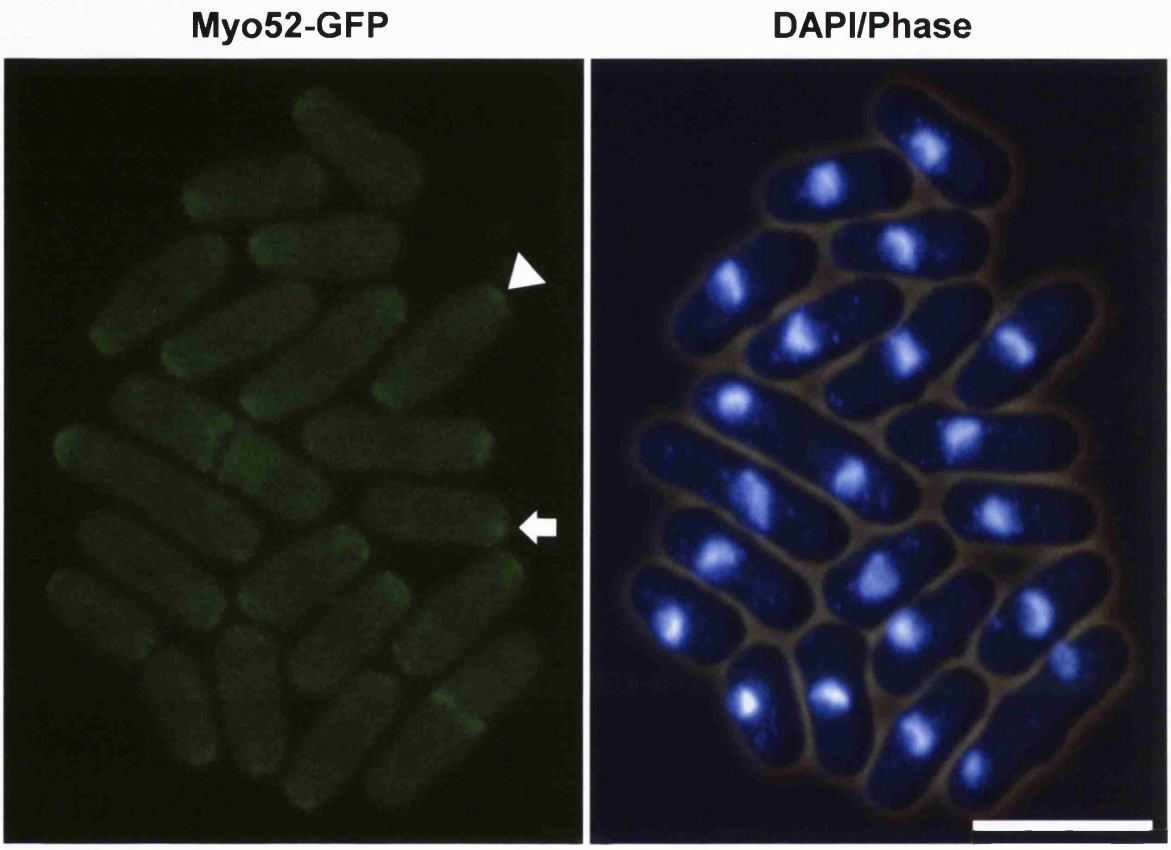

Figure 6.4 Localisation of Myo52-GFP Expressed from the *myo52*$^{+}$ Promoter

Myo52 tagged at the C-terminus with GFP localises to the poles and equator of fission yeast. Bipolar (arrow head) and monopolar (arrow) staining can be distinguished when the tagged gene is expressed from the native *myo52*$^{+}$ promoter. The panel on the right is the same field of cells viewed with a DAPI filter. Cells were grown in liquid YES medium at 25°C. Bar = 10 μm.

6.2.3 Localisation of Myo52 Correlates with the Distribution of Actin

Since the localisation of Myo52 resembled the distribution of actin during different stages of the cell cycle, simultaneous localisation of the two proteins was carried out to investigate the spatial and temporal relationship between Myo52 and actin. This was performed by probing *myo52Δ* cells expressing GFP-Myo52 from a plasmid with an anti-actin antibody. A secondary antibody conjugated to rhodamine was used to detect the localisation of the primary antibody by immunofluorescence microscopy. The distribution of actin and Myo52 were then visualised by exciting the rhodamine and GFP fluorophores with green and blue light respectively.

Microscopic examination of these cells showed that the bipolar localisation of actin as observed using the rhodamine filter of the microscope correlated with the bipolar distribution of GFP-Myo52 when the same cells were viewed through the FITC filter to visualise GFP (Figure 6.5A). Although the bipolar distribution of actin and GFP-Myo52 occurred at the same time the spatial localisation of the two proteins was not identical. Actin staining appeared punctate and actin patches were observed in places other than at the very tips of cells. The localisation of GFP-Myo52 did not show the punctate staining pattern to that observed for actin, instead GFP-Myo52 appeared to be localised as one continuous cap at the cell poles.

The equatorial localisation of GFP-Myo52 also correlated with the medial localisation of actin because the GFP-Myo52 equatorial band was present about the same time and place as the actin ring (Figure 6.5B).

6.2.4 Myo52 Relocates from the Poles to the Equator at Late Anaphase

Myo52 was seen to relocate from the poles to the equator in cells undergoing mitosis. To determine the precise stage of mitosis at which Myo52 relocated from the poles, tubulin staining was performed to relate the location of Myo52 in the cell to that of the mitotic spindle. This was achieved by processing *myo52Δ* cells transformed with

pREP41GFP-*myo52*$^+$ with the TAT1 anti-tubulin antibody for immunofluorescence microscopy and observing the distribution of microtubules, GFP-Myo52 and nuclei.

Microscopic observation of the cells showed that in small newly divided cells GFP-Myo52 was present at only one end (Figure 6.6). As cells progressed through the cell cycle and became longer GFP-Myo52 was seen at both poles. The tips of the interphase array of microtubules which extended from one pole to the other seemed to overlap with the polar localisation of GFP-Myo52. When interphase microtubules depolymerised to form the mitotic spindle GFP-Myo52 remained at the poles. At mid-anaphase as the mitotic spindle elongated to separate the daughter nuclei GFP-Myo52 was still present at the poles. Only at late-anaphase GFP-Myo52 was observed to localise from the poles to the equator. Analysis of 38 mitotic spindles showed that GFP-Myo52 relocated to the equator at late-anaphase when the mean spindle length was 9.4 μm (standard deviation: 1.1 μm). No equatorial GFP-Myo52 was observed at spindle lengths less than 9.4 μm indicating that cells must pass through a certain point in the cell cycle before its relocation to the equator. At the end of mitosis when the interphase array of microtubules started to reform in daughter cells the single ring of GFP-Myo52 became two bands.

6.2.5 Myo52 Relocates to the Equator Before Septation

The fact that the localisation of Myo52 to the poles and equator coincided with the timing of cell growth and division indicated that Myo52 may some how be involved in cell growth. To further investigate this point, *cdc25-22* cells were transformed with pREP41GFP-*myo52*$^+$ and synchronised by temperature block and release (Moreno et al., 1989). The results showed that nearly all cells in the population had a bipolar localisation of GFP-Myo52 following incubation at 36°C for 4 hours (Figure 6.7). Even in these highly elongated cells GFP-Myo52 localised to the very tips of growing cells. The culture was then returned to 25°C and samples were taken every 10 minutes to determine the frequency of cells showing an equatorial ring of GFP-Myo52 as well as scoring for the presence of septa. Following release from their cell cycle arrest, the

frequency of cells with an equatorial ring of GFP-Myo52 steadily increased which peaked 50 minutes after incubation at 25°C. The frequency of septated cells, on the other hand, reached its peak only after 70 minutes at 25°C indicating that GFP-Myo52 localised to the equator before septation.

Figure 6.7 summarises the temporal relationship between the distribution of GFP-Myo52 and septation in a synchronous culture of *cdc25-22* cells. Similar results were obtained when the experiment was repeated in a *cdc25-22* strain integrated with a GFP tagging module at the *myo52*$^{+}$ locus (data not shown).

6.2.6 Myo52 Localises to Sites of Septation

The localisation of GFP-Myo52 in *cdc25-22* cells showed that the protein localised to the equator as a single band before septation but occurred as a double band after septation (Figure 6.7). Furthermore, the septum that formed appeared to be "sandwiched" in between the two GFP-Myo52 bands. To further investigate the relationship between Myo52 and septation the localisation of the protein was investigated in the *cdc16-116* mutant which forms multiple septa at the restrictive temperature (Fankhauser et al., 1993). This was performed to test whether the association between Myo52 and septation remained when a protein involved in the regulation of septum formation was inactivated.

Figure 6.8 shows that at 25°C *cdc16-116* cells transformed with pREP41GFP-*myo52*$^{+}$ grew relatively normally and formed a single septum in each cell cycle. However, after 1 hour at the restrictive temperature *cdc16-116* cells formed multiple septa which coincided with the localisation of GFP-Myo52. The distribution of GFP-Myo52 also coincided with septa which did not form at the equator. Thus, Myo52 is intimately involved in septation. Similar results were obtained when the experiment was repeated in a *cdc16-116* strain in which expression of Myo52-GFP was controlled from the *myo52*$^{+}$ promoter (data not shown).

6.2.7 Myo52 Localises to Growing Poles

The localisation of Myo52 in wild type and *cdc25-22* cells showed that the protein localised to sites of growth. To investigate the polar localisation of Myo52, the protein was localised in the *tea1-3* temperature-sensitive mutant which exhibits defects in defining the site of growth and produces T-shaped cells with more than two poles at the restrictive temperature (Verde et al., 1995; Mata and Nurse, 1997).

Microscopic observation of *tea1-3* cells transformed with pREP41GFP-*myo52*$^{+}$ showed that GFP-Myo52 localised to both poles in cells undergoing bipolar growth at 25°C (Figure 6.9). The bipolar localisation of GFP-Myo52 also corresponded to the distribution of actin patches at the two growing poles.

At the restrictive temperature, however, the *tea1-3* mutant defines a new site of growth and produces cells with an extra pole. As well as defining an extra pole, the *tea1-3* mutant also has defects in undergoing new end take off and fails to activate growth at other poles (Verde et al., 1995). Thus, *tea1-3* cells grow only from one pole at 36°C even though cells may have more than two poles. This is consistent with the monopolar actin distribution in T-shaped cells (Figure 6.9). Interestingly, GFP-Myo52 localised to the single growing pole of *tea1-3* cells where actin was present, but significantly, was absent from the non-growing poles. These results confirm the association between Myo52, actin and cell growth.

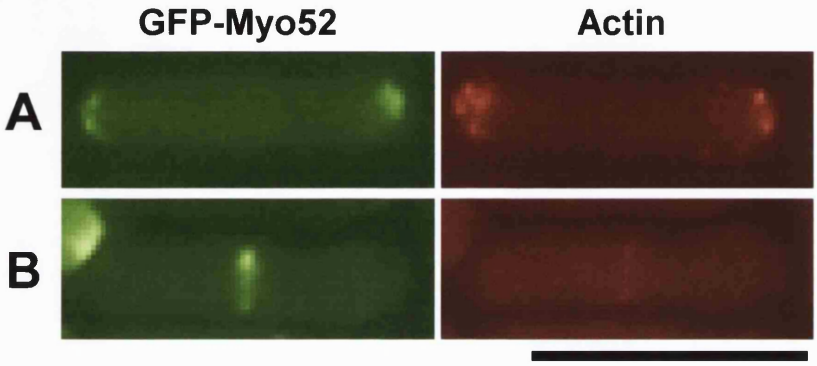

Figure 6.5 The Localisation of Myo52 Correlates with the Distribution of Actin

(A) GFP-Myo52 localises to both poles in cells undergoing bipolar growth.

(B) GFP-Myo52 localises to the equator in cells undergoing cytokinesis.

The panels on the left shows the localisation of GFP-Myo52 viewed with a FITC filter and the panels on the right shows the same cells viewed with a rhodamine filter to reveal the distribution of actin. *myo52Δ* cells transformed with pREP41GFP-*myo52*$^{+}$ were processed for immunofluorescence microscopy from cultures grown in liquid minimal medium in the absence of thiamine at 25°C for 20 hours to induce the expression of the gene from the *nmt1*$^{+}$ promoter. The N-350 anti-actin antibody was used to probe the localisation of actin. Note the distribution of GFP-Myo52 and actin at the cell poles does not precisely coincide. Bar = 10 μm.

Figure 6.6 Myo52 Relocates from the Poles to the Equator at Late Anaphase

A series of images of fission yeast cells at different stages of the cell cycle arranged to illustrate the distribution of GFP-Myo52 through a single cell cycle.

(a) At the beginning of the sequence GFP-Myo52 is found only at one pole of a newly divided cell.

(b) As the cell cycle progresses GFP-Myo52 is present at both poles and the interphase array of microtubules extends from one pole to the other.

(c) When mitosis is initiated and the interphase microtubules disappear to form the mitotic spindle GFP-Myo52 remains at the poles.

(d) As mitosis proceeds (mid-anaphase) and the spindle elongates to separate the daughter nuclei GFP-Myo52 is still present at the poles.

(e) Only at a critical point in mitosis (late-anaphase) GFP-Myo52 starts to relocate from the poles to the equator.

(f) During the transition from anaphase to telophase the spindle is fully extended and polar staining of GFP-Myo52 completely disappears to form an equatorial ring of GFP-Myo52.

(g) The single ring of GFP-Myo52 becomes two bands as the interphase array of microtubules starts to reform in the daughter cells.

The above sequence of images were obtained from *myo52Δ* cells transformed with pREP41GFP-*myo52*$^{+}$ which was processed for immunofluorescence microscopy after 20 hours growth in liquid minimal medium in the absence of thiamine at 25°C. The TAT1 anti-tubulin antibody was used to localise microtubules and the mitotic spindle. The distribution of GFP-Myo52 is shown in green, tubulin staining is shown in red, DAPI staining is shown in blue and the composite images is shown on the far right. Bar = 10 μm.

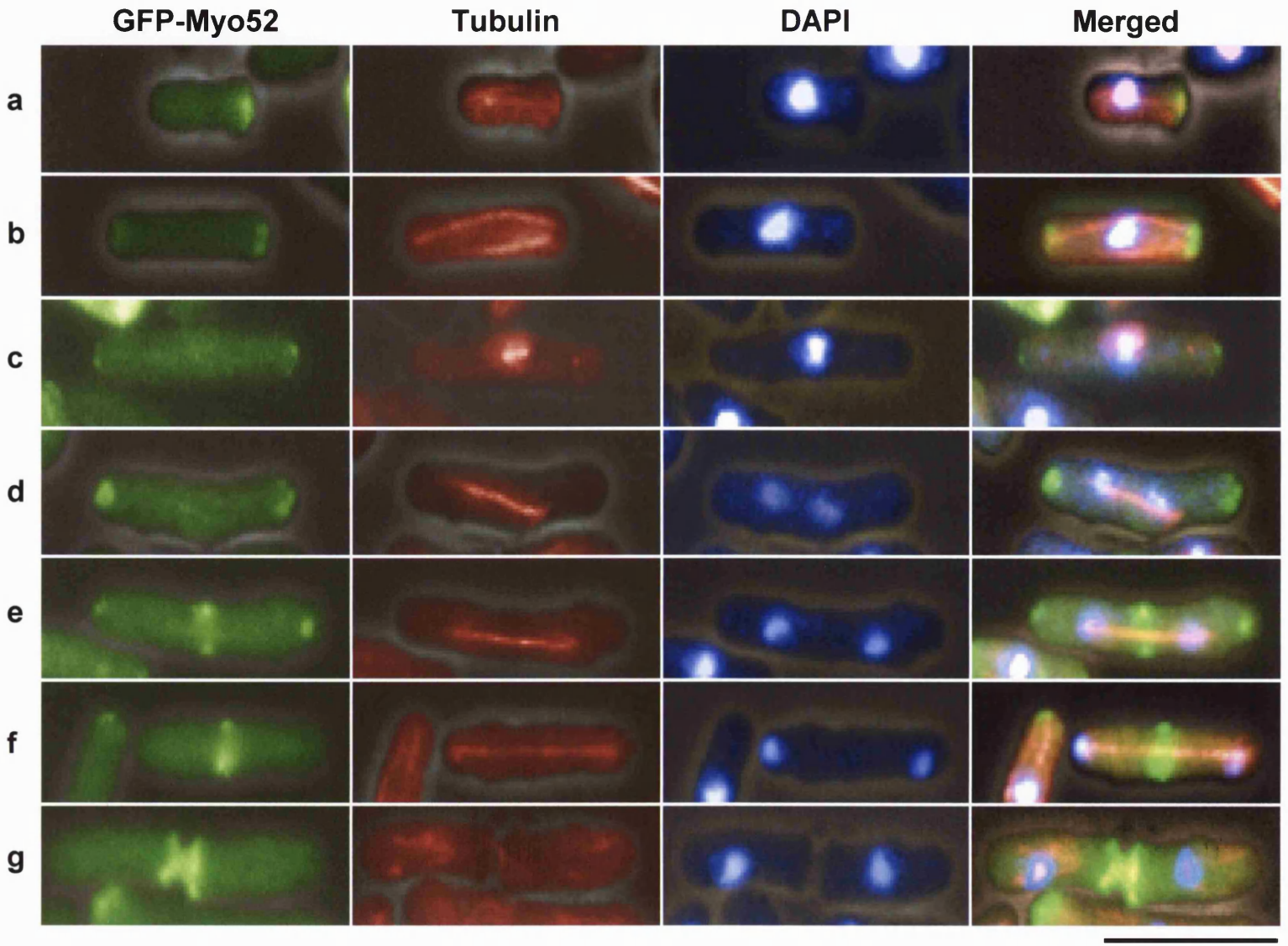
GFP-Myo52
Tubulin
DAPI
Merged
a
b
c
d
e
f
g

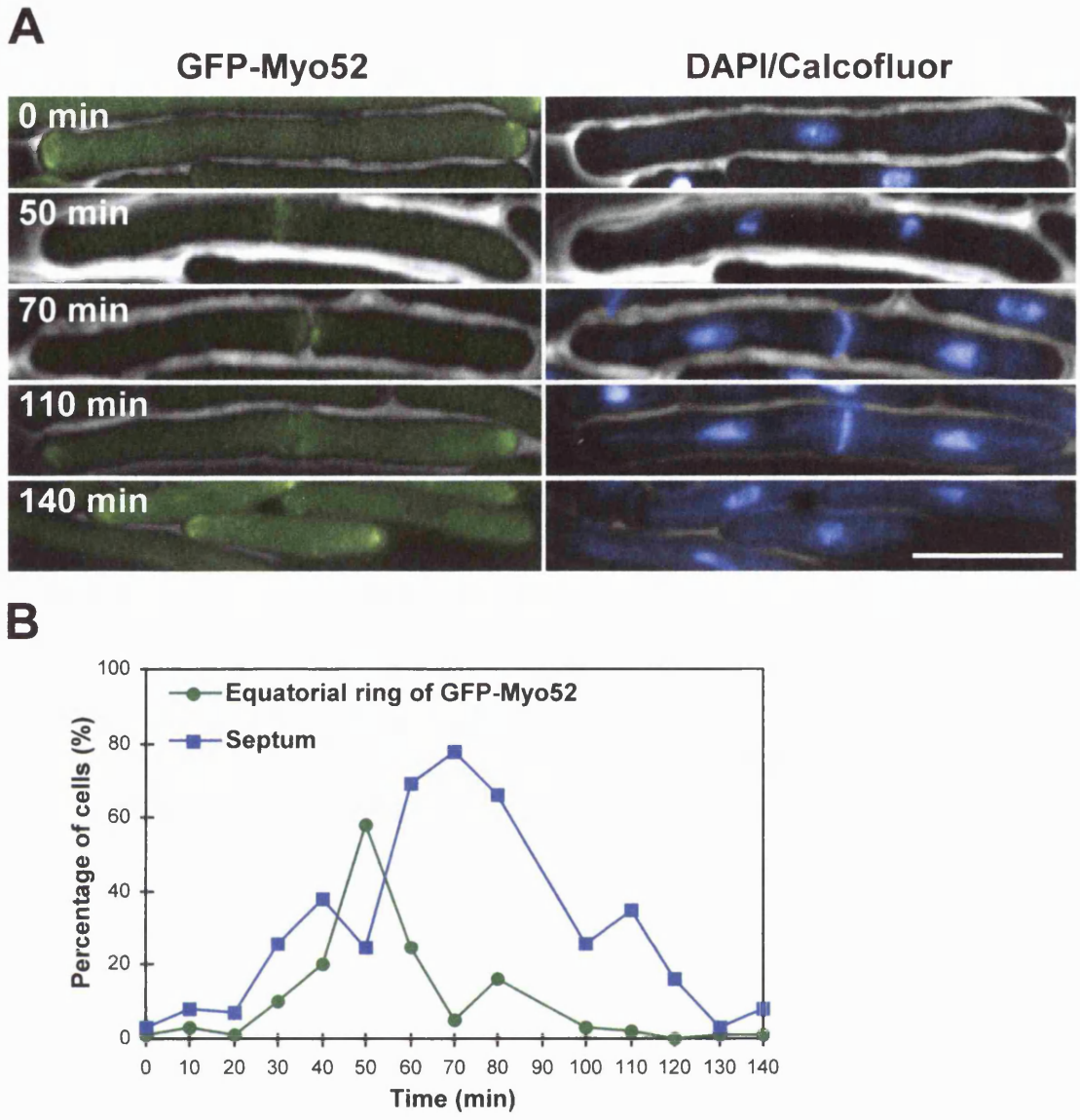

Figure 6.7 Localisation of Myo52 in *cdc25-22*

(A) GFP-Myo52 localises to both poles in *cdc25-22* cells arrested in the cell cycle at 36°C for 4 hours (top panel). When the culture is shifted to the permissive temperature most of the *cdc25-22* cells display an equatorial ring of GFP-Myo52 after 50 minutes at 25°C. A double band of GFP-Myo52 is observed at the equator after 70 minutes which coincides with the distribution of the septum. After 110 minutes GFP-Myo52 relocates to the poles and most of the *cdc25-22* cells display bipolar GFP-Myo52 staining after 140 minutes at 25°C. Bar = 10 μm.

(B) Graphical representation of the localisation of GFP-Myo52 in a population of *cdc25-22* cells after release from cell cycle arrest. A peak of GFP-Myo52 staining at the equator (50 minutes) is observed prior to the peak of septation (70 minutes).

For this experiment, *cdc25-22* cells transformed with pREP41GFP-*myo52*$^{+}$ were grown in liquid minimal medium for 20 hours at 25°C in the absence of thiamine to induce expression of the gene. Thiamine was added when GFP-Myo52 was observed in cells to stop further production of the protein. The culture was then incubated at 36°C for 4 hours to arrest *cdc25-22* in the cell cycle. After incubation at 36°C the culture was grown at 25°C to release the cells from their cell cycle arrest and the distribution of GFP-Myo52 was followed by taking samples every 10 minutes. For each time point, at least 100 cells were scored for the presence of equatorial GFP-Myo52 and septa.

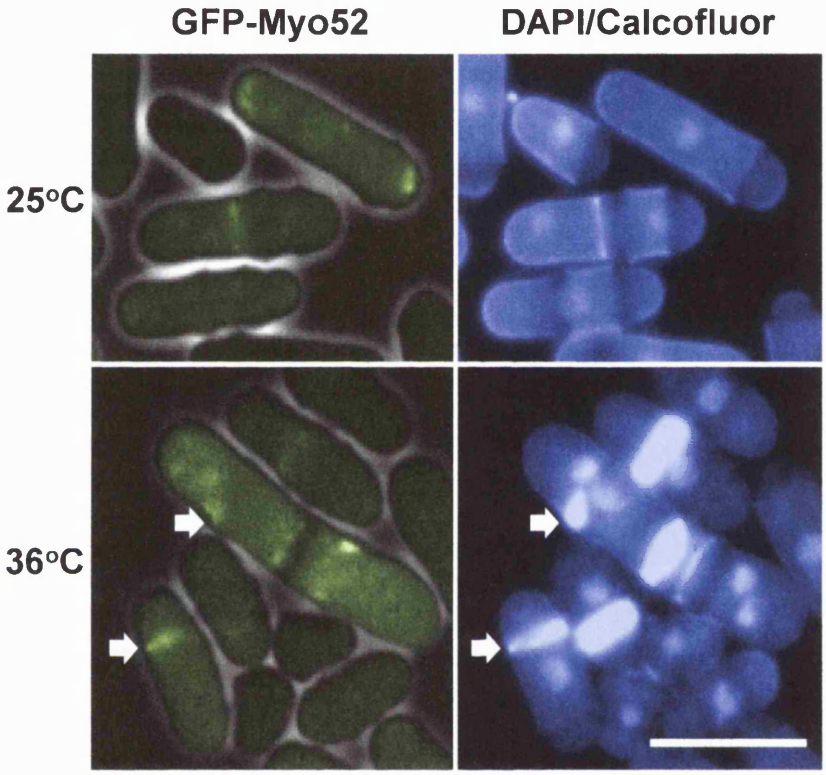

Figure 6.8 Localisation of Myo52 in *cdc16-116*

At the permissive temperature of 25°C GFP-Myo52 localises to the poles of growing cells and to the equator of cells undergoing septation. When the temperature is raised to 36°C for 1 hour the *cdc16-116* mutant forms multiple septa and the localisation of GFP-Myo52 correlates with the distribution of septa even when they are misplaced (arrows).

cdc16-116 cells transformed with pREP41GFP-*myo52*$^{+}$ were grown in liquid minimal medium in the absence of thiamine at 25°C for 20 hours after which thiamine was added. The culture was then split into two and one half was incubated at 25°C and the other half at 36°C for 1 hour before microscopic examination. Bar = 10 μm.

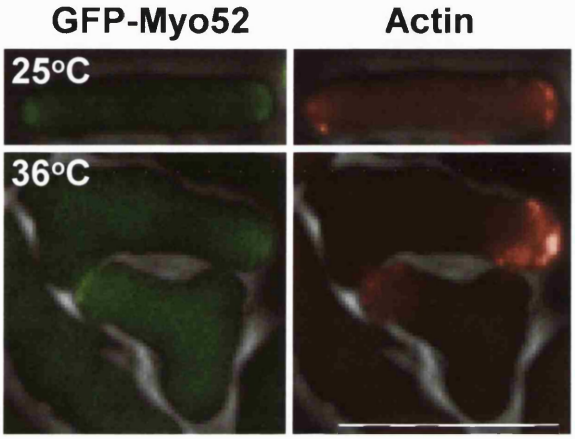

Figure 6.9 Localisation of Myo52 in *tea1-3*

GFP-Myo52 localises to both poles in cells undergoing bipolar growth at the permissive temperature of 25°C in *tea1-3* cells. When the temperature is raised to 36°C for 4 hours Tea1 is inactivated and new tips are generated, thus forming T-shaped cells. GFP-Myo52 is only found at the poles where actin is present.

tea1-3 cells transformed with pREP41GFP-*myo52*$^{+}$ were grown in liquid minimal medium in the absence of thiamine at 25°C for 20 hours after which thiamine was added to stop further production of GFP-Myo52. The culture was then split into two and one half was incubated at 25°C and the other half at 36°C for 4 hours before processing for immunofluorescence microscopy. The N-350 anti-actin antibody was used to probe the localisation of actin. Bar = 10 μm.

6.2.8 Localisation of Myo52 is Dependent on an Intact Actin Cytoskeleton

In the studies carried out so far Myo52 localised to the growing poles of wild type and *cdc25-22* cells and to the single actin-associated pole in *tea1-3* cells at the restrictive temperature. Furthermore, an equatorial band of Myo52 was observed with the occurrence of the medial actin ring in dividing cells (Figure 6.5). These studies indicated that the localisation of Myo52 and actin were intimately linked. To investigate whether Myo52 localisation was dependent on actin, treatments which disrupted the actin cytoskeleton were used to study their effects on the localisation of Myo52. This was carried out in a variety of ways, either using drugs to depolymerise actin or using an actin mutant to disrupt the actin cytoskeleton.

a. Treatment with Cytochalasin A

The first method was to use the actin-depolymerising drug cytochalasin A which has been shown to be effective in disrupting the fission yeast actin cytoskeleton (Kanbe et al., 1993). When *myo52Δ* cells transformed with pREP41GFP-*myo52*$^{+}$ were treated with cytochalasin A, numerous small dots of fluorescence were seen to be distributed throughout the cytoplasm of growing cells (Figure 6.10A). In dividing cells, patches of GFP-Myo52 were observed at the incipient site of division but were irregularly formed and not organised into an equatorial band. The disruption of the polar and equatorial localisation of GFP-Myo52 in cells treated with cytochalasin A indicated that actin was required for both its polar localisation in growing cells and its organisation into an equatorial band in dividing cells. When the drug was washed out and cells incubated in fresh medium the polar caps and equatorial bands of GFP-Myo52 returned, indicating that the effect of cytochalasin A was reversible.

b. Localisation of Myo52 in cps8^{-}

As a further test to show that Myo52 required an intact actin cytoskeleton for its localisation, Myo52 was localised in the temperature-sensitive actin mutant *cps8*$^{-}$ (Ishiguro and Kobayashi, 1996). At the permissive temperature *cps8*$^{-}$ cells transformed with pREP41GFP-*myo52*$^{+}$ localised GFP-Myo52 to the poles and

equator (Figure 6.10B). Fluorescence was sometimes observed in places other than these sites indicating that the actin cytoskeleton was not entirely normal in the *cps8*⁻ mutant even at the permissive temperature. At 36°C, large dots of fluorescence distributed throughout the cytoplasm was observed. In addition, filaments of GFP-Myo52 were also observed, perhaps decorating the actin cables that have been reported in fission yeast (Marks and Hyams, 1985; Arai et al., 1998).

c. Treatment with Latrunculin B

To more clearly demonstrate that the polar localisation of Myo52 depended on actin, *cdc25-22* cells arrested in the cell cycle at 36°C were treated with the actin-depolymerising drug latrunculin B (Ayscough et al., 1997). After 4 hours at this temperature *cdc25-22* arrested as cells undergoing bipolar growth and localised GFP-Myo52 at the two growing poles (Figure 6.10C). Addition of DMSO had no effect on the polar localisation of GFP-Myo52. However, when latrunculin B was added the polar caps of GFP-Myo52 dispersed into numerous small dots reminiscent of those observed in cells treated with cytochalasin A (Figure 6.10A).

6.2.9 Polar Localisation of Myo52 is Dependent on an Intact Microtubule Cytoskeleton

To investigate whether microtubules were also important for the localisation of Myo52, cells were treated with thiabendazole (TBZ) a drug which has been shown to be effective in depolymerising microtubules in fission yeast (Sawin and Nurse, 1998). When cells were treated with TBZ the polar caps of GFP-Myo52 were dislodged from the poles (Figure 6.11). Unlike treatments using actin-depolymerising drugs, the polar cap of GFP-Myo52 did not disperse into numerous small dots but instead remained intact as one large patch displaced to one side of the cell. The GFP-Myo52 band, however, was observed in cells in the process of division and appeared to be unaffected by TBZ. To confirm that microtubules had depolymerised using this treatment cells were processed for immunofluorescence microscopy and stained with the TAT1 anti-tubulin antibody. Microscopic observation showed that cells treated

with TBZ contained short microtubules that did not extend from one pole to the other but appeared as short stumps around the nucleus (data not shown).

To test the reversibility of TBZ treatment, one hour after the addition of the drug cells were washed free of TBZ and incubated for 30 minutes in fresh medium. After incubation in fresh medium GFP-Myo52 caps were once again observed at the poles.

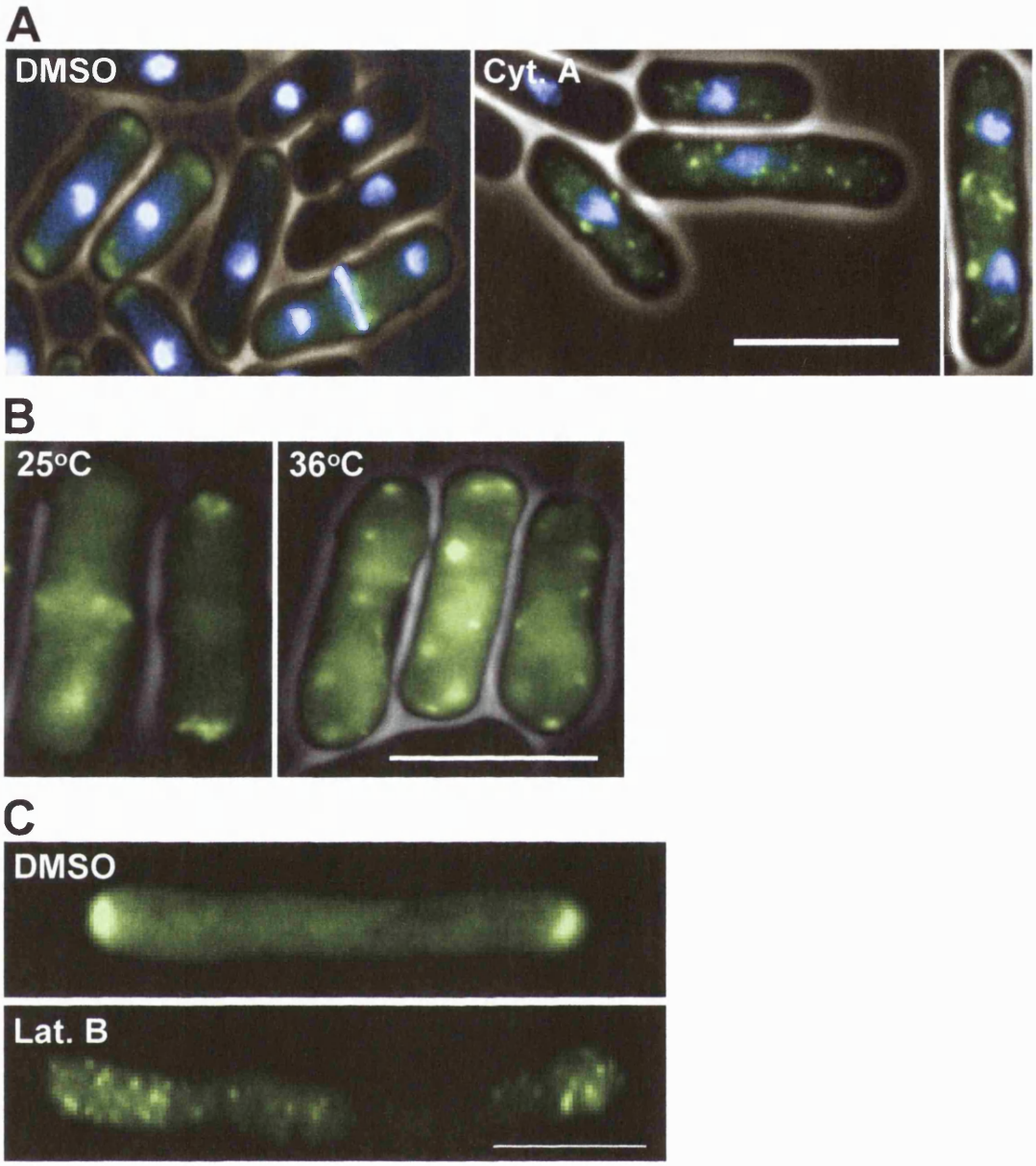

Figure 6.10 Localisation of Myo52 is Dependent on an Intact Actin Cytoskeleton

(A) Treatment of cells with the actin-depolymerising drug cytochalasin A disperses the polar cap of GFP-Myo52 into numerous small dots (middle panel) and disrupts the formation of the GFP-Myo52 ring in dividing cells (right panel). Treatment of cells with the DMSO solvent alone does not disrupt the polar and equatorial localisation of GFP-Myo52 (left panel). Cells were incubated in the presence of 5 μg/ml cytochalasin A at room temperature for 5 minutes to depolymerise actin. DAPI and Calcofluor staining is also shown to reveal nuclei and septa.

(B) GFP-Myo52 localises to the poles and equator in the *cps8*$^{-}$ temperature-sensitive actin mutant at 25°C but forms large dots throughout the cytoplasm after 1 hour at 36°C.

(C) The polar caps of GFP-Myo52 is unaffected in *cdc25-22* cells arrested at 36°C for 4 hours upon treatment with DMSO but disperses into numerous small dots after treatment with the actin-depolymerising drug latrunculin B. Cells were incubated in the presence of 10 μM latrunculin B at room temperature for 5 minutes to depolymerise actin.

Cells in (A), (B) and (C) all contain the pREP41GFP-*myo52*$^{+}$ plasmid and were grown in liquid minimal medium in the absence of thiamine at 25°C for 20 hours to induce the production of GFP-Myo52. After this period thiamine was added to stop further production of the protein before the described treatment. Bars = 10 μm.

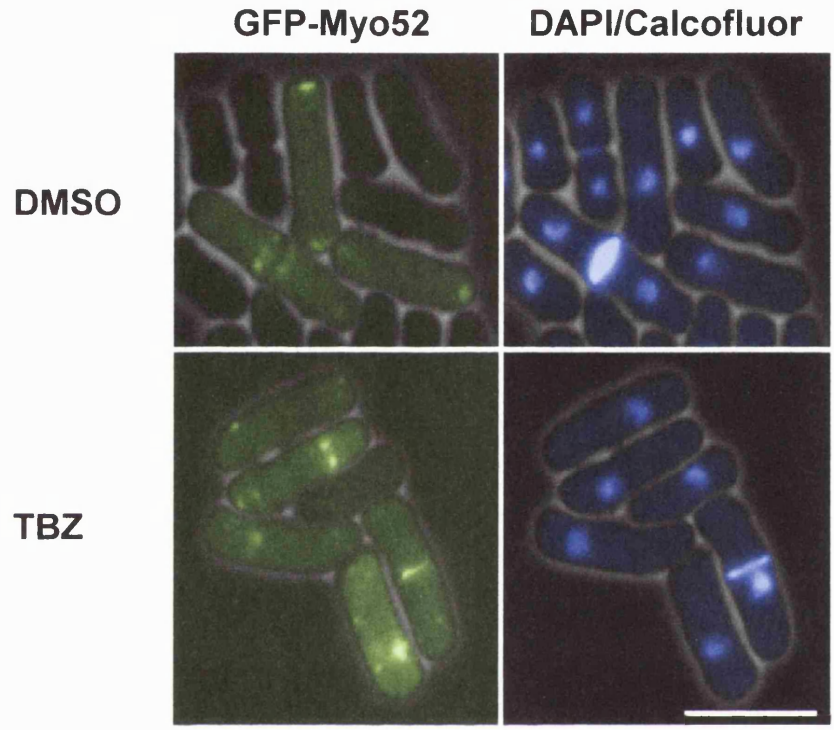

Figure 6.11 Polar Localisation of Myo52 is Microtubule-Dependent

Treatment of cells with the microtubule-depolymerising drug thiabendazole (TBZ) causes the displacement of GFP-Myo52 from the poles. However, the equatorial GFP-Myo52 remains in place and corresponds to the location of the septum.

myo52Δ cells transformed with pREP41GFP-*myo52*$^{+}$ were grown at 25°C in liquid minimal medium in the absence of thiamine for 20 hours to induce the production of GFP-Myo52 after which thiamine was added. TBZ was then added to a final concentration of 300 μg/ml and the culture was incubated at 25°C for 1 hour before microscopic observation. Control cells incubated in the presence of DMSO is also shown. Bar = 10 μm.

6.3 DISCUSSION

This chapter describes the preliminary localisation of Myo51 and a more detailed analysis of the localisation of Myo52. The results showed that the two fission yeast class V myosins have distinct patterns of localisation: Myo51 localises to one pole of fission yeast cells whereas Myo52 localises to both poles of growing cells and to the equator in cells undergoing division. Furthermore, Myo52 is intimately associated with actin and evidence is provided to show that an intact actin cytoskeleton is required for both the polar and equatorial localisation of Myo52. In addition, microtubules may also be required for certain aspects of Myo52 localisation.

6.3.1 Myo51 Localisation

Myo51 was localised by indirect immunofluorescence microscopy using an anti-myc antibody to probe the distribution of myc-Myo51 which was expressed from a plasmid. The results showed that myc-Myo51 was present at one end of cells indicating that the protein was asymmetrically localised.

Recently a different localisation of Myo51 to that reported here has been shown (Win et al., 2001). In this study Myo51 was found to have no specific localisation in interphase cells but was associated with the cytokinetic actin ring during cell division. The differences may lie in the way protein localisation was carried out in the two studies. Win et al. (2001) localised Myo51 in two ways: the first method was to tag Myo51 at the C-terminus with GFP in which expression of the protein was controlled by the native *myo51*$^+$ promoter and the second method by tagging the protein at the N-terminus in which expression was controlled by the *nmt1*$^+$ promoter on a plasmid.

Several factors could account for the distinct localisation of Myo51 reported here. The first is that the presence of a large tagging molecule such as GFP, which is 27 kD in size (Prasher et al., 1992), either at the N- or C-terminus might interfere with localisation. The second is that tip localisation may be an artefact of the high levels of myc-Myo51 when it was expressed from a plasmid. This may be the likely

explanation since diffuse fluorescence reminiscent to that described in this chapter was observed when GFP-Myo51 was overexpressed from a plasmid but was not observed when the expression of the protein was controlled from the *myo51*$^+$ promoter in the genome (D. Mulvihill, personal communication). The third possibility is that myc-Myo51 equatorial rings may have been present but the formaldehyde-glutaraldehyde fixation method may not have preserved these rings during the process of immunological detection and consequently was not observed upon microscopic examination. This issue might be finally resolved with the production of Myo51 specific antibody to detect native protein at physiological concentrations.

6.3.2 Myo52 Localisation

The polar and equatorial localisation of Myo52 was demonstrated in three ways; by means of N-terminal myc or GFP tags expressed from a plasmid or as a C-terminal GFP fusion under the control of the *myo52*$^+$ promoter. All of these different approaches gave similar results and therefore one can be reasonably confident that the localisation of Myo52 reported in this chapter represents the normal localisation of Myo52 in fission yeast cells.

a. Myo52 and Polarised Growth

Actin staining showed that the localisation of Myo52 and actin were closely correlated. Myo52 formed a discrete cap at the pole where actin patches were present and formed an equatorial band that coincided with the occurrence of the medial actin ring. The association between actin and Myo52 was not disrupted in *tea1-3* cells, a mutant which shows defects in defining the site of growth and is unable to switch from monopolar to bipolar growth (Verde et al., 1995). In these cells Myo52 remained associated with actin at the single growing pole and was absent from poles where growth did not take place. In contrast, Myo52 was found at both poles in *cdc25-22* cells undergoing bipolar growth.

The fact that Myo52 associates with sites of active growth indicates that this class V myosin may be involved in the recruitment of components to the growing pole. In budding yeast the homologue of Myo52, Myo2, also localises to sites of active growth (Catlett and Weisman, 1998; Reck-Peterson et al., 1999) and has been implicated in the targeting of secretory vesicles to the growing bud (Pruyne et al., 1998; Schott et al., 1999). If Myo52 does act as a motor, like other class V myosins, one candidate protein that could be transported by Myo52 is the product of the *mok1*$^+$ gene (Katayama et al., 1999; also known as *ags1*$^+$, Hochstenbach et al., 1998). Mok1 is an α-glucan synthase which is involved in the deposition of cell wall material and localises to sites of active growth. Like Myo52, Mok1 shows a similar distribution to actin in fission yeast cells and, furthermore, treatments that disrupt the actin cytoskeleton also disrupt the localisation of Mok1. Whether Myo52 is associated with vesicles containing material required for cell wall synthesis, like its counterpart in budding yeast (Schott et al., 1999) is suggested by the dispersal of Myo52 into small vesicle-like dots following actin depolymerisation (see below).

b. Myo52 and Cell Division

Most actin patches relocate from the poles immediately after entry into mitosis to form an equatorial band of actin (Marks and Hyams, 1985). This is followed by the recruitment of the fission yeast class II myosins to the cell middle. A ring of Myo2 is formed during metaphase/anaphase A and then later by a ring of Myp2 at the end of anaphase B (Kitayama et al., 1997; Bezanilla et al., 2000). The fission yeast class II myosin rings are thus seen to colocalise at some point in mitosis to form the actin based contractile ring (Motegi et al., 2000). In this context, a ring of Myo52 is observed at late anaphase, after the formation of the contractile ring. Interestingly, the Myo52 ring does not contract, unlike the Myo2 and Myp2 rings (Bezanilla et al., 2000; Motegi et al., 2000; Mulvihill et al., 2000). On this basis Myo52 does not appear to be the motor that powers the constriction of the actin ring but instead may be associated with the septum that forms centripetally as the actin ring contracts.

One possibility is that Myo52 brings components required for septation to the division site. This is consistent with the observation that Myo52 is seen at the incipient division site prior to the appearance of the septum, most clearly demonstrated in *cdc25-22* cells released from cell cycle arrest. Interestingly, the single Myo52 ring becomes two bands after septum formation and is reminiscent of the double bands of Mok1 α-glucan synthase staining during cell division (Katayama et al., 1999).

In the mutant *cdc16-116*, multiple septa and Myo52 bands are formed at the restrictive temperature and the localisation of Myo52 remains associated with septation even when septa do not form at the equator. The fact that Myo52 is observed with septa that do not form in the middle suggests that factors responsible for the placement of septa are also responsible for the placement of Myo52.

Interestingly, septum formation at the cell equator occurs in *myo52Δ* cells (Chapter 4), indicating that Myo52 is not essential for either the correct placement or synthesis of septa. Perhaps Myo52-independent mechanisms exist by which septal components are brought to the division site. Alternatively, Myo52 may bring a minor component to the site of septation. Although *myo52Δ* cells form septa, these cells display a higher septation index than wild type cells (Chapter 4) indicating that the process of septum synthesis or cleavage occur more efficiently in the presence of Myo52.

c. Myo52 and the Fission Yeast Cytoskeleton

Treatments with actin-depolymerising drugs showed that the polar cap of Myo52 disperse into numerous small dots, indicating that an intact actin cytoskeleton was required for the polar localisation of Myo52. Electron microscopy studies have shown the presence of a system of Golgi-derived vesicles associated with sites of cell wall deposition (Kanbe et al., 1989; Robinow and Hyams, 1989) and that the distribution of this vesicle system through the cell cycle parallels that of the actin cytoskeleton (Marks and Hyams, 1985). Interestingly, treatment of fission yeast with cytochalasin

A causes vesicles to be dissociated away from the growing poles such that they accumulate in the cytoplasm (Kanbe et al., 1993). Perhaps the dots of fluorescence that are observed, represent Myo52-associated vesicles that disperse into the cytoplasm upon disruption of the actin cytoskeleton.

The polar localisation of Myo52 also seems to be microtubule-dependent because treatment with the microtubule-depolymerising drug TBZ dislodged the polar cap of Myo52 from the poles as one large patch although it did not disperse. One possible explanation on the displacement of Myo52 from the poles is that the microtubule filament system may be required for the integrity of the cortical actin cytoskeleton and treating cells with TBZ may have had an effect on the cortical actin cytoskeleton which consequently disrupted the polar localisation of Myo52. Indeed, treatments with TBZ has been shown to disrupt cortical actin patches in fission yeast (Sawin and Nurse, 1998) indicating that the microtubule and actin cytoskeleton functionally interact.

TBZ did not disrupt the equatorial localisation of Myo52 and the cells were able to form complete bands of Myo52 in the presence of the drug. In contrast, treatments which disrupted the actin cytoskeleton also disrupted the equatorial localisation of Myo52 indicating that an intact actin cytoskeleton was required for both the polar and equatorial localisation of Myo52 which is consistent with the localisation of Myo52 with cortical actin patches and the medial actin ring.

Chapter 7
Myo52 and Cell Wall Synthesis

7.1 INTRODUCTION

The cell wall of *Schizosaccharomyces pombe* is composed of galactomannan, α-1,3-linked glucans, β-1,3-linked glucans and β-1,6-linked glucans (Osumi et al., 1998). Fission yeast cells are thought to grow by incorporating new cell wall material into cuts made in the pre-existing glucan molecules (Johnson et al., 1989). Turgor pressure stretches the weakened cell wall to make room for the insertion of new cell wall components resulting in the extensile growth of fission yeast.

Actin appears to be intimately associated with cell growth and localises to sites of cell wall synthesis (Marks and Hyams, 1985). This is supported by the observation that the cell wall of the *cps8*⁻ actin mutant is disorganised (Osumi et al., 1998). Perhaps the actin cytoskeleton provides a scaffold that localises factors involved in cell wall synthesis, such as the Mok1 α-glucan synthase, to sites of cell wall deposition (Katayama et al., 1999). Indeed, treatments with drugs which depolymerise the actin cytoskeleton delocalise Mok1 from the poles and equator where it is normally localised (Katayama et al., 1999).

Actin is also important for the formation of the division septum and it has been suggested that the deposition of cell wall material may be guided by the cytokinetic actin ring (Marks and Hyams, 1985; Eng et al., 1998). Observations from mutants in the *cdc3*, *cdc4*, *cdc8*, *cdc12* and the *rng2* genes which show defects in the organisation of the cytokinetic actin ring also exhibit defects in septum formation (Balasubramanian et al., 1994; McCollum et al., 1995; Balasubramanian et al., 1992; Chang et al., 1997; Eng et al., 1998). The products of these genes have been localised and found to be essential for cytokinetic actin ring formation.

The signal that triggers actin ring constriction and septum formation is thought to be mediated by a signaling cascade defined by the *sid* genes (septum initiation defective) (Balasubramanian et al., 2000). These include *cdc7*, *cdc11*, *cdc14*, *spg1*, *sid1*, *sid2* and *sid4* (Guertin et al., 2000). Mutations in these genes prevent cytokinesis but,

interestingly, show normal medial actin ring assembly at mitosis and redistribution of actin patches at the cell poles during interphase. However, their failure to undergo cytokinesis and cell cleavage results in the formation of multinucleate and highly elongated cells which eventually causes them to lyse (Guertin et al., 2000).

The product of the *spg1*$^+$ gene appears to be of key importance in the activation of actin ring constriction and septum formation (Schmidt et al., 1997). Spg1 is a GTPase and the proteins ability to control septation is determined by the state of the guanine nucleotide. GTP bound Spg1 is the biologically active form and induces septum formation when it is overexpressed. The effects of GTP bound Spg1 are mediated through its effector protein kinase Cdc7 and require the function of Sid1, Sid2, and Cdc14 which are downstream in the septation signaling cascade (Schmidt et al., 1997; Sparks et al., 1999; Balasubramanian et al., 1998; Guertin et al., 2000). Cdc16 and Byr4 which form a two component GTPase activating protein complex for Spg1 negatively regulate the septation induction pathway, presumably by converting Spg1 into its inactive GDP bound form (Cerutti and Simanis, 1999). The observation that mutants in *cdc16* and *byr4* form multiple septa is consistent with these genes having a role in negatively regulating septation (Fankhauser et al., 1993; Song et al., 1996).

This chapter further explores the role of Myo52 in tip growth and septation. This is based on the fact that Myo52 localises to sites of active growth (Chapter 6) and is supported by the observation that *myo52Δ* cells display various morphological abnormalities (Chapter 4), consistent with the possibility that these cells are defective in localising growth at defined sites.

In this chapter I present evidence that *myo52Δ* interacts with mutants in the pathway that regulates septation and with mutants defective in the organisation of the cytokinetic actin ring. Colocalisation of Myo52 with the cell wall synthesis enzyme, Mok1, will be shown. I will also present data which suggests that the cell wall of *myo52Δ* is different from that of wild type and show that the Mok1 α-glucan

synthase is highly abundant in *myo52Δ* cells. These results implicate a role for Myo52 in cell wall synthesis and septation. The possible nature of the relationship between Myo52 and cell growth in fission yeast will be discussed and compared to that in other organisms.

7.2 RESULTS

7.2.1 *myo52Δ* Exhibits a Genetic Interaction with Components of the Pathway that Regulates Septation

Localisation studies showed that Myo52 formed a single band at the incipient site of septation in dividing wild type cells whilst in the *cdc16-116* mutant, multiple bands of Myo52 were observed to coincide with the distribution of the multiple septa that formed (Chapter 6). These results indicated that the equatorial localisation of Myo52 responded to signals from the pathway that regulated septation. To investigate whether *myo52Δ* exhibited a genetic interaction with components of the pathway that regulated septation *myo52Δ cdc16-116* and *myo52Δ spg1-B8* double mutants were constructed.

The results of the genetic analysis showed that the *myo52Δ spg1-B8* double mutant grew very poorly at temperatures which was permissive for the growth of the *myo52Δ* and *spg1-B8* single mutants (Figure 7.1A) indicating that the combination of the two mutations was synthetically lethal. Microscopic examination of the double mutant revealed the presence of many lysed cells and few cells with septa were observed at either 25°C or 29°C. The genetic interaction between *myo52Δ* and *spg1-B8* was supported by the observation that *myo52Δ* also exhibited a similar lethal interaction with a mutation in the gene (*cdc7-24*) directly regulated by Spg1 (data not shown).

Analysis of the *myo52Δ cdc16-116* double mutant showed that *myo52Δ* also exhibited

a strong genetic interaction with *cdc16-116* resulting in the death of the double mutant at 29°C (Figure 7.1B). Unlike the interaction with *spg1-B8* and *cdc7-24*, the *myo52Δ cdc16-116* double mutant died as septated cells with oval and rod-shaped morphology.

7.2.2 *myo52Δ* Cells Form Multiple Septa Upon Overexpression with *spg1*$^+$

myo52Δ cells form septa, indicating that septation occurs in the absence of *myo52*$^+$ function (Chapter 4). To further investigate the role of *myo52*$^+$ in septum formation, the *spg1*$^+$ septum inducing gene was overexpressed in *myo52Δ* and wild type cells (Schmidt et al., 1997). If *myo52*$^+$ is involved in septation then it might be expected that the efficiency of septation caused by *spg1*$^+$ overexpression would be reduced in the absence of Myo52.

To test this, *myo52Δ* and wild type cells were transformed with the pREP41-*spg1*$^+$ plasmid. Transformants were grown in minimal medium in the absence of thiamine for 30 hours to induce the expression of *spg1*$^+$, after which they were harvested and approximately 500 cells were scored for the presence of septa (Figure 7.2A). The results showed that overexpression of *spg1*$^+$ caused *myo52Δ* cells to form multiple septa at about the same frequency to wild type cells. For example, the percentage of the *myo52Δ* and wild type population with a single septum was 30% and 36% respectively. The percentage of cells with two septa was 17% in the *myo52Δ* population and 12% in wild type cells whereas the proportion of cells with three or more septa was approximately 5% in both populations. The fact that wild type and *myo52Δ* cells formed septa at about the same frequency when *spg1*$^+$ was overexpressed indicated that Spg1 was still able to activate septum formation in the absence of Myo52.

To examine whether there were any qualitative differences in the septa formed, wild type and *myo52Δ* cells were stained with the cell wall dye, Calcofluor (Figure 7.2B).

Microscopic examination of *myo52Δ* cells showed the presence of septa that were more intensely stained with Calcofluor than in wild type controls perhaps indicating that the septa in *myo52Δ* were thicker than normal or that the bright staining may be a consequence of septa having to span a wider girth in *myo52Δ* cells. Septa were able to span the entire diameter of the cell on most occasions although in about 1% of the *myo52Δ* population short incomplete stumps of septa were observed.

7.2.3 *myo52Δ* Exhibits a Genetic Interaction with Mutants that are Defective in Actin Organisation

Since *myo52Δ* cells exhibit a genetic interaction with components of the pathway that regulate septation, genetic crosses were carried out to investigate whether *myo52Δ* also interacts with mutants defective in the organisation of the cytokinetic actin ring. Genetic crosses were performed with *cdc3-6*, *cdc4-8* and *cdc8-110* which have mutations in the fission yeast profilin, myosin light chain and tropomyosin genes respectively (Balasubramanian et al., 1994; McCollum et al., 1995; Balasubramanian et al., 1992). The characteristic feature of all these mutants is that they grow normally at permissive temperature (25°C) but display disorganised contractile actin rings when the temperature is raised to 36°C. Additionally, mutations in the actin binding proteins, profilin and tropomyosin, also display delocalised actin patches suggesting that these proteins are important for the general organisation of actin in the cell (Chang and Nurse, 1996).

The genetic cross between *myo52Δ* x *cdc3-6* yielded no viable *myo52Δ cdc3-6* progeny out of the sixteen tetrads dissected. All the *myo52Δ cdc3-6* double mutants died as germinated spores which failed to divide at 25°C, a temperature which permitted the growth of *myo52Δ* and *cdc3-6* single mutant members of the tetrads. Thus, *myo52Δ* exhibited a synthetic lethal interaction with a mutation in the profilin gene.

When the *myo52Δ* x *cdc4-8* cross was performed viable *myo52Δ cdc4-8* double mutants were obtained at 25°C. However, when these mutants were incubated at the semi-permissive temperature of 29°C they were unable to form colonies (Figure 7.3A) and died as elongated cells with aberrant septa indicating that *myo52Δ* also exhibited a synthetic lethal interaction with *cdc4-8*.

Viable *myo52Δ cdc8-110* double mutants were obtained from the cross between *myo52Δ* and *cdc8-110* cells. The *myo52Δ cdc8-110* double mutant was able to grow at temperatures (25°C and 29°C) which permitted the growth of *myo52Δ* and *cdc8-110* single mutants indicating that the combination of these mutations was not synthetically lethal. The *myo52Δ cdc8-110* double mutant was morphologically indistinguishable from the *myo52Δ* single mutant but grew more slowly than either single mutant at both 25°C and 29°C. These results indicate that *myo52Δ* exhibited only a weak genetic interaction with the *cdc8-110* tropomyosin mutation compared to the synthetic lethality obtained with the *cdc3-6* (profilin) and *cdc4-8* (myosin light chain) mutations.

7.2.4 Moderate Expression of Myo52 is Toxic to *cdc4-8* Cells

cdc3-6 and *cdc4-8* mutants exhibited a synthetic lethal interaction with *myo52Δ*. To investigate the effect of *myo52*$^+$ gene dosage in these mutants, pREP41GFP-*myo52*$^+$ was transformed into *cdc3-6*, *cdc4-8* and also *cdc8-110*.

Transformation of the plasmid into *cdc3-6* and *cdc8-110* mutants yielded cells with a wild type morphology in medium supplemented with thiamine at 25°C. In conditions when the *nmt1*$^+$ promoter from pREP41GFP-*myo52*$^+$ was induced, both the *cdc3-6* and *cdc8-110* mutants produced cells that gave an overexpression phenotype similar to that observed in wild type cells at 25°C (Chapter 5).

Curiously, the presence of pREP41GFP-*myo52*$^+$ plasmid in the *cdc4-8* mutant

appeared to be toxic even in medium supplemented with thiamine. These transformants grew more slowly than *cdc4-8* control cells containing the empty pREP41GFP plasmid. Microscopic inspection of the *cdc4-8* cells transformed with pREP41GFP-*myo52*$^+$ showed that their slow growth was a consequence of their abnormal morphology and highly elongated cells up to 70 μm in length were often observed (data not shown). These long cells also formed three to four branches spaced along the main cell axis such that they resembled the hyphae of filamentous fungi rather than the morphology of a unicellular yeast. Surprisingly, these morphological defects were observed in thiamine-supplemented medium - conditions in which the *nmt1*$^+$ promoter was largely suppressed, suggesting that even a moderate increase in the expression of *myo52*$^+$ was toxic to *cdc4-8* cells.

Since moderate overexpression of *myo52*$^+$ in *cdc4-8* produced abnormal cells at 25°C, it was envisaged that by raising the temperature to 29°C a more severe phenotype should be observed in this temperature-sensitive mutant. Figure 7.3B shows that *cdc4-8* cells transformed with the pREP41GFP-*myo52*$^+$ was unable to grow at this temperature whereas control cells formed colonies in the same conditions. The experiment was also repeated using *cdc4-8* cells transformed with pREP41myc-*myo52*$^+$ plasmid and identical results were observed. At 25°C *cdc4-8* cells containing pREP41myc-*myo52*$^+$ formed abnormally shaped cells in medium supplemented with thiamine and at 29°C they were unable to form colonies and died as highly elongated and branched cells that accumulated multiple nuclei.

To investigate whether this phenotype was specific to *myo52*$^+$, the other type V myosin, *myo51*$^+$, was also overexpressed in *cdc4-8* cells using the pREP41myc-*myo51*$^+$ plasmid. Unlike *cdc4-8* cells containing plasmids with the *myo52*$^+$ gene, *cdc4-8* cells containing the pREP41myc-*myo51*$^+$ were viable at both 25°C and 29°C and displayed wild type morphology in minimal medium supplemented with thiamine. These results indicate that the *cdc4-8* mutant is highly sensitive to Myo52 levels in the cell.

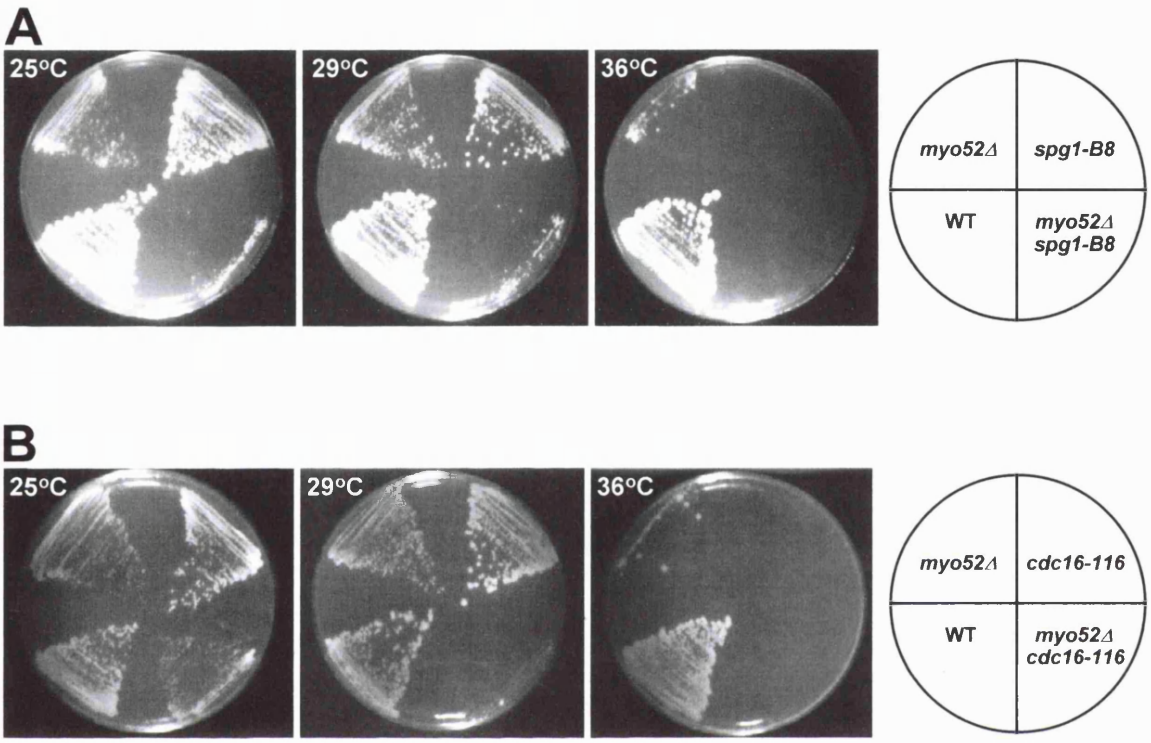

Figure 7.1 *myo52Δ* Exhibits a Genetic Interaction with Components of the Pathway that Regulates Septation

(A) The *myo52Δ spg1-B8* double mutant grows very poorly at temperatures which is permissive for the growth of *myo52Δ* and *spg1-B8* single mutants (25°C and 29°C).

(B) The *myo52Δ cdc16-116* double mutant is unable to grow at 29°C a temperature which is permissive for the growth of *myo52Δ* and *cdc16-116* single mutants.

For both (A) and (B) cells were incubated on YES plates for three days.

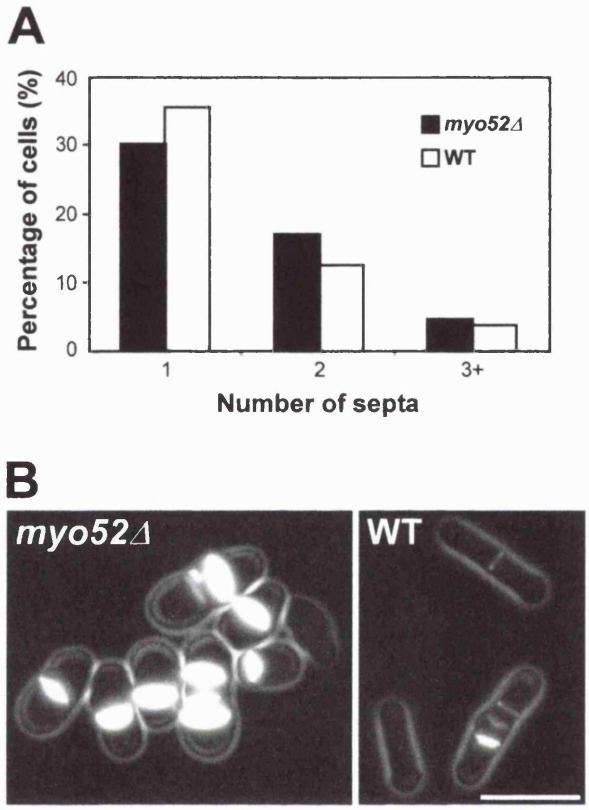

Figure 7.2 Overexpression of *spg1*$^+$ in *myo52Δ* and Wild Type Cells

(A) The bar chart shows the percentage of cells with one, two, three or more septa after overexpressing *spg1*$^+$ in *myo52Δ* and wild type cells. *myo52Δ* cells form multiple septa at a similar frequency to wild type cells.

(B) Calcofluor staining of *myo52Δ* and wild type cells after *spg1*$^+$ overexpression. The septa formed in *myo52Δ* are more intensely stained with Calcofluor than in wild type cells. Bar = 10 μm.

For both (A) and (B) cells transformed with pREP41-*spg1*$^+$ were grown in minimal medium in the absence of thiamine for 30 hours at 25°C.

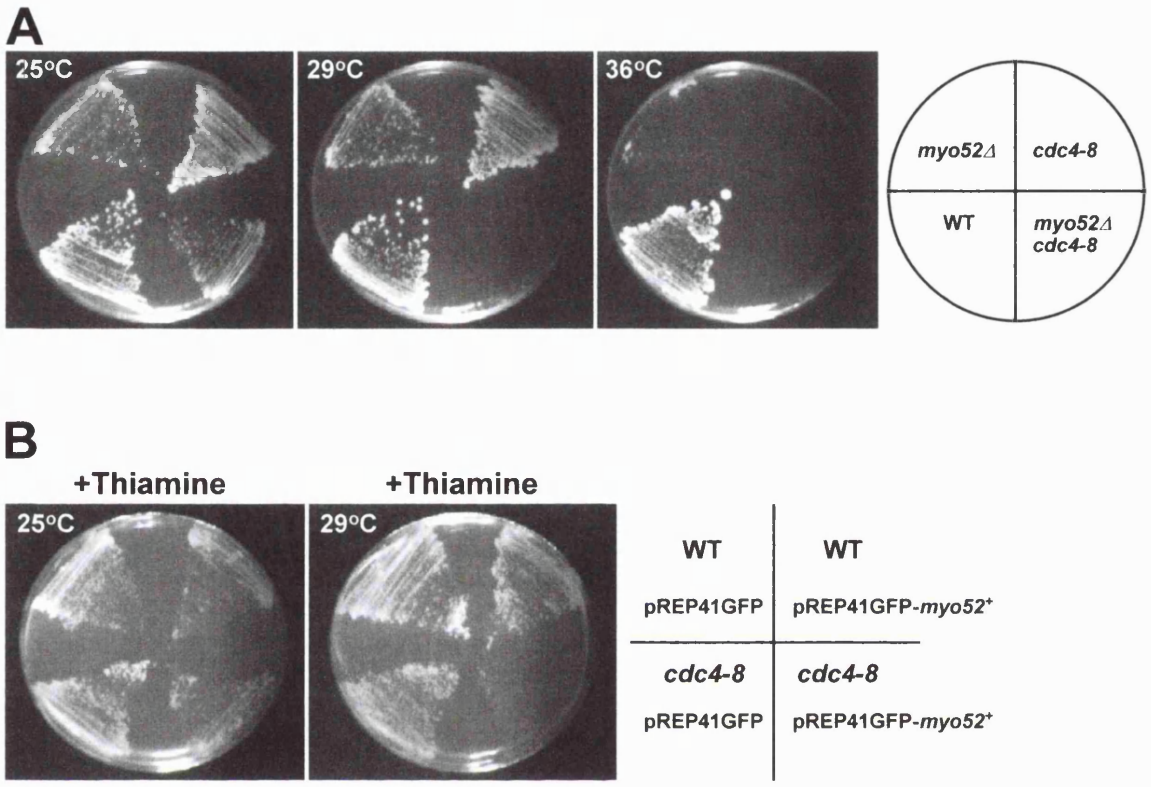

Figure 7.3 Myo52 Exhibits an Interaction with Cdc4

(A) The *myo52Δ cdc4-8* double mutant is unable to grow at 29°C a temperature which is permissive for the growth of *myo52Δ* and *cdc4-8* single mutants. Cells were incubated on YES plates for three days.

(B) Increased levels of Myo52 is toxic to *cdc4-8* cells. *cdc4-8* cells transformed with pREP41GFP-*myo52*$^{+}$ plasmid are unable to grow at 29°C whereas cells containing pREP41GFP vector alone form colonies at this temperature. Cells were incubated on minimal medium in the presence of thiamine and therefore relied on the basal level of transcription initiation from the *nmt1*$^{+}$ promoter to express *myo52*$^{+}$. The photographs show plates after three days of incubation.

7.2.5 Myo52 Colocalises with Mok1 α-Glucan Synthase

Localisation studies showed that Myo52 was present at sites of cell wall deposition, similar to the distribution of the previously described Mok1 α-glucan synthase (Katayama et al., 1999). To investigate whether the two proteins colocalised, *myo52Δ* cells expressing GFP-Myo52 from the pREP41GFP-*myo52*$^{+}$ plasmid were stained with the anti-Mok1 polyclonal antibody. The results of the immunofluorescence microscopy showed that Mok1 localised at both poles in interphase cells as a discrete cap at the very tip of each growing pole (Figure 7.4). When the same cells were examined for the distribution of GFP-Myo52, green fluorescence was observed at the poles which resembled the caps of red fluorescence from the Mok1 staining, indicating that GFP-Myo52 and Mok1 staining overlapped. To investigate whether the two proteins precisely occupied the same space in the cell, the images taken under FITC (GFP-Myo52) and rhodamine (Mok1) fluorescence were merged. Interestingly, yellow spots of fluorescence was observed at points in the cell where GFP-Myo52 and Mok1 colocalised in the merged image (green + red). However, some green and red fluorescence was observed in the merged image, indicating that not all the GFP-Myo52 are associated with Mok1.

Colocalisation of GFP-Myo52 with Mok1 at the equator of dividing cells was less clear. Although yellow spots of fluorescence were observed at the equator where the two proteins colocalised (Figure 7.4), no equatorial rings of Mok1, as reported by Katayama et al. (1999), was observed when GFP-Myo52 rings were formed. This may be as a consequence of the poor preservation of the Mok1 rings using the formaldehyde-glutaraldehyde method used to fix the cells for immunofluorescence microscopy. Alternatively, this may indicate that the Mok1 and GFP-Myo52 equatorial rings form at distinct times in the cell.

7.2.6 Mok1 is Delocalised in *myo52Δ* Cells

myo52Δ cells exhibit morphological defects resulting from their inability to undergo polarised growth (Chapter 4). To investigate whether this was due to defects in the localisation of factors involved in cell wall deposition, *myo5Δ* cells were stained for the Mok1 α-glucan synthase. Mok1 was chosen since Myo52 colocalised with the α-glucan synthase in wild type cells and therefore might play some role in its localisation.

Immunofluorescence microscopy with the anti-Mok1 polyclonal antibody showed that Mok1 was delocalised in round *myo52Δ* cells (Figure 7.5). Partial Mok1 localisation at the poles was observed in *myo52Δ* cells that retained the rod-shaped fission yeast morphology but discrete polar caps of staining were not observed. In most cells the polar Mok1 staining appeared diffuse and occupied most of the polar region instead of forming a distinct cap at the very tip of each pole. Equatorial localisation of Mok1 also appeared diffuse and a wide belt of staining was observed at the equator of dividing cells. In some cells polar and equatorial localisation of Mok1 occurred at the same time.

7.2.7 Myo52 Localisation does not Require Mok1

Mok1 staining in *myo52Δ* showed that Mok1 was delocalised in these cells. To investigate whether the localisation of Myo52 required Mok1, the distribution of GFP-Myo52 was studied in the *mok1-664* temperature-sensitive mutant. At the permissive temperature GFP-Myo52 localised to the poles of growing cells and to the equator of dividing cells (Figure 7.6). When the temperature was raised to 36°C for 4 hours green fluorescence was still observed at the growing poles and at the equator of cells undergoing division. The fact that GFP-Myo52 was correctly localised in the *mok1-664* mutant indicated that Mok1 was not required for the localisation of Myo52 although this does not exclude the possibility that Myo52 may be important for the localisation of Mok1.

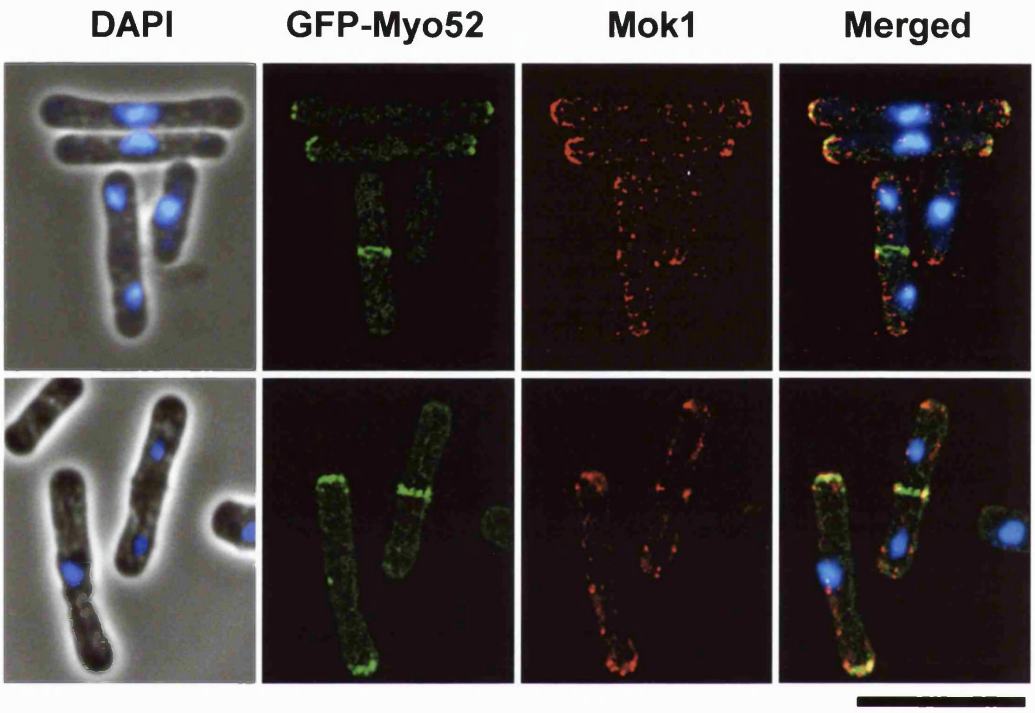

Figure 7.4 Myo52 Colocalises with Mok1 in Fission Yeast Cells

myo52Δ cells transformed with pREP41GFP-*myo52*$^{+}$ were probed with the anti-Mok1 polyclonal antibody to investigate the localisation of GFP-Myo52 and Mok1. The top and lower panels represent two fields of cells showing the distribution of GFP-Myo52 (green) and Mok1 (red). Yellow dots (green + red) are found wherever GFP-Myo52 and Mok1 colocalise (merged image). The figure shows deconvolved images of Mok1 staining and GFP-Myo52. Bar = 10 μm.

Cells were grown in liquid minimal medium in the absence of thiamine at 25°C for 20 hours to induce the expression of GFP-Myo52. Cells were fixed with formaldehyde-glutaraldehyde before processing for immunofluorescence microscopy.

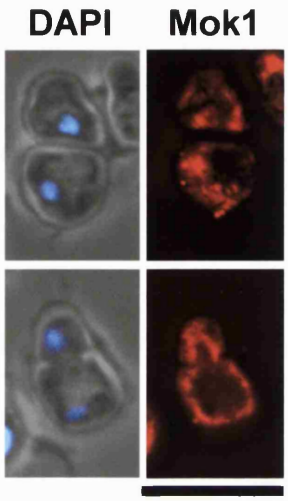

Figure 7.5 Mok1 Localisation in *myo52Δ* Cells

Mok1 staining shows that the the α-glucan synthase is partially localised in *myo52Δ* cells at sites of cell wall deposition. Two typical *myo52Δ* cells are shown. The top panel shows a septating cell with some Mok1 staining at the equator. The bottom panel shows another cell with Mok1 staining at the cell periphery. The figure shows deconvolved images of Mok1 staining. Bar = 10 μm.

myo52Δ cells were grown at 25°C in liquid YES medium to exponential phase and fixed with formaldehyde-glutaraldehyde before processing for immunofluorescence microscopy with the anti-Mok1 polyclonal antibody.

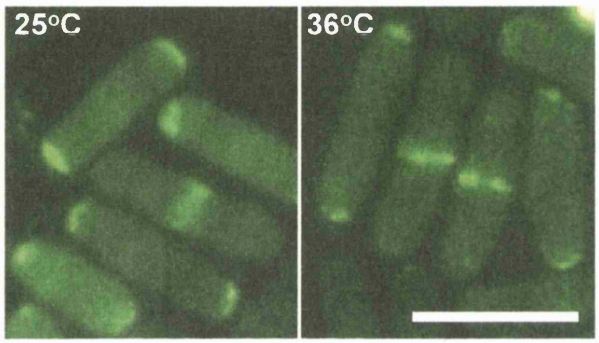

Figure 7.6 Myo52 Localisation does not Require Mok1

GFP-Myo52 localises to the poles and equator in the *mok1-664* temperature-sensitive mutant at 25°C and 36°C. *mok1-664* cells transformed with pREP41GFP-*myo52*$^{+}$ were grown at 25°C for 20 hours in liquid minimal medium in the absence of thiamine to induce the production of GFP-Myo52. Following growth, thiamine was added to the medium to stop further production of the protein. The culture was then split in two and one half was incubated at 25°C and the other half at 36°C for a further 4 hours before microscopy. Bar = 10 μm.

7.2.8 *myo52Δ* Exhibits a Synthetic Lethal Interaction with *pck2-8*

Genetic studies showed that *myo52Δ* interacted with components of the pathway that regulated septation and additionally with structural mutants defective in maintaining the integrity of the cytokinetic actin ring. To investigate whether *myo52Δ* also exhibited a genetic interaction with mutants defective in cell wall synthesis, *myo52Δ* was crossed with *mok1-664* and a mutant in the protein kinase C gene (*pck2-8*) which has been shown to be a regulator of Mok1 (Katayama et al., 1999).

Analysis of the *myo52Δ pck2-8* double mutant showed that the combination of the two mutations was highly deleterious even at the permissive temperature of 25°C (Figure 7.7A). The *myo52Δ pck2-8* double mutant barely grew at this temperature and microscopic inspection revealed large round cells that had completely lost the characteristic rod-shaped morphology of fission yeast (data not shown). Double mutants between *myo52Δ* and a null allele of *pck2* (*pck2Δ*) was also constructed to confirm the genetic interaction with *pck2-8*. The *myo52Δ pck2Δ* double mutant also produced large round cells that grew very poorly at 25°C. Thus, *myo52Δ* exhibited a strong genetic interaction with *pck2* mutants.

A synthetic lethal interaction between *myo52Δ* and *mok1-664*, however, was not observed and the *myo52Δ mok1-664* double mutant was viable at temperatures permissive for the growth of the single mutants (Figure 7.7B). The double mutant was also morphologically indistinguishable from the *myo52Δ* single mutant.

7.2.9 *myo52Δ* is Resistant to Zymolyase Cell Wall Digestion

Localisation of Mok1 showed that the α-glucan synthase was delocalised in *myo52Δ* cells. To assess whether Mok1 delocalisation reduced the integrity of the *myo52Δ* cell wall, *myo52Δ* cells were treated with Zymolyase - an enzyme which has been shown to digest the fission yeast cell wall (Hochstenbach et al., 1998; Katayama

et al., 1999). The sensitivity of *myo52Δ* to Zymolyase was compared to wild type cells and to two mutants known to be sensitive to this enzyme, *mok1-664* and *pck2Δ* (Katayama et al., 1999).

As a measure of the progress of cell wall digestion, the change in optical density of cultures treated with Zymolyase was followed. Surprisingly, the results showed that *myo52Δ* cells were significantly more resistant to Zymolyase cell wall digestion than to wild type cells (Figure 7.8A). There was virtually no change in optical density in *myo52Δ* cells treated with Zymolyase whereas wild type cells showed a steady decrease in optical density over the 4 hour period in which the experiment was conducted. When *myo51Δ* cells were digested with Zymolyase, they too showed a steady decline in optical density similar to that of wild type cells (data not shown). However, *mok1-664* and *pck2Δ* cells exhibited a more rapid decrease in optical density, diminishing to half its original value in less than 50 minutes incubation in Zymolyase, indicating that these mutants underwent cell lysis as a consequence of their fragile cell walls.

To investigate whether Zymolyase had any morphological effect on *myo52Δ*, Zymolyase treated cells were examined microscopically. In agreement with the optical density results, intact *myo52Δ* cells were observed even after 4 hours in the enzyme (Figure 7.8B). In contrast, wild type, *mok1-664* and *pck2Δ* showed cell lysis and only the cellular debris of these cells were observed after 4 hours incubation in Zymolyase.

To investigate whether the intact *myo52Δ* cells were viable after Zymolyase digestion, the experiment was repeated and a viability assay was performed by spreading a sample of cells onto YES plates at intervals during enzyme treatment. After allowing the cells to grow up into colonies onto YES plates the number of colonies obtained were scored. The results of the viability assay showed that more viable *myo52Δ* cells survived the Zymolyase treatment than in other fission yeast strains tested (Figure

7.8C). However, the viability of *myo52Δ* cells decreased with increasing incubation with Zymolyase perhaps indicating that the cell walls of these cells were being damaged by the enzyme which was not detected through spectroscopic or microscopic examination.

7.2.10 Mok1 is Highly Abundant in *myo52Δ* Cells

To determine an explanation for the resistance of *myo52Δ* cells to Zymolyase digestion it was reasoned that the composition of the *myo52Δ* cell walls must have been different that made it so refractile to Zymolyase treatment. To assess whether this might have been as a consequence of the different levels of cell wall synthesis enzymes in *myo52Δ*, the level of one of the cell wall synthesis enzymes (Mok1) was investigated in *myo52Δ* and compared to that of wild type cells.

This was achieved by preparing total protein extracts from *myo52Δ* and wild type cells and running 50 μg samples on an 7% SDS polyacrylamide gel. The resulting immunoblot with the anti-Mok1 polyclonal antibody showed that the antibody detected a band approximately 280 kD in size which corresponded to the molecular weight of Mok1 (Figure 7.9). Comparison of the bands from *myo52Δ* and wild type protein extracts indicated that Mok1 was estimated to be over three times more abundant in *myo52Δ* than in wild type cells (as judged by eye). To confirm that protein samples from *myo52Δ* and wild type cells were loaded in equal amounts the membrane was probed with the TAT1 anti-tubulin antibody as a protein loading control. The intensity of the tubulin bands in the immunoblot were about the same indicating that equal amounts of protein were loaded from the *myo52Δ* and wild type protein extracts.

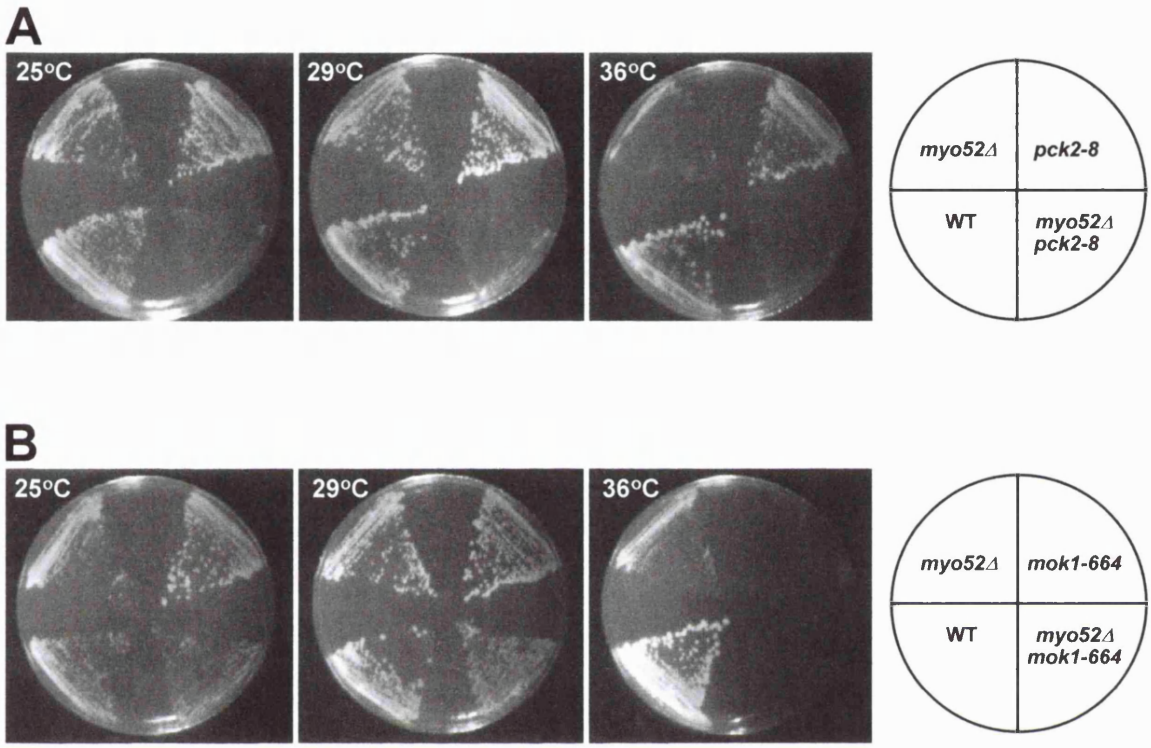

Figure 7.7 *myo52Δ* Exhibits a Synthetic Lethal Interaction with *pck2-8* but not *mok1-664*

(A) The *myo52Δ pck2-8* double mutant grows very poorly at temperatures which is permissive for the growth of *myo52Δ* and *pck2-8* single mutants (25°C and 29°C). Note *pck2-8* single mutant also grows at 36°C although they grow with morphological defects at this temperature.

(B) The *myo52Δ mok1-664* double mutant grows at temperatures which is permissive for the growth of *myo52Δ* and *mok1-664* single mutants.

For both (A) and (B) cells were incubated on YES plates for three days.

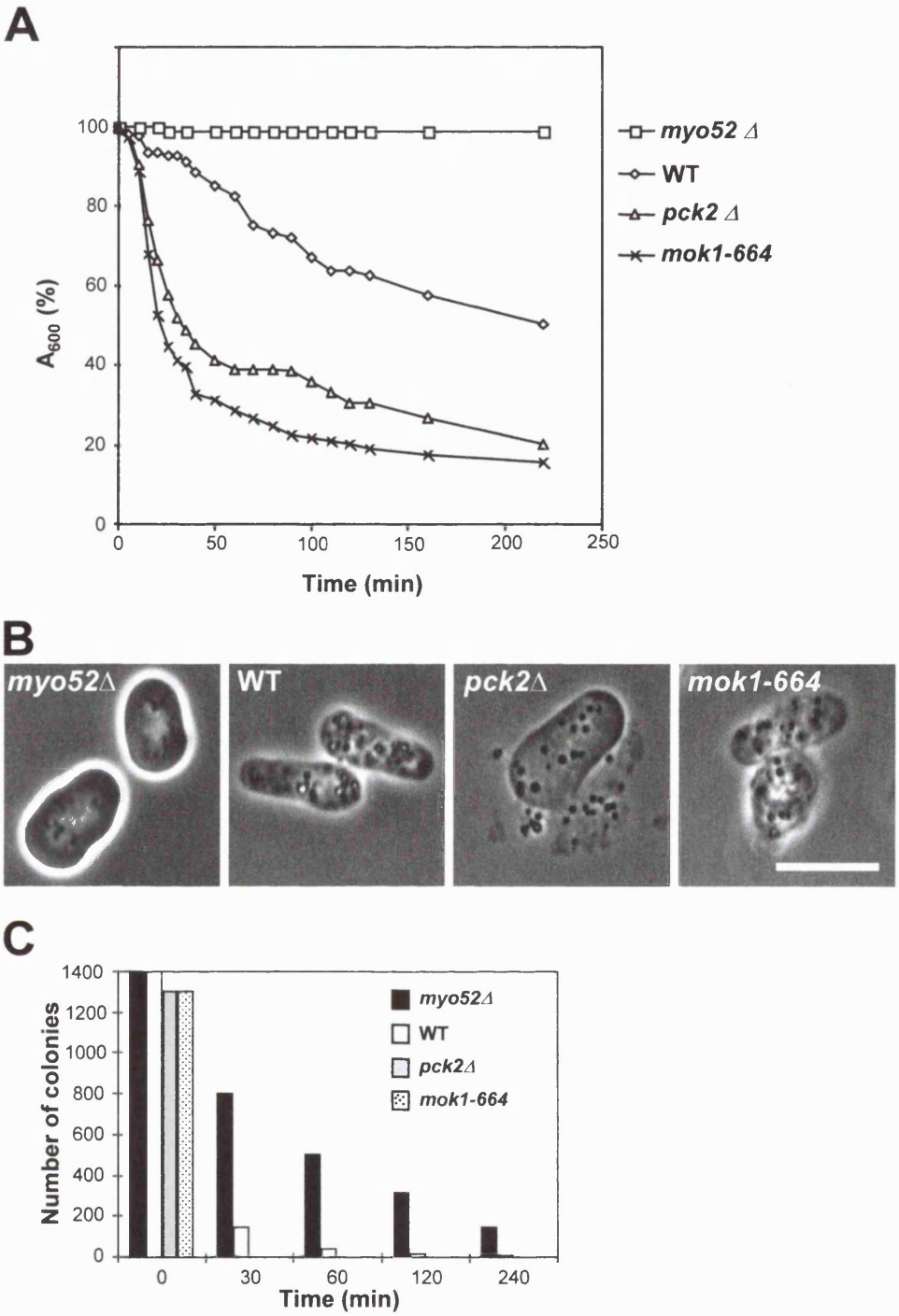

Figure 7.8 *myo52Δ* Cells are More Resistant to Zymolyase Cell Wall Digestion than Wild Type Cells

(A) *myo52Δ* , wild type, *pck2Δ* and *mok1-664* cells were incubated in the presence of 300 μg/ml Zymolyase cell wall digesting enzyme at room temperature. The change in optical density with time was used as a measure of the progress of cell wall digestion. *myo52Δ* cells were more resistant to Zymolyase than the other fission yeast strains tested.

(B) Phase contrast microscopy of cells in (A) after 220 minutes in Zymolyase. Note the bright phase ring around *myo52Δ* cells indicating an intact cell wall. Bar = 10 μm.

(C) A viability assay was performed on the cells described in (A) by spreading approximately 1500 cells onto YES plates at intervals during Zymolyase digestion. The bar chart shows the mean number of colonies per plate after 4 days incubation at 25°C.

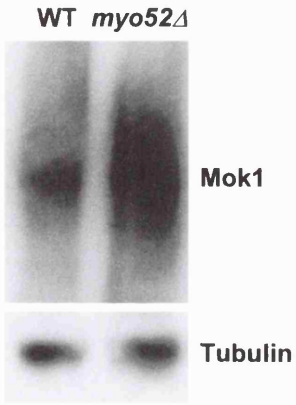

Figure 7.9 *myo52Δ* Cells have a Greater Abundance of the Mok1 α-Glucan Synthase than Wild Type Cells

Immunoblot of wild type and *myo52Δ* protein extracts with the anti-Mok1 polyclonal antibody (top panel) and TAT1 anti-tubulin monoclonal antibody (lower panel) as a protein loading control. Mok1 is highly abundant in *myo52Δ* cells. The immunoblot was performed on total protein extracts from *myo52Δ* and wild type cells grown to exponential phase in YES medium at 25°C.

7.3 DISCUSSION

7.3.1 Myo52 and Septation

myo52Δ cells form septa in the absence of *myo52*$^+$ function. Overexpression of the *spg1*$^+$ septum inducing gene (Schmidt et al., 1997) results in the formation of multiple septa at a frequency that was similar to that of wild type cells. At first, this may suggest that Myo52 had no role in septation. However, localisation studies showed that Myo52 was present at the equator as a single band prior to septation and as a double band after a septum had formed, indicating that the protein had some function at the equator of dividing cells. One possibility is that Myo52 may be important in the centripetal degradation of the primary septum to bring about the physical separation of sister cells (Gould and Simanis, 1997). This may explain why a proportion of *myo52Δ* cells were multiseptate (Chapter 4). However, Myo52 was always found at the equator before septum formation and if Myo52 had a role in septum degradation it might be expected that the protein localised at the equator after a septum had formed. This indicates that Myo52 might play an early role in some aspect of septation.

Alternatively, the fact that *myo52Δ* cells were able to form septa may indicate that other factor(s) could assume the function carried out by Myo52 at the cell equator in its absence. One such candidate is Myo51 and the recent localisation of Myo51 to the cytokinetic actin ring (Win et al., 2001; D. Mulvihill, personal communication) suggests that this could be possible. However, the observation that the *myo51Δ myo52Δ* double mutant forms septa and is viable (Chapter 4) indicates that there may be a myosin V independent mechanism of septum synthesis in *S. pombe*. As another explanation, Myo52 might play a minor role in septum synthesis and its presence in wild type cells merely increases the efficiency of septation. In the absence of Myo52, however, the efficiency of septation or cell cleavage is reduced, resulting in the observation of some multiseptate *myo52Δ* cells.

The synthetic lethal interaction of *myo52Δ* with *spg1-B8* and *cdc7-24* septation initiation mutants (Schmidt et al., 1997; Fankhauser and Simanis, 1994) provide further evidence of a role for Myo52 in cell division. The fact that the *myo52Δ spg1-B8* and *myo52Δ cdc7-24* double mutants die in the absence of a functional *myo52*$^{+}$ gene imply that Myo52 is required when the Spg1/Cdc7 septation induction pathway is impaired. Perhaps Myo52 is one of many downstream effectors of Spg1/Cdc7 which might explain why cells were still capable of septation in the absence of Myo52. However, when the function of an upstream regulator of septation is compromised, septum formation may be reduced to such an extent that results in the death of *spg1-B8* and *cdc7-24* mutants in a *myo52Δ* genetic background. Interestingly, the two class II myosin null mutants, *myo2Δ* and *myp2Δ*, and the other class V myosin null mutant, *myo51Δ*, also display a synthetic lethal interaction with *cdc7-24* (May et al., 1997; Mulvihill et al., 2000; T. Z. Win, unpublished results) indicating that these myosins are also regulated by the same pathway which regulate Myo52.

In addition to its interaction with *spg1-B8* and *cdc7-24*, *myo52Δ* also exhibited a genetic interaction with *cdc16-116*, a mutation which causes cells to undergo uncontrolled septation (Fankhauser et al., 1993). In the absence of *myo52*$^{+}$, cells show defects in localising growth at the tips resulting in the observation of round and pear-shaped *myo52Δ* cells (Chapter 4). Perhaps the *cdc16-116* allele in *myo52Δ* cells further disrupts tip growth in *myo52Δ* by diverting resources to the formation of septa. Alternatively, the synthetic lethality of the *myo52Δ cdc16-116* double mutant might reflect the poor organisation of septa that form in *myo52Δ* cells when septation is unregulated. This is supported by the observation that overexpression of the *spg1*$^{+}$ septum inducing gene in *myo52Δ* resulted in a proportion of cells with incomplete stumps of septa.

Genetic analyses also showed that *myo52Δ* exhibited a synthetic lethal interaction with *cdc3-6* profilin and *cdc4-8* myosin light chain mutants (Balasubramanian et al.,

1994; McCollum et al., 1995). *myo52Δ* also showed a weak genetic interaction with the *cdc8-110* tropomyosin mutant (Balasubramanian et al., 1992). The common feature of *cdc3-6*, *cdc4-8* and *cdc8-110* mutants is that they display a disorganised actin ring and the genetic interaction between *myo52Δ* and these mutants suggest that the actin ring defect might be aggravated in the absence of *myo52*$^{+}$. Whether *myo52Δ* also genetically interacts with other actin ring mutants, such as *cdc12*$^{-}$ and *rng2*$^{-}$ (Chang et al., 1997; Eng et al., 1998) remains to be investigated.

Interestingly, mutations in the genes encoding profilin (*cdc3-6*) and tropomyosin (*cdc8-110*) show that these genes are also important for the organisation of actin patches (Balasubramanian et al., 1992, 1994). *myo52Δ* cells display an abnormal organisation of actin and also exhibit a synthetic lethal interaction with the actin mutant *cps8*$^{-}$ (Chapter 4). Perhaps the observed genetic interaction between *myo52Δ* and mutants in profilin and tropomyosin might be a consequence of a general failure to organise actin in the *myo52Δ cdc3-6* and *myo52Δ cdc8-110* double mutants. These results further demonstrate the importance of a functional actin cytoskeleton for the survival of fission yeast cells.

Analysis of *cdc4-8* transformed with plasmids containing *myo52*$^{+}$ showed that *myo52*$^{+}$ expression was more toxic to *cdc4-8* cells than to wild type, *cdc3-6* or *cdc8-110* cells. In the absence of *myo52*$^{+}$ ectopic expression, *cdc4-8* cells divide normally at 25°C. However, moderate ectopic expression of *myo52*$^{+}$ had a severe effect on the *cdc4-8* mutant producing highly elongated and multinucleate cells, even in medium supplemented with thiamine. Perhaps increased levels of Myo52 reduced the pool of available functional Cdc4 giving rise to the observed phenotype at 25°C and the death of cells at 29°C due to further depletion of the residual Cdc4 activity by heat inactivation. Cdc4 has been shown to be the light chain that associates with the two class II myosins, Myo2 and Myp2 (Naqvi et al., 1999; Motegi et al., 2000). The ability of Myo52 to lower the pool of functional Cdc4 could be envisaged if Myo52

also had the capability to bind to Cdc4 and thus sequester it from cellular functions. Observations from budding yeast suggests that this is possible since a myosin light chain (Mlc1) which displays homology to Cdc4 (May et al., 1998) has been found to associate with a class V myosin (Stevens and Davis, 1998). Further work will have to be carried out to establish the light chains that associate with Myo52 and indeed Myo51. The localisation of fission yeast calmodulin, Cam1, to active growth sites (Moser et al., 1997) and the association of Cdc4 to the class II myosins provide an indication of the candidate proteins which could bind to Myo52 and Myo51.

7.3.2 Myo52 and Polarised Cell Growth

In other organisms the class V myosins serve as molecular motors that transport cargoes to their target destination (Titus, 1997a, 1997b). For example, the colour changes that occur in *Xenopus laevis* pigment cells have been partly attributed to the function of a myosin V motor protein which has been demonstrated to bind to melanosomes and these pigment organelles move along actin filaments in *in vitro* motility assays (Rogers et al., 1999). In the case of the budding yeast class V myosin, Myo2, the cellular cargoes that seems to be transported are vacuoles and secretory vesicles which are targeted to the growing bud (Schott et al., 1999). In the *myo2-66* budding yeast mutant, enlarged unbudded cells are observed at the restrictive temperature suggesting a defect in the localisation of cell growth (Johnston et al., 1991). The fact that *myo52Δ* also display morphological abnormalities indicative of a defect in localising growth suggest that a similar situation analogous to the vesicle transport function of Myo2 in budding yeast may also operate with Myo52 in fission yeast. This is supported by the observation that Myo52, like its budding yeast homologue (Catlett and Weisman, 1998; Reck-Peterson et al., 1999), localises to sites of active growth.

Interestingly, Myo52 colocalises with the Mok1 α-glucan synthase at the cell poles during interphase and to a certain extent at the equator in dividing cells. The observation that Mok1 is delocalised in *myo52Δ* but Myo52 is properly localised in

the *mok1-664* mutant suggest that Myo52 is required for the localisation of Mok1 but not vice versa. These results are consistent with the possibility that Myo52 may be the motor that localises its cargo (Mok1) to growing sites but the cargo is not important for the localisation of the motor. Further work will have to be carried out to establish whether Myo52 associates with Mok1 biochemically and whether Myo52 also colocalises with other cell wall synthesis enzymes such as the 1,3-β-glucan synthase subunit Drc1/Cps1 (Liu et al., 1999).

The observation that *myo52Δ* cells are more resistant to Zymolyase cell wall digestion than wild type cells provide further evidence of a role for Myo52 in cell morphogenesis. Zymolyase is a mixture of cell wall digesting enzymes that has β-1,3-glucanase activity (Ovalle et al., 1998). The fact that mutants defective in the synthesis of α-glucan such as *ags1-1*, *mok1-664* and *pck2Δ* are hypersensitive to Zymolyase (Hochstenbach et al., 1998; Katayama et al., 1999) indicate that both α-glucan and β-glucan are important in maintaining the integrity of fission yeast cells. Interestingly, *myo52Δ* cells exhibited a higher abundance of the Mok1 α-glucan synthase suggesting that the possible mechanism by which *myo52Δ* cells were resistant to Zymolyase was that the architecture of *myo52Δ* cell walls was different from that of wild type cells. Perhaps a higher abundance of Mok1 may have resulted in the incorporation of more α-glucan and consequently a thicker cell wall in *myo52Δ* cells. Electron microscopy will be useful in determining the nature of the *myo52Δ* cell wall.

One question remains: why does *myo52Δ* have a higher abundance of Mok1? A tentative model is that a feedback mechanism that requires precise localisation of Mok1 to target sites may be operating. In wild type cells Mok1 localises correctly to the poles and equator and the localisation of Mok1 to these sites may signal the cell to prevent further targeting of Mok1 to growth sites. However, in *myo52Δ*, Mok1 is delocalised which prevents the feedback mechanism from working. The cell senses

that little or no Mok1 is reaching the target destination and attempts to resolve this by upregulating the production of Mok1.

Interestingly, *myo52Δ* cells exhibited a synthetic lethal interaction with *pck2* mutants (*pck2-8* and *pck2Δ*). Pck2 has been suggested to be a positive regulator of Mok1 activity since *pck2Δ* cells have a reduced level of α-glucan and is resistant to toxic overproduction of Mok1 (Katayama et al., 1999). However, *pck2Δ* cells also have a lower level of β-glucan and galactomannan. Furthermore, overproduction of Pck2 have been shown to increase 1,3-β-glucan synthase activity (Arellano et al., 1999). These results indicate that Pck2 is involved in the coordinated regulation of the levels of various cell wall components by affecting the activity of a number of cell wall metabolic enzymes (Katayama et al., 1999). The synthetic lethality of the *myo52Δ pck2-8* and *myo52Δ pck2Δ* strains may therefore reflect a general failure in cell wall organisation in the double mutants perhaps as a consequence of the lack of active cell wall enzymes and their inability to localise these enzymes to target sites. However, no synthetic lethal interaction between *myo52Δ* and *mok1-664* was observed possibly because the high levels of Mok1 which was present in *myo52Δ* cells may have also been present in *myo52Δ mok1-664* to ensure sufficient α-glucan synthesis in the double mutant. Alternatively, since $pck2^{+}$ was still functional in *myo52Δ mok1-664* the integrity of the double mutant may have been maintained by modulating the activity of other cell wall metabolic enzymes such as those involved in β-glucan synthesis.

The work presented here shows that the cell wall of *myo52Δ* is different from that of wild type cells resulting in its substantial resistance to the Zymolyase cell wall digestion. This work also shows that one of the cell wall synthesis enzymes, Mok1 α-glucan synthase, is upregulated in *myo52Δ* suggesting a possible mechanism of resistance to Zymolyase. Further work will have to be carried out to determine

whether the abundance of Mok1 correlates with an increase in the levels of α-glucan in *myo52Δ* cell walls. Indeed, the level of other cell wall components, β-glucan and galactomannan, and the activity of β-glucan synthases should also be determined to investigate their contribution in altering the composition of the *myo52Δ* cell wall.

Chapter 8
Summary and Discussion

In this thesis I have reported the identification of two new myosin genes in the fission yeast, *Schizosaccharomyces pombe*. Both genes encode class V myosins and were named *myo51*$^+$ and *myo52*$^+$. Phylogenetic analysis of the head domains places Myo51 and Myo52 with other members of the class V group of the myosin superfamily. Myo51 and Myo52 are most similar to their budding yeast homologues, Myo2 and Myo4, which lie on the same branch of the phylogenetic tree.

The class V myosins are generally regarded as motor proteins that transport cellular cargoes to their sites of destination along tracks of actin filaments (Titus 1997a, 1997b; Reck-Peterson et al., 2000; Wu et al., 2000). Observations from several model systems have led to this view. *In vitro* studies of isolated actin filaments and myosin V molecules have shown that class V myosins are (+) end directed actin motors (Wells et al., 1999). Analysis of purified frog melanosomes have revealed that these organelles are associated with a myosin V motor (Rogers and Gelfand, 1998). Furthermore, these organelles exhibit directed movement along actin filaments *in vitro*, indicating that a myosin V motor contributes towards the localisation of melanosomes in frog melanophores. Studies of the budding yeast class V myosins, Myo2 and Myo4, show that these motors have distinct functions (Brown, 1997). Myo2 is required for the localisation of secretory vesicles and vacuoles to the growing bud (Johnston et al., 1991; Govindan et al., 1995; Hill et al., 1996) and that this localisation is dependent on the integrity of actin cables that connect the mother to the bud (Hill et al., 1996; Pruyne et al., 1998). Myo4, however, is required for the localisation of *ASH1* mRNA to the growing bud (Long et al., 1997; Takizawa et al., 1997) and the physical interaction between *ASH1* mRNA and Myo4 is mediated by the adapter protein She3 (Takizawa and Vale, 2000). It is possible that, like their homologues in other organisms, the fission yeast class V myosins may also be involved in the transport of various cargoes in the cell.

Several lines of evidence suggest that *myo51*$^+$ and *myo52*$^+$ have non-overlapping functions in *S. pombe*. Deletion analysis of *myo51*$^+$ have shown that it encodes a non-

essential gene that gives rise to cells that are indistinguishable from wild type cells under laboratory conditions. Deletion of *myo52*$^{+}$, however, produces cells with defects in morphology and *myo52Δ* cells are rounded and pear-shaped in appearance. Combination of the *myo51Δ* and *myo52Δ* null mutations in the same strain reveal that the *myo51Δ myo52Δ* double mutant has the characteristics of the *myo52Δ* single mutant. Assuming that there are no other myosin V genes in *S. pombe*, the fact that the *myo51Δ myo52Δ* double mutant remain viable indicates that fission yeast cells can survive without the function of class V myosin motors, albeit with morphological defects and slow growth rates. This is in contrast to the synthetic lethal interaction observed between *myo2-E1* and *myp2Δ* which show that the function of class II myosin motors are required for the viability of fission yeast cells (Bezanilla and Pollard, 2000; Motegi et al., 2000; Mulvihill et al., 2000). However, the finding that the *myo51Δ cps8*$^{-}$ and *myo52Δ cps8*$^{-}$ mutants are synthetically lethal suggests that myosin V proteins are required under certain conditions, in this case myosin V function is required when the actin cytoskeleton is compromised.

Overexpression studies show that *myo51*$^{+}$ and *myo52*$^{+}$ give distinct overexpression phenotypes. Overproduction of Myo51 gives rise to elongated cells with multiple nuclei whereas overproduction of Myo52 results in branched cells with aberrant septa. Localisation studies also show that Myo51 and Myo52 are localised to different sites in the cell. These results, taken together with the phenotypes of the *myo51Δ* and *myo52Δ* cells, suggest that *myo51*$^{+}$ and *myo52*$^{+}$ perform distinct and non-overlapping functions in *S. pombe*. The function of Myo51 is unclear although Win et al. (2001) have proposed that the protein may have a non-essential role in cytokinesis as a component of the cytokinetic actin ring. The finding by Win et al. (2001) that Myo51 is a component of the cytokinetic actin ring suggests a novel role for a myosin V motor in cytokinesis. At present we can only speculate what Myo51 does at the division site. Perhaps Myo51 is required under certain conditions for cytokinesis or perhaps it localises some non-essential factor to the cytokinetic actin

ring. In this thesis I have reported that Myo51 is localised asymmetrically and is present at one of the cell poles, indicating that the protein may have some function in this region of the cell. The reasons why Myo51 is found to localise differently between this study to that of Win et al. (2001) is discussed in Chapter 6.

In comparison to *myo51*$^{+}$, much more is known about *myo52*$^{+}$. Deletion of *myo52*$^{+}$ shows that the gene product is required to maintain the rod shape morphology of *S. pombe* cells. Myo52 localises at the single growing pole before new end take off (NETO) and is present at both poles after activation of bipolar growth. Myo52 localises to the equator prior to septation as an equatorial ring at late anaphase. After septation Myo52 is localised in juxtaposition with the septum on both sides of the cross wall. In the following cell cycle, Myo52 disappears from the division site to relocate to the old end. The localisation of Myo52 correlates with the distribution of actin and is dependent on actin. The observation that Myo52 is intimately associated with sites of cell wall deposition and the finding that *myo52Δ* cells have aberrant cell morphology strongly indicates that Myo52 is required for localising growth at defined sites. The observation that Myo52 colocalises with the Mok1 α-glucan synthase at the cell poles and to some extent at the equator suggest that the role of Myo52 is to localise factors involved in cell growth, such as Mok1, to sites of cell wall deposition. This is supported by the observation that in the absence of *myo52*$^{+}$ function, Mok1 is delocalised. It is not known whether Myo52 uses an active transport mechanism to localise factors involved in cell growth to sites of cell wall deposition since the results presented in this thesis do not exclude the possibility that Myo52 may play an anchoring role in the localisation of these factors to sites of growth. Creation of an ATPase dead Myo52 mutant protein and testing its ability to complement the morphological defects of *myo52Δ* cells will be useful in determining whether the motor activity of Myo52 is required for its function.

Treatments with drugs which depolymerise actin results in the delocalisation of Myo52 from sites of cell wall deposition. Interestingly, fluorescent images of Myo52

localisation show that the polar caps of Myo52 disperse into numerous cytoplasmic dots following treatment with actin-depolymerising drugs. These cytoplasmic dots may represent Myo52-associated vesicles which are normally localised to growing sites by the interaction between Myo52 and the actin cytoskeleton. This hypothesis is consistent with electron microscopy studies which have shown that vesicles are present at the poles of fission yeast and that their polar localisation is dependent on an intact actin cytoskeleton (Kanbe et al., 1989, 1993).

In filamentous fungi there is a vesicle rich body known as the "Spitzenkorper" found at the growing tips of hyphae (Seiler et al., 1997; Lehmler et al., 1997) and the Myo52 cap at the poles of a fission yeast cell is reminiscent of this body. The Spitzenkorper is dependent on an intact microtubule cytoskeleton and in particular the function of the microtubule motor protein, kinesin (Seiler et al., 1997; Lehmler et al., 1997). Some class V myosins have been found to be physically associated with a kinesin-related motor protein (Huang et al., 1999; Beningo et al., 2000) and a microtubule associated protein (Yin et al., 2000) but whether Myo52 falls into this category remains to be investigated. Interestingly, the polar caps of Myo52 are dislodged from the poles when fission yeast cells are treated with the microtubule-depolymerising drug thiabendazole (TBZ), although, unlike treatments which depolymerise actin, the Myo52 caps do not disperse into dots upon microtubule depolymerisation. Whether this represents a true dependence of Myo52 on microtubules for the protein's polar localisation or whether the displacement of the Myo52 cap is a consequence of the effect of TBZ on the normal organisation of actin at the cell poles (Sawin and Nurse, 1998) is unclear. The use of other microtubule-depolymerising drugs such as carbendazim (MBC) (Brunner and Nurse, 2000) which does not disturb the actin cytoskeleton (D. Brunner, personal communication) may be useful in distinguishing between these two possibilities.

Interestingly, analysis of the integrity of the *myo52Δ* cell walls show that they are substantially more resistant to the cell wall digesting enzyme Zymolyase than wild

type cells. This indicates that the *myo52Δ* cell walls must necessarily be different from that of wild type cells. In *myo52Δ*, the Mok1 α-glucan synthase is upregulated suggesting a mechanism for resistance to Zymolyase, perhaps by altering the composition of the *myo52Δ* cell wall. In budding yeast, mutants in the class V myosin gene, *MYO2*, display defects in the deposition of chitin in their cell walls (Johnston et al., 1991; Santos and Snyder, 1997). In these mutants chitin deposition is delocalised and chitin is present throughout the cell surface instead of being deposited at the incipient bud site and bud neck where it is normally localised. This has been partly attributed to the delocalisation of the chitin synthase, Chs3, in *myo2* mutants (Santos and Snyder, 1997). Studies of the budding yeast class II myosin, Myo1, have shown that it too may be involved in the deposition of chitin since *myo1* mutants have defects in the deposition of chitin and cell wall components (Watts et al., 1987; Rodriguez and Paterson, 1990; Brown, 1997). Mutants in *MYO1* have elevated levels of chitin in their cell walls (Rodriguez-Medina et al., 1998) and display increased activities in enzymes involved in chitin synthesis (Cruz et al., 2000). These observations in budding yeast suggests that cell wall metabolism is deregulated in *myo1* mutants. In fission yeast, Pck1 and Pck2 have been found to be important in the control of cell wall metabolism (Kobori et al., 1994). Pck1 and Pck2 are targets of the Rho GTPases, Rho1 and Rho2 (Arellano et al., 1999). It will be interesting to investigate the role of these proteins in the regulation of cell wall synthesis in *myo52Δ* cells, particularly since *myo52Δ* exhibits a synthetic lethal interaction with mutants in $pck2^{+}$. As a first step towards the understanding of these proteins in cell wall metabolism, the amount of Mok1 in $pck1^{-}$ and $pck2^{-}$ mutants should be investigated. If the level of Mok1 is reduced in these mutants, it will suggest that the synthetic lethal interaction between *myo52Δ* and $pck2^{-}$ may be a consequence of the lack of active cell wall enzymes in the double mutant and their inability to localise these enzymes to target sites.

Comparisons between Myo52 and the budding yeast class V myosin, Myo2, show that these proteins share homology in primary sequence and have similar coiled-coil predictions (Chapter 3). It appears that the homology between the two protein sequences also extend to cellular function. Like Myo52, Myo2 is also localised to sites of active growth, that is to the bud tip of small budded cells and then later to the mother-bud neck during cytokinesis (Lillie and Brown, 1994). Mutants in *MYO2* display defects in growth and the temperature-sensitive *myo2-66* mutant grows isotropically to produce unbudded, enlarged cells at the restrictive temperature (Johnston et al., 1991). Consistent with the growth defects, *myo2-66* mutants display defects in the localisation of secretory vesicles and vacuoles (Johnston et al., 1991; Govindan et al., 1995; Hill et al., 1996). Recently, two distinct regions in the C-terminal globular domain of Myo2 have been identified to be important for the interaction between Myo2 and its cargoes (Catlett et al., 2000). Further work will have to be carried out to determine the exact cargoes that associate with Myo52 and the region of the Myo52 molecule that mediate the interaction between the motor and cargo. The observation in budding yeast that Myo2 has distinct regions for cargo binding will be useful in determining the cargo binding domains of Myo52. Another line of suggested work is to investigate the ability of Myo2 to complement the morphological defects of *myo52Δ* cells. This will be the ultimate test of whether the budding yeast class V myosin is the functional homologue of Myo52.

REFERENCES

Adachi, Y., Toda, T., Niwa, O., and Yanagida, M. (1986). Differential expression of essential and non-essential α-tubulin genes in *Schizosaccharomyces pombe*. *Molecular Cell Biology* **6:**2168-2178.

Alberts, B., Bray, D., Lewis, J., Raff, M., Roberts, K., and Watson, J. D. (1994). The cytoskeleton. In "Molecular biology of the cell." 3rd edn. pp. 786-861. Garland Publishing Inc., New York.

Alfa, C. E., Fantes, P., Hyams, J. S., Mcleod, M., and Warbrick, E. (1993). "Experiments with fission yeast: a laboratory course manual." Cold Spring Harbor Press, New York.

Alfa, C. E., and Hyams, J. S. (1990). Distribution of tubulin and actin through the cell division cycle of the fission yeast *Schizosaccharomyces japonicus* var. *versatilis*: a comparison with *Schizosaccharomyces pombe*. *Journal of Cell Science* **96:**71-77.

Anderson, B. L., Boldogh, I., Evangelista, M., Boone, C., Greene, L. A., and Pon, L. A. (1998). The src homology domain 3 (SH3) of a yeast type I myosin, Myo5p, binds to verprolin and is required for targeting to sites of actin polarization. *Journal of Cell Biology* **141(6):**1357-1370.

Arai, R., Nakano, K., and Mabuchi, I. (1998). Subcellular localization and possible function of actin, tropomyosin and actin-related protein 3 (Arp3) in the fission yeast *Schizosaccharomyces pombe*. *European Journal of Cell Biology* **76:**288-295.

Arellano, M., Duran, A., and Perez, P. (1996). Rho1 GTPase activates the (1-3)beta-D-glucan synthase and is involved in *Schizosaccharomyces pombe* morphogenesis. *EMBO Journal* **15(17):**4584-4591.

Arellano, M., Duran, A., and Perez, P. (1997). Localisation of the *Schizosaccharomyces pombe* rho1 GTPase and its involvement in the organisation of the actin cytoskeleton. *Journal of Cell Science* **110:**2547-2555.

Arellano, M., Valdivieso, M. H., Calonge, T. M., Coll, P. M., Duran, A., and Perez, P. (1999). *Schizosaccharomyces pombe* protein kinase C homologues, pck1p and pck2p, are targets of rho1p and rho2p and differentially regulate cell integrity. *Journal of Cell Science* **112:**3569-3578.

Atkinson, S. J., and Stewart, M. (1991). Molecular basis of myosin assembly: coiled-coil interactions and the role of charge periodicities. *Journal of Cell Science Supplement* **4:**7-10.

Ayscough, K., Hajibagheri, N. M., Watson, R., and Warren, G. (1993). Stacking of Golgi cisternae in *Schizosaccharomyces pombe* requires intact microtubules. *Journal of Cell Science* **106:**1227-1237.

Ayscough, K. R., Stryker, J., Pokala, N., Sanders, M., Crews, P., and Drubin, D. G. (1997). High rates of actin filament turnover in budding yeast and roles for actin in establishment and maintenance of cell polarity revealed using the actin inhibitor latrunculin-A. *Journal of Cell Biology* **137(2):**399-416.

Bahler, J., and Pringle, J. R. (1998). Pom1p, a fission yeast protein kinase that provides positional information for both polarized growth and cytokinesis. *Genes and Development* **12:**1356-1370.

Bahler, J., Steever, A. B., Wheatley, S., Wang, Y., Pringle, J. R., Gould, K. L., and McCollum, D. (1998). Role of polo kinase and Mid1p in determining the site of cell division in fission yeast. *Journal of Cell Biology* **143(6):**1603-1616.

Bahler, J., Wu, J., Longtine, M. S., Shah, N. G., McKenzie III, A., Steever, A. B., Wach, A., Philippsen, P., and John R. Pringle. (1998). Heterologus modules for efficient and versatile PCR-based gene targeting in *Schizosaccharomyces pombe*. *Yeast* **14:**943-951.

Bahler, M. (2000). Are class III and class IX myosins motorized signalling molecules? *Biochimica et Biophysica Acta* **1496:**52-59.

Baker, J. P., and Titus, M. A. (1998). Myosins: matching functions with motors. *Current Opinion in Cell Biology* **10:**80-86.

Balasubramanian, M. K., Helfman, D. M., and Hemmingsen, S. M. (1992). A new tropomyosin essential for cytokinesis in the fission yeast *S. pombe*. *Nature* **360:**84-87.

Balasubramanian, M. K., Hirani, B.R., Burke, J. D., and Gould, K. L. (1994). The *Schizosaccharomyces pombe cdc3*$^{+}$ gene encodes a profilin essential for cytokinesis. *Journal of Cell Biology* **125(6):**1289-1301.

Balasubramanian, M. K., McCollum, D., Chang, L., Wong, K. C. Y, Naqvi, N. I., He, X., Sazer, S., and Gould, K. L. (1998). Isolation and characterisation of new fission yeast cytokinesis mutants. *Genetics* **149:**1265-1275.

Balasubramanian, M. K., McCollum, D., and Gould, K. L. (1997). Cytokinesis in fission yeast *Schizosaccharomyces pombe*. *Methods in Enzymology* **283:**494-506.

Balasubramanian, M. K., McCollum, D., and Surana, U. (2000). Tying the knot: linking cytokinesis to the nuclear cycle. *Journal of Cell Science* **113:**1503-1513.

Barylko, B., Binns, D. D., and Albanesi, J. P. (2000). Regulation of the enzymatic and motor activities of myosin I. *Biochimica et Biophysica Acta* **1496:**23-35.

Basi, G., Schmid, E., and Maundrell, K. (1993). TATA box mutations in the *Schizosaccharomyces pombe nmt1* promoter affect transcription efficiency but not transcription start point or thiamine repressibility. *Gene* **123:**131-136.

Batra, R., Geeves, M. A., and Manstein, D. J. (1999). Kinetic analysis of *Dictyostelium discoideum* myosin motor domains with glycine-to-alanine mutations in the reactive thiol region. *Biochemistry* **38:**6126-6134.

Bauer, C. B., Kuhlman, P. A., Bagshaw, C. R., and Rayment, I. (1997). X-ray crystal structure and solution fluorescence characterization of Mg 2'(3')-O-(N-methylanthraniloyl) nucleotides bound to the *Dictyostelium discoideum* myosin motor domain. *Journal of Molecular Biology* **274:**394-407.

Bement, W. M., Wirth, J. A., and Mooseker, M. S. (1994). Cloning and mRNA expression of human unconventional myosin I-C. A homologue of amoeboid myosins-I with a single IQ motif and an SH3 domain. *Journal of Molecular Biology* **243:**356-363.

Beningo, K. A., Lillie, S. H., and Brown, S. S. (2000). The yeast kinesin related protein Smy1p exerts its effects on the class V myosin Myo2p via a physical interaction. *Molecular Biology of the Cell* **11:**691-702.

Berger, B., Wilson, D. B., Wolf, E., Tonchev, T., Milla, M., and Kim, P. S. (1995). Predicting coiled-coils by use of pairwise residue correlations. *Proceedings of the National Academy of Sciences USA* **92:**8259-8263.

Bezanilla, M., Forsburg, S. L., and Pollard, T. D. (1997). Identification of a second myosin-II in *Schizosaccharomyces pombe*: Myp2p is conditionally required for cytokinesis. *Molecular Biology of the Cell* **8:**2693-2705.

Bezanilla, M., and Pollard, T. D. (2000). Myosin-II tails confer unique functions in *Schizosaccharomyces pombe*: characterisation of a novel myosin-II tail. *Molecular Biology of the Cell* **11:**79-91.

Bezanilla, M., Wilson, J. M., and Pollard, T. D. (2000). Fission yeast myosin-II isoforms assemble into contractile rings at distinct times during mitosis. *Current Biology* **10:**397-400.

Bi, E., Maddox, P., Lew, D. J., Salmon, E. D., McMillan, J. N., Yeh, E., and Pringle, J. R. (1998). Involvement of an actomyosin contractile ring in *Saccharomyces cerevisiae* cytokinesis. *Journal of Cell Biology* **142(5):**1301-1312.

Block, S. M. (1996). Fifty ways to love your lever: myosin motors. *Cell* **87:**151-157.

Bloom, K., and Beach, D. L. (1999). mRNA localization: motile RNA, asymmetric anchors. *Current Opinion in Microbiology* **2:**604-609.

Blotnick, E., and Muhlrad, A. (1992). Effect of actin on the tryptic digestion of myosin subfragment 1 in the weakly attached state. *European Journal of Biochemistry* **210:**873-879.

Bobola, N., Jansen, R. P., Shin, T. H., and Nasmyth, K. (1996). Asymmetric accumulation of Ash1p in postanaphase nuclei depends on a myosin and restricts yeast mating-type switching to mother cells. *Cell* **84:**699-709.

Bremer, A., and Aebi, U. (1992). The structure of the F-actin filament and the actin molecule. *Current Opinion in Cell Biology* **4:**20-6.

Bridgman, P. C. (1999). Myosin Va movements in normal and dilute-lethal axons provide support for a dual filament motor complex. *Journal of Cell Biology* **146(5):**1045-1060.

Brockerhoff, S. E., Stevens, R. C., and Davis, T. N. (1994). The unconventional myosin, Myo2, is a calmodulin target at sites of cell growth in *Saccharomyces cerevisiae*. *Journal of Cell Biology* **124(3):**315-323.

Brown, S. S. (1997). Myosins in yeast. *Current Opinion in Cell Biology* **9:**44-48.

Brunner, D., and Nurse, P. (2000). CLIP170-like tip1p spatially organizes microtubular dynamics in fission yeast. *Cell* **102:**695-704.

Catlett, N. L., Duex, J. E., Tang, F., and Weisman, L. S. (2000). Two distinct regions in a yeast myosin-V tail domain are required for the movement of different cargoes. *Journal of Cell Biology* **150(3):**513-525.

Catlett, N. L., and Weisman, L. S. (1998). The terminal tail region of a yeast myosin-V mediates its attachment to vacuole membranes and sites of polarized growth. *Proceedings of the National Academy of Sciences USA* **95:**14799-14804.

Catlett, N. L., and Weisman, L. S. (2000). Divide and multiply: organelle partitioning in yeast. *Current Opinion in Cell Biology* **12:**509-516.

Cerutti, L., and Simanis, V. (1999). Asymmetry of the spindle pole bodies and spg1p GAP segregation during mitosis in fission yeast. *Journal of Cell Science* **112:**2313-2321.

Chang, E. C., Barr, M., Wang, Y., Jung, V., Xu, H. P., and Wigler, M. H. (1994). Cooperative interaction of *S. pombe* proteins required for mating and morphogenesis. *Cell* **79:**131-141.

Chang, F. (1999). Movement of a cytokinesis factor cdc12p to the site of cell division. *Current Biology* **9:**849-852.

Chang, F., Drubin, D., and Nurse, P. (1997). cdc12p, a protein required for cytokinesis in fission yeast, is a component of the cell division ring and interacts with profilin. *Journal of Cell Biology* **137(1):**169-182.

Chang, F., and Nurse, P. (1996). How fission yeast fission in the middle. *Cell* **84:**191-194.

Chang, F., Woollard, A., and Nurse P. (1996). Isolation and characterization of fission yeast mutants defective in the assembly and placement of the contractile actin ring. *Journal of Cell Science* **109:**131-142.

Chang, L., and Gould, K. L. (2000). Sid4p is required to localize components of the septation initiation pathway to the spindle pole body in fission yeast. *Proceedings of the National Academy of Sciences USA* **97(10):**5249-5254.

Chant, J. (1996). Septins scaffolds and cleavage planes in *Saccharomyces. Cell* **84:**187-190.

Cheney, R. E. (2000). A new direction for myosin. *Trends in Cell Biology* **10:**307-311.

Cheney, R. E., and Mooseker, M. S. (1992). Unconventional myosins. *Current Biology* **4:**27-35.

Cheney, R. E., O'Shea, M. K., Heuser, J. E., Coelho, M. V., Wolenski, J. S., Espreafico, E. M., Forscher, P., Larson, R. E., and Mooseker, M. S. (1993b). Brain Myosin-V is a two-headed unconventional myosin with motor activity. *Cell* **75:**13-23.

Cheney, R. E., Riley, M. A., and Mooseker, M. S. (1993a). Phylogenetic analysis of the myosin superfamily. *Cell Motility and the Cytoskeleton* **24:**215-223.

Cohen, C, Szent-Gyorgyi, A. G., and Kendrick-Jones, J. (1971). Paramyosin and the filaments of molluscan "catch" muscles. I. paramyosin: structure and assembly. *Journal of Molecular Biology* **56:**223-237.

Conrad, P. A., Guiliano, K. A., Fisher, G., Collins, K., Matsudaira, P. T., and Taylor, D. L. (1993). Relative distribution of actin, myosin I, and myosin II during the wound healing response of fibroblasts. *Journal of Cell Biology* **120:**1381-1391.

Cooper, J. A. (1987). Effects of cytochalasin and phalloidin on actin. *Journal of Cell Biology* **105:**1473-1478.

Cope, M. J. T. V., Whisstock, J., Rayment, I., and Kendrick-Jones, J. (1996). Conservation within the myosin motor domain: implications for structure and function. *Structure* **4:**969-987.

Craig, R., and Megerman, J. (1977). Assembly of smooth muscle myosin into side polar filaments. *Journal of Cell Biology* **75:**990-996.

Craven, R. A., Griffiths, D. J. F., Sheldrick, K. S., Randall, R. E., Hagan, I. M., and Carr, A. M. (1998). Vectors for the expression of tagged proteins in *Schizosaccharomyces pombe. Gene* **221:**59-68.

Crozet, F., Amraoui, A. E., Blanchard, S., Lenoir, M., Ripoll, C., Vago, P., Hamel, C., Fizames, C., Levi-Acobas, F., Depetris, D., Mattei, M., Weil, D., Pujol, R., and Petit, C. (1997). Cloning of the genes encoding two murine and human cochlear unconventional type I myosins. *Genomics* **40:**332-341.

Cruz, J. A., Garcia, R., Rodriguez-Orengo, J. F., and Rodriguez-Medina, J. R. (2000). Increased chitin synthesis in response to type II myosin deficiency in *Saccharomyces cerevisiae*. *Molecular Cell Biology Research Communications* **3(1):**20-25.

Cubitt, A. B., Heim, R., Adams, S. R., Boyd, A. E., Gross, L. A., and Tsien, R. Y. (1995). Understanding, improving and using green fluorescent proteins. *Trends in Cell Biology* **20:**448-455.

Ding, R., West, R. R., Morphew, M., and McIntosh, J. R. (1997). The spindle pole body of *Schizosaccharomyces pombe* enters and leaves the nuclear envelope as the cell cycle proceeds. *Molecular Biology of the Cell* **8:**1461-1479.

Dominguez, R., Freyzon, Y., Trybus, K. M., and Cohen, C. (1998). Crystal structure of a vertebrate smooth muscle myosin motor domain and its complex with the essential light chain: visualisation of the pre-power stroke state. *Cell* **94:**559-571.

D'Urso, G., and Nurse, P. (1995). Checkpoints in the cell cycle of fission yeast. *Current Opinion in Genetics and Development* **5:**12-16.

Egel, R. (1989). Mating-type genes, meiosis, and sporulation. In "Molecular biology of the fission yeast", A. Nasim, P. Young and B. F. Johnson, eds. pp. 31-73. Academic Press Inc., London.

Elledge, S. J. (1996). Cell cycle checkpoints: preventing an identity crisis. *Science* **274:**1664-1671.

Eng, K., Naqvi, N. I., Wong, K. C. Y., and Balasubramanian, M. K. (1998). Rng2p, a protein required for cytokinesis in fission yeast, is a component of the actomyosin ring and the spindle pole body. *Current Biology* **8:**611-621.

Epp, A. J., and Chant, J. (1997). An IQGAP-related protein controls actin-ring formation and cytokinesis in yeast. *Current Biology* **7:**921-929.

Erickson, H. P. (2000). Gamma-tubulin nucleation: template or protofilament? *Nature Cell Biology* **2(6):**93-96.

Erickson, H. P., and O'Brien, E. T. (1992). Microtubule dynamic instability and GTP hydrolysis. *Annual Review of Biophysics and Biomolecular Structure* **21:**145-166.

Espindola, F. S., Espreafico, E. M., Coelho, M. V., Martins, A. R., Costa, F. R. C., Mooseker, M. S., and Larson, R. E. (1992). Biochemical and immunological characterization of p190-Calmodulin complex from vertebrate brain: a novel calmodulin-binding myosin. *Journal of Cell Biology* **118(2):**359-368.

Espreafico, E. M., Cheney, R. E., Matteoli, M., Nascimento, A. A. C., De Camilli, P. V., Larson, R. E., and Mooseker, M. S. (1992). Primary structure and cellular localization of chicken brain myosin-V (p190), an unconventional myosin with calmodulin light chains. *Journal of Cell Biology* **119(6):**1541-1557.

Espreafico, E. M., Coling, D. E., Tsakraklides, V., Krogh, K., Wolenski, J. S., Kalinec, G., and Kachar, B. (1998). Localization of myosin-V in the centrosome. *Proceedings of the National Academy of Sciences USA* **95:**8636-8641.

Evangelista, M., Klebl, B. M., Tong, A. H., Webb, B. A., Leeuw, T., Leberer, E., Whiteway, M., Thomas, D. Y., and Boone, C. (2000). A role for myosin-I in actin assembly through interactions with Vrp1p, Bee1p, and the Arp2/3 complex. *Journal of Cell Biology* **148(2):**353-362.

Fankhauser, C., Marks, J., Reymond, A., and Simanis, V. (1993). The *S. pombe cdc16* gene is required both for maintenance of $p34^{cdc2}$ kinase activity and regulation of septum formation: a link between mitosis and cytokinesis? *EMBO Journal* **12(7):**2697-2704.

Fankhauser, C., Reymond, A., Cerutti, L., Utzig, S., Hofmann, K., and Simanis, V. (1995). The *S. pombe cdc15* gene is a key element in the reorganization of F-actin at mitosis. *Cell* **82:**435-444.

Fankhauser, C., and Simanis, V. (1994). The cdc7 protein kinase is a dosage dependent regulator of septum formation in fission yeast. *EMBO Journal* **13(13):**3011-3019.

Fantes, P. (1989). Cell cycle controls. In "Molecular biology of the fission yeast", A. Nasim, P. Young and B. F. Johnson, eds. pp. 127-204. Academic Press Inc., London.

Field, C., Li, R., and Oegema, K. (1999). Cytokinesis in eukaryotes: a mechanistic comparison. *Current Opinion in Cell Biology* **11:**68-80.

Fisher, A. J., Smith, C. A., Thoden, J. B., Smith, R., Sutoh, K., Holden, H. M., and Rayment, I. (1995). X-ray structures of the myosin motor domain of *Dictyostelium discoideum* complexed with $MgADP{\cdot}BeF_x$ and $MgADP{\cdot}AlF_4^-$. *Biochemistry* **34:**8960-8972.

Forsburg, S. L. (1993). Comparison of *Schizosaccharomyces pombe* expression systems. *Nucleic Acids Research* **21(12):**2955-2956.

Friedrich, P., and Azodi, A. (1991). MAP2: a sensitive cross-linker and adjustable spacer in dendritic architecture. *FEBS Letters* **295:**5-9.

Fuchs, E., and Cleveland, D. W. (1998). A structural scaffolding of intermediate filaments in health and disease. *Science* **279:**514-519.

Furge, K. A., Cheng, Q., Jwa, M., Shin, S., Song, K., and Albright, C. F. (1999). Regions of Byr4, a regulator of septation in fission yeast, that bind Spg1 or Cdc16 and form a two-component GTPase-activating protein with Cdc16. *Journal of Biological Chemistry* **274(16):**11339-11343.

Furge, K. A., Wong, K., Armstrong, J., Balasubramanian, M., and Albright, C. F. (1998). Byr4 and Cdc16 form a two-component GTPase-activating protein for the Spg1 GTPase that controls septation in fission yeast. *Current Biology* **8(17):**947-954.

Gabriel, M., Horky, D., Svoboda, A., and Kopecka, M. (1998). Cytochalasin D interferes with contractile actin ring and septum formation *in Schizosaccharomyces japonicus var. versatilis. Microbiology* **144:**2331-2344.

Garces, J., and Gavin, R. H. (1998). A PCR screen identifies a novel, unconventional myosin heavy chain gene (*MYO1*) in *Tetrahymena thermophila. Journal of Eukaryote Microbiology* **45(3):**252-259.

Geli, M. I., and Riezman, H. (1996). Role of type I myosins in receptor-mediated endocytosis in yeast. *Science* **272:**533-535.

Gerisch, G., and Weber, I. (2000). Cytokinesis without myosin II. *Current Opinion in Cell Biology* **12:**126-132.

Glotzer, M. (1997). The mechanism and control of cytokinesis. *Current Opinion in Cell Biology* **9:**815-823.

Goldman, Y. E. (1998). Wag the tail: structural dynamics of actomyosin. *Cell* **93:**1-4.

Goldschmidt-Clermont, P. J., Furman, M. I., Wachsstock, D., Safer, D., Nachmias, V. T., and Pollard, T. D. (1992). The control of actin nucleotide exchange by thymosin β4 and profilin. A potential regulatory mechanism for actin polymerization in cells. *Molecular Biology of the Cell* **3:**1015-1024.

Goode, B. L., Drubin, D. G., and Barnes, G. (2000). Functional cooperation between the microtubule and actin cytoskeletons. *Current Opinion in Cell Biology* **12:**63-71.

Goodson, H. V., Anderson, B. L., Warrick, H. M., Pon, L. A., and Spudich, J. A. (1996). Synthetic lethality screen identifies a novel yeast myosin I gene (*MYO5*): myosin I proteins are required for polarization of the actin cytoskeleton. *Journal of Cell Biology* **133(6):**1277-1291.

Goodson, H. V., and Spudich, J. A. (1993). Molecular evolution of the myosin family: relationships derived from comparisons of amino acid sequences. *Proceedings of the National Academy of Sciences USA* **90:**659-663.

Goodson, H. V., and Spudich, J. A. (1995). Identification and molecular characterization of a yeast myosin I. *Cell Motility and the Cytoskeleton* **30:**73-84.

Gould, K. L., and Simanis, V. (1997). The control of septum formation in fission yeast. *Genes and Development* **11:**2939-2951.

Govindan, B., Bowser, R., and Novick, P. (1995). The role of Myo2, a yeast class V myosin, in vesicular transport. *Journal of Cell Biology* **128(6):**1055-1068.

Guertin, D. A., Chang, L., Irshad, F., Gould, K. L., and McCollum, D. (2000). The role of the Sid1p kinase and Cdc14p in regulating the onset of cytokinesis in fission yeast. *EMBO Journal* **19(8):**1803-1815.

Gulick, A. M., Bauer, C. B., Thoden, J. B., and Rayment, I. (1997). X-ray structures of the MgADP, MgATPγS, and MgAMPPNP complexes of the *Dictyostelium discoideum* myosin motor domain. *Biochemistry* **36:**11619-11628.

Guo, S., and Kemphues, K. J. (1996). A non-muscle myosin required for embryonic polarity in *Caenorhabditis elegans*. *Nature* **382:**455-458.

Haarer, B. K., Petzold, A., Lillie, S. H. and Brown, S. S. (1994). Identification of *MYO4*, a second class V myosin gene in yeast. *Journal of Cell Science* **107:**1055-1064.

Hagan, I. M. (1998). The fission yeast microtubule cytoskeleton. *Journal of Cell Science* **111:**1603-1612.

Hagan, I. M., and Hyams, J. S. (1988). The use of cell division cycle mutants to investigate the control of microtubule distribution in the fission yeast *Schizosaccharomyces pombe*. *Journal of Cell Science* **89:**343-357.

Hagan, I. M., and Hyams, J. S. (1996). Forces acting on the fission yeast anaphase spindle. *Cell Motility and the Cytoskeleton* **34:**69-75.

Hagan, I. M., Riddle, P. N., and Hyams, J. S. (1990). Intramitotic controls in the fission yeast *Schizosaccharomyces pombe*: the effect of cell size on spindle length and the timing of mitotic events. *Journal of Cell Biology* **110:**1617-1621.

Hagan, I. M., and Yanagida, M. (1997). Evidence for cell cycle-specific, spindle pole body-mediated, nuclear positioning in the fission yeast *Schizosaccharomyces pombe*. *Journal of Cell Science* **110:**1851-1866.

Haimo, L., and Thaler, C. (1994). Regulation of organelle transport: lessons from color change in fish. *BioEssays* **16:**727-733.

Hall, A. (1998). Rho GTPases and the actin cytoskeleton. *Science* **279:**509-514.

Hanson, J., and Huxley, H. E. (1953). Structural basis of the cross-striations in muscle. *Nature* **172:**530-532.

Hart, M. J., Cowan, M. G., Souza, B., and Polakis, P. (1996). IQGAP1, a calmodulin-binding protein with a ras GAP-related domain, is a potential effector for Cdc42Hs. *EMBO Journal* **15:**2997-3005.

Highsmith, S. (1999). Lever arm model of force generation by actin-myosin-ATP. *Biochemistry* **38:**9791-9797.

Hill, K. L., Catlett, N. L., and Weisman, L. S. (1996). Actin and myosin function in directed vacuole movement during cell division in *Saccharomyces cerevisiae*. *Journal of Cell Biology* **135(6):**1535-1549.

Hiraoka, Y., Toda, T., and Yanagida, M. (1984). The *NDA3* gene of fission yeast encodes beta-tubulin - a cold-sensitive *nda3* mutation reversibly blocks spindle formation and chromosome movement in mitosis. *Cell* **39:**349-358.

Hirata, D., Masuda, H., Eddison, M., and Toda, T. (1998). Essential role of tubulin-folding cofactor D in microtubule assembly and its association with microtubules in fission yeast. *EMBO Journal* **17:**658-666.

Hirata, D., Nakano, K., Fukui, M., Takenaka, H., Miyakawa, T., and Mabuchi, I. (1998). Genes that cause aberrant cell morphology by overexpression in fission yeast: a role of a small GTP-binding protein Rho2 in cell morphogenesis. *Journal of Cell Science* **111:**149-159.

Hirokawa, N., Hisanaga, S. I., and Shiomura, Y. (1988). MAP2 is a component of crossbridges between microtubules and neurofilaments in the neuronal cytoskeleton: quick-freeze, deep-etch immunoelectron microscopy and reconstitution studies. *Journal of Neuroscience* **8:**2769-2779.

Hochstenbach, F., Klis, F. M., van den Ende, H., van Donselaar, E., Peters, P. J., and Klausner, R. D. (1998). Identification of a putative alpha-glucan synthase essential for cell wall construction and morphogenesis in fission yeast. *Proceedings of the National Academy of Sciences USA* **95:**9161-9166.

Hodge, T., and Cope, M. J. T. V. (2000). A myosin family tree. *Journal of Cell Science* **113:**3353-3354.

Hoppe, P. E., and Waterson, R. H. (1996). Hydrophobicity variations along the surface of the coiled-coil rod may mediate striated muscle myosin assembly in *Caenorhabditis elegans*. *Journal of Cell Biology* **135:**371-382.

Horio, T., Uzawa, S., Jung, M. K., Oakley, B. R., Tanaka, K., and Yanagida, M. (1991). The fission yeast gamma-tubulin is essential for mitosis and is localized at microtubule organising centres. *Journal of Cell Science* **99:**693-700.

Houdusse, A., and Cohen, C. (1995). Target sequence recognition by the calmodulin superfamily: implications from light chain binding to the regulatory domain of scallop myosin. *Proceedings of the National Academy of Sciences USA* **92:**10644-10647.

Houdusse, A., Kalabokis, V. N., Himmel, D., Szent-Gyorgyi, A. G., and Cohen, C. (1999). Atomic structure of scallop myosin subfragment S1 complexed with MgADP: a novel conformation of the myosin head. *Cell* **97:**459-470.

Houdusse, A., Silver, M., and Cohen, C. (1996). A model of Ca^{2+}-free calmodulin binding to unconventional myosins reveals how calmodulin acts as a regulatory switch. *Structure* **4:**1475-1490.

Huang, J-D., Brady, S. T., Richards, B. W., Stenoien, D., Resau, J. H., Copeland, N. G., and Jenkins, N. A. (1999). Direct interaction of microtubule-and actin-based transport motors. *Nature* **397:**267-270.

Huang, J-D., Cope, M. J. T. V., Mermall, V., Strobel, M. C., Kendrick-Jones, J., Russell, L. B., Mooseker, M. S., Copeland, N. G., and Jenkins, A. (1998). Molecular genetic dissection of mouse unconventional myosin-VA: Head region mutations. *Genetics* **148:**1951-1961.

Huxley, A. F., and Simmons, R. M. (1971). Proposed mechanism of force generation in striated muscle. *Nature* **233:**533-538.

Huxley, H. E. (1963). Electron microscopic studies on the structure of natural and synthetic protein filaments in striated muscle. *Journal of Molecular Biology* **7:**281-308.

Huxley, H. E. (1969). The mechanism of muscular contraction. *Science* **164:**1356-1366.

Iacovoni, J. S., Russell, P., and Gaits, F. (1999). A new inducible protein expression system in fission yeast based on the glucose-repressed *inv1* promoter. *Gene* **232:**53-58.

Ikebe, M., Mitra, S., and Hartshorne, D. J. (1993). Cleavage at site A, Glu-642 to Ser-643, of the gizzard myosin heavy chain decreases affinity for actin. *Journal of Biological Chemistry* **268:**25948-25951.

Ikura, M. (1996). Calcium binding and conformational response in EF-hand proteins. *Trends in Biological Sciences* **21(January):**14-17.

Ishiguro, J., and Kobayashi, W. (1996). An actin point-mutation neighboring the hydrophobic plug causes defects in the maintenance of cell polarity and septum organization in the fission yeast *Schizosaccharomyces pombe. FEBS Letters* **392:**237-241.

Ishijima, S. A., Konomi, M., Takagi, T., Sato, M., Ishiguro, J., and Osumi, M. (1999). Ultrastructure of cell wall of the *cps8* actin mutant cell in *Schizosaccharomyces pombe. FEMS Microbiology Letters* **180:**31-37.

Jansen, R., Dowzer, C., Michaelis, C., Galova, M., and Nasmyth, K. (1996). Mother cell-specific *HO* expression in budding yeast depends on the unconventional myosin Myo4p and other cytoplasmic proteins. *Cell* **84:**687-697.

Jochova, J., Rupes, I., and Streiblova, E. (1991). F-actin contractile rings in protoplasts of the yeast *Schizosaccharomyces*. *Cell Biology International Reports* **15:**607-610.

Johnson, B. F., Miyata, M., and Miyata, H. (1989). Morphogenesis of fission yeasts. In "Molecular biology of the fission yeast", A. Nasim, P. Young and B. F. Johnson, eds. pp. 331-366. Academic Press Inc., London.

Johnson, B. F., Yoo, B. Y., and Calleja, G. B. (1973). Cell division in yeasts: movement of organelles associated with cell plate growth of *Schizosaccharomyces pombe*. *Journal of Bacteriology* **115:**358-366.

Johnston, G. C., Predergast, J. A., and Singer, R. A. (1991). The *Saccharomyces cerevisiae MYO2* gene encodes an essential myosin for vectorial transport of vesicles. *Journal of Cell Biology* **113(3):**539-551.

Joshi, H. C. (1994). Microtubule organizing centres and γ-tubulin. *Current Opinion in Cell Biology* **6:**55-62.

Jurado, L. A., Chockalingam, P. S., and Jarrett, H. W. (1999). Apocalmodulin. *Physiological Reviews* **79(3):**661-682.

Kabsch, W., Mannherz, H. G., Suck D., Pai, E. F., and Holmes, K. C. (1990). Atomic structure of the actin-DNAse-I complex. *Nature* **347:**37-44.

Kabsch, W., and Vandekerckhove. (1992). Structure and function of actin. *Annual Review of Biophysics and Biomolecular Structure* **21:**49-76.

Kanbe, T., Akashi, T., and Tanaka, K. (1993). Effect of cytochalasin A on actin distribution in the fission yeast *Schizosaccharomyces pombe* studied by fluorescent and electron microscopy. *Protoplasma* **176:**24-32.

Kanbe, T., Kobayashi, I., and Tanaka, K. (1989). Dynamics of cytoplasmic organelles in the cell cycle of the fission yeast *Schizosaccharomyces pombe*. *Journal of Cell Science* **94:**647-656.

Karess, R. E., Chang, X., Edwards, K. A., Kulkarni, S., Aguilera, I., and Kiehart, D. P. (1991). The regulatory light chain of nonmuscle myosin is encoded by *Spaghetti-squash*, a gene required for cytokinesis in *Drosophila*. *Cell* **65:**1177-1189.

Katayama, S., Hirata, D., Arellano, M., Perez, P., and Toda, T. (1999). Fission yeast α-glucan synthase Mok1 requires the actin cytoskeleton to localize the sites of growth and plays an essential role in cell morphogenesis downstream of protein kinase C function. *Journal of Cell Biology* **144(6):**1173-1186.

Keating, T. J., and Borisy, G. G. (2000). Immunostructural evidence for the template mechanism of microtubule nucleation. *Nature Cell Biology* **2(6):**352-357.

Kitayama, C., Sugimoto, A., and Yamamoto, M. (1997). Type II myosin heavy chain encoded by the *myo2* gene composes the contractile ring during cytokinesis in *Schizosaccharomyces pombe*. *Journal of Cell Biology* **137(6):**1309-1319.

Kliche, W., Pfannstiel, J., Tiepold, M., Stoeva, S., and Faulstich, H. (1999). Thiol-specific cross-linkers of variable length reveal a similar separation of SH1 and SH2 in myosin subfragment 1 in the presence and absence of MgADP. *Biochemistry* **38:**10307-10317.

Kobori, H., Toda, T., Yaguchi, H., Toya, M., Yanagida, M., and Osumi, M. (1994). Fission yeast protein kinase C gene homologues are required for protoplast regeneration: a functional link between cell wall formation and cell shape control. *Journal of Cell Science* **107:**1131-1136.

Koslovsky, J. S., Qian, C., Jiang, X., and Mercer, J. A. (1993). Molecular cloning of a mouse myosin I expressed in brain. *FEBS Letters* **320(2):**121-124.

Kuznetsov, S. A., Langford, G. M., and Weiss, D. G. (1992). Actin-dependent organelle movement in squid axoplasm. *Nature* **356:**722-725.

Lechler, T., Shevchenko, A., and Li, R. (2000). Direct involvement of yeast type I myosins in Cdc42-dependent actin polymerization. *Journal of Cell Biology* **148(2):**363-373.

Lee, G. (1993). Non-motor microtubule-associated proteins. *Current Opinion in Cell Biology* **5:**88-94.

Le Goff, X., Utzig, S., and Simanis, V. (1999). Controlling septation in fission yeast: finding the middle, and timing it right. *Current Genetics* **35:**571-584.

Lehmler, C., Steinberg, G., Snetselaar, K. M., Schliwa, M., Kahmann, R., and Bolker, M. (1997). Identification of a motor protein required for filamentous growth in *Ustilago maydis*. *EMBO Journal* **16:**3464-3473.

Levine, R. J. C., Elfvin, M., Dewey, M. M., and Walcott, B. (1976). Paramyosin in invertebrate muscles II. Content in relation to structure and function. *Journal of Cell Biology* **70:**273-279.

Li, C., Furge, K. A., Cheng, Q., and Albright, C. F. (2000). Byr4 localizes to spindle-pole bodies in a cell cycle-regulated manner to control Cdc7 localization and septation in fission yeast. *Journal of Biological Chemistry* **275(19):**14381-14387.

Lillie, S. H., and Brown, S. S. (1994). Immunofluorescence localization of the unconventional myosin, Myo2p, and the putative kinesin-related protein, Smy1p, to the same regions of polarized growth in *Saccharomyces cerevisiae*. *Journal of Cell Biology* **125:**825-842.

Lippincott, J., and Li, R. (1998). Sequential assembly of myosin II, an IQGAP-like protein, and filamentous actin to a ring structure involved in budding yeast cytokinesis. *Journal of Cell Biology* **140(2):**355-366.

Liu, J., Wang, H., and Balasubramanian, M. K. (2000). A checkpoint that monitors cytokinesis in *Schizosaccharomyces pombe. Journal of Cell Science* **113:**1223-1230.

Liu, J., Wang, H., McCollum, D., and Balasubramanian, M. K. (1999). Drc1p/Cps1p, a 1,3-β-glucan synthase subunit, is essential for division septum assembly in *Schizosaccharomyces pombe. Genetics* **153:**1193-1203.

Long, R. M., Singer, R. H., Meng, X. Gonzalez, I., Nasmyth, Jansen, R. (1997). Mating type switching in yeast controlled by asymmetric localization of *ASH1* mRNA. *Science* **277:**383-387.

Lowey, S., Waller, G. S., and Trybus, K. M. (1993). Skeletal muscle myosin light chains are essential for physiological speeds of shortening. *Nature* **365:**454-456.

Madden, K., and Snyder, M. (1998). Cell polarity and morphogenesis in budding yeast. *Annual Review of Microbiology* **52:**687-744.

Mandelkow, E., and Mandelkow, E-M. (1994). Microtubule structure. *Current Opinion in Structural Biology* **4:**171-179.

Mandelkow, E., and Mandelkow, E-M. (1995). Microtubules and microtubule-associated proteins. *Current Opinion in Cell Biology* **7:**72-81.

Marcus, S., Polverino, A., Chang, E., Robbins, D., Cobb, M. H., and Wigler, M. H. (1995). Shk1, a homolog of the *Saccharomyces cerevisiae* Ste20 and mammalian p65PAK protein kinases, is a component of a Ras/Cdc42 signalling module in the fission yeast *Schizosaccharomyces pombe. Proceedings of the National Academy of Sciences USA* **92:**6180-6184.

Marks, J., Fankhauser, C., and Simanis, V. (1992). Genetic interactions in the control of septation in *Schizosaccharomyces pombe. Journal of Cell Science* **101:**801-808.

Marks, J., Hagan, I. M., and Hyams, J. S. (1986). Growth polarity and cytokinesis in fission yeast: the role of the cytoskeleton. *Journal of Cell Science Supplement* **5:**229-241.

Marks, J., Hagan, I. M., and Hyams, J. S. (1987). In "Spatial organization in eukaryotic microbes", R. K. Poole and A. P. C. Trinki, eds. pp. 119-135. IRL Press, Oxford.

Marks, J., and Hyams, J. S. (1985). Localization of F-actin through the cell division cycle of *Schizosaccharomyces pombe. European Journal of Cell Biology* **39:**27-32.

Mata, J., and Nurse, P. (1997). Tea1 and the microtubular cytoskeleton are important for generating global spatial order within the fission yeast cell. *Cell* **89:**939-949.

Mata, J., and Nurse, P. (1998). Discovering the poles in yeast. *Trends in Cell Biology* **8:**163-167.

Maundrell, K. (1990). *nmt1* of fission yeast. A highly transcribed gene completely repressed by thiamine. *Journal of Biological Chemistry* **265(19):**10857-10864.

Maupin, P., Phillips, C. L., Adelstein, R. S., and Pollard, T. D. (1994). Differential localisation of myosin-II isozymes in human cultured cells and blood cells. *Journal of Cell Science* **107:**3077-3090.

May, K. M., and Hyams, J. S. (1998). The yeast cytoskeleton: the closer we look, the more we see. *Fungal Genetics and Biology* **24:**110-122.

May, K. M., Watts, F. Z., Jones, N., and Hyams, J. S. (1997). Type II myosin involved in cytokinesis in the fission yeast, *Schizosaccharomyces pombe*. *Cell Motility and the Cytoskeleton* **38:**385-396.

May, K. M., Win, T. Z., and Hyams, J. S. (1998). Yeast myosin II: a new subclass of unconventional conventional myosins? *Cell Motility and the Cytoskeleton* **39:**195-200.

McCollum, D., Balasubramanian, M., and Gould, K. (1999). Identification of cold-sensitive mutations in the *Schizosaccharomyces pombe* actin locus. *FEBS Letters* **451(3):**321-326.

McCollum, D., Balasubramanian, M. K., Pelcher, L. E., Hemmingsen, S. M., and Gould, K. L. (1995). *Schizosaccharomyces pombe cdc4*$^{+}$ gene encodes a novel EF-hand protein essential for cytokinesis. *Journal of Cell Biology* **130(3):**651-660.

McCollum, D., Feoktistova, A., Morphew, M., Balasubramanian, M., and Gould, K. L. (1996). The *Schizosaccharomyces pombe* actin-related protein, Arp3, is a component of the cortical actin cytoskeleton and interacts with profilin. *EMBO Journal* **15:**6438-6446.

McGoldrick, C. A., Gruver, C., and May, G. S. (1995). *myoA* of *Aspergillus nidulans* encodes an essential myosin I required for secretion and polarized growth. *Journal of Cell Biology* **128(4):**577-587.

McLachlan, A. D., and Karn, J. (1982). Periodic charge distributions in the myosin rod amino acid sequence match cross-bridge spacings in muscle. *Nature* **299:**226-231.

Mehta, A. D., Rock, R. S., Rief, M., Spudich, J. A., Mooseker, M. S., and Cheney, R. E. (1999). Myosin V is a processive actin-based motor. *Nature* **400:**590-593.

Mercer, J. A., Seperack, P. K., Strobel, M. C., Copeland, N. G., and Jenkins, N. A. (1991). Novel myosin heavy chain encoded by murine dilute coat colour locus. *Nature* **349:**709-713.

Mermall, V., Post, P. L., and Mooseker, M. S. (1998). Unconventional myosins in cell movement, membrane traffic, and signal transduction. *Science* **279:**527-533.

Mertins, P., and Gallwitz, D. (1987). A single intronless actin gene in fission yeast *Schizosaccharomyces pombe*: nucleotide sequence and transcripts formed in homologous and heterologous yeast. *Nucleic Acids Research* **15:**7369-7379.

Miller, P. J., and Johnson, D. I. (1994). Cdc42p GTPase is involved in controlling polarized cell growth in *Schizosaccharomyces pombe*. *Molecular Cell Biology* **14(2):**1075-1083.

Mitchison, J. M., and Nurse, P. (1985). Growth in cell length in the fission yeast *Schizosaccharomyces pombe*. *Journal of Cell Science* **75:**357-376.

Moores, S. L., Sabry, J. H., and Spudich, J. A. (1996). Myosin dynamics in live *Dictyostelium* cells. *Proceedings of the National Academy of Sciences USA* **93:**443-446.

Mooseker, M. S., and Cheney, R. E. (1995). Unconventional myosins. *Annual Review of Cell and Developmental Biology* **11:**633-675.

Moreau, V., and Way, M. (1999). *In vitro* approaches to study actin and microtubule dependent cell processes. *Current Opinion in Cell Biology* **11:**152-158.

Moreno, S., Hayles, J., and Nurse, P. (1989). Regulation of $p34^{cdc2}$ protein kinase during mitosis. *Cell* **58:**361-372.

Moreno, S., Klar, A., and Nurse, P. (1991). Molecular genetic analysis of fission yeast *Schizosaccharomyces pombe*. *Methods in Enzymology* **194:**795-823.

Morishita, M., and Shimoda, C. (2000). Positioning of medial actin rings affected by eccentrically located nuclei in a fission yeast mutant having large vacuoles. *FEMS Microbiology Letters* **188:**63-67.

Moritz, M., Braunfeld, M. B., Guenebaut, V., Heuser, J., and Agard, D. A. (2000). Structure of the gamma-tubulin ring complex: a template for microtubule nucleation. *Nature Cell Biology* **2(6):**365-370.

Mornet, D., Bertrand, R., Pantel, P., Audemard, E., and Kassab, R. (1981). Proteolytic approach to structure and function of actin recognition site in myosin heads. *Biochemistry* **20:**2110-2120.

Morrell, J. L., Morphew, M., and Gould, K. L. (1999). A mutant of Arp2p causes partial disassembly of the Arp2/3 complex and loss of cortical actin function in fission yeast. *Molecular Biology of the Cell* **10:**4201-4215.

Moser, M. J., Flory, M. R., and Davis, T. N. (1997). Calmodulin localizes to the spindle pole body of *Schizosaccharomyces pombe* and performs an essential function in chromosome segregation. *Journal of Cell Science* **110:**1805-1812.

Motegi, F., Nakano, K., Kitayama, C., Yamamoto, M., and Mabuchi, I. (1997). Identification of Myo3, a second type-II myosin heavy chain in the fission yeast *Schizosaccharomyces pombe. FEBS Letters* **420:**161-166.

Motegi, F., Nakano, K., and Mabuchi, I. (2000). Molecular mechanisms of myosin-II assembly at the division site in *Schizosaccharomyces pombe. Journal of Cell Science* **113:**1813-1825.

Mulvihill, D. P., Petersen, J., Ohkura, H., Glover, D. M., and Hagan, I. M. (1999). Plo1 kinase recruitment to the spindle pole body and its role in cell division in *Schizosaccharomyces pombe. Molecular Biology of the Cell* **10:**2771-2785.

Mulvihill, D. P., Win, T. Z., Pack, T. P., and Hyams, J. S. (2000). Cytokinesis in fission yeast: a myosin pas de deux. *Microscopy Research and Technique* **49:**152-160.

Munchow, S., Sauter, C., and Jansen, R. (1999). Association of the class V myosin Myo4p with a localised messenger RNA in budding yeast depends on She proteins. *Journal of Cell Science* **112:**1511-1518.

Munz, P., Wolf, K., Kohli, J., and Leupold, U. (1989). Genetics overview. In "Molecular biology of the fission yeast", A. Nasim, P. Young and B. F. Johnson, eds. pp. 1-30. Academic Press Inc., London.

Murray, A. W. (1992). Creative blocks: cell-cycle checkpoints and feedback controls. *Nature* **359:**599-604.

Nakano, K., Arai, R., and Mabuchi, I. (1997). The small GTP-binding protein Rho1 is a multifunctional protein that regulates actin localization, cell polarity, and septum formation in the fission yeast *Schizosaccharomyces pombe. Genes to Cells* **2(11):**679-694.

Nakano, K., and Mabuchi, I. (1995). Isolation and sequencing of two cDNA clones encoding Rho proteins from the fission yeast *Schizosaccharomyces pombe. Gene* **155(1):**119-122.

Naqvi, N. I., Eng, K., Gould, K. L. and Balasubramanian, M. K. (1999). Evidence for F-actin-dependent and -independent mechanisms involved in assembly and stability of the medial actomyosin ring in fission yeast. *EMBO Journal* **18(4):**854-862.

Nascimento, A. A. C., Amaral, R. G., Bizario, J. C. S., Larson, R. E., and Espreafico, E. M. (1997). Subcellular localization of myosin-V in the B16 melanoma cells, a wild type cell line for the *dilute* gene. *Molecular Biology of the Cell* **8:**1971-1988.

Nascimento, A. A. C., Cheney, R. E., Tauhata, S. B. F., Larson, R. E., and Mooseker, M. S. (1996). Enzymatic characterization and functional domain mapping of brain myosin-V. *Journal of Biological Chemistry* **271:**17561-17569.

Nasmyth, K., and Jansen, R. (1997). The cytoskeleton in mRNA localization and cell differentiation. *Current Opinion in Cell Biology* **9:**396-400.

Nitao, L. K., and Reisler, E. (1998). Probing the conformational states of the SH1-SH2 helix in myosin: a cross-linking approach. *Biochemistry* **37:**16704-16710.

Novak, K. D., Peterson, M. D., Reedy, M. C., and Titus, M. A. (1995). *Dictyostelium* myosin I double mutants exhibit conditional defects in pinocytosis. *Journal of Cell Biology* **131(5):**1205-1221.

Novak, K. D., and Titus, M. A. (1997). Myosin I overexpression impairs cell migration. *Journal of Cell Biology* **136(3):**633-647.

Novak, K. D., and Titus, M. A. (1998). The myosin I SH3 domain and TEDS rule phosphorylation site are required for in vivo function. *Molecular Biology of the Cell* **9:**75-88.

Nurse, P. (1997). CDKs and cell-cycle control in fission yeast: relevance to other eukaryotes and cancer. *International Journal of Cancer* **71:**707-708.

Nurse, P., Thuriaux, P., and Nasmyth, K. (1976). Genetic control of the cell division cycle in the fission yeast *Schizosaccharomyces pombe*. *Molecular General Genetics* **146:**167-178.

Obar, R. A., Dingus, J., Bayley, H., and Vallee, R. B. (1989). The RII subunit of cAMP-dependent protein kinase binds to a common amino-terminal domain on microtubule-associated proteins 2A, 2B, and 2C. *Neuron* **3:**639-645.

Ohkura, H., Hagan, I. M., and Glover, D. M. (1995). The conserved *Schizosaccharomyces pombe* kinase plo1, required to form a bipolar spindle, the actin ring, and septum, can drive septum formation in G1 and G2 cells. *Genes and Development* **9:**1059-1073.

Osumi, M., Sato, M., Ishijima, S. A., Konomi, M., Takagi, T., and Yaguchi, H. (1998). Dynamics of cell wall formation in fission yeast, *Schizosaccharomyces pombe*. *Fungal Genetics and Biology* **24:**178-206.

Ottilie, S., Miller, P. J., Johnson, D. I., Creasy, C. L., Sells, M. A., Bagrodia, S., Forsburg, S. L., and Chernoff, J. (1995). Fission yeast *pak1*$^{+}$ encodes a protein kinase that interacts with Cdc42p and is involved in the control of cell polarity and mating. *EMBO Journal* **14(23):**5908-5919.

Otto, J. J. (1994). Actin-bundling proteins. *Current Biology* **6:**105-109.

Ovalle, R., Lim, S. T., Holder, B., Jue, C. K., Moore, C. W., and Lipke, P. N. (1998). A spheroplast rate assay for determination of cell wall integrity in yeast. *Yeast* **14:**1159-1166.

Paluh, J. L., Nogales, E., Oakley, B. R., McDonald, K., Pidoux, A. L., and Cande, W. Z. (2000). A mutation in g-tubulin alters microtubule dynamics and organization and is synthetically lethal with the kinesin-like protein Pkl1p. *Molecular Biology of the Cell* **11:**1225-1239.

Panataloni, D., and Carlier, M. F. (1993). How profilin promotes actin filament assembly in the presence of thymosin β4. *Cell* **75:**1007-1014.

Paoletti, A., and Chang, F. (2000). Analysis of mid1p, a protein required for placement of the cell division site, reveals a link between the nucleus and the cell surface in fission yeast. *Molecular Biology of the Cell* **11:**2757-2773.

Petersen, J., Nielsen, O., Egel, R., and Hagan, I. M. (1998). F-actin distribution and function during sexual differentiation in *Schizosaccharomyces pombe. Journal of Cell Science* **111:**867-876.

Peterson, M. D., Urioste, A. S., and Titus, M. A. (1996). *Dictyostelium discoideum* myoJ: a member of a broadly defined myosin V class or a class XI unconventional myosin? *Journal of Muscle Research and Cell Motility* **17:**411-424.

Pollard, T. D. (1986). Assembly and dynamics of the actin filament system in nonmuscle cells. *Journal of Cellular Biochemistry* **31:**87-95.

Pollard, T. D., Blanchoin, L., and Mullins, R. D. (2000). Molecular mechanisms controlling actin filament dynamics in nonmuscle cells. *Annual Review of Biophysics and Biomolecular Structure* **29:**545-576.

Pollard, T. D., and Craig, S. W. (1982). Mechanism of actin polymerization. *Trends in Biological Science* **7(February):**55-58.

Pollard, T. D., Doberstein, S. K., and Zot, H. G. (1991). Myosin-I. *Annual Review of Physiology* **53:**653-681.

Pollard, T. D., and Korn, E. D. (1973). *Acanthamoeba* myosin. *Journal of Biological Chemistry* **248:**4682-4690.

Prasher, D. S., Eckenrode, V. K., Ward, W. W., Predergast, F. G., and Cormier, M. J. (1992). Primary structure of the *Aquorea victoria* green-fluorescent protein. *Gene* **111:**229-233.

Prekeris, R., and Terrian, D. M. (1997). Brain myosin V is a synaptic vesicle-associated motor protein: evidence for a Ca^{2+}-dependent interaction with synaptobrevin-synaptophysin complex. *Journal of Cell Biology* **137(7):**1589-1601.

Provance, D. W., Wei, M., Ipe, V., and Mercer, J. A. (1996). Cultured melanocytes from dilute mutant mice exhibit dendritic morphology and altered melanosome distribution. *Proceedings of the National Academy of Sciences* **93:**14554-14558.

Pruyne, D., and Bretscher, A. (2000a). Polarization of cell growth in yeast. *Journal of Cell Science* **113:**365-375.

Pruyne, D., and Bretscher, A. (2000b). Polarization of cell growth in yeast. *Journal of Cell Science* **113:**571-585.

Pruyne, D. W., Schott, D. H., and Bretscher, A. (1998). Tropomyosin-containing actin cables direct the Myo2p-dependent polarized delivery of secretory vesicles in budding yeast. *Journal of Cell Biology* **143(7):**1931-1945.

Quinlan, R., Hutchinson, C., and Lane, B. (1995). Intermediate filament proteins. *Protein Profiles* **2:**801-832.

Radcliffe, P., Hirata, D., Childs, D., Vardy, L., and Toda, T. (1998). Identification of novel temperature-sensitive lethal alleles in essential β-tubulin and nonessential α2-tubulin genes as fission yeast polarity mutants. *Molecular Biology of the Cell* **9:**1757-1771.

Rayment, I., Rypniewski, W. R., Schmidt-Base, K., Smith, R., Tomchick, D. R., Benning, M. M., Winkelmann, D. A., Wesenberg, G., and Holden, H. M. (1993). Three-dimensional structure of myosin subfragment-1: a molecular motor. *Science* **261:**50-58.

Reck-Peterson, S. L., Novick, P. J., and Mooseker, M. S. (1999). The tail of a yeast class V myosin, Myo2p, functions as a localization domain. *Molecular Biology of the Cell* **10:**1001-1017.

Reck-Peterson, S. L., Provance Jr, D. W., Mooseker, M. S., and Mercer, J. A. (2000). Class V myosins. *Biochimica et Biophysica Acta* **1496:**36-51.

Rhoads, A. R., and Friedberg, F. (1997). Sequence motifs for calmodulin recognition. *FASEB Journal* **11:**331-340.

Robinow, C. F., and Hyams, J. S. (1989). General cytology of fission yeasts. In "Molecular biology of the fission yeast", A. Nasim, P. Young and B. F. Johnson, eds. pp. 273-330. Academic Press Inc., London.

Rodionov, V. I., Hope, A. J., Svitkina, T. M., and Borisy, G. G. (1998). Functional coordination of microtubule-based and actin-based motility in melanophores. *Current Biology* **8:**165-168.

Rodriguez, J. R., and Paterson, B. M. (1990). Yeast myosin heavy chain mutant: maintenance of the cell type specific budding pattern and the normal deposition of chitin and cell wall components requires an intact myosin heavy chain. *Cell Motility and the Cytoskeleton* **17:**301-308.

Rodriguez-Medina, J. R., Cruz, J. A., Robbins, P. W., Bi, E., and Pringle, J. R. (1998). Elevated expression of chitinase 1 and chitin synthesis in myosin II-deficient *Saccharomyces cerevisiae*. *Cell and Molecular Biology* **44(6):**919-925.

Rogers, S. L., and Gelfand, V. I. (1998). Myosin cooperates with microtubule motors during organelle transport in melanophores. *Current Biology* **8:**161-164.

Rogers, S. L., Karcher, R. L., Roland, J. T., Minin, A. A., Steffen, W., and Gelfand, V. I. (1999). Regulation of melanosome movement in the cell cycle by reversible association with myosin V. *Journal of Cell Biology* **146(6):**1265-1275.

Royzycki, M. D., Myslik, J. C., Schutt, C. E., and Lindberg, U. (1994). Structural aspects of actin-binding proteins. *Current Opinion in Cell Biology* **6:**87-95.

Ruppel, K. M., and Spudich, J. A. (1995). Myosin motor function: structural and mutagenic approaches. *Current Opinon in Cell Biology* **7:**89-93.

Ruppel, K. M., and Spudich, J. A. (1996). Structure-function analysis of the motor domain of myosin. *Annual Review of Cell Developmental Biology* **12:**543-573.

Russell, P. (1989). Gene cloning and expression in fission yeast. In "Molecular biology of the fission yeast", A. Nasim, P. Young and B. F. Johnson, eds. pp. 243-271. Academic Press Inc., London.

Salmon, E. D., and Way, M. (1999). Cytoskeleton. Editorial overview. *Current Opinion in Cell Biology* **11:**15-17.

Santos, B., and Snyder, M. (1997). Targeting of chitin synthase 3 to polarized growth sites in yeast requires Chs5p and Myo2p. *Journal of Cell Biology* **136:**95-110.

Saraste, M., Sibbald, P. R., and Wittinghofer, A. (1990). The P-loop a common motif in ATP- and GTP-binding proteins. *Trends in Biological Sciences* **15(November):**430-434.

Sawin, K. E. (1999). Some thoughts about microtubules and cell polarity in fission yeast. *Fungal Genetics and Biology* **27:**224-230.

Sawin, K. E., and Nurse, P. (1998). Regulation of cell polarity by microtubules in fission yeast. *Journal of Cell Biology* **142(2):**457-471.

Sayers, L. G., Katayama, S., Nakano, K., Mellor, H., Mabuchi, I., Toda, T., and Parker, P. J. (2000). Rho-dependence of *Schizosaccharomyces pombe* Pck2. *Genes to Cells* **5(1):**17-27.

Schaefer, D. A., and Schroer, T. A. (1999). Actin-related proteins. *Annual Review of Cell and Developmental Biology* **15:**341-363.

Schliwa, M. (1999). Molecular motors join forces. *Nature* **397:**204-205.

Schmidt, S., Sohrmann, M., Hofmann, K., Woollard, A., and Simanis, V. (1997). The Spg1p GTPase is an essential, dosage-dependent inducer of septum formation in *Schizosaccharomyces pombe. Genes and Development* **11:**1519-1534.

Schott, D., Ho, J., Pruyne, D., and Bretscher, A. (1999). The COOH-terminal domain of Myo2p, a yeast myosin V, has a direct role in secretory vesicle targeting. *Journal of Cell Biology* **147(4):**791-807.

Seiler, S., Nargang, F. E., Steinberg, G., and Schliwa, M. (1997). Kinesin is essential for cell morphogenesis and polarized secretion in *Neurospora crassa. EMBO Journal* **16:**3025-3034.

Sellers, J. R. (1999). "Myosins." 2nd edn. Oxford University Press, New York.

Sellers, J. R. (2000). Myosins: a diverse superfamily. *Biochimica et Biophysica Acta* **1496:**3-22.

Sellers, J. R., Goodson, H. V., Wang, F. (1996). A myosin family reunion. *Journal of Muscle Research and Cell Motility* **17:**7-22.

Shannon, K. B., and Li, R. (1999). The multiple roles of Cyk1p in the assembly and function of the actomyosin ring in budding yeast. *Molecular Biology of the Cell* **10:**283-296.

Shannon, K. B., and Li, R. (2000). A myosin light chain mediates the localization of the budding yeast IQGAP-like protein during contractile ring formation. *Current Biology* **10:**727-730.

Skoufias, D. A., and Scholey, J. M. (1993). Cytoplasmic microtubule-based motor proteins. *Current Opinion in Cell Biology* **5:**95-104.

Smith, C. A., and Rayment, I. (1995). X-ray structures of the magnesium(II)-pyrophosphate complex of the truncated head of *Dictyostelium discoideum* myosin to 2.7 A resolution. *Biochemistry* **34:**8973-8981.

Smith, C. A., and Rayment, I. (1996). X-ray structure of the magnesium(II)·ADP·vanadate complex of the *Dictyostelium discoideum* myosin motor domain to 1.9 A resolution. *Biochemistry* **35:**5404-5417.

Snell, V., and Nurse, P. (1994). Genetic analysis of cell morphogenesis in fission yeast - a role for casein kinase II in the establishment if growth polarity. *EMBO Journal* **13:**2066-2074.

Sohrmann, M., Fankhauser, C., Brodbeck, C., and Simanis, V. (1996). The *dmf1/mid1* gene is essential for correct positioning of the division septum in fission yeast. *Genes and Development* **10:**2707-2719.

Sohrmann, M., Schmidt, S., Hagan, I., and Simanis, V. (1998). Asymmetric segregation on spindle poles of the *Schizosaccharomyces pombe* septum-inducing protein kinase Cdc7p. *Genes and Development* **12:**84-94.

Soldati, T., Geissler, H., and Schwarz, E. C. (1999). How many is enough? Exploring the myosin repertoire in the model eukaryote *Dictyostelium discoideum*. *Cell Biochem Biophys* **30(3):**389-411.

Song, K., Mach, K. E., Chen, C., Reynolds, T., and Albright, C. F. (1996). A novel suppressor of *ras1* in fission yeast, *byr4*, is a dosage-dependent inhibitor of cytokinesis. *Journal of Cell Biology* **133(6):**1307-1319.

Sparks, C. A., Morphew, M., and McCollum, D. (1999). Sid2p, a spindle pole body kinase that regulates the onset of cytokinesis. *Journal of Cell Biology* **146(4):**777-790.

Spudich, J. A. (1994). How molecular motors work. *Nature* **372:**515-518.

Steinberg, G. (2000). The cellular roles of molecular motors in fungi. *Trends in Microbiology* **8(4):**162-168.

Stevens, R. C., and Davis, T. N. (1998). Mlc1p is a light chain for the unconventional myosin Myo2p in *Saccharomyces cerevisiae*. *Journal of Cell Biology* **142(3):**711-722.

Stow, J. L., Fath, K. R., and Burgess, D. R. (1998). Budding roles for myosin II on the Golgi. *Trends in Cell Biology* **8:**138-141.

Streiblova, E., Hasek, J., and Jelke, E. (1984). Septum pattern in *ts* mutants of *Schizosaccharomyces pombe* defective in genes *cdc3*, *cdc4*, *cdc8*, and *cdc12*. *Journal of Cell Science* **69:**47-65.

Strome, S. (1993). Determination of cleavage planes. *Cell* **72:**3-6.

Sutherland, J. D., and Witke, W. (1999). Molecular genetic approaches to understanding the actin cytoskeleton. *Current Opinion in Cell Biology* **11:**142-151.

Sutoh, K. (1982). An actin-binding site on the 20K fragment of myosin subfragment 1. *Biochemistry* **21:**4800-4804.

Szent-Gyorgyi, A. G., Cohen, C., and Kendrick-Jones, J. (1971). Paramyosin and the filaments of molluscan 'catch' muscles. II. Native filaments: isolation and characterization. *Journal of Molecular Biology* **56:**239-258.

Takizawa, P. A., Sil, A., Swedlow, J. R., Herskowitz, I., and Vale, R. D. (1997). Actin-dependent localization of an RNA encoding a cell-fate determinant in yeast. *Nature* **389:**90-93.

Takizawa, P. A., and Vale, R. D. (2000). The myosin motor, Myo4p, binds Ash1 mRNA via the adapter protein, She3p. *Proceedings of the National Academy of Sciences USA* **97(10):**5273-5278.

Titus, M. A. (1997a). Myosin V - the multi-purpose transport motor. *Current Biology* **7(5):**301-304.

Titus, M. A. (1997b). Unconventional myosins: new frontiers in actin-based motors. *Trends in Cell Biology* **7:**119-123.

Titus, M. A., Novak, K. D., Hanes, G. P., and Urioste, A. S. (1995). Molecular genetic analysis of *myoF*, a new *Dictyostelium* myosin I gene. *Biophysical Journal* **68:**152-157.

Toda. T., Adachi, Y., Hiraoka, Y., and Yanagida, M. (1984). Identification of the pleiotropic cell cycle gene *NDA2* as one of two different α-tubulin genes in *Schizosaccharomyces pombe*. *Cell* **37:**233-242.

Toda, T., Shimanuki, M., and Yanagida, M. (1993). Two novel protein kinase C-related genes of fission yeast are essential for cell viability and implicated in cell shape control. *EMBO Journal* **12:**1987-1995.

Toda, T., Umesono, K., Hirata, A., and Yanagida, M. (1983). Cold-sensitive nuclear division arrest mutants of the fission yeast *Schizosaccharomyces pombe*. *Journal of Molecular Biology* **168:**251-270.

Tsakraklides, V., Krogh, K., Wang, L., Bizario, J. C. S., Larson, R. E., Espreafico, E. M., and Wolenski, J. S. (1999). Subcellular localization of GFP-myosin-V in live mouse melanocytes. *Journal of Cell Science* **112:**2853-2865.

Umesono, K., Toda, T., Hiyashi, S., and Yanagida, M. (1983). Two cell division cycle genes *NDA2* and *NDA3* of the fission yeast *Schizosaccharomyces pombe* control microtubular organization and sensitivity to anti-mitotic benzimidazole compounds. *Journal of Molecular Biology* **168:**271-284.

Uyeda, T. Q. P., Abramson, P. D., and Spudich, J. A. (1996). The neck region of the myosin motor domain acts as a lever arm to generate movement. *Proceedings of the National Academy of Sciences USA* **93:**4459-4464.

Uyeda, T. Q. P., and Spudich, J. A. (1993). A functional recombinant myosin II lacking a regulatory light chain-binding site. *Science* **262:**1867-1870.

Vale R. D. (1994). Getting a grip on myosin. *Cell* **78:**733-737.

Vale, R. D. (1996). Switches, latches, and amplifiers: common themes of G proteins and molecular motors. *Journal of Cell Biology* **135(2):**291-302.

Vale, R. D., and Milligan, R. A. (2000). The way things move: looking under the hood of molecular motor proteins. *Science* **288:**88-95.

Veigel, C., Coluccio, L. M., Jontes, J. D., Sparrow, J. C., Milligan, R. A., and Molloy, J. E. (1999). The motor protein myosin-I produces its working stroke in two steps. *Nature* **398:**530-533.

Verde, F. (1998). On growth and form: control of cell morphogenesis in fission yeast. *Current Opinion in Microbiology* **1:**712-718.

Verde, F., Mata, J., and Nurse, P. (1995). Fission yeast cell morphogenesis: identification of new genes and analysis of their role during the cell cycle. *Journal of Cell Biology* **131(6):**1529-1538.

Verde, F., Wiley, D. J., and Nurse, P. (1998). Fission yeast orb6, a ser/thr protein kinase related to mammalian rho kinase and myotonic dystrophy kinase, is required for maintenance of cell polarity and coordinates cell morphogenesis with the cell cycle. *Proceedings of the National Academy of Sciences USA* **95:**7526-7531.

Verkhovsky, A. B., Svitkina, T. M., and Borisy, G. G. (1995). Myosin II filament assemblies in the active lamella of fibroblasts: their morphogenesis and role in the formation of actin filament bundles. *Journal of Cell Biology* **131:**989-1002.

Volkmann, N., and Hanein, D. (2000). Actomyosin: law and order in motility. *Current Opinion in Cell Biology* **12:**26-34.

Wade, R. H., and Hyman, A. A. (1997). Microtubule structure and dynamics. *Current Opinion in Cell Biology* **9:**12-17.

Walker, R., and Sheetz, M. P. (1993). Cytoplasmic microtubule-associated motors. *Annual Review of Biochemistry* **62:**429-451.

Watts, F. Z., Shields, G., and Orr, E. (1987). The yeast *MYO1* gene encoding a myosin-like protein required for cell division. *EMBO Journal* **6:**3499-3505.

Welch, M. D., Mallavarapu, A., Rosenblatt, J., and Mitchison, T. J. (1997). Actin dynamics *in vivo*. *Current Opinion in Cell Biology* **9:**54-61.

Welch, M. D., Rosenblatt, J., Skoble, J., Portnoy, D. A., and Mitchison, T. J. (1998). Interaction of human Arp2/3 complex of *Listeria monocytogenes* ActA protein in actin filament nucleation. *Science* **281:**105-108.

Wells, A. L., Lin, A. W., Chen, L., Safer, D., Cain, S. M., Hasson, T., Carragher, B. O., Milligan, R. A., and Sweeney, H. L. (1999). Myosin VI is an actin-based motor that moves backwards. *Nature* **401:**505-508.

Wells, J. A., and Yount, R. G. (1979). Active site trapping of nucleotides by crosslinking two sulfhydrils in myosin subfragment 1. *Proceedings of the National Academy of Sciences* **76:**4966-4970.

Wells, J. A., and Yount, R. G. (1980). Reaction of 5,5'-dithiobis(2-nitrobenzoic acid) with myosin subfragment one: evidence for formation of a single protein disulfide with trapping of metal nucleotide at the active site. *Biochemistry* **19:**1711-1717.

Wessels, D., Titus, M., and Soll, D. R. (1996). A *Dictyostelium* myosin I plays a crucial role in regulating the frequency of pseudopods formed on the substratum. *Cell Motility and the Cytoskeleton* **33:**64-79.

White, J., and Strome, S. (1996). Cleavage plane specification in *C. elegans*: how to divide the spoils. *Cell* **84:**195-198.

Wiese, C., and Zheng, Y. (2000). A new function for the gamma-tubulin ring complex as a microtubule minus-end cap. *Nature Cell Biology* **2(6):**358-364.

Win, T. Z., Gachet, Y., and Hyams, J. S. (1999a). Myo52: a type V myosin concerned with growth polarity and cell division in fission yeast. *Molecular Biology of the Cell* **10** 162a.

Win, T. Z., Gachet, Y., Mulvihill, D. P., May, K. M., and Hyams, J. S. (2001). Two type V myosins with non-overlapping functions in the fission yeast *Schizosaccharomyces pombe*: Myo52 is concerned with growth polarity and cytokinesis, Myo51 is a component of the cytokinetic actin ring. *Journal of Cell Science* **114:**

Win, T. Z., May, K. M., and Hyams, J. S. (1999b). Two type V myosins with distinct functions in fission yeast. *Molecular Biology of the Cell* **10** 162a.

Wolenski, J. S. (1995). Regulation of calmodulin-binding myosins. *Trends in Cell Biology* **5:**310-316.

Wong, K. C. Y., Naqvi, N. I., Iino, Y., Yamamoto, M., and Balasubramanian, M. K. (2000). Fission yeast Rng3p: an UCS-domain protein that mediates myosin II assembly during cytokinesis. *Journal of Cell Science* **113:**2421-2432.

Wu, X., Jung, G., and Hammer HI, J. A. (2000). Functions of unconventional myosins. *Current Opinion in Cell Biology* **12:**42-51.

Xie, X., Harrison, D. H., Schlichting, I., Sweet, R. M., Kalabokis, V. N., Szent-Gyorgyi, A. G., and Cohen, C. (1994). Structure of the regulatory domain of scallop myosin at 2.8 A resolution. *Nature* **368:**306-312.

Yaffe, M. P., Hirata, D., Verde, F., Eddison, M., Toda, T., and Nurse, P. (1996). Microtubules mediate mitochondrial distribution in fission yeast. *Proceedings of the National Academy of Sciences USA* **93:**11644-11668.

Yamashita, R. A., and May, G. S. (1998). Constitutive activation of endocytosis by mutation of *myoA*, the myosin I gene of *Aspergillus nidulans*. *Journal of Biological Chemistry* **273(23):**14644-14648.

Yanagida, T., Kitamura, K., Tanaka, H., Iwane, A. H., and Esaki, S. (2000). Single molecule analysis of the actomyosin motor. *Current Opinion in Cell Biology* **12:**20-25.

Yin, H., Pruyne, D., Huffaker, T. C., and Bretscher, A. (2000). Myosin V orientates the mitotic spindle in yeast. *Nature* **406:**1013-1015.

Young, P. E., Richman, A. M., Ketchum, A. S., and Kiehart, D. P. (1993). Morphogenesis in *Drosophila* requires nonmuscle myosin heavy chain function. *Genes and Development* **7:**29-41.

Zang, J., Cavet, G., Sabry, J. H., Wagner, P., Moores, S. L., and Spudich, J. A. (1997). On the role of myosin-II in cytokinesis: Division of *Dictyostelium* cells under adhesive and nonadhesive conditions. *Molecular Biology of the Cell* **8:**2617-2629.

Zhao, Y., and Lieberman, H. B. (1995). *Schizosaccharomyces pombe*: a model for molecular studies of eukaryotic genes. *DNA and Cell Biology* **14(5):**359-371.